Coastal Dynamics

Geology, Economy and Environment

Dr. Rosalin Das
Prof. Rabindra Nath Hota
Dr. Asim Amitabh Pradhan
Dr. Smruti Rekha Sahoo
Mr. Arun Kumar Naik
Dr. Pankajini Mahanta
Dr. Satyabrata Nayak

Publisher:
STRING PRODUCTION
2H, 1066, Preet Vihar Colony,
Roorkee, Uttarakhand – 247667
Email: stringproductionofficial@gmail.com

COASTAL DYNAMICS GEOLOGY, ECONOMY AND ENVIRONMENT

ISBN: 978-93-6048-921-2

Cover Design & Book Layout by **Divyansh Manral**

Printed in India

Table of Contents

A Note on Depositional Environment of Bhuj and Jhuran Formation of Kachchh Basin, Western India Using Ichnology and Sedimentology

Sneha Bhaumik[1], Asthajita Bhuyan[2], Kalyan Kumar Neog[3], Shreerup Goswami[4], Rosalin Das[5], Dhirendra Kumar Pandey [6]

1. Ph. D Research Scholar, Fakir Mohan University, Balasore

2, 3. K. S. K. V. Kachchh University, Gujarat

4. Professor, Ph. D., D. Sc Head of Geology Department Utkal University

5. Associate Professor, Head of Geology Department Fakir Mohan University

6. Professor, Head of Geology Department, Central University South Bihar

*Corresponding author's email: dbhaumik588@gmail. com

Abstract

In Kachchh Basin during middle Jurassic, a major transgression took place but the intensity of rift related subsidence decreased. In the north and centre of the basin marginal alluvial fans, tidal flat and shoreline systems developed. On the west, shallow marine and shoreline systems dominated. The Nirona Formation and the lower part of Kaladongar Formation shows fluvial characteristics. Continuous transgression resulted in deepening of the marine basin and the depositional systems. The Jhuran Formation indicates deltaic to marginal marine environment. Ichnological data shows moderate to high diversity trace fossils and they denote regime between fair-weather and storm-weather wave bases. Integration of ichnological data with sedimentological data indicates fluctuatig wave and storm energy environment within normal marine conditions. The repetitive bioturbated cycles indicates the availability of colonization window, which is a prime reason for preserving bioturbation in wave-dominated settings. There are presence of glauconite grains seen which indicate continental shelf marine depositional environments with slow rates of accumulation. The cyclic events of Ghuneri Member offer better insight into the ichnology of the Early Cretaceous wave-dominated deltaic environment. An ideal bioturbated cycle of coarsening-up/ thickening-up cycles, varying from shale/siltstone/fine-grained sandstone to medium/coarse-grained massive to cross-bedded sandstone. Presence of herringbone, cross stratification and large troughs in upward sequence indicating storm energy environment. Trace fossils play an important role for understanding sedimentological, geological, basin analysis and also stratigraphic boundaries.

Key words : Jurassic, Kachchh Basin, Bioturbation, transgression, trace fossils.

1. Introduction

Ichnology and sedimentology plays an amazing role in depositional environment analysis. Trace fossils are considered to be crucial parameter for understanding the geological, sedimentological and ecological palaeo-events and paleo-environments because they are preserved in-situ and rarely undergo post-death transport. Ichnology has an advantage over other parameters for interpreting the basins and this concept was successfully used for basin analysis (Bottjer and Droser, 1991). The Upper Jurassic rocks of Western Kachchh have been extensively studied for their stratigraphy (Rajnath, 1932; Biswas, 1978), depositional environment (Bose et al. 1986; Fürsich and Pandey, 2003) and biostratigraphy (Krishna et al. 2000; Prasad, 1998). However, studies concerning ichnology of Western Kachchh are sparse (Badve and Ghare, 1978). The purpose of this paper is to to reconstruct the depositional environment history of the selected sections of Jhuran and Bhuj formation using a combination of sedimentology, petrography and ichnology.

The Kachchh Basin is a western marginal peri-cratonic rift basin developed during the Mesozoic times. The Kachchh basin preserves about 2000 to 3000 m of Mesozoic and 1000 m of Cenozoic sediments (Biswas, 1977, 1982). The Tertiary rocks are exposed along the coastal belt of southern and western Kachchh bordering the Mesozoic rocks. The Jurassic rocks of the Kachchh Basin have a rich fossil assemblages, which range in age from Pliensbachian to Late Tithonian times (Fürsich et al., 2013). The Kachchh region forms a crucial geodynamic part of the western continental margin of India and is an important site of Mesozoic and Cenozoic tectonic sedimentation. The general form of the uplifts are marked by domes and asymmetrical anticlines. The Northern fringe of the rocky mainland is marked by The Kachchh Mainland Fault according to Biswas (1974, 2003). The tectonic and seismic evolution of Kachchh region have been co-insisted with differential movement along the E-W trending master faults and NW-SE to NE-SW transverse fault systems. The drainage patterns of mainland and behavior of river channels ideally reflect that Kachchh is tectonically active. Kachchh has been divided into five zones which are : Kachchh Mainland, Wagad uplift, Pachham island, Khadir island and Bela island.

Kachchh Basin is considered to be extension of the Indus shelf. Here Precambrian sediments forms basement. Nagarparkar Igneous complex forms the northern rift shoulder, Saurashtra uplift forms its southern rift shoulder. The Eastern margin of the basin is marked by a gravity subsurface high known as Radhanpur Arc,. According to Biswas (1993) the development of the Kachchh Rift occurred in two stages (1) opening of Banni Half Graben (BHG) towards the north followed by further opening of the rift and forming (2) Gulf of Kachchh Half Graben (GOKHG) in the south. Both half grabens, i. e., BHG and GOKHG have sepeate sedimentary facies because both opened separately.

The sedimentation in the Kachchh basin occurred in three distinct phases (1) Pre-Rift, (2) Syn-Rift and (3) Post-Rift. The Pre-Rift stage sediments or rift opening sediments are exposed in the Banni Half graben (especially in the island belt). The sediments deposited in the syn-rift stage are characterized by early syn-rift, rift climax and late syn rift stages. These sediments display evidences of four major transgressions associated with three regressive phases (Biswas, 1993). These transgressions occurred during Late Bathonian, Early Callovian, Early-Middle Oxfordian, and Tithonian Transgression. A fifth, short lived Early Aptian transgression was also ascertained in the western Kachchh recently (Desai, 2013). The early syn-rift basin fill is characterized by conglomerates and sandstones (Chariya Bet Conglomerate Member) deposited as fan and fluvial environment (Fursich et al., 2004). These are only exposed in the Island belt (Banni Half Graben). The end of the early syn-rift stage is marked by opening of GOKHG. Late syn rift stage is marked by the series of high frequency Transgressive-regressive cycles depositing Kimmerdigian and Tithonian sediments. The post rift stage is characterized by prograding deltaic system restricted in GOKHG.

2. Geological Setting

The Kachchh Mainland are classified into four formations viz., the Jhurio, Jumara, Jhuran and Bhuj formations in ascending order (Biswas, 1977) and is composed of repetitive transgressive-regressive cycle. The Bhuj formation is only established in Kachchh Mainland and further subdivided into Ghuneri, Ukra and the Upper Member (Biswas, 1977). Biswas (2016a) introduced the term "Group" within stratigraphy and included the basin in different basins and i. e Kachchh Mainland Group, Pachchham Island Group & Eastern Kachchh Group. The Ukra member of Bhuj Formation is marine transgressive unit which is mainly exposed in distal part of the deltaic environment in western side (Biswas, 1993; Desai, 2013)many years geologists have been using Biswas's classification, but many new member have been introduced but many of them have not been formalized (e. g., Fürsich et al*.,* 2013, 2020). The early biostratigraphy by Waagen (1873-75) was largely supported by Krishna and his coworkers (e. g., Krishna and Pathak, 1991; Krishna and Ojha, 1996; Krishna, 2005, 2017; Krishna et al., 2011) and also by others (e. g., Agrawal and Pandey1985; Bardhan and Datta, 1987; Pandey and Westermann, 1988; Jain and Pandey, 2000; Roy et al., 2007; Pandey et al*.,* 2012, 2016).

Sequence stratigraphy of Jurassic Successions were addressed by many workers (e. g., FürsichandOschmann, 1993; Fürsich et al., 2001; Fürsich and Pandey, 2003; Krishna, 2005, 2017, p. 150; Joseph and Patel, 2015;Desai et al., 2021).

The sections of the study area shows the coarsening upward sequence which starts with fine -medium grained sandstone. The basal part of each section starts with Jhuran formation which is mainly characterized by argillaceous siltstone and ferruginous

siltstone intercalations with ammonitic fragments. This is followed by fine grained sandstone which shows fine parallel laminations and also sometimes hummocky cross stratification which is alternate thin parallel laminated bioturbated sandstone. This is followed by highly bioturbated tabular planar cross stratified fine grained sandstoneintercalated with thinly laminated siltstone. These bioturbated sandstone is often appeared with alteration of ripple laminated sandstone *Gyrochorte*and also*Rhizocorallium*. The bioturbation increases in upward direction. Mainly the Ghuneri member of Bhuj formation is characterized by thick beds of sandstones with alteration of ferruginous siltstone and also shale. The sandstones are well sorted and on the basis of modal analysis the cementing percentage is much more in Bhuj formation rather in Jhuranformation. The sandstones of Bhuj formation are mainly quartz arenitic. In large coarse grained sandstones are characterized by herringbone cross stratification. In the uppermost part the coarse grained sandstone is also characterized by some deeper vertical burrows like *Diplocraterion*, *Skolithos*. The bed tops is characterized by linear wave ripples with crest bifurcation and also flat crests. The bioturbated sequences are also characterized by *Glossifungutes.* Previous works suggest that theGhuneri member of Bhuj Formation is mainly characterized with bioturbated cycles (Desai, 2016) and contains *Balanoglossites*from the *Glossofungites*ichnofacies (Desai and Saklani, 2012) and *Conichnusconicus*(Desai and Saklani, 2015). Other trace fossildiscoveries include *Thalassinoides*, *Skolithos*, *Chondrites*, *Ophiomorpha*, *Rhizocorallium*, *Aulichinites*from the Umiaformation (=Lower part Ghuneri Member) (Krishna, 1987). *Asteriacites quinquefolis*– starfish trace (Patel *et al*., 2008)

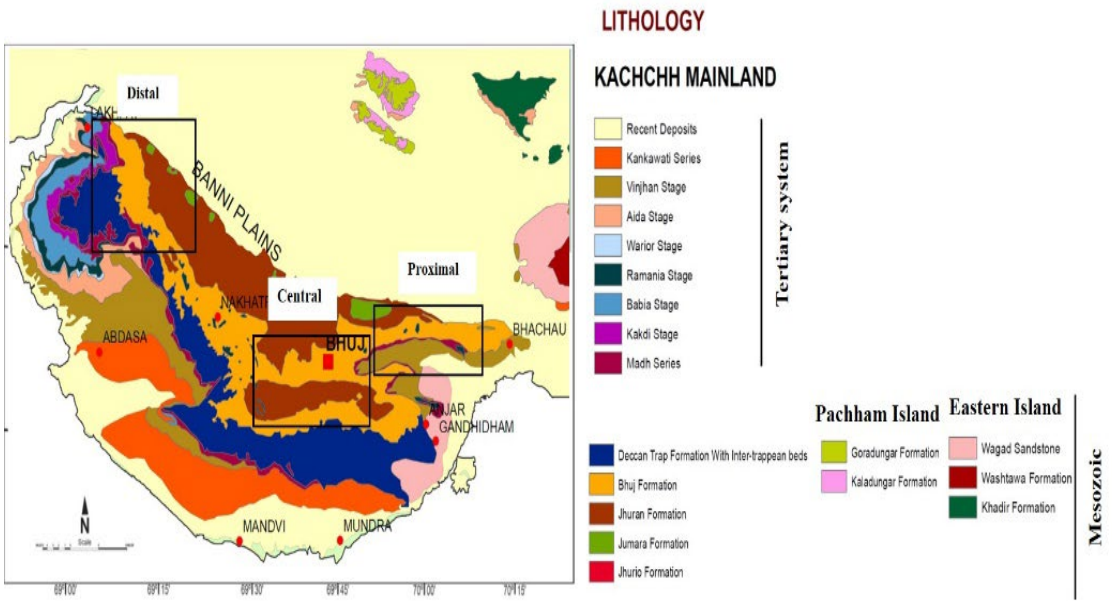

Figure 1. Location map of the Kachchh Basin along with outcrop exposures.

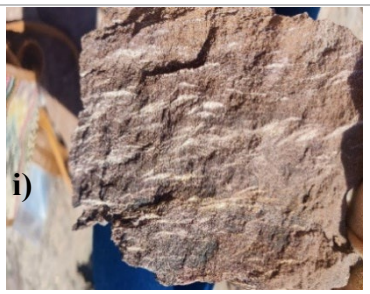
i)

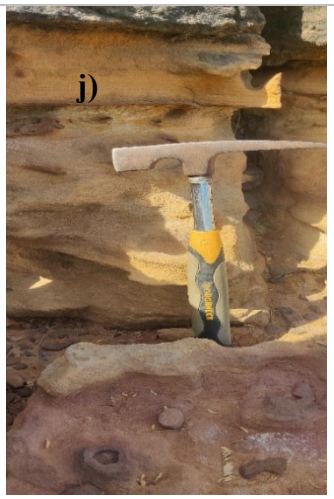
j)


k)


l)


m)

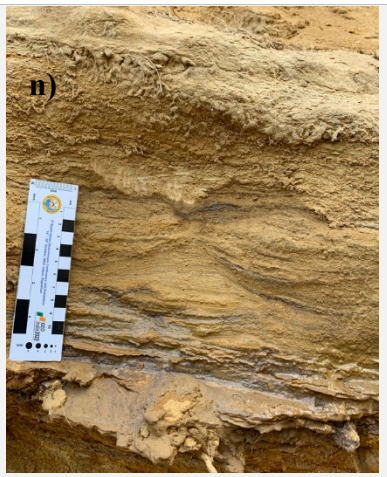

Fig:2 *: Field Photographs of different sedimentary structures a, e) herringbone cross stratification, b) large trough cross stratification, c) parallel lamination, d) oscillatory ripple marks, f) g) low angle cross stratification, h) presence of quartz pebbles along the troughs, i) medium grained, low angle cross stratified, thinly bedded, clay interbedded sst; upper surface of the sst bed is ripple laminated with horizontal burrows, j) fine-medium grained low angle cross stratified sandstone with rare vertical burrows and also iron concretions, k)thickly bedded medium- coarse grained sst along with large scale cross stratification and herringbone cross stratification, the upper surface is bioturbated, l) Trigonia bed below the basal part of Ghuneri Mb in Lakhapar, m) GAB III in Katesar, n) flaser bedding, o) lithology measurement in Tapkeshwari area.*

3. Materials And Methods

The present study involves the sections which are exposed at Tapkeshwari Section, Bhuj Mundra Section, Lakhapar Sections Katesar Dome Section. Within these sections detailed lithology, grain size, ichnology, sedimentary structures, diagenetic features have been studied to understand the sedimentary environment. The bed rock samples have also been collected from each bed to understand the porosity, matrix & cement percentage towards the younging direction of the formations. With the help of Dickinson et al (1983) Modal analysis identification and recording the amount of monocrystalline quartz (Qm), polycrystalline quartz (Qp), (Qm and Qp make together makes the total quartz Qt), feldspar (F), lithic sedimentary and metasedimentary clasts (Ls) and lithic volcanic clasts (Lv), (Ls and Lv constitute together with lithic clastics L) have been done. Sections were made with the help of Corel Draw Graphic Suit.

4 Localities and Sections

The cyclic sedimentation of Kachhchh Basin is mainly characterised by shallow water siliciclastic sedimentary cycles which are overlain by thick pebbly coarsening upward

sequence which are the part of shallowing sequence. They are reworked again during transgression event. Most of the bed represents are the part of Highstand System Tract (HST) where as the coarsening upward sequence Transgressive System Tract (TST). Fürsich& Oschmann (1993) said that the reworked concretions represent the lag deposits those show the period of non sedimentation phase, they are the part of transgressive system tract. TST-HST are mainly controlled by the accommodation space and rate of sedimentation.

The major transgression event was recorded Bajocian period which is represented by the marker horizon and i. e. Upper Bajocian *Leptosphinctes* PebblyRudstone which can be traced from island belt upto Kachchh Mainland (Fürsichetal. 2001; Fig. 4).

4. 1 Tapkeshwari Section

An ideal cycle which is coarsening upward from thin banded siltstone – shale -fine grained sandstone to coarse grained sandstones which are highly cross bedded and i. e indicative of high energy environment. The ichnological evidences indicate the regime between fair weather and storm weather wave base. Deltaic deposits are common in eastern part of the study area ; the succession varies from prodelta to delta front environment. The section lies in the south western part of Bhuj (co-ordinates: *N 23°10′, E 69°40′)*. In this section the Katrol Formation of Kimmeridgian age was observed which are dominated by fine grained parallel laminated argillaceous sandstone, they are bioturbated at the lower part. But in the upper part Hummocky Cross Stratification (HCS) was observed and the sandstones are being coarser which are indicative of higher energy environment. The Katrol formation is followed by Jhuran Formation which are dominated by intercalated sandstone-shale unit which are characterised by oscillatory ripple marks and becoming kaolinized in the upper part. It is believed that the lower part of Bhuj Formation starts where the grain size is becoming coarser and mainly chracterised by deeper burrows.

In addition to that presence of deeper burrows also indicate high energy environment. The *GyrochorteComosa* is very much common throughout the section. In the lower part *Rhyzocorallium* is very much common in thinly laminated sandstone which indicates the energy level is very much low. *Diplocraterion* is also observed in upper part of coarse grained sandstone unit.

Presence of *Skolithos* indicate high energy environment; at some places due to the lack of sediments or due to slow sedimentation they were able to build colony even within fine grained intercalated sandstone and shale unit. The bioturbated cycles have been deposited in wave deposited deltaic environment. The cycle is mainly defined by coarsening and thickening up cycle. The ichnological data shows theassemblages are in between fair weather andstorm – wave bases ; indicating the fluctuation of wave and storm energy within normal marine condition. In the southern part of Tapkeshwari

section around (co-ordinates: *N 23°8′, E 69°39′)*near river section*Asteriacites quinquefolius*are common in lower Bhuj formation which indicates intertidal environment. They are mainly exposed in ferruginous ripple marked sandstone.

4. 2 Bhuj-Mundra Road Section

As like the Tapkeshwari Section here we also have seen coarsening or thickening upward sequence of thinly bedded mudstone-siltstone to fine grained sandstone to coarse grained sandstones which indicates fluctuation of wave energy. Presence of herringbone structure, cross stratification, highly cross bedded sequences and large troughs are seen in upward sequences which indicates storm energy environment. This location is at one of the exposure of the Katrol Hill Range (Fault), co-ordinates:*N 23°10′, E 69°38′.* Just like Tapkeshwari section ichnologicalevidences indicates the regime between fair weather and storm weather wave base. In this section Katrol Formation of Kimmeridgian age was observed, characterised by fine grained sandstone or shale. Followed by Jhuran Formation of Tithonian age which are dominated by intercalated sandstone-shale unit and characterised by oscillatory ripple marks. Jhuran rocks were followed by coarse grained sandstones which contains some deeper burrows, *skolithos,* characteristic of Bhuj formation. Below this tiny flame structures were also seen. At the lower sequences repeated bioturbated beds are seen.

Almost at the boundary between Jhuran and Bhuj Formation a bioturbated zone seen where*skolithos,* Y shaped burrows indicates high energy environment, were present. In addition*GyrochorteComosa, Gyrochorte Variabilis,* brush or fan like, were seen at a high amount. It indicates shallow-marine storm dominated environment. Some ichnofossils like- *Paleophycus*indicator of marine or lacustrine environment, *Taenidium,* indicator of shallow to deep marine environment, *Balanoglossus,* indicator of shallow marine environment between tide marks, *Rhizocorallium,* indicator of shallower and high energy environment are found. The bioturbated cycles have been deposited in wave dominated deltaic environment. The ichnological data shows the assemblages are in between fair weather and storm – weather wave bases ; also indicates the fluctuation of wave and storm energy within normal marine condition.

4. 3 Lakhapar Section

Just like the previous sections here we have also seen a cyclic thickening or coarsening upward sequences from fine grained sandstone-shale to siltstone to coarse grained sandstones with cross stratifications. At the lowermost bed there have been fragments of Ammonites and lots of fragments of burrows were found. The bed is considered as Umia Ammonite Bed (co-ordinates: *N23°42′, E68°57′*), part of the Umia Formation belongs to Late Tithonian sediments. UAB is followed by a fine grained kaolinized sandstone bed where we have seen fragments of wood fossils which is sometimes called as umia plant bed. Following beds contains green coloured planar laminations or glauconitic

sandstone beds are found. As we were moving upward there is coarsening of grains. At the upward sequences there were presence of cross stratifications which indicates us high energy or storm energy environment. At the upward sequences we have found a bed of *GyrochorteComosa*which indicates us shallow marine storm dominated environment. At the atmost top, we have seen three *Trigonia*beds of Bhuj Formation of Early/Lower Cretaceous age, which indicates us warm-shallow marine environment. The beds which contain *Trigonia*are ferruginous and coarse grained.

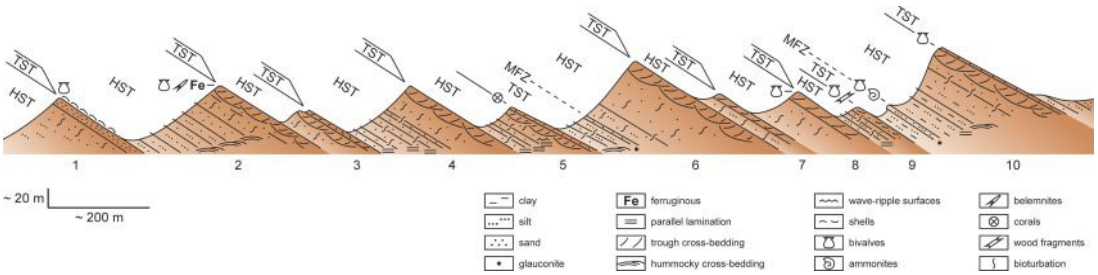

Fig. 3: Schematic cross-section through the Middle member of the Jhuran Formation north of the Lakhapar village with individual TST-HST sequence (modified from Fürsich& Pandey 2003: fig. 3).

4. 4 Katesar Section

At Katesar (co-ordinates: *N 23°46′, E 68°53′*)a section has been mapped across the strikefor stratigraphical, sedimentological, ichnological studies. The basal part of the section started with Green Ammonite Bed which is highly glauconitic in nature and that contains high concentration of biogenic parts which indicates that there's extensive sediment starvation which demarcates the maximum flooding zone. Concretions are the most important features in fine grained sediments of KatesarSection. Some concretions are autochthonous and some of them are reworked due to wave and current actions. At some places wave ripples are very much common. In the south western part the upper part of middle member of Jhuran Formation is exposed which is also highly bioturbated, kaolinized and ferruginous. That correspond to the highstand system tract of the cycle. *Gyrochorte*is encountered within ferruginous medium to fine grained poorly sorted sandstone. Towards the younging direction the sandstones are much more coarser and also quartz rich. These were devoid of marine fossils. Due to extensive weathering the burrows are not well preserved. In the uppermost part of this section some well preserved long vertical burrows of 3-4 cm in width and 10-15 cm in length have been observed which are believed to be *Skolithos* have been observed. These are formed due to slow sedimentation rate due to increase in water depth below the wave base. The strata was formed under the influence of high energy, fair weather wave base and tidal currents. The presence of such trace fossils reflect the changes in water depth and also the other ecological conditions. In southern part of Katesar Mahadev Temple (co-ordinates: *N 23°46′42", E 68°52′*)Ukra member of Bhuj Formation is exposed. The member is

fossiliferous calcareous glauconitic shales. Presence of glauconite indicates shallow to moderately deep marine environment with low sedimentation rate and low oxygen condition. The glaucotnitic fine grained sandstone is overlain by massive ferugenous sandstone

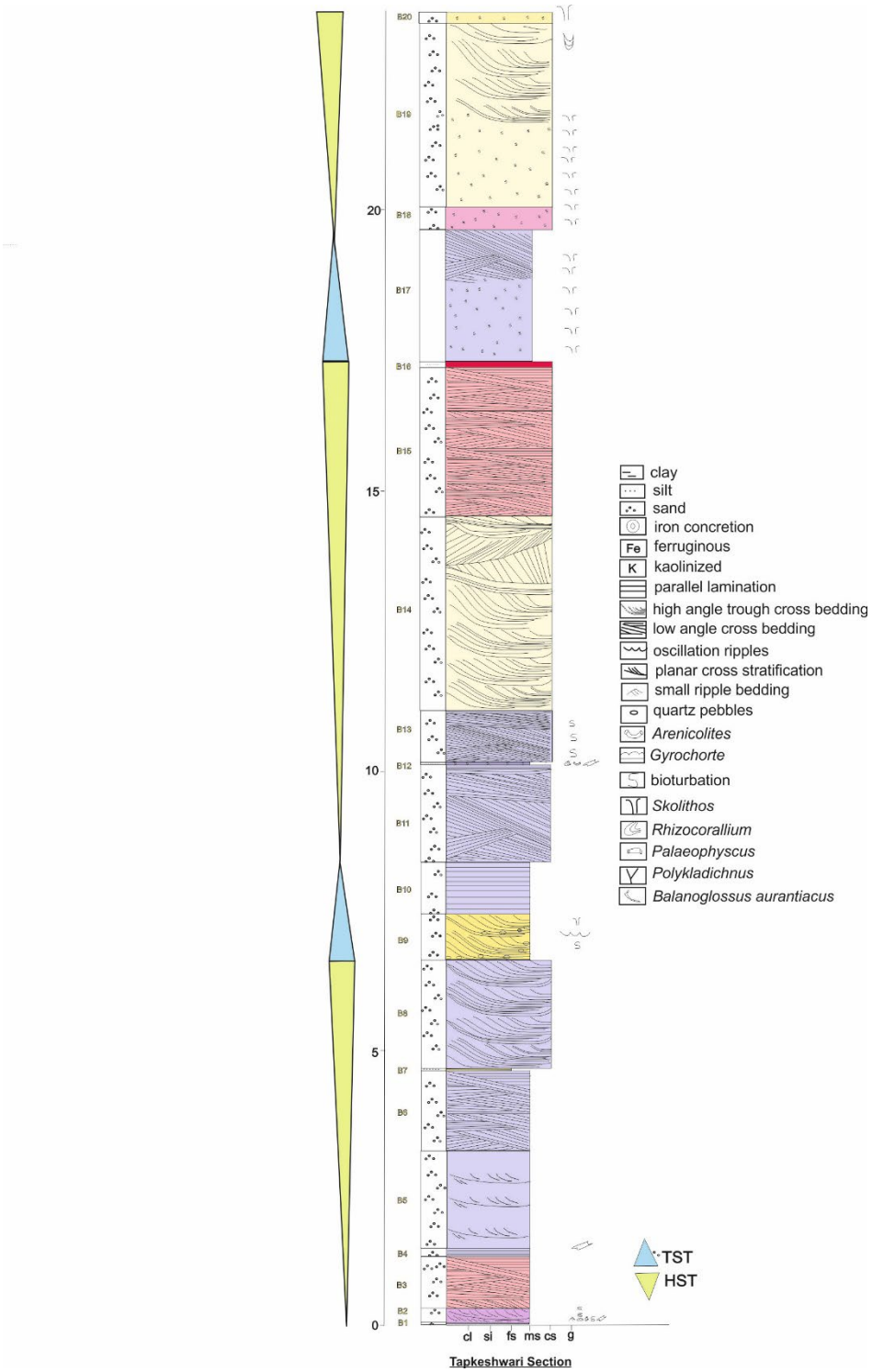

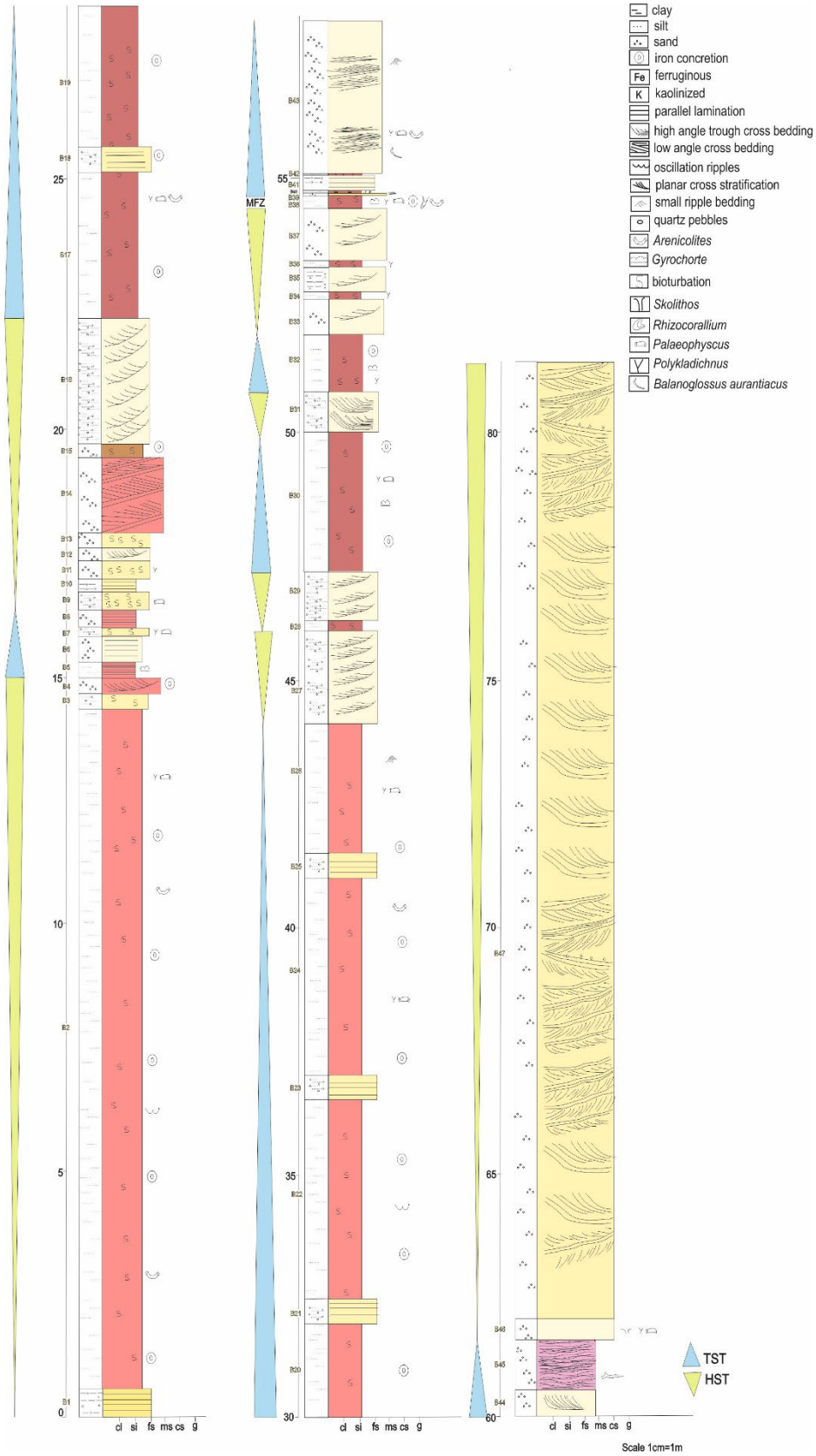
clay
silt
sand
iron concretion
Fe ferruginous
K kaolinized
parallel lamination
high angle trough cross bedding
low angle cross bedding
oscillation ripples
planar cross stratification
small ripple bedding
quartz pebbles
Arenicolites
Gyrochorte
bioturbation
Skolithos
Rhizocorallium
Palaeophyscus
Polykladichnus
Balanoglossus aurantiacus
MFZ
TST
HST
cl si fs ms cs g
Scale 1cm=1m

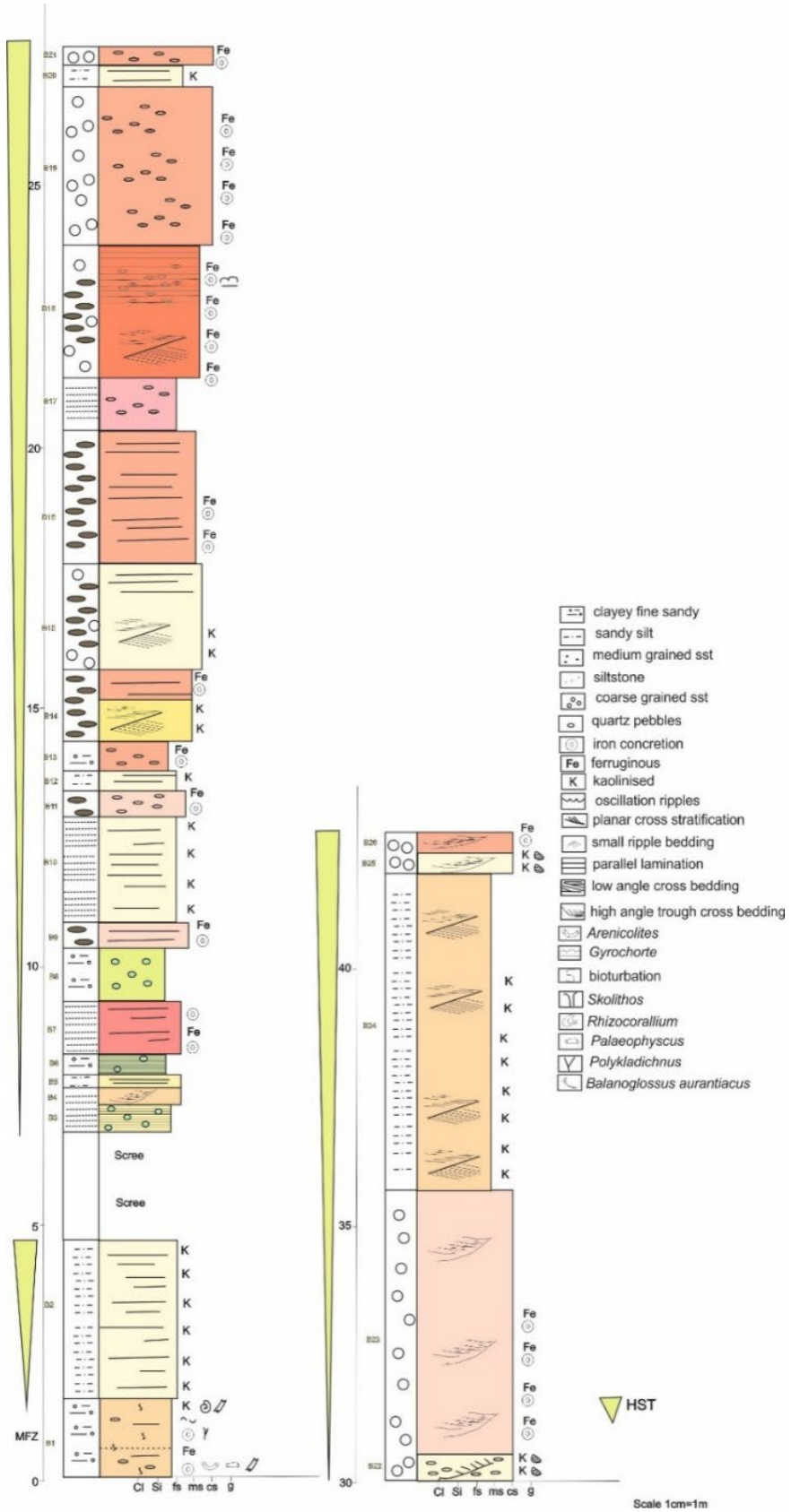
clayey fine sandy
sandy silt
medium grained sst
siltstone
coarse grained sst
quartz pebbles
iron concretion
Fe ferruginous
K kaolinised
oscillation ripples
planar cross stratification
small ripple bedding
parallel lamination
low angle cross bedding
high angle trough cross bedding
Arenicolites
Gyrochorte
bioturbation
Skolithos
Rhizocorallium
Palaeophyscus
Polykladichnus
Balanoglossus aurantiacus
Scree
Scree
MFZ
HST
Cl Si fs ms cs g
Scale 1cm=1m

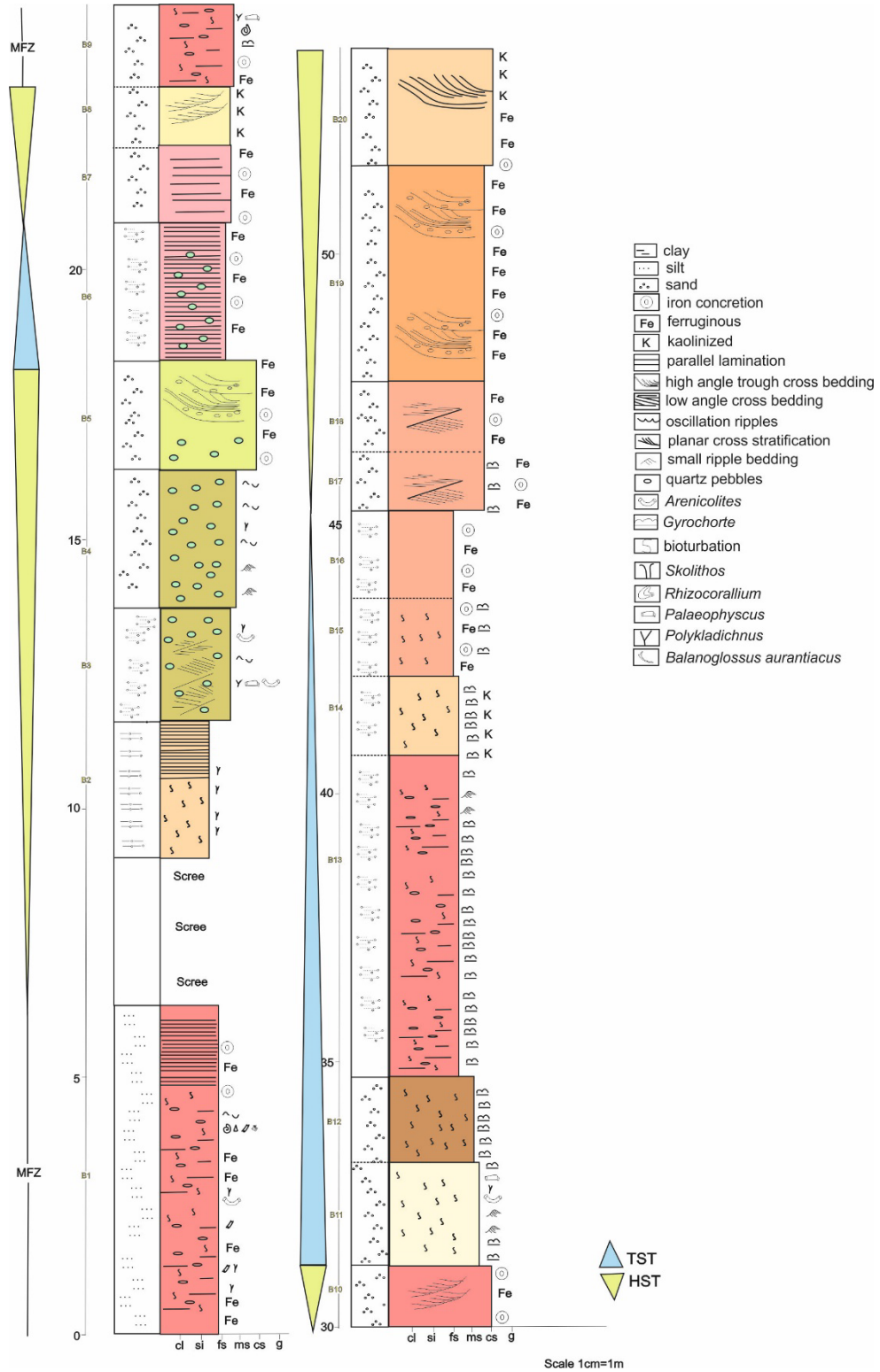

Figure 4 :Lithologs of the localities in the eastern & western part of Kachchh Basin;TST : Transgressive Systems tract; HST :High Stand Systems Tract; MFZ: Maximum Flooding Zone

Recent studies have shown that the threemembers are re-interpreted as, wave-dominated delta forGhuneri Member (Desai, 2016; Bhatt and Patel, 2017; Desaiand Chauhan, 2021), transgressive unit for Ukra Member (Desai, 2013, 2016; Bansal *et al.,* 2017) and fluvial dominateddelta for Upper Member (Biswas, 1993). The Ghuneri member of Bhuj formation shows asymmetric bioturbated zones. The Bhuj Formation is only exposed in the KachchhMainland and can be sub-divided into Ghuneri, UkraandUpper Member in ascending order (Biswas, 1977). The thickness of Ghuneri member thickens progressively from eastern to western part. In Tapkeshwari, Bhuj Mundra section the uppermost beds are characterised by medium to coarse grained sandstones which are mainly quartz arenites. The sandstones are dominated by large scale trough cross bedding at some places large hummocks can also be observed. These sandstones are highly bioturbated. They exhibit different types of *Glossifungites*ichnospecies. According to (Bose *et al*., 1986) the Ghunerimember of this formation is characterised by wave dominated delta. The Ukra member of the uppermost part of this formation is only exposed in the western part of the basin. Previously it was discovered that the Ghuneri member of the formation is characterised by contains*Balanoglossites*fromthe *Glossofungites*ichnofacies (Desai and Saklani, 2012) and *Conichnusconicus*(Desai and Saklani, 2015). Other trace fossildiscoveries include *Thalassinoides*, *Skolithos*, *Chondrites*, *Ophiomorpha*, *Rhizocorallium*, *Aulichinites*from the Umiaformation (=Lower part Ghuneri Member) (Krishna, 1987). *Asteriacitesquinquefolis*– starfish trace (Patel *et al*., 2008). In Lakhapar section a *Trigonia*shell beds have been observed. The basal boundary Ghuneri member is considered to be the part of short transgressive unit in deltaic progradation (Biswas, 1993; Desai, 2013).

Systematics :

Ichnogenus Arenicolites Salter, 1857

Arenicolites variabilisFürsich, 1974a

Pl. I Fig. I

Description: They are vertical or sometimes oblique U-shaped, rarely J-shaped burrows without spreite. Tubes are cylindrical has smooth walls. The arms of the U-tubes are straight to curved and parallel to each other. In cross-sections, they also appear as J-shaped. Has diameter between 9-30 mm, distance between two parallel arms between 20-40 mm and burrowing depth varies between 15 to 27 cm. Created by suspension feeding, dwelling, sound resonance (Wilson, 1971).

Discussion: The burrows has a high variety in morphology with narrower width of U tube and greater depth. *Arenicolites* are considered as a dwelling, sound resonance and feeding structure of suspension-feeding (Hakes, 1976) or crustaceanlike organisms (Goldring, 1962). *Arenicolites* are distinguished from *Diplocraterion* by the absence of spreiten in *Arenicolites*(Fürsich, 1974a). Although known to occur in diverse

environments, including eolian (Ekdale et al., 2007), non-marine (Guillette et al., 2003), marine, freshwater lacustrine and fluvial (Eager et al., 1985), it is typical of shallowmarine settings (Crimes, 1977). Commonly occur as a post-depositional features and passively filled with coarse-grained sediments, but the Kachchh specimens lack retrusive structures. Arenicolites are interpreted as a work of suspension-feeding polychaetes (Fürsich, 1974a; Patel and Desai, 2009).

Asteriacites Quinquefolius*,* Quenstedt 1876

Description : These are star-like trace fossils consisting of five tapering arms which radiates outwards from the centre. They are conical or sub-conical or sub-cylindrical biogenic structures with pentamerous symmetry. They are transversely striated with double row of nodes or rounded radial grooves. They occur in the form of depression or concave epirelief on the casting material.

Discussion : Four *Asteriacites* are recognised viz. *Asteriacites stelliformis Osgood*, 1970, *A. quinquefolius Quenstedt*, 1876, *A. lumbricalis von Schlotheim*, 1822 and *A. aberensis* Crimes and Crossley, 1991. *A. quinquefolius Quenstedt*, 1876 is larger and has broader arms and a "shaggy" (zotting) appearance rather than with transverse striations. The star fish (Asteroids) is virtually a symbol of sea life and are found more on hard rocky bottom or shelly bottom. Sometimes the species that live more or less buried necessarily occur on the sandy bottom. The resting traces of *A. quinquefolius* is identical to star fish- *Astropecten* (Asteroids) and repetitive arm movement intergrades with crawling traces. The animal is stranded on sandy sediments making an impression on sediments and departs from the same route during fluctuations of the water level conditions in tidal flat environment. *Asteriacites* most commonly has been reported from shallow marine deposit of presumed normal marine salinity (Miller and Knox, 1985).

The specimens from Bhuj Formation suggest intertidal environment and They are mainly exposed in ferruginous ripple marked sandstone.

Ichnogenus BalanoglossitesMägdefrau, 1932

BalanoglossitestriadicusMägdefrau, 1932

Pl. I Fig. II

Description: *B. triadicus*are irregularly oriented, branched tunnels, does not have faecal pellets and forms a complex three-dimensional network. Shows U, J, Y, or I shape in a vertical section. All burrows are of diameter 10-28 mm and unlined with sharp margins. The cross-section of the lower part of the burrows are circular to elliptical. The burrow has large width towards the top of the bed, shaping into funnels forms a wider irregular opening. The burrows are structureless, contrasts with the host rock and passively filled of mediumto coarse-grained sand grains. Locally burrows are filled with purple to reddish coloured ferruginous rims or halos.

Discussion: *B. triadicus* (Mägdefrau, 1932) was first studied from the Middle Triassic sediments of Germany, which Knaust (2008) re-described as a complex type of trace caused by both burrowing and boring behaviour. Also, the ichnospecies *B. eurystomus* (Mägdefrau, 1932) is considered as junior synonymy under *B. triadicus*. The present specimens lack faecal pellets and give indications of firmground (Desai and Saklani, 2012). *B. triadicus*has irregular branching with a complex pattern of burrows. They indicates environment of shallow waters between tide marks along the coast of warm oceans.

EXPLANATION OF PLATE I

I) *Arenicolites variabilis*in fine to medium grained sandstoneII)*Balanoglossitesramosus*s in highly bioturbated sandstone III)*DiplocraterionParallelum* - medium –coarse grained trough cross bedded bioturbated sstIV)*GyrochorteComosa*found in ferruginous medium to fine grained sandstone of all the sections V)*Fan* like structure of *Gyrochorte variabilis* occurring in

Balanoglossitesramosus Knaust, 2008

Description: Complex three-dimensional burrow network comprises of vertical to inclined shafts connected to horizontal tunnels. In cross-section the tunnels and shafts are seen circular to elliptical and at some places irregular. Tunnels are local blind-ended and sometimes show side branching. Shafts are straight or curved and sometimes bifurcate and continued as inclined or horizontal tunnels. They has unlined tunnels and shafts, and has clean and sharp margins. Burrows are filled with medium to coarsesand grains, structureles sediments.

Discussion: Stratigraphically, the trace fossils range from Ordovician (Knaust, 2008; Dronov, 2011) to Holocene and also in recent deposits (Patel and Desai, 2009). They are more abundant and widely reported from the Triassic carbonate successions of the German Basin (Kazmierczak and Pszczołkowski,


II

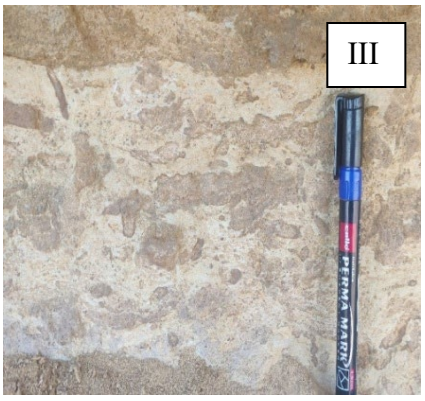
III
PERMA MARK


IV

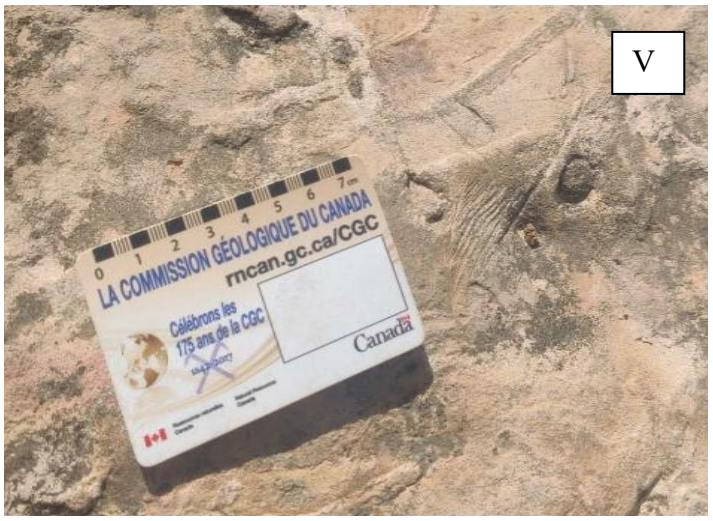
V
LA COMMISSION GÉOLOGIQUE DU CANADA
rncan.gc.ca/CGC
Célébrons les 175 ans de la CGC
Canada

1969; Knaust, 2008). These trace fossils are reported shallow marine condition (Knaust, 2008), lower intertidal zone (Kazmierczak and Pszczołkowski, 1969), storm dominated shallow marine environment (Dronov, 2011), intertidal lagoon (Patel and Desai, 2009).

Ichnogenus Chondrites Sternberg, 1833

Chondrites intricatus Brongniart, 1823

Description: Regularly branching tunnel systems, consisting of a small number of sub vertical shafts, dichotomously branched burrows, bifurcating at an angle >45° with 1st or 2nd order of branching. Branches rarely interconnected with each other. Tunnels are straight with a rounded or tapering end, and in cross-section seen elliptical. Tunnel diameter varies from 4 to 10 mm. Burrows fills both active or passive and fills different from the host sediment.

Discussion: *C. intricatus* distinguished from other species in the angle of branching and diameter of the burrow. *C. intricatus* are more slender than other specimens. Mono-species occurrence of Chondrites is indicative of anoxic conditions (Bromley and Ekdale, 1984). These are considered as a burrows of a deposit feeding worm like organism. Possible trace-makers are *Sipuncuild* or marine worm organism similar to modern *polychaetes*. *Chondrites* trace makers are also considered chemo symbiotic organisms (Seilacher, 1990; Fu, 1991). They indicates fully marine, low oxygen environment. In recent intertidal zones of Mandvi, Gulf of Kachchh, the trace makers of Chondrites shows changes in feeding strategies during reversal of flow during changing tidal condition (Patel and Desai, 2009).

DiplocraterionParallelum Torell, 1870

Pl. I. Fig. III

Description: Vertical, U-shaped burrow with retrusive spreiten between vertical arms, unlined burrow fill, and spreite sediments are similar to the host sediments. Burrrow top forms a relatively wide semi-spherical bulb or dumb bell shape in plain view. The arms

of the burrows are straight and parallel to each other. The tubes has diameter between 1 to 3 mm, with inter-tube distance 7 to 10 mm with a depth of burrow up to 60 cm.

Discussion: *D. parallelum* is characterized by straight and parallel arms of the burrows and have little distance. They are created by dwelling behaviour of a suspension feeder. *Diplocraterion* is considered as the work of the suspension-feeding organisms (Fursich, 1974b). *D. parallelum* is probably produced by worms which occurs commonly in Paleozoic, Mesozoic and Cenozoic sediments (Gerard and Bromley, 2008). The retrusive spreite structure is mainly related to the impermeability of sediments or perturbation in sediments. They indicates marine intertidal, shallow subtidal environments and deep-water environments, such as fans and distal shelves.

Ichnogenus Gyrochorte Heer, 1865

GyrochorteComosa(Heer, 1865)

Pl. I. Fig. IV

Description: *G. Comosa*are straight to sinuous oriented horizontal burrows consisting of smooth ridges with a median furrow and has two lobes. Burrows have both positive and negative epirelief preservation. In the upper surface its curved bilobate ribbon type, it is called as epirelief and the lower portion is known as hyporelief. There are fine striations along the ribbon and also form wide V type shape above the surface. The width of *G. Comosa*trail ranges from 3 to 6 mm and the length is approximately 40 cm. The *Gyrochorte* is a deposit feeder which is used to move obliquely along the sediment. In cross section it gives an expression of double arches and it is generally deposited in storm dominated or high energy, near-shore or shallow-marine environment in fine grained planar laminated sandstone along with *Pascichnia*and *Fodinichnia*. In parallel laminated, HCS and also in oscillatory ripple surfaced sandstone *GyrochorteComosa*is common.

Discussion: *Gyrochorte* is the burrow of an animal that selects food from the sediments through their entire body (Powell, 1992). This kind of traces commonly occurs throughout the almost entire Mesozoic sediments of the Kachchh Basin. *Gyrochorte* is characterized by the vertical dimension of convex epirelief and the corresponding hypo reliefs in the same bed (de Gibert and Benner, 2002). These traces are called as the work of an opportunistic organism from high energy, shallow marine environment (de Gibert and Benner, 2002). *Gyrochorte*typically occurs in sandy facies of moderately energetic, near-shore and shallow marine environments (de Gibert and Benner, 2002)

Ichnogenus Gyrochorte Heer, 1865

Gyrochortevariabilis (Fürsich Alberti and Pandey, 2017

Pl. I. Fig. V

Description:*Gyrochorte variabilis* shows distinct morphology and also shows a distinct feeding behaviour. It shows lateral displacements along the ribbon which some authors called as brushes and some as fan type. Due to lateral movement the fans start to appear generally by arthropods or worm like organisms. The feature of fan indicate that the organisms scooped out the sediment for sometime and then dragged its body to construct new shape of fan. Mainly there are five types of morphological expressions generally observed. Franz T. Fürsich et. al, Matthias Alberti et. al and Dhirendra K. Pandey et. al 2016 explained the following types Type 1: predominantly transverse ridges and biserially arranged pads. Type 2: biserially arranged pads, elongated in the direction of the ribbon and oblique with respect to the horizontal plane. Type 3: biserially arranged elongated pads, long axis of pads forming an angle with the direction of the ribbon. Type 4: Elongated pads forming an oblique angle with the direction of the ribbon. A biserial arrangement is no longer visible. Type 5: fan-like arrangement of bilobate rays. Types 3 to 5 are stages of a morphological continuum.

Discussion: The *Gyrochorte Variabilis* has fan-like or brush like arrangements of bilobed trraces which distinguished it from other species of *Gyrochorte* (Fürsich et al., 2017). In general, polychaetes or worm-like organisms makes these types of traces (Seilacher, 2007). The "brushes" forming fanning pattern is considered a behavioural variant of the trace makers (Weiss, 1949; Seilacher, 2007). The brushes or fan-like structures occurred both in one direction and in sideways movement and is considered a behavioural variant for the exploitation of organic matter in the substrate (Fürsich et al., 2017).

Ichnogenus Ophiomorpha Lundgren, 1891

Ophiomorpha nodosa Lundgren, 1891

Description: Simple to complex branched burrow system, distinctly smooth lined with sediments, with vertical shafts and interconnected horizontal to inclined tunnels. Vertical shafts are straight, but horizontal tunnels may be straight to curve. Walls are thickly lined with a smooth interior and outer

EXPLANATION OF PLATE II

I), VI)*Skolithosverticalis* in Ghuneri member in southern part of Tapkeshwari section II) *Rhizocorallium* irregular in Tapkeshwari section III)*Paleophycustubularis* onwave rippled surface of medium grained sandstone in Ghuneri member in southern part of Tapkeshwari section IV) *Rhizocoralliumjenense* in Bhuj Airport section V) *Taenidiumserpentinium* in ferruginous sandstone in Bhuj Mundra Section VII) Thalassinoidessuevicus

walls with nodular structure. Burrow fill is similar to the host sediment. Diameter of the burrrows varies from 24 mm to 35 mm, with a width of the outer wall of 5-6 mm thick.

Sometimes the nature of the burrow wall changes vertically, from irregular to nodular outer wall.

Discussion: Distinguished based on a thick-lined wall with nodular structures and interpreted as dwelling burrow or filter-feeding organisms. *Ophiomorpha* is a characteristic trace fossil for the clastic, litoral-sublitoral-shelfal environments, typically belonging to a subtidal region (Chamberlain and Baer, 1973; Frey et al., 1978) or lower intertidal zone (Patel and Desai, 2001). They appear as dominantly vertically branched when associated with firmgroundGlossifunguitesichnofacies surface.

Ichnogenus Palaeophycus Hall, 1847

Palaeophycustubularis Hall, 1847

Pl. I. Fig. VI, Pl. II. Fig. III

Description: Predominantly horizontal, straight to sinuous, lined, smoothly walled and unbranched burrows. Cross-sections are circular to oval shapes. Diameter varying between 6 to 15 mm. Fills with structureless passive fill similar to host rocks.

Discussion: *P. tubularis*has thin lining, gently curved, smooth walls. The burrow morphology is described by Fillion and Pickerill (1984). The trace is interpreted to be a dwelling structure. *Palaeophycus* are thinly-walled with no striations. *P. tubularis* produced probably by polychaetes worms, which occurs from the Precambrian to Recent (Pemberton and Frey, 1982). These denotes us marine to continental including alluvial and lacustrine environment.

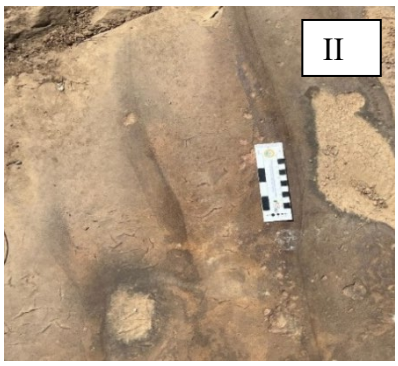

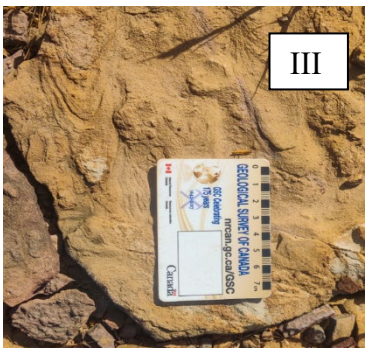

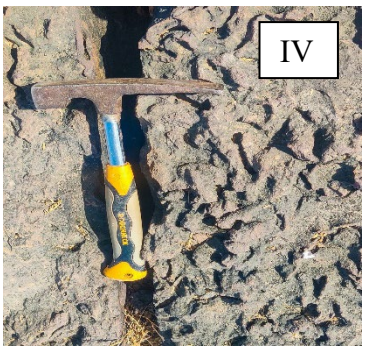

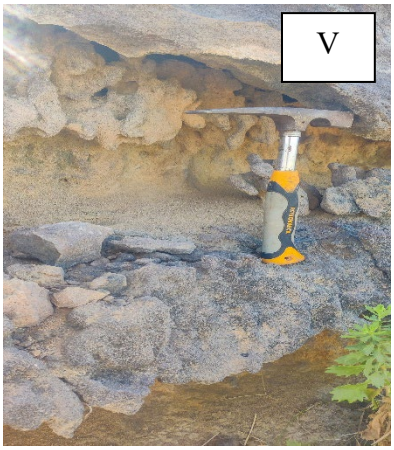

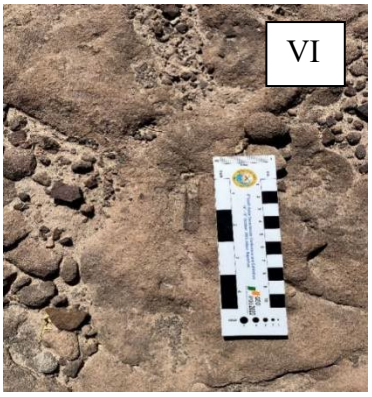

Ichnogenus Planolites Nicholson, 1873

Planolitesbeverleyensis Billings, 1862

Description : Simple, unbranched, unlined cylindrical or subcylindrical infilled burrows. They are straight to gently curved, cylindrical to elliptical in cross-section and horizontal to oblique to the bedding plane. Burrows may cross-over. These are found throughout the Ediacaran and the Phanerozoic that is made during the feeding process of worm-like animals. The traces are generally small, diameter ranges from 7 to 10 mm, the maximum observed length is up to 150 mm, unlined and rarely branched and they are filled with materials different from the host rocks.

Discussion: P. beverleyensis is of larger size than P. montanus(Pemberton and Frey, 1982). Planolites is interpreted to be made by active backfilling of deposit feeder (Uchman, 1995). According to Desai (2016) the ichnospecies are generally developed from distal to proximal part of deltaic environment and developed in low energy environment. These types of organisms have the ability to manipulate sedimentary substrate and they are mainly dominant bioturbators. They are ceated by animals during deposit feeding and dwelling (Nicholson, 1873). Shallow marine - deep marine environment to continental, terrestrial and aquatic, in alluvial, lacustrine settings (Nicholson, 1873).

Ichnogenus PolykladichnusFürsich, 1981

Polykladichnus irregularis Fürsich, 1981

Description: Simple, slender, infaunal burrow with vertical shafts, which branches upward near the bedding surface in a Y shape. Burrow is thinly lined, and branches in upward oriented Y. Burrow fill is different in texture and colour from the host sediment. Burrows are seen circular in cross-section and do not have wide junctions at bifurcation points. Diameter varies from 3-5 mm and length or depth of the burrow is at least 15 cm.

Discussion: Traces are made by domichnia and Fodichniabehaviour of suspension feeders. Traces are caused by *Polychaete* worm or other wormlike organisms in marine environments. These were earlier reported from the recent intertidal zone of Mandvi and the Gulf of Kachchh (Patel and Desai, 2009).

Ichnogenus Rhizocorallium Zenker, 1836

Rhizocoralliumirregulare Mayer, 1954

PL. II. Fig. II

Description: Epichnial, semi to full-relief preservation of large U-shaped, unbranched, horizontal to sub horizontal spreiteburrows. Burrows are elongate, bandlike, straight or winding. More than 45 cm long, curved to slightly sinuous and occasionally branched. The width of the U ranges from 70-80 mm, with a diameter of marginal tubes ranging from 10-20 mm. The spreiten are well preserved, and burrow filled with same sediments as of the host rock.

Discussion: The *R. irregulare* can distinguished from other species of *Rhizocorallium* by long and curved to even bifurcating burrows. They indicates depositional environments of shallow marine to deep marine. The specimens of Kachchh is characterized by its long and curved nature matches well with specimens described by *R. irregulare* (Fürsich, 1974b). These are considered as dwelling of a suspension feeder and burrow of a deposit feeder (Fürsich, 1974b) and are characteristic trace fossils indicating low energy hydrodynamic conditions (Rodríguez-Tovar and Pérez-Valera, 2008).

Rhizocoralliumjenense Zenker, 1836

PL. II. Fig. IV

Description: Epichnial, full relief, simple, horizontal to slightly inclined sprieten, unbranched, U-shaped burrow tube. Width ranges from 80-100 mm. Tubes are parallel to each other and relatively thick up to 25 mm with distinctly "Protrusive", with retrusive limbs. Distinct, curved packets of spreiten fill the inter-tube areas, each nearly 5-9 mm thick.

Discussion: The ichnospecies *R. jenense* characterized by having short retrusive tube which is vertically retrusive. Seilacher (2007) extensively discussed the taxonomic status of *Rhizocorallium* and Fürsich (1974b), who concluded that short oblique, vertically retrusive forms should be interpreted as burrows of suspension feeders. It is typically found in Jurassic sediments deposited in high energy shallow marine conditions (Patel et al., 2008) and from Lower Cambrian sediments (Jensen, 1997).

Ichnogenus Skolithos Haldeman, 1840

Skolithos linearis Haldeman, 1840

Description: Straight vertical to slightly inclined cylindrical burrows. Has very thin, discontinuous linings. Burrows sometimes seen slightly J-shaped. Burrows are parallel and unbranched. Occurs densely, unornamented, lined with a diameter ranging from 10-17 mm. Length up to several decimeters. The walls of burrow are distinct, smooth, does not have fill structures and appears as a small ring-like projection on the top of the bed. Burrow fill coarser than host rock.

Discussion: Skolithos commonly occurs in every type of environment from marine to continental terrestrial and aquatic. Present in shallow marine high energy environments and is produced by a wide range of trace makers: woms, arthropods, annelids or phoronids (Alpert, 1974; Fillion and Pickerill, 1990). The dense occurrence of Skolithos is interpreted as a domichnion of suspension-feeding organisms like polychaetes (Alpert, 1974, Patel and Desai, 2009).

Skolithosverticalis Hall, 1943

PL. II. Fig. IV

Description: Vertical to slightly inclined, straight, cylindrical burrows with diameter ranging from 6 to 10 mm and length up to 7 cm. Burrow walls are distinct, smooth, structureless and fills with sediments similar to the host rock.

Discussion: *S. verticalis* is characterized by inclined shorter burrows, and the field specimens are similar to that of specimens described by Alpert (1974) for *S. verticalis*. It has greater length than *S. linearis*. As compared to *S. verticalis*, *S. magnus* has indistinct burrow walls, have slight bulges at irregular intervals, and *S. annulatus* have ring line annulations (Alpert, 1974). Skolithos are interpreted as dwelling burrows of suspension-feeders (Patel and Desai, 2009) and commonly occurs in high-energy shallow marine nearshore environments (Knaust, 2017).

Ichnogenus Taenidium Heer, 1877

Taenidiumserpentinium (Brady, 1947)

Pl. II. Fig. V

Description: These are cylindrical, unbranched, unlined or sometimes thinly lined, simple burrows, parallel to inclined to the bedding plane with a maniscate backfill. The burrows can be straight, curved or sinuous. The diameter of the burrows areof 10 to 17 mm wide. It is developed by deposite feeder organisms and indicates shallow to deep marine environment. These fossils are developed in fine to medium grained sandstones belong to Jhuran formation. It is a meniscus horizontal tube without any ornamentation and on bioturbation scale it is moderately to heavily bioturbated. On the basis of field appearance it belongs to *Taenidium* cf. *diesingi* ichhnospecies.

Discussion: Taenidiumserpentinium is distinguished by its sinuous burrows which has distinct well-spaced arcuate meniscate (D'Alessandro and Bromley, 1987). Taenidium

is produced by deposit feeder organisms such as pascichnia (D'Alessandro and Bromley, 1987). During Jurassic, the ichnospecies occurs in wide energy conditions in Kachchh, varying from the shallow marine storm-influenced environment (Fürsich et al. 2018); lowto-intermediate energy ramp (Fürsich, 1998) to inner shelf/ prodelta environment (Desai et al. 2008).

Ichnogenus TeredolitesLeymerie, 1842

TeredolitescalvatusLeymerie, 1842

Description: Clusters of elongate to short, calvate shaped boring, oriented perpendicular to oblique to the woody substrate. Specimens were preserved essentially as complete relief and semi relief as incomplete to variably preserved clavate tubes. Borings are moderately lined with ferruginous material and burrow-fill consists of the same. Sometimes burrow linings were calcareous and burrow fill consist of glauconitic material. In cross-section mainly seen as circular to elliptical, a diameter of the neck region ranges from 3- 5 mm, linings are up to 1 mm thick. The base of the boring is smooth with a turbinate shape.

Discussion: Ichnogenus Teredolites comprises of two species, namely *T. calvatus* and *T. logissimus*. The species differ mainly in (1) the nature of the orientation regarding the grain/substrate, (2) it's width/length ratio. *T. calvatus* are oriented perpendicular or slightly oblique to the substrate, has width/length ratio less than 5 (Kelley and Bromley, 1984). The borings are considered permanent domicile structures of filter-feeding worms (Savrda and Smith, 1996). They are caused by dwelling and feeding behaviour of suspension feeders. Possible tracemakers are shipworms, wood boring bivalves.

Ichnogenus Thalassinoides Ehrenberg, 1944

Thalassinoidessuevicus (Rieth, 1932)

Pl. II. Fig. VII

Description: Three-dimensional predominantly horizontal system of lined burrows which has smooth burrow walls. Burrows has both irregular to dichotomous branching. They formed typically in Y and T shapes in a horizontal plane and enlargements at bifurcations. Basically burrows has bifurcation angle of about 120°. Burrows are oriented parallel to the bedding planes, dominantly has horizontal component and also has minor vertical component. In cross-sections, they are seemed to be circular to elliptical burrows, with a diameter ranging between 20 to 30 mm. The burrows are 1 cm in diameter, occasionally exhibit meniscate backfill structures, and are usually filled with the same material as the surrounding matrix.

Discussion: *Thalassinoidessuevicus* is characterised by its burrow enlargement at bifurcation dominance of horizontal components (Myrow, 1995 and reference therein). It occurs in depositional environments ranging from marginal marine to deep marine

(Fürsich, 1974a; Knaust, 2017 pg. 160). Organisms like crustaceans make these kind of burrows and these burrows are made as a combined dwelling and feeding activity of crustaceans (Frey et al., 1984).

Discussion and Conclusion

During the middle Jurassic, a major marine transgression took place whilst rift related subsidence decreased in intensity. Marginal alluvial fans, tidal flat and shoreline systems developed in the north and centre of the basin. Further west, shallow marine and shoreline systems dominated. The Nirona Formation and the lower part of Kaladongar Formation show fluvial characteristics. Continued transgression resulted in deepening of the marine basin and the depositional systems; the Juran Formation indicates a deltaic to marginal marine environment. Ichnological data shows a moderate to high diversity trace fossils corresponding to ichno-assemblages of regim between fair-weather and storm-wave bases. Integration of ichnological data with sedimentological data indicates fluctuating wave and storm energy within normal marine conditions. The bioturbation style signifies the availability of colonization window as a prime reason for preserving bioturbation in wave-dominated settings. Thus, the cyclic units of Ghuneri Member offer better insight into the ichnology of the Early Cretaceous wave-dominated deltaic environment. The post-rift sediments of GhuneriMember comprised asymmetrical bioturbated cycles deposited in a wave-dominated deltaic environment. An ideal bioturbated cycle included coarsening-up thickening-up cycles, varying from shale/siltstone/fine-grained sandstone to medium/coarse-grained massive to cross-bedded sandstone.

Acknowledgements

Authors gratefullyacknowledges Dr. Bhawani Singh Desai, Dr. Suraj Bhosale, Ketan Chaskar for helping us out during the field days. Authors would also like to sincerely thank to Dr. J P. Mohakul, Director, GSI & Ms. Sayani Khan, Senior Geologist for encouraging us in completing our project.

References

- Alberti M, Chauhan D, Fürsich FT, Mukherjee D, Pandey DK(2020) Stratigraphic architecture and palaeoenvironments in the Kachchh rift basin during the Jurassic. In: 36th International Geological Congress, Field Trip Guide WR010, p 143
- BHAWANISINGH G. DESAI, DARSHIT PADIA, SURAJ BHOSALE, SURUCHI CHAUHAN (2022); Ichnology of Early Cretaceous, cyclic bioturbated Ghuneri Member (Bhuj Formation) from the Kachchh Basin, western India, ISSN 0552-9360.

- BHAWANISINGH G. DESAI, (2016)*;* Ichnological Events Associated with Evolution of Kachchh Rift Basin, Western India;SPECIAL PUBLICATION OF THE GEOLOGICAL SOCIETY OF INDIA No. 6, pp. 114-128
- Biswas, S. K. 1993. Geology of Kutch. KD Malaviya institute of petroleum exploration, Dehradun, 450.
- Bromley, R. G. and Ekdale, A. A. 1984. Chondrites: a trace fossil indicator of anoxia in sediments. Science, 224 (4651): 872-874.
- Crimes, T. P. 1977. Trace fossils of an Eocene deep-sea fan, northern Spain. In: Crimes, T. P., Harper, J. C. (Eds.), Trace fossils 2, Geological Journal Special Issue, 9: 71–90.
- D'Alessandro, A. and Bromley, R. G. 1987. Meniscate trace fossils and the Muensteriab –Taenidium problem. Palaeontology 30: 743-763.
- de Gibert, J. M. and Benner, J. S. 2002. The trace fossil "Gyrochorte": etology and paleoecology. Revista Espanola de paleontologia, 17 (1): 1-12.
- Desai, B. G. and Biswas, S. K. 2018. Postrift deltaic sedimentation in western Kachchh Basin: Insights from Ichnology and sedimentology. Palaeogeography, Palaeoclimatology, Palaeoecology, 504: 104-124.
- Desai, B. G. and Saklani, R. D. 2012. Significance of the trace fossil BalanoglossitesMägdefrau, 1932 from the Lower Cretaceous Guneri member (Bhuj formation) of the Guneri dome, Kachchh, India. Swiss Journal of Palaeontology, 131 (2): 255-263.
- Desai, B. G., Patel, S. J., Shukla, R. and Surve, D. 2008. Analysis of ichnoguilds and their significance in interpreting ichnological events: A study from Jhuran Formation (Upper Jurassic), western Kachchh, India. Journal of the Palaeontological Society of India, 72: 458-466
- Dhirendra K. Pandey, Franz T. Fürsich1 & Matthias Alberti (2017); Behavioural variants of the trace fossil Gyrochorte ; ISSN 0373-9627
- Frey, R. W., Curran, H. A. and Pemberton, S. G. 1984. Tracemaking activities of crabs and their environmental significance: the ichnogenus Psilonichnus. Journal of Paleontology, 58: 333-350
- Fu, S. 1991. Funktion, Verhalten, und Einteilungfucoider und lophocteniiderLebensspuren. Courier Forschungs-InstitutSenckenberg, 135, Frankfurt, 79.
- Fürsich, F. T. 1974a. Corallian (Upper Jurassic) trace fossils from England and Normandy. Stuttgarter BeiträgezurNaturkunde, 13: 1–52 Serie B.

- Fürsich, F. T. 1974b. Ichnogenus Rhizocorallium. PaläontologischeZeitschrift, 48 (1-2): 16-28.
- Goldring, R. 1962. The trace fossils of the Baggy Beds (Upper Devonian) of North Devon, England. PaläontologischeZeitschrift, 36 (3-4): 232- 251.
- Guillette, L., Pemberton, S. G. and Sarjeant, W. A. S. 2003. A Late Triassic invertebrate ichnofauna from Ghost Ranch, New Mexico. Ichnos. 10: 141-151.
- Hakes, W. G. 1976. Trace fossils and depositional environment of four clastic units, Upper Pennsylvanian megacyclothems, northeast Kansas: The University of Kansas Paleontological Contributions, 63: 1-46.
- Jensen, S. 1997. Trace fossils from the Lower Cambrian Mickwitzia sandstone, south-central Sweden. Fossils and Strata, 42: 1–110.
- Kazmierczak, J. and Pszczóåkowski, A. 1969. Burrows of enteropneusta in Muschelkalk (Middle Triassic) of the Holy Cross Mountains, Poland: Acta Palaeontologica Polonica, 14, 299-318.
- Knaust, D. 2008. BalanoglossitesMägdefrau, 1932 from the Middle Triassic of Germany: part of a complex trace fossil probably produced by burrowing and boring polychaetes. PaläontologischeZeitschrift, 82 (4): 347-372.
- Knaust, D. 2017. Atlas of Trace Fossils in Well Core: Appearance, Taxonomy and Interpretation. Springer, 209.
- Mägdefrau, K. 1932. ÜbereinigeBohrgängeaus dem unterenMuschelkalk von Jena. PaläontologischeZeitschrift, 14 (3): 150-160.
- Myrow, P. M. 1995. Thalassinoides and the enigma of Early Paleozoic openframework burrow systems. Palaios, 10: 58-74
- Pandey D. K., Fürsich F. T., Alberti Matthias, Bhaumik Sneha and Wagih ayoubhannaa. 2016. A review of the tithonian ammonites from the Kachchh Basin, Western India. ISSN 0522-9630
- Patel, S. J. and Desai, B. G. 2009. Animal-sediment relationship of the crustaceans and polychaetes in the intertidal zone around Mandvi, Gulf of Kachchh, Western India. Journal of the Geological society of India, 74 (2): 233-259.
- Pemberton, S. G. and Frey, R. W. 1982. Trace fossil nomenclature and the Planolites-Palaeophycus dilemma. Journal of Paleontology, 56: 843- 881.
- *Planolites*Nicholson, 1873 in GBIF Secretariat (2003). GBIF Backbone Taxonomy.

- Powell, J. H. 1992. Gyrochorte burrows from the Scarborough Formation (Middle Jurassic) of the Cleveland Basin, and their sedimentological setting. Proceedings of the Yorkshire Geological Society, 49 (1): 41-47.
- Rodríguez-Tovar, F. J. and Pérez-Valera, F. 2008. Trace fossil Rhizocorallium from the Middle Triassic of the Betic Cordillera, Southern Spain: characterization and environmental implications. Palaios, 23 (2): 78- 86.
- Seilacher, A. 1990. Aberrations in bivalve evolution related to photo and chemosymbiosis Historical Biology, 3 (4): 289-311.
- Uchman, A. 1995. Taxonomy and palaeoecology of flysch trace fossils: the Marnoso-arenacea Formation and associated facies (Miocene, northern Appenines, Italy). Beringeria, 15: 1 -115.

Note on the Emerging Mouth Bar of Budhabalanga River at Chandipur, Balasore, Odisha

G. P. Mohapatra, B. M. Faruque, M. Mohanty and J. N. Das

Institution of Geoscientists Odisha (IGO), Bhubaneswar

The Budhabalanga River is a perennial river stretching approximately for 198. 75 Km from its origin in the Similipal range of hills in Odisha's Mayurbhanj district to its confluence with the Bay of Bengal at Balaramgarhi. With a total catchment area of 4, 840 Km^2, the river is fed by major tributaries, including the Sone, Gangadhar, and Katra. Historically, the Budhabalanga River played a crucial role in trade duringthe 17^{th} and 18^{th} centuries. It facilitated cargo transport from the Bay of Bengal to Balasore, attracting European traders such as the British, Dutch, and Danish. The first English factory was established in Balasore in 1640, followed by a British settlement in 1642. Dutch and Danish trading centres were also established during this

period. Balasore thrived as a centre for shipbuilding and textile manufacturing. However, over time, rising waters and sediment accumulation at the river's mouth led to its decline as a navigable port.

Geographically, Balasore town is situated in the northern coastal plain (the Balasore Plain) comprising the flood plain of the meandering Budhabalang river. The various features reported from the coastal plain are alluvial flood plains, natural levees, palaeochannels, active channels, recent and palaeo beach and beach ridges, tidal flats, mangrove swamps, spits, bars and lakes. The area is considered to have been built initially by marine deposits in the form of a broad continental shelf, and subsequently by fluviatile deposits after upliftment. The soil composition varies from fine silt in the vicinity of rivers to coarse silt in farther regions and belong to the Present day surface (Present to Late Holocene age). Red soil with low fertility occurring towards western plains in proximity to the Simlipal hills possibly belongs to the Kaimundi Surface (Late Pleistocene to Early Holocene age) (Mishra et al., 2002). The development of a tidal flat at Chandipur at the confluence of the Budhabalanga river and the sea (Fig. 1a & b) is a remarkable geological feature and forms a major tourist spot in the State. The ~ 5 km long area with a slender beach of approximately 40 m features a wide tidal flat of 4 km and comprises a network of bars and inter-bars (Mondal et al., 2010).

In recent decades, satellite imagery has revealed the formation of a unique bar at the mouth of the Budhabalanga River. This bar, located on a mesotidal coast with tidal ranges exceeding 2 metres, has been emerging over the past 25 years. The river's

mouth lies within a distinct curvilinear bay, bordered by the tidal deltas of the Ganges to the north and the Brahmani-Baitarani system to the south.

Observation from Satellite Imagery

The study of sequential satellite images taken over a span of 50 years indicate following significant geomorphological changes:

• North-Eastern Flank**:** Features a beach with swell patterns.

• South-Eastern Flank**:** Largely barren, with visible traces of bar formation offshore.

Burhabalang River.

•The river's flow shows a northward migration, evidenced by meandering patterns and an abandoned oxbow lake.

• Tidal incursions have caused a distinctive bend in the beach along the southern bank.

The southern sand-bar on the mouth of the Budhabalanga River has a narrow zone influenced by aeolian process, forming ripple marks. Heavies can be seen as lags between two crests of light minerals. Whereas the sandy sediments located below the swash-spread have developed ripples due to hydrodynamics.

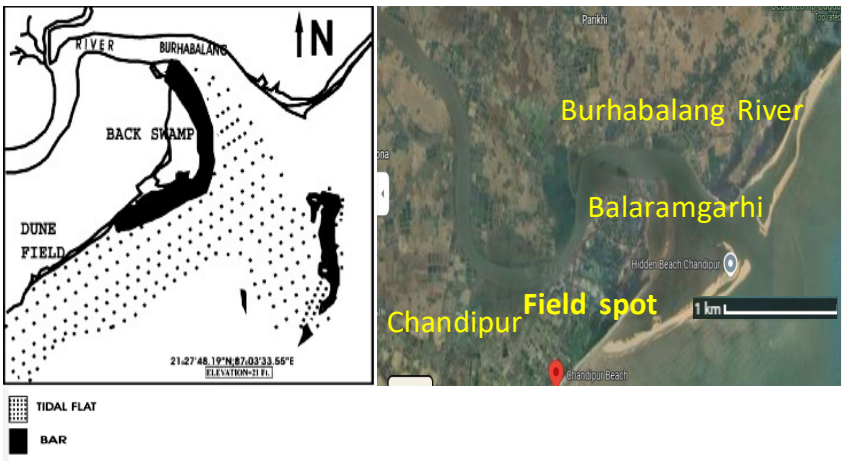

Fig. 1 a. Chandipur Tidal Flat at the confluence of River Budabhalang with the sea

Figure 1b: Google satellite imagery of

Budhabalanga River mouth bars (2025)

The study of the recent satellite imagery (Fig. 1b) highlights further developments such as:

• The southern bar now features a protected lagoon, while another offshore bar is forming. This bar is curvilinear, with noticeable wave refraction patterns on its submerged surface.

These observations suggest the river mouth is undergoing rapid progradation, which is going to advance further in the near future.

Factors Driving Progradation

Since 1993, rapid sediment deposition at the river mouth has led to the formation of prominent bars on both flanks. The contributing factors include:

1. **Increased Sediment Input** of the Budhabalang river originating from the Similipal complex, as its catchment area.

2. **Enhanced River Flow:** Stronger discharge into the sea, is apparently amplified during the northwest monsoon.

3. **Coastal Current Dynamics:** A reversal of the usual southwest monsoon currents may have

reworked sediment deposits. As noted by Dan et al. (2011), spit formation and evolution at river mouths occur when sediment supply surpasses wave-induced transport capacity. This process facilitates deltaic progradation, but reduced sediment input combined with increased wave dynamics can hinder spit formation.

Further Study and Monitoring

For understanding the provenance of the bar the following studies may be taken up:

• **Mineral Analysis:** Examination of heavy mineral assemblages is an ideal tool to trace sediment sources. Mishra et al (2024) reported the following composition of heavy minerals, from Chandipur beach sands, in decreasing order of abundance.

biotite (27. 39%), chlorite (17. 22%), sillimanite (12. 49%), garnet (11. 49%),

muscovite(10. 14%), sphene (8. 23%) and zircon (6. 01%) with minor hypersthene (2. 63), epidote (1. 21%), tourmaline (1. 02%), hornblende (0. 56%), spinel (0. 44%), andalusite (0. 33%), rutile (0. 31%), staurolite (0. 2%), enstatite (0. 18%) and actinolite (0. 13). They concluded that the sillimanite and garnet do not have their provenance in the vicinity of Chandipur, thus attributing the transportation of these two minerals from the southern coast, due to the long shore current running from south to north.

• **Profile Studies:** Analysis of seasonal and annual deposition patterns.

• **Clay Mineral Studies:** Assessment of the influence of Gangetic sediments.

• **Grain Size Analysis:** Current sediments are fine to very fine with minimal heavy mineral content.

• **Growth of Bar**: Granulometric study along the length of the sand bar will indicate the direction of deposition or growth

• **Direction of current/tide/wind flow**

Ripple marks on the bar indicate wind and sediment movement patterns. Comprehensive monitoring using satellite imagery is essential to track changes at

the river mouth and assess the impacts of cyclones, sea level rise, and climate change on the region.

Field Observation:

The southern sand-bar on the mouth of the Budhabalanga River at Chandipur is separated from the western mainland by a narrow stream of water flowing from north to south. It forms a narrow zone above the high tide water level. The bar formed by several cycles of deposition is mainly composed of fine sand often influenced by aeolian process, forming ripple marks (Fig

2). Heavies can be seen as lags between two crests of light minerals. Whereas the sandy sediments located below the swash-spread have developed ripples due to hydrodynamics, and show multiple directions of flow (Fig. 3) due to tidal influence and swash back. The longitudinal alignment of shells indicates the direction of flow current, prevalent at present in the area. The northern bar appears to be hinged with the shore at its northern end.

The offset of the flow towards NE between the mouth of the river and the opening between the two sand bars (Fig. 1) is due to long shore current from south to north at this location.

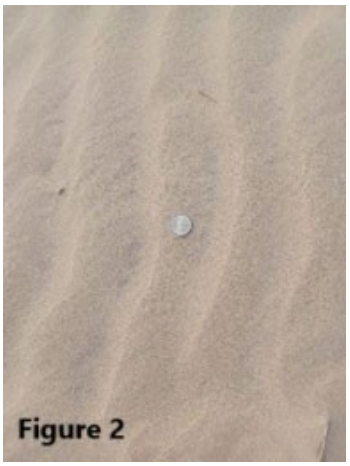

Figure 2 Aeolian ripple marks, regular pattern, unidirectional, with very low incidence of heavies in the trough.

Figure 3. Subaqueous ripple marks, chaotic due to interference of multiple direction of flow, scanty heavies in the trough.

Foot Notes

Bar/Sand bar: The term “bar” may be used in a generic sense to include the various types of submerged or emergent embankments of sand and gravel built on the seafloor by waves and currents (Fig. 4). Granulometric study along the length of the sand bar

will indicate the direction of deposition or growth. They may be emergent at low tide and partially (or fully) buried in high tide.

Spit: As defined by Evans (1942) it is a type of sand bar, a ridge or embankment of sediment, attached to the land at one end and terminating in open water at the other. Most commonly the axis of a spit will extend in a straight line parallel to the coast, but, where currents are deflected landward, with the resulting creation of a recurved spit.

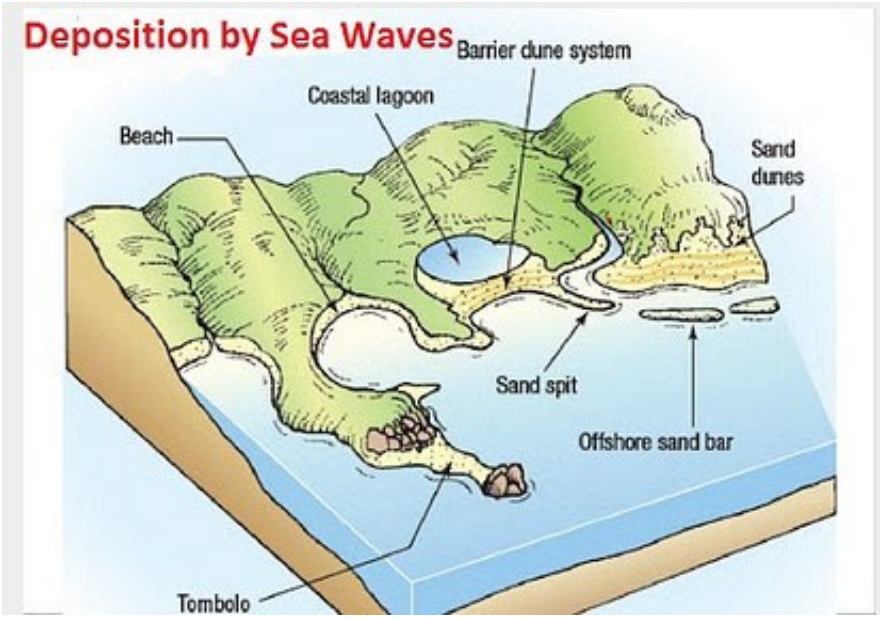

Fig. 4: Model of depositional features by sea waves (Source: Internet)

Flaser Bedding/Lenticular Bedding: Flaser bedding and lenticular bedding are both sedimentary bedding patterns that involve alternating layers of mud and sand (Fig. 5). Flaser bedding is a type of ripple cross-lamination where thin streaks of mud occur between sets of ripple laminae mostly made of sand. Lenticular bedding on the other hand is classified by its large quantities of mud relative to sand and the sand formations within the bedding display a

'lens-like' shape. They are commonly found in high-energy environments such as the intertidal and supratidal zones and show evidence of tidal rhythm, tidal currents and tidal slack.

Ripples: Commonly known as sand waves, ripples are undulatory structures produced by a current (water or wind) on the surface of a sandy sediment. In general, these structures are known as bedforms, as they form at the bottom of a basin at the contact between the sediment and air/water. When ripples are produced by a unidirectional current, they show an asymmetric shape with a gentler and a steeper side. On the other hand, oscillatory currents like waves often produce symmetric ripples and are controlled by the speed of the current, depth, grain size, and direction of flow. The internal structure

of ripples is characterized by foreset laminae that lean in the direction of the flow and are hence useful paleocurrent indicators when observing fossil ripple marks or cross-bedding preserved in rocks (Fig. 7).

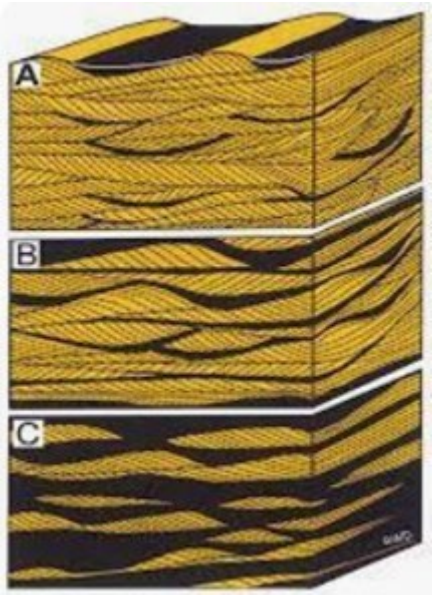

Figure 5: Flaser Bedding and Lenticular Bedding after Raineck and Singh (1980)

Straight ripples (or, at large scale, dunes) are linked to the formation of planar cross-bedding. At higher flow velocity or lower water depth, ripple crests become progressively more sinuous, then catenary (like the Greek letter ω), and finally highly irregular (linguoid, tongue shaped, or lunate, crescent shaped) (Fig. 6a). The difference between the linguoid and lunate ripples is the orientation of the concavity, opposite to the direction of the current in linguoid ripples, in favor of it in lunate ripples.

Interference Ripples: Sedimentary structure made up of two sets of ripples formed at right- angles to each other as a result two dominant paleocurrents (Fig. 6b).

Fig 6a: Irregular Sinous Ripples at Chandipur Fig. 6b: Ripple interference

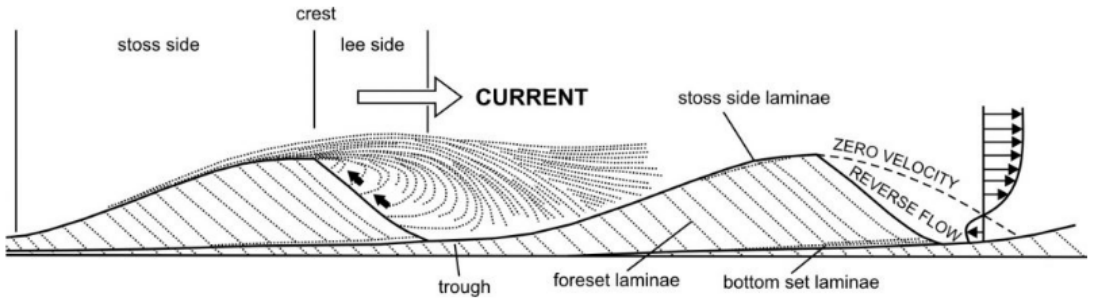

Fig. 7: Illustrative cross section of ripples (Source: Internet)

References

- Evans, O. F. (1942) The origin of spits, bars and related Structures, Jour. of Geology, v. 50 (7).
- Mondal, S., Bardhan, S. and Sarkar, D. (2010) Testability of energy maximization model
- (Kitchell et al., 1981) of naticid predation on two bivalve prey from eastern coast of India. Nautilus. v. 124, pp. 1–14.
- Mishra, A. K., Mohanty, B. K. and Om Prakash (2002) Quaternary sedimentation, stratigraphy and neotectonics along the coastal tract and river valleys of Orissa. Proc. GEOSAS– IV, pp. 128-133.
- Mishra, S., Hota, R. N. and Nayak, B. (2024) Comparative study of heavy minerals of Chandipur and Chandrabhaga beaches of Odisha, SGAT Bulletin, v. 25(2), Dec. 2024, pp. 110-118
- Reineck, H. E. and Singh, I. B. (1980) Depositional Environments. In:Depositional Sedimentary Environments. Springer Study Edition. Springer, Berlin, Heidelberg. https://doi. org/10. 1007/978-3-642-81498-3_2.

Glacio-eustasy and Shelf Sediments off Indian Coastal zone

B. M. Faruque

Plot 68, Zahirland, TinkoniaBagicha, Cuttack

Email: bmfaruquegeo@gmail. com

The studies on the glacio-eustasy, tectono-eustasy and radiocarbon measures of major events of the Last Glacial Cycle (LGC) along the continental shelves of India are rather sketchy. However, the impressions of sea level changes along the Indian coasts and shelf, including Andaman and Lakshadweep islands, have been documented by several workers and the details are available from the studies of Vaz, (1996), Brückner (1989), Mohapatra et al (2001), Banerjee & Sengupta, 1992), Vohra, (1996), Hashimi et al (1995), Faruque et al (2014), Faruque et al (2008), in shelf area. The Holocene Sea Level Curve observed for the east coast of India (Faruque et al. 2008) appears broadly identical with the global sea level curve proposed by Fairbridge (1965). The present study analyses the impact of glacio-eustasy on the shelf sediments off Indian coasts and the influence of sea level fluctuations on onshore landform. One of the conclusions drawn from studies of seabed sediments from shelf edge to the beach, for east coast region of India is that at 18ka-14ka BP the sea level had a phase of glaciation leading to regression of the sealevel to -122 m below present sea level (psl). Due to deglaciation sea level transgression led to the rise of sea level to the present sea level around 6 ka BP. The transgression of the sea from LGM to present gave rise to various types of sediments controlled by the nature of provenance, chemical properties of the sea water and the marine biota and above all theclimate. The sediments near the shelf edge and around palaeobeach ridges at -95 m, and -86 m were coarser, rich in skeletal residues of biota and more calcareous than the midshelf swales composed of lime mud, calcareous ooids (Fig. 1), skeletal remains of marine biota.

A series of submarine ridge-like features occurring along the shelf edges are due to the development of colonial coral-algal growths related to lowered palaeosea stands. About four (Andhra-Odisha shelf) to seven (Kerala shelf) such linear beach-ridge structures have been recorded at depths between 63. 5 m and 122 m on the shallow seismic records across the shelf. Their relief calculated from the echograms, are 3 to 17. 6 m from the base. The most prominent of these ridges is located at -122 m depth and is full of coralline debris besides coarse sand, ooids and skeletal clastic remains, which is contrary to the expectation of fine silt and clay at depth with low energy environment. The anomaly in the physical and chemical characters, were attributes of

the sea level changes of the Last Glacial Cycle. It is observed how sediment characters of the shelf change considerably in composition and texture due to impact of glacio-eustasy. The outershelf and parts of continental slope off Gujrat is found to be occupied by lime mud with 71% to 96% Calcium Carbonate. Outer shelf off north Andhra between -90 m and -

110 m depth is also composed of lime, and the sediments are rich in Calcium Carbonate. The lime mud is formed by combination of biogenic material with chemogenic precipitates. The absence of lime mud in the inner shelf is explained by the fact that the sea level, during its transgression reached a depth of say -30 m was due to deglaciation and warming of Earth's climate. Warm climate led to melting of the glacier which reduced the salinity of the sea water and increased influx of terrigenous material into the shelf. Low salinity is not congenial for precipitation of salt. The climate was cold and arid during the periods 18 ka and 14 ka B. P. at the peak of glaciation. Last Glacial Maxima (LGM) (Fairbridge, 1961). Aridity caused the drainage systems going dry, which prevented terrigenous clastic sediments from reaching the sea. The sea level lowered at -122 m depth gave rise to coarse sandy beach which became ridges, due to high energy depositional environment of surf zone, where most of the turbulence and churning takes place. Corals do not survive at -122 m depth of the sea, but sea level only when lowered at -122 m could support rich growth of coral reef which grew into a 300m wide coral reef at LGM. The sediments off Krishna-Godavari delta is composed of terrigenous material consisting of smectite, from the breakdown of Deccan basalt. Core samples from several locations in the shelf contained higher percentage of smectite as against absence of smectite at -2 m below the seafloor. The -2 m stratigraphically lower sediment was deposited at colder and arid climatic condition. Whereas modern sediments deposited on the seafloor carry considerably high proportion of smectite due to advent of interglacial hot and humid phase, which is conducive to help break down of basic rock, the Deccan basalt. It can be compared with another similar impact of glaciation in Antarctica. The khondalite rocks occurring in Antarctica have not developed laterite or bauxite, whereas in the hot and humid tropics khondalite hills of Odisha and Andhra Pradesh have given rise to the formation of thick horizon of laterite and bauxite. Fig. 2 Wave cut notch near Collinpur. S. Andaman. In the continental shelf off southern Odisha coast terrigenous sediments are derived from physical and chemical breakdown of khondalite, granite and acid to basic charnockite rocks of Eastern Ghats Supergroup formation. The sediments in the Sonapurpeta to Puri sector of the coast and shelf are characterized by the presence of heavy minerals like: sillimanite, garnet, ilmenite, rutile, zircon and monazite. The heavy minerals are carried by rivers like Vamsadhara, Nagavalli, Mahendratanaya and Rushikulya. The longshore current support the transportation of light minerals while increasing the concentration and gradual transportation (Natalia,

2009) in the northeastward direction of the heavies. When the sea level was lowered during Last Glacial Cycle, the distribution of sediments with heavies also shifted seaward, gradually, commensurate with the regressed position of the sea level in the mid-shelf. Heavy minerals have been sampled from upto water-depths of 25m to 30m in the shelf, but beyond 70m water- depth the heavies almost disappear and the sediment is enriched in calcareous material derived from skeletal remains of fauna and precipitated calcareous ooids. The ooid grains are invariably coated with iron oxide (Fig. 1), as seen under scanning electron microscope (Faruque etal, 2008). Following global warming and deglaciation the sea plunged into a transgressive phase and the rise was also punctuated by short episodes of cooling where the sea level stands occurred giving rise to formation of beach rocks and beach ridges, defining the paleo-shoreline. Around 6 ka the sea reached the present level and due to further warming it reached almost 5m above the present level, indicated in the formation of beach rocks and wave cut notches. Rocky promontories, vulnerable to chemical and mechanical breakdown, give in to high energy wave action and develop concave notches (Fig, 2) at higher level than the psl, leaving behind signatures of high sea stands. The sediments on the beach often get cemented with calcareous matrix to form beach rocks. Formed at higher sea stands of Late Holocene the beach rocks survive low energy aeolian processes and in most cases contain skeletal remains of biota, which help in calculation of radiocarbon dates for the high sea stand of the past. Beach rocks have been recorded from Rameshwaram, Kanya Kumari, Andhra Pradesh in the east coast and from South Andaman Island. There is, however, a caveat here, wave cut notches on rocky promontories without organic remains cannot give the date of sea level high. At present we are in an interglacial with hot and humid climate which culminates in a trend of sea level rise.

Towards Sustainable Coastal Management: Insights from Odisha's Tourism and Geological Dynamics

Biswanath Sahoo* and Asim Amitabh Pradhan

Department of Geology, Fakir Mohan University, Balasore- 756089 (India)

Email: biswanathsahoo164@gmail. Com

Abstract

Sustainable coastal management is essential for preserving biodiversity, promoting economic stability, and addressing the impacts of climate change. Odisha, a coastal state in eastern India, offers valuable insights into the balance between tourism development and environmental preservation along its 480 km coastline. This study explores the complex challenges in tourism while safeguarding the coastal environment, examining geomorphological, ecological, and socio-economic factors.

Odisha's coastline is home to diverse ecosystems, including sandy beaches, estuarine systems, deltaic plains, mangroves, barrier islands, and Chilika Lake. These ecosystems are crucial for biodiversity conservation and providing storm protection. However, the region faces significant environmental vulnerabilities due to frequent cyclones, storm surges, rising sea levels, and coastal erosion triggered due to one cause which is climate change. The research integrates various methodologies, such as field studies, remote sensing data, and stakeholder interviews, to assess coastal dynamics. Key focus areas include sediment transport patterns, shoreline changes, and the influence of geological features, such as the Eastern Ghats Mobile Belt and the deltaic systems of the various river systems on coastal resilience. Understanding these processes is vital for managing the impacts of coastal erosion and storm surges.

Tourism is a major economic driver in Odisha, especially in destinations like Puri, Konark, and Gopalpur, which attract large numbers of visitors annually. However, tourism also presents challenges, including overcrowding, waste management issues, and resource depletion, further exacerbating environmental degradation. The study emphasizes the need for sustainable tourism practices that minimize ecological impact while fostering economic growth.

The research also examines community-led conservation initiatives as models for balancing development and environmental preservation. Examples include mangrove conservation efforts in Bhitarkanika and ecotourism projects around Chilika Lake. These

initiatives show how local communities can contribute to sustainable coastal management by protecting ecosystems and promoting eco-friendly tourism alternatives.

The study concludes by advocating for an integrated, multi-pronged approach to coastal management. This includes adopting sustainable tourism practices, implementing coastal zoning regulations, and restoring natural ecosystems such as mangroves and wetlands. Zoning regulations are critical for controlling unregulated development and protecting sensitive coastal areas. Additionally, the restoration of natural buffers like mangroves and sand dunes is essential for strengthening the region's resilience to climate risks. The research stresses the importance of incorporating geological and ecological knowledge, alongside traditional practices, to improve decision-making and planning for long-term coastal sustainability. By adopting collaboration among policymakers, scientists, and local communities, the study argues that Odisha can serve as a model for sustainable coastal management.

Keywords: Sustainable coastal management, coastal erosion, climate change, Chilika Lake, mangrove restoration, shoreline changes

1. Introduction

Odisha's coastline is an important geographical feature, providing ecological, economic, and cultural significance. However, this region is increasingly vulnerable to climate change, coastal erosion, and unregulated tourism development. Addressing these challenges requires a balanced approach integrating geological, environmental, and socio-economic strategies. This paper investigates the impacts of tourism and geological processes on Odisha's coastal sustainability and proposes solutions for effective management.

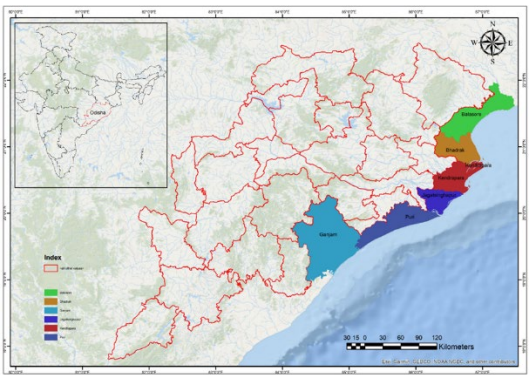

Fig. 1 Coastal districts of Odisha

2. Tourism and Its Environmental Impact

2. 1 Tourism Growth and Economic Contributions

Tourism plays a significant role in Odisha's economy, particularly in coastal regions, where popular destinations like Puri, Konark, and Gopalpur attract millions of visitors

annually. In 2023, Odisha recorded an impressive 15. 6 million domestic tourists and 0. 3 million foreign tourists, contributing substantially to the state's revenue. Coastal tourism hotspots such as Puri, Konark, and Gopalpur account for nearly 40% of Odisha's total coastal tourism revenue, underscoring the economic importance of these areas. However, the growth of tourism in these regions is not evenly distributed throughout the year. Seasonal fluctuations, particularly during major festivals like the Rath Yatra in Puri, cause an influx of tourists, leading to overcrowding, increased waste generation, and excessive pressure on local resources. Conversely, during off-peak seasons, businesses struggle with reduced income, leading to economic instability among local communities dependent on tourism-related activities.

Additionally, the rapid expansion of tourism has led to an increase in infrastructure development, including hotels, resorts, and commercial establishments along the coast. While these developments support economic growth, they often encroach upon ecologically sensitive areas, such as sand dunes and coastal wetlands, which serve as natural buffers against erosion and storm surges. Furthermore, unregulated tourism has exacerbated environmental challenges, including waste mismanagement, depletion of freshwater resources, and habitat destruction. Without sustainable tourism policies and conservation efforts, Odisha's coastal regions risk long-term ecological degradation, which could undermine both biodiversity and the tourism industry itself. Implementing responsible tourism strategies that balance economic benefits with environmental sustainability is crucial for the long-term viability of Odisha's coastal tourism sector.

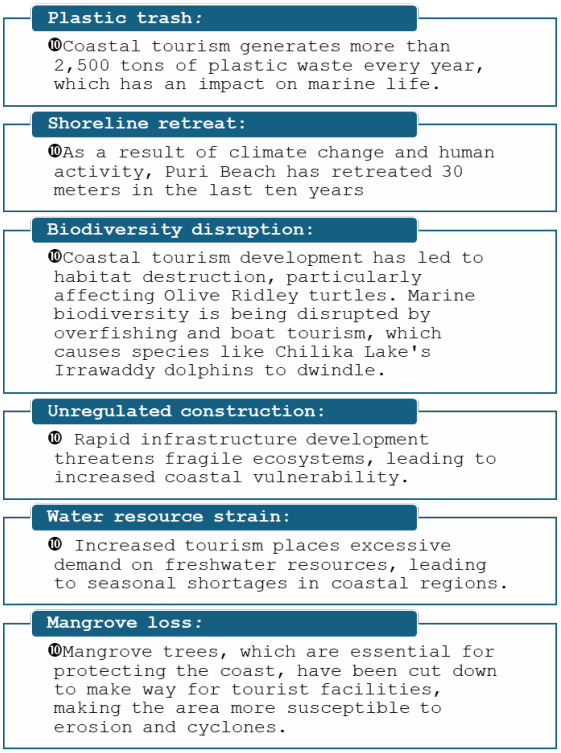

2. 2 Environmental Challenges

3. Geomorphological and Geological Dynamics

3.1 Shoreline Changes and Erosion Trends

The coastal dynamics of Odisha have undergone significant transformations over the past few decades. Shoreline change along Odisha coast using statistical and geo-spatial techniques reveals that approximately 30% of Odisha's coastline is experiencing significant erosion (Kar et al., 2021). Among the most affected areas are the Puri and Ganjam districts, where erosion poses severe risks to infrastructure, coastal settlements, and economic activities. The erosion in these regions is primarily driven by a combination of natural and anthropogenic factors, including rising sea levels, increased wave action, and human-induced modifications such as sand mining and construction of coastal structures.

Puri district records the highest erosion rate at 3. 2 m/year, followed by Ganjam at 2. 8 m/year. In other districts like Kendrapara, Balasore, and Jagatsinghpur, the erosion rates range between 1. 5 and 2. 1 m/year. The high erosion rates in Puri and Ganjam can be attributed to their geomorphological setting, wherein strong wave action and sediment transport imbalance accelerate coastal retreat. Furthermore, coastal engineering interventions, such as groynes and breakwaters, have altered natural sediment dynamics, leading to localized erosion.

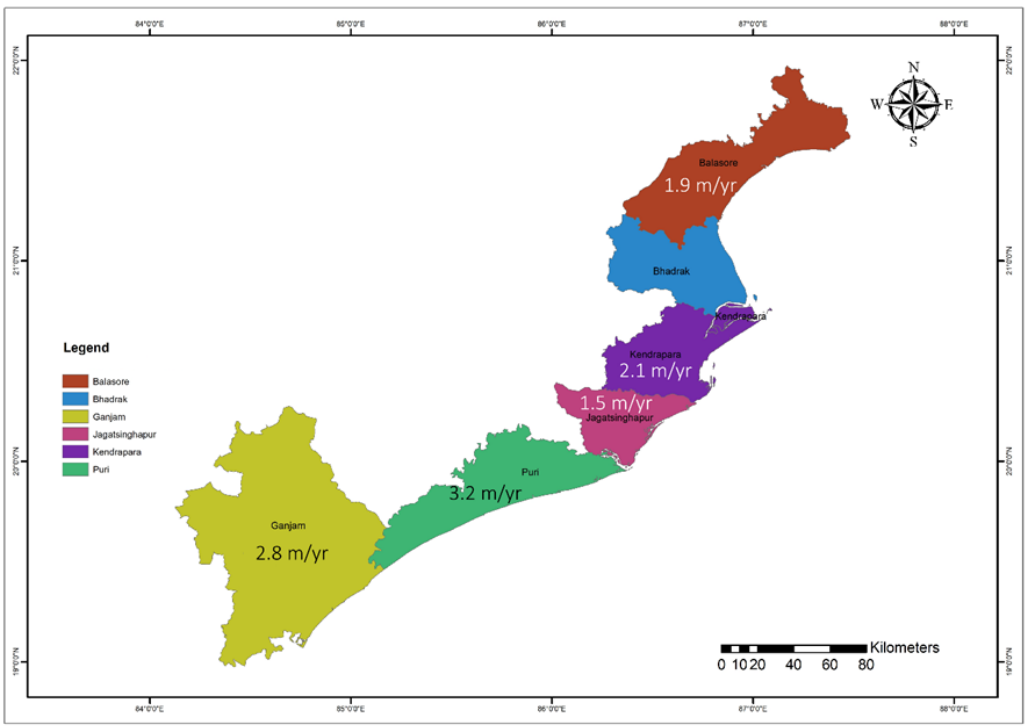

Fig. 2 Erosion rates across various coastal districts of Odisha

3. 2 Riverine and Deltaic Influences

The Mahanadi, Brahmani, and Baitarani rivers play a crucial role in shaping Odisha's coastal sediment deposition and erosion patterns. These rivers transport vast amounts of sediment, which help maintain the stability of the coastline and support diverse ecosystems. However, the construction of dams and other upstream modifications has significantly reduced sediment supply, leading to increased coastal retreat and heightened risks of flooding. This disruption in sediment flow has weakened natural coastal defenses, making the region more vulnerable to extreme weather events. Additionally, sand dune degradation has emerged as a pressing concern, primarily due to human-induced activities such as unregulated tourism, infrastructure development, and sand mining. The destabilization of these dunes not only threatens the coastal landscape but also diminishes their ability to act as protective barriers against storm surges and sea-level rise. Addressing these challenges requires a comprehensive approach that balances development with conservation efforts to ensure the long-term sustainability of Odisha's coastal environment. Significant sand displacement from Puri Beach to Chilika Lake's inlet is caused by longshore drift, which has a major impact on sediment transport and periodically closes and opens the lake's mouth.

3. 3 Sea-level Rise and Climate Change Effects

Recent studies indicate that Odisha's coastline is experiencing a sea-level rise of approximately 2. 5 mm per year, posing significant challenges to coastal communities and ecosystems (Das & Mohapatra, 2020). The rising sea levels have intensified the impact of cyclonic activity, leading to higher storm surges that severely affect agricultural lands, displace communities, and damage infrastructure. The increased frequency and intensity of these storms have heightened the vulnerability of Odisha's coastal population, particularly in low-lying regions. Additionally, saltwater intrusion into groundwater has emerged as a serious environmental concern, deteriorating drinking water quality and rendering agricultural lands unsuitable for cultivation. This has had dire consequences for local farmers, whose livelihoods depend on coastal agriculture. A striking example of the destructive impact of these climatic events was Cyclone Fani in 2019, which resulted in storm surges displacing over 1. 5 million people in Odisha (IMD Report, 2019).

4. Sustainable Coastal Management Strategies

4. 1 Eco-tourism initiatives

Eco-tourism has emerged as a key strategy for promoting sustainable coastal management in Odisha, with Chilika Lake serving as a prime example of its success. The implementation of eco-tourism initiatives in Chilika has led to a 15% increase in biodiversity conservation, particularly benefiting migratory bird populations and aquatic species. This conservation success is largely attributed to the shift towards low-impact

tourism activities, such as birdwatching, boating, and guided nature trails, which minimize environmental disturbances while enhancing visitor experiences. Additionally, revenue generated from eco-tourism in Chilika has been reinvested into local community development, fostering improved livelihoods for residents engaged in sustainable fishing, handicrafts, and tourism services.

4. 2 Community-based conservation programs

Community-based conservation programs have played a significant role in enhancing environmental resilience and local livelihoods. For instance, mangrove restoration initiatives in Bhitarkanika have effectively mitigated cyclone-related damages by approximately 30%, demonstrating the protective role of coastal vegetation in disaster-prone regions. Additionally, conservation efforts actively involve local fishermen by promoting eco-friendly livelihood alternatives, ensuring both sustainable resource management and economic stability. Furthermore, wetland restoration projects in Chilika have led to notable improvements in fishery resources, directly contributing to increased local incomes. These initiatives highlight the critical intersection between ecological conservation and socio-economic benefits.

Below are the corresponding pie charts visualizing the impact of these conservation efforts:

1. Cyclone damage reduction due to mangrove restoration
2. Eco-friendly livelihood participation among fishermen
3. Economic benefits from wetland restoration in Chilika

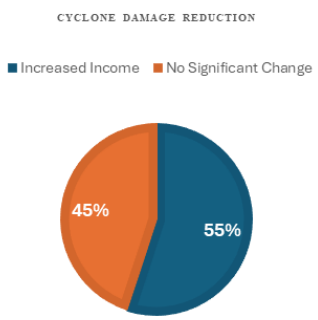

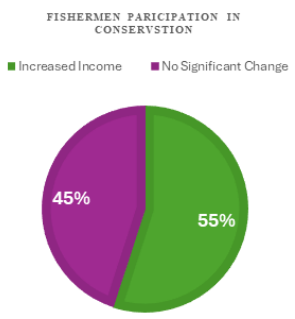

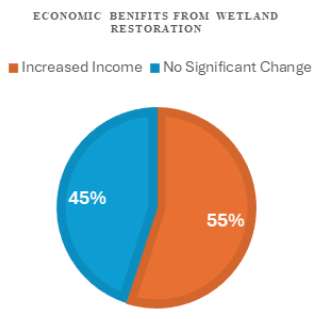

4. 3 Implementation of coastal zoning and regulations

Implementing coastal zoning and regulations in Odisha is crucial for safeguarding ecologically sensitive areas, mitigating coastal erosion, and promoting sustainable tourism. Below is an overview of Odisha's initiatives in this regard, supported by research-based data and visual representations.

Designation of buffer zones to protect ecologically sensitive areas:

Odisha adheres to the Coastal Regulation Zone (CRZ) Notification of 2019 issued by the Ministry of Environment, Forest, and Climate Change. This notification classifies coastal stretches into different zones to regulate development activities:

- CRZ-I: Ecologically sensitive areas where no new construction is permitted, except projects related to the Department of Atomic Energy, defense requirements, or for maintaining existing structures.
- CRZ-II: Areas that have already been developed up to or close to the shoreline. Construction and reconstruction of buildings are allowed, subject to local town and country planning rules, without altering the existing land-use pattern.
- CRZ-III: Relatively undisturbed areas that do not fall under CRZ-I or CRZ-II. Here, the area up to 200 meters from the High Tide Line (HTL) is earmarked as a "No Development Zone, " with certain exceptions for specific activities.

Strict enforcement of building regulations to prevent coastal erosion and habitat loss

The Odisha Development Authority (Planning and Building Standards) Rules, 2020, emphasize compliance with the CRZ Notification. Specifically, plots located within the Coastal Regulation Zone are subject to restrictions to prevent unauthorized construction that could lead to coastal erosion and habitat degradation.

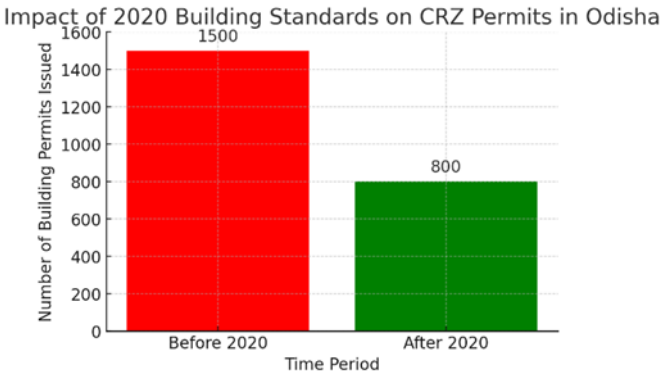

Fig. 3 Impact of 2020 building standards on CRZ permits in Odisha.

Adoption of waste management protocols for tourist hotspots

Odisha has adopted the Solid Waste Management Rules, 2016, which include provisions for establishing buffer zones around waste processing and disposal facilities. These buffer zones serve as no-development areas to minimize environmental impact, especially in regions exceeding five tonnes per day of waste processing capacity.

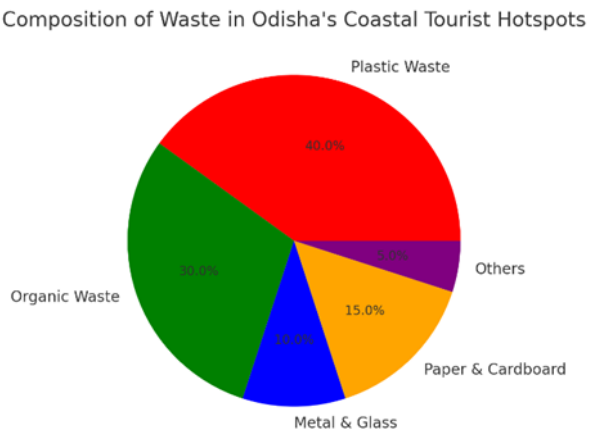

Fig. 4 Proportion of different waste types in Odisha's coastal tourist hotspots

Odisha's implementation of coastal zoning and regulations, including the establishment of buffer zones, enforcement of building standards, and adoption of waste management protocols, plays a crucial role in preserving its coastal ecosystems and promoting sustainable development.

5. Policy Recommendations

Effective coastal management in Odisha requires a comprehensive strategy that integrates scientific monitoring, sustainable tourism, environmental conservation, and multi-stakeholder collaboration. The following policy recommendations are essential for ensuring long-term coastal sustainability:

- Strengthening coastal monitoring systems: Implementing GIS and remote sensing technologies can significantly enhance coastal hazard assessment, erosion trend analysis, and land-use mapping (Das and Chatterjee, 2020).
- Expanding eco-tourism zones: Establishing community-based eco-tourism initiatives around fragile ecosystems like Chilika Lake and Bhitarkanika can promote sustainable tourism while conserving biodiversity (Das and Chatterjee, 2020).
- Enriching waste management infrastructure: Introducing waste segregation, recycling programs, and biodegradable alternatives in coastal tourist hubs can mitigate environmental degradation (Bahinipati & Sahoo 2012).
- Restoring natural buffers: Increasing mangrove plantation efforts and wetland conservation in critical areas like Kendrapara and Balasore can reduce cyclone-related damages and coastal erosion (Bahinipati & Sahoo 2012).
- Promoting stakeholder collaboration: Establishing coastal management committees with government agencies, research institutions, and local communities can lead to more effective and sustainable policies (Das and Chatterjee, 2020).

6. Conclusion

Odisha's coastal sustainability is at a crossroads, requiring immediate action to address environmental degradation and ensure long-term resilience. By adopting integrated geological, ecological, and tourism management strategies, Odisha can achieve a balance between economic growth and environmental protection. Strengthening zoning laws, improving community-based conservation, and expanding eco-tourism initiatives are essential steps toward sustainable coastal development. Collaboration among policymakers, scientists, and local communities will be key in transforming Odisha into a model for responsible coastal management.

References

- Bahinipati, C. S. and Sahu, N. C. (2012). Mangrove Conservation as Sustainable Adaptation to Cyclonic Risk in Kendrapada District of Odisha, India. Asian Journal of Environment and Disaster Management, Vol. 4, No. 2, pp. 183–202.
- Bakshi, A., & Panigrahi, A. K. (2022). Study on Climate Change and Its Impact on Coastal Habitats with Special Reference to Ecosystem Vulnerability of the Odisha Coastline, India. Applied Geomorphology and Contemporary Issues. doi:10. 1007/978-3-031-04532-5_25
- Das, M., and Chatterjee, B. (2020) Community Empowerment and Conservation through Ecotourism: A case of Bhitarkanika wildlife Sanctuary, Odisha, India. Tourism Review International, Vol. 24, pp. 215–231.
- Das, S., & Mohapatra, P. (2020). Sea-Level Rise and Its Impact on Coastal Odisha. Journal of Climate Studies, 15(3), 45-58.
- Dash, T., Patel, A., & Sinha, R. (2022). Mangrove Restoration and Climate Resilience in Odisha. Environmental Sustainability, 29(1), 102-118.
- IMD Report (2019). Cyclone Fani: Impact Assessment and Response Strategies. India Meteorological Department, New Delhi.
- Jena, R., & Chand, B. (2019). Coastal Erosion and Mitigation Strategies in Odisha. Journal of Marine Geology, 17(2), 78-94.
- Kar, P. K., Mohanty, P. K., Pradhan, S., Behera, B., Padhi, S. K. and Mishra, P. (2021). Shoreline change along Odisha coast using statistical and geo-spatial techniques. J. Earth Syst. Sci. pp. 190-209.
- Mahapatra, A., Rao, K., & Mishra, P. (2021). Coastal Erosion Trends in Odisha: A Satellite-Based Analysis (1990-2020). Geoscience Journal, 25(4), 132-148.
- Mishra, R., Tripathy, S., & Nanda, P. (2021). Tourism and Environmental Challenges in Odisha. International Journal of Environmental Policy, 34(5), 213-227.
- Mohanty, L., Das, B., & Nayak, K. (2018). Climate Change and Coastal Vulnerability in Odisha. Earth Science Review, 40(1), 21-37.

- Pattnaik, S., & Kumar, P. (2019). Community-Based Coastal Conservation Initiatives in Odisha. Sustainability Science, 14(3), 175-189.
- Rao, V. R., Murty, P. L. N., & Jain, I. (2017). Coastal erosion and accretion in Odisha: A study based on remote sensing and GIS techniques. Journal of Coastal Conservation, 21(6), 797-811.
- Sahu, D., Behera, S., & Pradhan, P. (2023). GIS-Based Coastal Monitoring in Odisha. Journal of Remote Sensing Applications, 28(2), 89-104.
- Tripathy, G. R., Singh, S. K., & Ramaswamy, V. (2018). Distribution and provenance of trace metals in sediments of the Mahanadi, Brahmani, and Baitarani River systems, India: Implications for coastal sediment deposition and erosion patterns. Journal of Coastal Research, 34(2), 334-347.

Mangroves of Western Coastal Maharashtra, Challenges and Opportunities

Archana Godbole & Jayant Sarnaik

Applied Environmental Research, Pune, India

Abstract

Mangroves are unique natural ecosystems that provide home and breeding ground to many marine resources like fish and crustaceans. Livelihoods of coastal communities are dependent on mangroves, as they utilize resources for food, livelihood, non-timber forest produce (NTFP), as well as they are the major source of firewood. Since the last couple of decades mangroves have been identified as main barriers for natural disasters like tsunami and are considered as best ecosystems to build resilience against climate change.

In western Coastal Maharashtra three districts, Raigad, Ratnagiri and Sindhudurg, have significant mangrove cover along the river creeks. The area under mangroves has increased since the last three decades, due to ingress of sea water on agricultural lands and livelihood patterns have changed due to loss of paddy farming. It is very interesting to understand in depth such recently developed land use change and its impact on coastal communities. In India the policies for mangrove conservation, especially CRZ regulations and current status of mangroves on privately owned erstwhile paddy lands, are a case in point where opportunities and challenges of coastal communities and climate resilience are concerned. The present paper examines the challenges, historical perspective, current measures by the State and Central Government for addressing the issue of sea water ingress and its impact on people's lives. Similarly how the current situation has brought many new opportunities for livelihoods and biodiversity conservation have also been discussed here.

Key words: Mangrove, western coast, socio-economic challenges

Introduction

Mangroves, situated at the confluence of the land and the open sea, mostly at river mouths and around lagoons with brackish water, protect the coastline against strong wave action, sand erosion, and winds. Mangroves are specialized salt-tolerant ecosystems that have been safeguarding tropical coastal regions around the world. They have an important ecological function to support marine biodiversity by providing breeding ground for fishes and crustaceans. Coastal communities are also largely

dependent on the mangroves for obtaining non-timber forest produce (NTFP), and firewood for a long time. Unfortunately they were not valued enough until recently when tropical cyclones hitting the coastal regions became frequent in India due to rising sea surface temperatures and changes in wind patterns (Najah et al. 2025). Ongoing reclamation activities for settlements and industrialization, together with sewage and industrial effluents being discharged in the rivers upstream of the mangrove ecosystem pose a serious threat for them.

According to global mangrove maps released by the Global Mangrove Watch, the estimated global mangrove forest cover in 2020 was 147, 359 km². Of this, 51% was located in the Asia-Pacific region, 29% in the Americas, and 20% in Africa. Comparing this to the baseline year of 1996, there has been a net loss of 5, 245 km² (3. 4%) of mangrove forests over the 24-year period. However, recent satellite data indicates that the global loss of mangroves has stabilized, with some gains observed around major rivers, estuaries, and deltas worldwide (UNEP, 2023). The stabilization can be attributed to the global sea levels rising at an unprecedented rate over the past 2500 years as a result of global warming (climate. nasa. gov).

Sea-level rise poses a major threat to mangrove ecosystems. Models predict that, if current trends continue, 25% of the global mangrove area could be submerged over the next 50 years. Additionally, one-third of the world's mangrove ecosystem regions will face severe impacts from rising sea levels; however the effects of sea-level rise will vary by region (IUCN). Overall, the mangrove ecosystem on the western coast of India is categorized as vulnerable (as seen in the map below), with the South India and Sri Lanka, and Maldives mangrove ecosystem as Critically Endangered (CR) (Selvam et al. 2024).

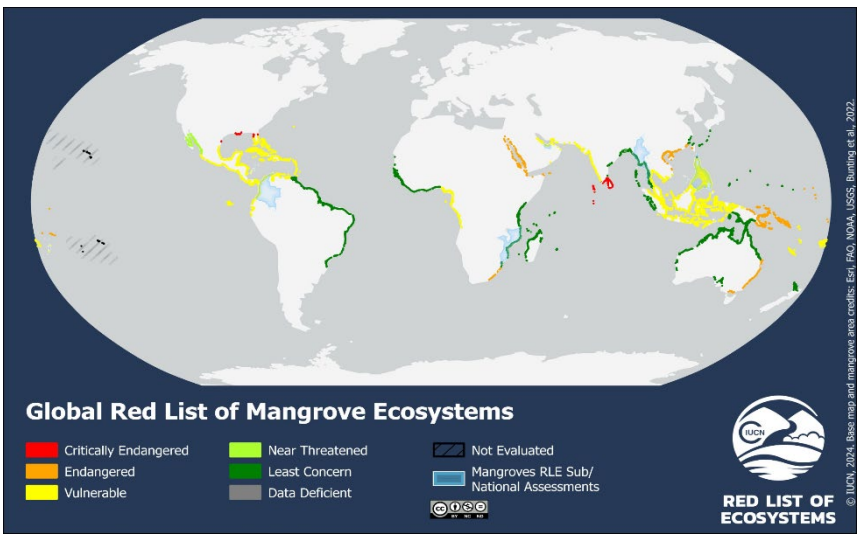

Mangroves and its challenges in the Indian scenario

As per Global forest Resource assessment, 2020 (FRA 2020), India holds three percent of the world's mangroves. The mainland peninsular India along with Andaman and

Nicobar Islands, and Lakshadweep host mangroves. Sunderbans- the largest mangrove ecosystem situated on the eastern coast of India along the coasts of Bay of Bengal is recognized as the World Heritage Site. India has been vulnerable to natural disasters due to its distinctive geo-climatic conditions; with floods, droughts, cyclones, earthquakes, and landslides have been a recurring phenomena.

The importance of the mangrove ecosystem came to light globally after one of the most devastating tsunamis the Indian Ocean tsunami which hit countries such as Indonesia, Thailand, Sri Lanka, India, and several other countries in 2004. Consequently the incidences of cyclonic storms also saw significant rise, one of the recent examples is of Nisarg cyclone which hit the western coast of India in 2020. The coastal areas with long stretches of mangroves were comparatively less affected in both the instances. The landfall of the Nisarg Cyclone was in Alibaug. However, dense mangrove patches along its coast protected the coastal communities from major losses.

The Indian Government issued Coastal Regulation Zone Notification, 2011 categorizing the coastal areas according to their risk of collapse. The Government of India exercising the power vested under EPA and Environment (Protection) Rules, 1986, issued notification in 1991 which was subsequently revised 2011 and 2019 with emphasis on the conservation and protection of coastal stretches, its unique environment and its marine area and promotion of development through sustainable approach based on scientific principles taking into account the dangers of natural hazard in coastal areas, sea level rise due to global warming. Accordingly the mangroves- one of the ecologically sensitive areas; categorized as CRZ 1 (Coastal Regulation Zone Notification, 2011) had legal protection. The Ministry of Environment, Forest and Climate Change (MoEF&CC) also allocated funds through the Central Sector Scheme for the conservation and management of mangroves and coral reefs in coastal states and Union Territories (UTs). As part of this initiative, 38 mangrove sites and 4 coral reef sites have been selected for on-ground intervention.

Mangroves of the western coast of India

As a direct consequence of rising sea levels, there is significant sea water ingression on the coastal lands of Konkan particularly in Ratnagiri, Raigad, Sindhudurg districts. The villagers in these areas had a well established traditional dykes system to arrest the water incoming from the Arabic ocean into their paddy fields. These were very efficiently managed by village communities and repaired in the event of breakage for generations. Afterwards the management of these dykes was legally handed over to the village Gram Panchayats; gradually leading to their mismanagement and most of the dykes are now broken. As a result, there is a consistent salt water ingression in the area. The local community has been completely dependent on the paddy crop in many coastal regions and ongoing salt water ingress poses a serious problem for the farmers as it is not only

responsible for barrening of land but also for making the groundwater saline. Due to this, countless farmers had to substitute their traditional agricultural practices with fishing and aquaculture for earning their livelihood. The shift was challenging for the local community.

Approximately forty percent of the human population lives within hundred kilometers in the coastal areas around the world. Obviously, the demand for freshwater required for drinking and sanitation is more causing heavy extraction of groundwater. This makes room for the salt water to ingress in the emptied aquifers. Thus as per the National Water Policy-2002 "over-exploitation of groundwater should be avoided, especially near the coast to prevent the ingress of seawater into sweet water/ freshwater aquifers" (Prusty & Farooq 2020).

In addition to being a barrier to arrest high tides from entering the coastal regions, the mangroves are also looked up as a source for climate change mitigation owing to its linkage to the blue carbon economy. In recent years, many studies have demonstrated a high potential of mangroves to sequester atmospheric carbon. The blue carbon financial market showed promising opportunities to earn incentives from the standing mangrove forests. Later on it was learnt that earning blue carbon credits is tricky since it largely relies on the additionality factor (Houston et al. 2024). Due to its complex nature, knowledge gap and lack in demonstrating direct benefit (including compensation) policy-level notifications or regulations are still in the primitive stage. The need to improve our understanding of this novel avenue is essential considering its positive implications in mitigating and adapting to climate change.

Understanding biodiversity profile and interdependency of the species is crucial in filling this knowledge gap. Thus, AERF identified four river estuaries namely Amba, Patalganga, Bhogawati, and Kundalika in Raigad which originate in the Sahyadri mountain ranges and meet Arabian sea forming estuaries along the western coast of Maharashtra. The estuaries harbour a vast area of mangroves along the banks stretching inwards into the terrestrial land. AERF team surveyed the area and prepared a comprehensive report with details on biodiversity profile with support from Apple Inc.

Salt marshes and mudflats, two different kinds of coastal wetlands, form the integral part of the ecologically sensitive mangrove ecosystem and hence categorized as CRZ 1 as per the Coastal Regulation Zone Notification, 2011 issued by Government of India.

They act as breeding and food grounds for the sand dwellers and the birds. The team documented thirteen species of plants, one species of Platyhelminthes, fifteen species of gastropods, thirty four species of Arthropods, twenty four species of fish and hundred species of birds.

The Socio-economic scenario of mangroves

Ongoing saltwater ingress has resulted in making the agricultural land unavailable for cultivation. Moreover, owing to the ecological importance of mangroves, farmers are banned from logging them off. This makes their situation worrisome as their sole livelihood earning resource is at loss. In order to compensate for the loss of paddy field by the villagers in the coastal lands of Raigad, AERF adopted a strategy to sign Mangrove Conservation Agreements. Through this approach, the AERF team identifies the farmers affected by salt water ingress and provides them incentives on the condition of not harming the mangroves. This helps the farmers to offset their hampered earning from agriculture, without causing damage to the unique mangrove ecosystem. Till date AERF has been successful in conserving about 1500 acres of coastal mangroves of Raigad through this approach.

Starting from about 60 miles south of Mumbai, AERF is implementing a conservation project aimed at safeguarding mangroves on private land while enhancing the resilience of local communities in the Pen, Alibag, and Roha blocks of Raigad district, up to the Mangangad and Dapoli blocks of Ratnagiri district in Maharashtra. Through an incentive-based mechanism, nearly 1500 acres of mangroves are being protected by more than 200 direct beneficiaries of the project.

While the focus is on incentivizing conservation, AERF also addresses cross-cutting issues and mainstreams mangrove conservation as a trade-off. This includes developing a waste treatment plant to prevent the garbage from entering mangrove areas, installing a desalination unit to provide clean drinking water to communities facing water scarcity, constructing a mangrove safari boat to promote ecotourism as a source of income, providing safety gear to fisherwomen who collect bivalves for their livelihood, and offering improved cooking stoves to reduce firewood consumption compared to traditional chulhas.

To conclude, conserving sensitive ecosystems such as mangroves is paramount and challenging at the same time owing to its linkage with the local stakeholders. The conservation strategy should be able to provide precise solutions giving due weightage to the local dynamics. Research encompassing various biodiversity components of the mangrove ecosystem is necessary to formulate the blue carbon trade-off in the Indian scenario. Policy-level reforms at the government level are essential as and when required since we have still not reached complete understanding of conserving this specialized ecosystem.

References

- Houston A, Kennedy H, Austin W E N (2024). Additionality in Blue Carbon Ecosystems: Recommendations for a Universally Applicable Accounting Methodology, Global Change Biology, 10. 1111/gcb. 17559, 30, 11

- IUCN redlist of Ecosystems https://iucn. org/resources/conservation-tool/iucn-red-list-ecosystems/red-list-mangrove-ecosystems
- Najah A, van der Merwe R & Al Shehhi M R (2025) Review of tropical cyclones impacting the Western Arabian Sea and Oman, Journal of Operational Oceanography, 18:1, 21-39, DOI: 10. 1080/1755876X. 2024. 2444753
- Prusty, Pintu & Farooq, Syed Hilal. (2020). Seawater intrusion in the coastal aquifers of India - A review. HydroResearch. 3. 61-74. 10. 1016/j. hydres. 2020. 06. 001.
- Selvam, V., Ramasubramanian, R., Kathiresan, K., Manoj Prasanna, M. G., Kodikara, K. A. S., Amarasinghe, M. D. & Suárez, E. L., (2024). IUCN Red List of Ecosystems, Mangroves of the South India, Sri Lanka and Maldives. EcoEvoRxiv.
- United Nations https://www.un.org/esa/sustdev/natlinfo/indicators/methodology_sheets/oceans_seas_coasts/pop_coastal_areas. pdf
- United Nations Environment Programme (2023). Decades of mangrove forest change: what does it mean for nature, people and the climate? UNEP, Nairobi

Sustainable Energy Transitions: Bridging the Gap with Geoscience

Satyabrata Nayak

satyabrata.nayak@inbox. Com

Abstract

As the world faces the challenges of climate change and the urgent need for a sustainable energy future, geoscience plays a pivotal role in advancing the transition to a net-zero carbon world. This shift requires innovative approaches to decarbonization, critical mineral exploration, energy storage, and renewable energy generation. The integration of artificial intelligence (AI) and machine learning (ML) is revolutionizing geoscientific methodologies, enhancing efficiency, and opening new opportunities for sustainable resource management. Carbon capture and storage (CCS) has become a crucial tool for reducing industrial greenhouse gas emissions by securely storing CO_2 in geological formations, with geoscientists contributing through reservoir identification, capacity assessment, and storage integrity monitoring. Likewise, the growing demand for critical minerals, such as cobalt, nickel, and lithium—essential for renewable energy technologies—is driving advancements in AI-driven exploration and sustainable mining practices. Hydrogen and geothermal energy are also emerging as key components of the clean energy transition, with geoscientists playing a vital role in hydrogen exploration, underground storage solutions, and geothermal system optimization. AI/ML further enhances resource discovery, reservoir modeling, and risk assessment, ensuring more efficient and sustainable energy production. The convergence of geoscience and emerging technologies is reshaping the energy landscape, fostering sustainability, and mitigating environmental impacts. Through interdisciplinary collaboration and technological innovation, geoscientists are shaping a resilient and equitable net-zero future, with their expertise in subsurface exploration, resource management, and environmental monitoring remaining essential in driving the global energy transition.

Keywards: Net-zero carbon, Climate change, Carbon capture and storage (CCS), Critical minerals, Renewable energy

Introduction

As the world confronts the challenges of climate change and the pressing need for a sustainable energy future, geoscience plays a crucial role in the transition to a net-zero carbon world (Intergovernmental Panel on Climate Change [IPCC], 2021). This dynamic landscape necessitates innovative approaches to decarbonization, critical mineral exploration, energy storage solutions, and sustainable energy generation

(International Energy Agency [IEA], 2022). Advances in technology, including artificial intelligence (AI) and machine learning (ML), are revolutionizing geoscientific methodologies, improving efficiency, and unlocking new opportunities in the pursuit of a greener future (Goodall et al., 2020; Zhang et al., 2023).

Carbon Capture and Storage

Carbon capture and storage (CCS) has emerged as a crucial technology for mitigating greenhouse gas emissions and addressing climate change (Intergovernmental Panel on Climate Change [IPCC], 2022). By utilizing deep geological formations, CCS enables the secure storage of captured CO_2, effectively reducing emissions from industrial sources (International Energy Agency [IEA], 2021). Geoscientists play a vital role in identifying suitable reservoirs, evaluating their storage capacity, and ensuring site integrity to minimize environmental risks (Benson & Cole, 2008). Advances in seismic imaging, reservoir simulation, and risk assessment have significantly improved our ability to monitor CO_2 behavior and prevent potential leakage. Additionally, the integration of artificial intelligence (AI) and machine learning (ML) is enhancing site selection processes and improving predictions of long-term storage performance, positioning CCS as a cornerstone technology for achieving net-zero carbon goals.

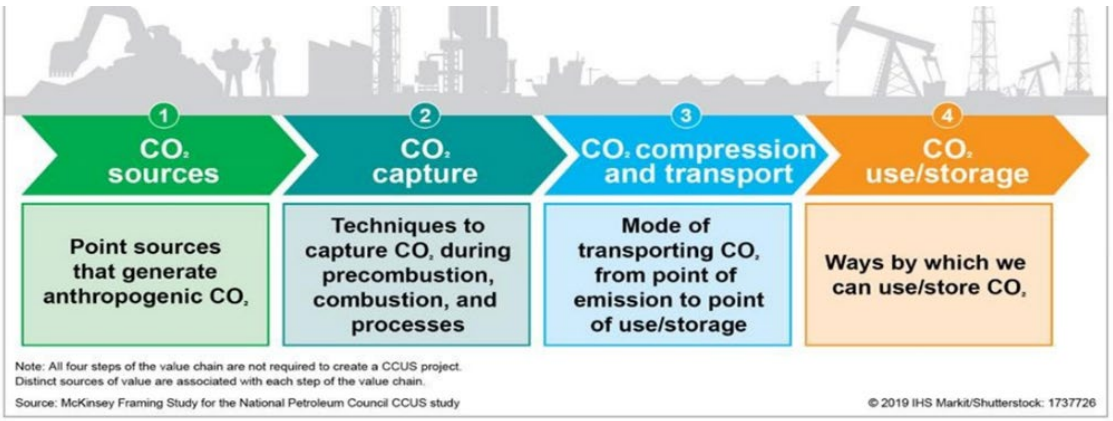

Figure 1: Critical steps of Carbon Capture and Storage (IHS 2019)

Critical Mineral

The global energy transition requires a substantial increase in the supply of critical minerals such as cobalt, nickel, rare earth elements, and copper, which are essential for renewable energy technologies and energy storage systems (International Energy Agency [IEA], 2021). Geoscientists are leveraging advanced exploration techniques, including geochemical analysis, remote sensing, and artificial intelligence (AI)-driven data analytics, to identify and assess new mineral deposits (Hofmann et al., 2022). However, the challenge lies in meeting the escalating demand for these resources while addressing environmental and social sustainability concerns (World Bank, 2020). Innovations in exploration methodologies, coupled with sustainable mining practices,

are crucial for ensuring that critical mineral supply chains remain resilient, ethically sourced, and environmentally responsible.

Lithium

Lithium, a critical component of rechargeable batteries, is essential for the electrification of transportation and grid-scale energy storage (International Energy Agency [IEA], 2022). Geoscientists play a key role in identifying lithium-rich brine deposits and hard-rock resources by utilizing hydrogeological modeling, isotopic analysis, and geophysical surveys (Kesler et al., 2012). The application of artificial intelligence (AI) and machine learning (ML) to analyze large geospatial and geochemical datasets is accelerating the discovery and development of economically viable lithium sources (Hofmann et al., 2022). Furthermore, advancements in sustainable extraction technologies, such as direct lithium extraction (DLE), are reducing environmental impacts and water consumption, aligning lithium production with broader sustainability objectives (Vikström et al., 2013).

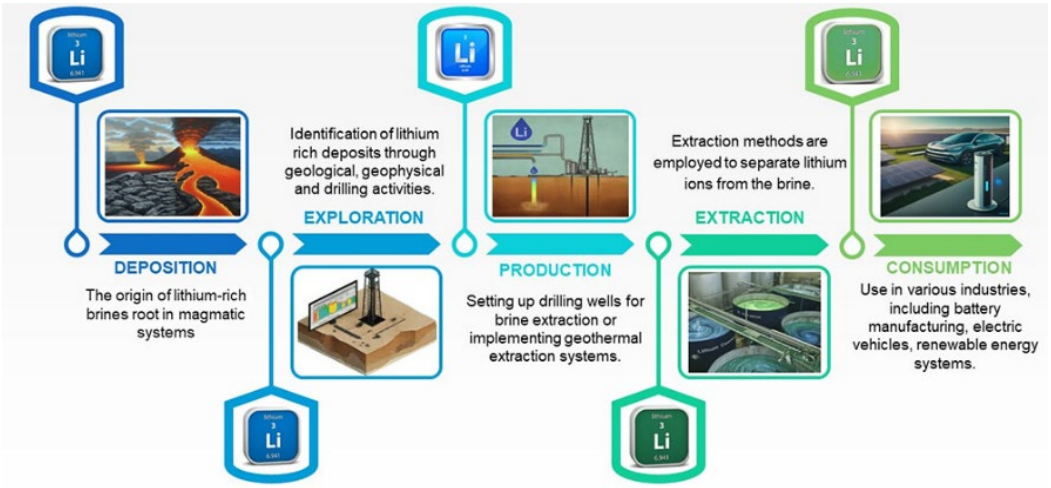

Figure 2: Full cycle for Lithium exploration and extraction (Ettehadi et al 2024)

Hydrogen

Hydrogen is increasingly recognized as a versatile energy carrier with the potential to decarbonize industries and the transportation sector (International Energy Agency [IEA], 2021). Geoscience plays a critical role in the exploration and development of natural hydrogen sources, as well as the underground storage of hydrogen in depleted reservoirs and salt caverns (Cuzens et al., 2023). Accurate geological modeling and risk assessments are essential to ensuring the safety and efficiency of hydrogen storage systems, mitigating potential leakage and maintaining long-term stability (Heinemann et al., 2021). Furthermore, artificial intelligence (AI) and machine learning (ML) algorithms enhance the interpretation of subsurface data, enabling precise mapping of storage capacities and monitoring hydrogen behavior under varying pressure and

temperature conditions. These advancements support the development of a robust hydrogen economy, which is integral to achieving global net-zero emissions targets.

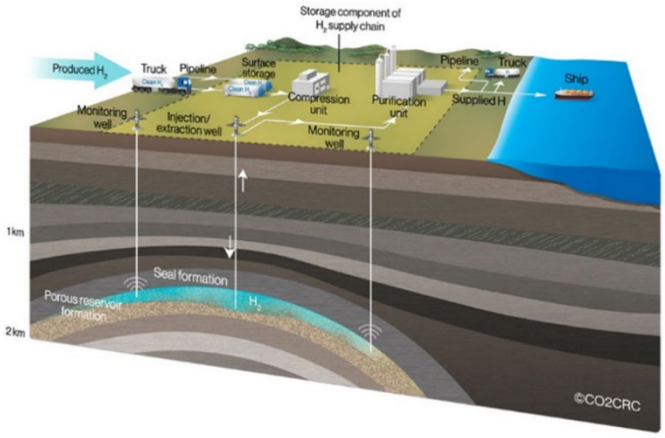

Figure 3 : Concept of Hydrogen storage (CO2 CRC)

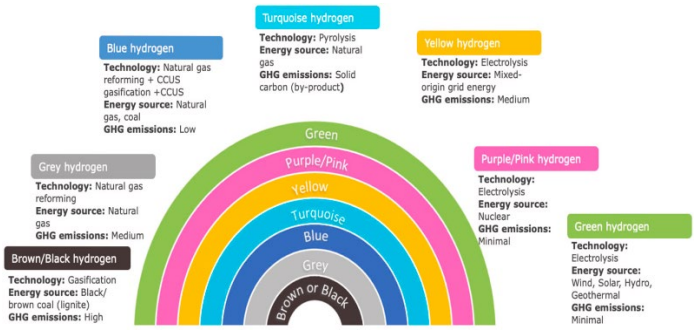

Figure 4: Different types of Hydrogen or the Color spectrum of hydrogen and the levels of GHG emissions (Rodríguez M, 2022)

Geothermal Energy

Geothermal energy provides a sustainable and reliable source of clean energy, with the potential to support global decarbonization efforts (International Energy Agency [IEA], 2022). Geoscientists play a crucial role in identifying and developing geothermal resources by employing advanced geophysical and geochemical techniques to locate and assess heat reservoirs (Tester et al., 2006). Enhanced Geothermal Systems (EGS), which leverage artificial intelligence (AI) and machine learning (ML) for optimizing drilling and reservoir management, are expanding the feasibility of geothermal energy in regions with less favorable geological conditions. By integrating geoscience expertise with technological innovation, geothermal energy can significantly reduce dependence on fossil fuels and contribute to long-term energy security.

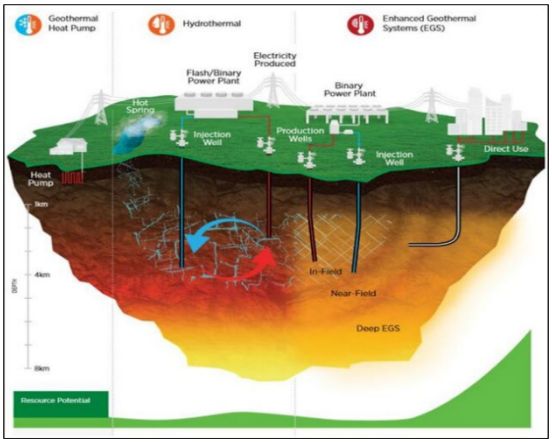

Figure 5: Operation conditions in different geothermal systems

(Dogdu 2023, Roberts et al 2020)

AI/ML

The integration of artificial intelligence (AI) and machine learning (ML) is transforming geoscience by enabling the rapid and accurate analysis of complex datasets (Libraries et al., 2020). AI/ML technologies are revolutionizing various applications, from automating seismic interpretation to predicting reservoir behavior and identifying mineral deposits, thereby enhancing decision-making processes across all aspects of the energy transition. Machine learning models can process vast volumes of geological, geophysical, and geochemical data, uncovering patterns and insights that would otherwise remain undetected (Bergen et al., 2019). Furthermore, AI-driven predictive analytics improve resource estimation, reduce exploration risks, and optimize production efficiency, ensuring that geoscience remains at the forefront of energy innovation.

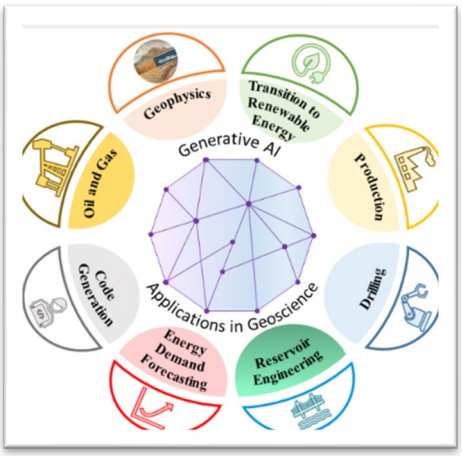

Figure 6: Some potential application domains of generative AI in geoscience.

(Hadid et al 2024)

Conclusion

The transition to a net-zero energy landscape is underpinned by the integration of geoscience with emerging technologies and interdisciplinary collaboration. Geoscientists are not only addressing technical challenges but are also playing a crucial role in fostering sustainability, minimizing environmental impacts, and ensuring equitable resource distribution. By leveraging expertise in subsurface exploration, resource management, and environmental monitoring, geoscience continues to shape the future of energy.

Geoscience is at the heart of the energy transition, driving advancements in decarbonization, critical mineral exploration, energy storage, and renewable energy solutions. The integration of AI/ML technologies is further enhancing the efficiency and sustainability of geoscientific practices. As the energy landscape continues to evolve, the role of geoscience will remain indispensable in achieving a net-zero carbon future, ensuring that the transition is both equitable and environmentally responsible. By embracing innovation and collaboration, geoscientists are paving the way for a sustainable and resilient energy future.

References

- Benson, S. M., & Cole, D. R. (2008). CO_2 sequestration in deep sedimentary formations. Elements, 4(5), 325-331. https://doi. org/10. 2113/gselements. 4. 5. 325
- Bergen, K. J., Johnson, P. A., de Hoop, M. V., & Beroza, G. C. (2019). Machine learning for data-driven discovery in solid Earth geoscience. Science, 363(6433), eaau0323. https://doi. org/10. 1126/science. aau0323
- Cuzens, P., Boreham, C., & Golding, S. D. (2023). Natural hydrogen: Geological sources, occurrences, and exploration potential. Earth-Science Reviews, 240, 104325. https://doi. org/10. 1016/j. earscirev. 2023. 104325
- Doğdu, N., Çelmen, O. (2023). Importance of reinjection in sustainability of geothermal resources and reinjection well location. Bulletin of the Mineral Research and Exploration 171, 159-175. https://doi. org/10. 19111/bulletinofmre. 1316785
- Ettehadi A, Chuprin M, Mokhtari M, Gang D, Wortman P, and Heydari E (2024). Geological Insights into Exploration and Extraction of Lithium from Oilfield Produced-Water in the USA: A Review. Energy & Fuels 2024 38 (12), 10517-10541. DOI: 10. 1021/acs. energyfuels. 4c00732
- Goodall, J. L., Bejarban, A., & Morsy, M. M. (2020). Advances in machine learning applications for geoscience: Opportunities and challenges. Computers & Geosciences, 140, 104489. https://doi. org/10. 1016/j. cageo. 2020. 104489

- Hadid, A., Chakraborty, T., & Busby, D. (2024). When geoscience meets generative AI and large language models: Foundations, trends, and future challenges. Expert Systems, 41(10), e13654. https://doi. org/10. 1111/exsy. 13654
- Heinemann, N., Booth, M. G., Haszeldine, R. S., Wilkinson, M., Scafidi, J., & Edlmann, K. (2021). Hydrogen storage in porous geological formations: Capacity, containment, and economic challenges. International Journal of Hydrogen Energy, 46(45), 23581-23606. https://doi. org/10. 1016/j. ijhydene. 2021. 04. 235
- Hofmann, M., Wellmann, F., & Jessell, M. W. (2022). Artificial intelligence in mineral exploration: Current state and future trends. Ore Geology Reviews, 144, 104832. https://doi. org/10. 1016/j. oregeorev. 2022. 104832 https://co2crc. com. au/
- International Energy Agency (IEA). (2022). The role of critical minerals in clean energy transitions. IEA Publications. https://www. iea. org/reports/the-role-of-critical-minerals-in-clean-energy-transitions
- Intergovernmental Panel on Climate Change (IPCC). (2022). Climate change 2022: Mitigation of climate change. Cambridge University Press. https://www. ipcc. ch/report/ar6/wg3/
- International Energy Agency (IEA). (2021). Carbon capture, utilization and storage: A critical tool in the climate challenge. IEA Publications. https://www. iea. org/reports/carbon-capture-utilisation-and-storage
- International Energy Agency (IEA). (2022). Global supply chains of EV batteries. IEA Publications. https://www. iea. org/reports/global-supply-chains-of-ev-batteries
- International Energy Agency (IEA). (2021). The future of hydrogen: Seizing today's opportunities. IEA Publications. https://www. iea. org/reports/the-future-of-hydrogen
- International Energy Agency (IEA). (2022). Global geothermal energy report: Opportunities and challenges in scaling up deployment. IEA Publications. https://www. iea. org/reports/global-geothermal-energy-report
- International Energy Agency (IEA). (2021). The role of critical minerals in clean energy transitions. IEA Publications. https://www. iea. org/reports/the-role-of-critical-minerals-in-clean-energy-transitions
- Intergovernmental Panel on Climate Change (IPCC). (2021). Climate change 2021: The physical science basis. Cambridge University Press. https://www. ipcc. ch/report/ar6/wg1/
- Kesler, S. E., Gruber, P. W., Medina, P. A., Keoleian, G. A., Everson, M. P., & Wallington, T. J. (2012). Global lithium resources: Relative importance of

pegmatite, brine, and other deposits. Ore Geology Reviews, 48, 55-69. https://doi. org/10. 1016/j. oregeorev. 2012. 05. 006

- Libraries, C. U. (2020). Artificial intelligence in geosciences: Emerging trends and applications. Earth Science Reviews, 210, 103382. https://doi. org/10. 1016/j. earscirev. 2020. 103382
- Rodríguez M. (2022). Hydrogen present and future. Part 2 – T´ecnicas Reunidas. Hydrogen Present and Future Part 2 2022. https://www. tecnicasreunidas. es/artic ulo/hydrogen-present-and-future-part-2/
- Roberts, D. (2020). Geothermal energy is poised for a big breakout, www. vox. com
- Tester, J. W., Anderson, B. J., Batchelor, A. S., Blackwell, D. D., DiPippo, R., Drake, E. M.,... & Veatch, R. W. (2006). The future of geothermal energy: Impact of enhanced geothermal systems (EGS) on the United States in the 21st century. Massachusetts Institute of Technology. https://www1. eere. energy. gov/geothermal/pdfs/future_geo_energy. pdf
- Vikström, H., Davidsson, S., & Höök, M. (2013). Lithium availability and future production outlooks. Applied Energy, 110, 252-266. https://doi. org/10. 1016/j. apenergy. 2013. 04. 005
- World Bank. (2020). Minerals for climate action: The mineral intensity of the clean energy transition. World Bank Group. https://pubdocs. worldbank. org/en/961711588875536384/Minerals-for-Climate-Action-The-Mineral-Intensity-of-the-Clean-Energy-Transition. pdf
- Zhang, X., Li, Y., & Wang, J. (2023). Artificial intelligence-driven innovations in geosciences and sustainable energy solutions. Renewable and Sustainable Energy Reviews, 180, 113168. https://doi. org/10. 1016/j. rser. 2023. 113168

A Comprehensive Review of Heavy Mineral Deposits in Coastal Environments

Smruti Rekha Sahoo, Indira Priyadarshini*, Rabindra Nath Hota and Pankajini Mahanta

Department of Geology, Fakir Mohan University, Balasore, Odisha

*Corresponding author: indirap.darshini@gmail.com

Abstract

The heavy mineral deposits in Odisha are found in beach and dune sand and are made up of a variety of minerals. The heavy mineral content in these deposits mineral content in these deposit ranges from 2. 9% to 20. 4%. Odisha is endowed with a number of multi-mineral placer deposits of beach and dune sand origin. Out of 470 km coastal length, 43 km has been evaluated under detailed and 62 km under scout-drilling programs of AMD. A heavy mineral reserve of 76. 74 million tonnes (mt) under indicated and 29. 22 mt under inferred category has been established till date. Composition of these deposits is nearly uniform, comprising ilmenite, garnet, sillimanite, rutile, zircon, monazite, magnetite and pyriboles. Based on coastal geomorphology, the entire coast is divided into three segments such as northern, central and southern, for describing the heavy mineral distribution and potentiality.

Southern segment of 108 km has been extensively explored in detail, and scout drilling has brought out three potential deposits. The largest of these, the Chhatrapur mineral sands deposit, with a heavy mineral reserve of 62 mt at an average grade of 18. 50%, is under active exploitation by the Indian Rare Earth Limited (IREL). Central segment of 230 km consists of deltaic sediments of the Mahanadi River system of Holocene age with the widest beach and dune complex. Northern segment of 132 km is a complex, low-lying coast of tidal flats, Recent beach and dune sands, and shore parallel palaeo-beach ridges deep inland. Singhbhum Group, Dhanjori and Dalma volcanic rocks and meta-sediments form the provenance for the heavy minerals.

The beach placer minerals in the chandipur area of the baleswar district on the north east Odisha coast of india, Beach and dune sands are ubiquitous along the 1 to 1. 5 km-wide. The heavy mineral assemblages, are comprised of 55% ilmenite, 25% sillimanite, 11% pyriboles and others, 5. 9% rutile, 1. 5% leucoxene, 1. 2% garnet, 0. 5% zircon, and 0. 4% magnetite. RiverBudhabalanga, source of sediments and heavy minerals in this area, is flowing roughly NW-SE to converge with the Bay of Bengal, developing prominent estuary and mouth bars at chandipur coast. The present study addresses which corroborate the deposition of sediments in low energy condition in a fluctuating

shoreline along the Chandipur coast. The perennial (Panchpara River) and the ephemeral drainage systems (Dubdubi River) played a dominant role in transporting and supplying sediment flux consisting of radioactive mineral (monazite) assemblages in chandipur coast. A tidal flat approx. 4km wide is found in Chandipur Odisha. NE part of this area with prominent heavy mineral lamina and SW part there are large scale aeolian dunes with heavy minerals concentrated along aeolian super- surfaces as well as in foreshore and backshore region.

This area lies in the coastal tract of Puri city in the northeast up to Ichchapuram in the southwest. The major river Rushikulya is flowing towards SE and merging with Bay of Bengal near Ganjam town. The Geomorphology map for the entire coastal stretch up to the limit of oldest / extreme inland palaeo - shoreline (Beach Ridge) is an important aspect for prospecting of heavy mineral deposits. Demarcation of the probable landforms such as Beach Ridge, Planated Beach Ridge, Dune Complex, Sand Dune.

The Brahmagiri placer deposits of puri district showing that the deposit contains potential amount of heavy mineral. The dune sands contain higher heavy minerals than that of beach sand. The main minerals in the Brahmagiri beach placer deposits are garnet, ilmenite, and sillimanite, with zircon, rutile, and monazite as minor minerals. Dune sands in the Brahmagiri area contain higher concentrations of heavy minerals than beach sands. The heavy minerals in the Brahmagiri area are well liberated, have uniform shapes, and have variable densities.

The Chatrapur area in Odisha, India, is known for its rich deposits of heavy minerals. These minerals are found in abundance in the beach sands along the Chatrapur coast, with high concentrations of titanium dioxide (TiO2) and thorium phosphate (ThP04). Some heavy minerals, like monazites and zircons, contain higher concentrations of radioactive elements like Th and U. The monazite sands in the Chhatrapur beach placer deposit have an average rare- earth element (REE) content of 56. 75 wt. %. The ilmenite mineral in the area has altered to secondary phases like pseudorutile, leucoxene, and rutile.

The intertidal zone as well as sand dunes of Gopalpur coast, Odisha contains heavy minerals of varying proportions ranging from 6. 51 to 8. 45wt% out of > 63 μm fractions. The heavy mineral assemblages are ilmenite, magnetite, garnet, sillimanite, zircon, rutile and hornblende of which ilmenite is dominant. The concentration of heavy minerals in Gopalpur is higher than in Paradeep. Scanning electron microscope images of ilmenite grains in Gopalpur show that they are sub-rounded to rounded, with some having angular or sub-angular features. The micro morphological features indicate the effects of mechanical and chemical weathering. The Mn/Mg ratios of most ilmenite grains in Gopalpur are low, indicating a basic rock source. However, some ilmenite grains have higher Mn/Mg ratios, which may indicate a source of charnockite or khondalites. The

Gopalpur beach and its adjacent area has a high content of sillimanite followed by garnet, pyroxene, rutile, sphene, biotite, hornblende, zircon and monazite.

Keywords: Beach Placers, Odisha, Coast, Heavy Mineral

Introduction:

Heavy mineral deposits found in coastal areas are important both economically and geologically. These minerals, such as ilmenite, zircon, rutile, garnet, and monazite, are mainly derived from igneous and metamorphic rocks. They are transported by rivers, waves, and coastal currents and get concentrated on beaches due to natural sorting processes. Coastal regions worldwide, particularly in India and Odisha, are known for their rich placer deposits, which play a vital role in the mineral industry.

Globally, placer deposits have been documented in various coastal settings, including Kerala's black sand deposits, which exhibit a three-stage depositional model influenced by wave and current activity (T. K. Mallik et al.). The study of these deposits helps in understanding sediment movement and their potential for mineral extraction. India has many coastal areas rich in heavy minerals. The formation and distribution of these heavy mineral deposits are influenced by various factors including provenance, hydrodynamic conditions, geomorphology, and climatic variations (M. Suresh Gandhi & M. Raja, 2014). The Tamil Nadu coastline, for instance, has high concentrations of garnet, zircon, and hypersthene, which are sourced from charnockite and granulite gneiss rocks (Suresh Gandhi & Raja, 2014). Similarly, the Kerala coastline contains valuable minerals like monazite, zircon, and ilmenite, which are sorted by waves and currents over time (Sundararajan et al., 2009). Additionally, studies in Bhimunipatnam's red sediments have confirmed the presence of high ilmenite concentrations, transported over long distances by riverine and coastal processes before being deposited on beaches (Sundararajan, 2009). The Neendakara–Kayamkulam belt in southwest India found large reserves of ilmenite, with wave energy playing a key role in mineral concentration (Anitha et. al, 2020).

India's east coast, particularly Odisha, is well-known for its extensive heavy mineral placer deposits. The heavy mineral deposits in Odisha are found in beach and dune sand and are made up of a variety of minerals. The heavy mineral content in these deposits mineral content in these deposit ranges from 2. 9% to 20. 4%. Odisha is endowed with a number of multi-mineral placer deposits of beach and dune sand origin. Out of 470 km coastal length, 43 km has been evaluated under detailed and 62 km under scoutdrilling programs of AMD. A heavy mineral reserve of 76. 74 million tonnes (mt) under indicated and 29. 22mt under inferred category has been established till date. Composition of these deposits is nearly uniform, comprising ilmenite, garnet, sillimanite, rutile, zircon, monazite, magnetite and pyriboles. Based on coastal

geomorphology, the entire coast is divided into three segments such as northern, central and southern, for describing the heavy mineral distribution and potentiality. These deposits are largely derived from the Eastern Ghats' charnockitic and khondalitic formations, with ilmenite, garnet, sillimanite, and monazite being the primary minerals (Ganapati Rao et al., 2019).

This literature review aims to provide a comprehensive understanding of the global distribution of heavy mineral deposits in coastal environments, with a special focus on India and Odisha. By analyzing previous research findings, mineral composition, depositional processes, and economic potential, this study will contribute to future exploration and sustainable management of these valuable coastal resources.

The Zones of Heavies in Odisha

The heavy mineral placers along the Gopalpur coast in southern Odisha, focusing on ilmenite as an indicator of provenance, which is the south segment (Chakraborty and Saha et. al, 2021). The dominant heavy minerals include ilmenite, magnetite, garnet, sillimanite, zircon, rutile, and hornblende, with ilmenite being the most abundant. Methodology mainly used as Electron Probe Micro Analysis (EPMA) for Geochemical analysis. Mn/Mg ratio was used to trace the provenance of ilmenite, distinguishing sources from basic igneous (pyroxene granulites) and metamorphic (khondalite and charnockite) rocks. Scanning Electron Microscope (SEM)captured ilmenite grains and observe micro-morphological features For heavy mineral sparation and identification using bromoform separation for heavy mineral extraction. For grain size analysis polarizing microscope used for mineral grain analysis. The study attributes the concentration and distribution of heavy minerals in the region to both riverine and marine processes, with sediment input primarily from the Rushikulya and Bahuda rivers.

Monazite, a significant rare earth and thorium phosphate mineral, has been documented in the heavy mineral-bearing sands of Chhatrapur coast, Odisha, with an estimated 62 million tonnes of heavy minerals at an average grade of 18. 50%, with concentrations varying between 0. 09% and 0. 16% (Rao, A. Y., Panda, N. K., Kumar, K. R. et al., 2022). The study of monazite has gained attention due to its economic importance as a source of rare earth elements (REEs), thorium (Th), and uranium (U), which are essential for various industrial and technological applications. monazite grains exhibit color variations ranging from colorless to different shades of yellow, green, and brown. The electron probe micro analysis (EPMA) of monazite grains has demonstrated that distinct chemical compositions correlate with differences in rare earth element (REE) concentrations and Th and U content. The occurrence of monazite and other heavy minerals along the Paradeep and Chhatrapur coast is documented by Behera, 2003. Viswanathan and Murthy, 1964 studied the geochemistry and provenance of monazite in coastal deposits of eastern India, emphasizing its derivation from khondalite and

charnockite rocks. Acharya et al., 2009 focuses on evaluating the heavy mineral placer sand deposits in the Kontiagarh area, Ganjam district, Odisha, India. The study revealed that the heavy mineral content in the beach and dune system varies from 9. 38% to 24. 20%, with heavy minerals primarily composed of ilmenite, garnet, sillimanite, rutile, monazite, and zircon, along with trace amounts of magnetite, hornblende, diopside, sphene, tourmaline, and epidote. The mineral composition was determined using optical microscopy, X-ray diffraction (XRD), and EPMAThe chemical composition of ilmenite, hematite, and other minerals was analyzed to understand their alteration and economic viability. These minerals were transported through fluvial systems such as the Rushikulya River and deposited along the coastal environment due to wave action and littoral currents.

The coastal deposits of Central Odisha host a significant concentration of heavy mineral placers, primarily derived from the Eastern Ghat Mobile Belt (EGMB). paleo-beach ridges in this area exhibited heavy mineral concentrations ranging from 2% to 64%, with an inferred reserve of 12. 89 million tonnes at an average grade of 10. 48%. These deposits contain minerals such as ilmenite, zircon, rutile, monazite, and sillimanite, which are economically valuable for various industrial applications. The provenance study indicates that the majority of the placer deposits in Central Odisha are derived from the charnockite, migmatite, and khondalite rocks of the EGMB. The heavy mineral sands in Central Odisha are considered economically viable due to their high ilmenite, zircon, and monazite content. The study highlights the potential for mining and resource utilization, emphasizing the need for sustainable extraction practices to prevent environmental degradation. (Ghosal et al., 2022).

Central segment of coastal deposits of 230 km consists of deltaic sediments of the Mahanadi river system of Holocene age with the widest beach and dune complex. (Behera, P. et. al 2003) conducted study on Astaranga Beach, Puri, investigates the distribution, concentration, and alteration of heavy minerals, particularly ilmenite, using Scanning Electron Microscope (SEM) and Energy Dispersive Spectrometer (EDS) techniques. The dominant heavy minerals occurs as ilmenite > zircon > sillimanite > garnet > rutile > pyroxene > monazite > others. Hydrodynamic sorting mechanisms play a key role in depositing heavy minerals in finer fractions, with ilmenite dominating the mineral assemblage. Routray et al., 2018 conducted a study on the placer deposits of the Brahmagiri coast, Odisha, focusing on their mineral composition, distribution, and beneficiation potential by conducting an assessment of the heavy mineral content in beach and dune sands and evaluating their recovery potential using gravity separation techniques. Their study concluded that the Brahmagiri placer deposits have significant economic potential for the extraction of ilmenite, rutile, zircon, garnet, monazite, and sillimanite. Rout et al. 2018 conducted a study on heavy mineral placer sand deposits along the Puri to Ichchapuram coastal tract of Odisha, India. The major river Rushikulya

is flowing towards SE and merging with Bay of Bengal near Ganjam town. The Geomorphology map for the entire coastal stretch up to the limit of oldest / extreme inland palaeo - shoreline (Beach Ridge) is an important aspect for prospecting of heavy mineral deposits. Demarcation of the probable landforms such as Beach Ridge, Planated Beach Ridge, Dune Complex, Sand Dune.

The northern segment of 132 km is a complex, low-lying coast of tidal flats, Recent beach and dune sands, and shore parallel palaeo-beach ridges deep inland. Singhbhum Group, Dhanjori and Dalma volcanic rocks and meta-sediments form the provenance for the heavy minerals. Bhattacharjee and Sarkar et. al., 2018 conducted a detailed study on the tidal flats of Chandipur, focusing on the formation of heavy mineral laminations, highlighted that the river. River Budhabalanga, source of sediments and heavy minerals in this area, is flowing roughly NW-SE to converge with the Bay of Bengal, developing prominent estuary and mouth bars at Chandipur coast. The total estimated reserves for these minerals are substantial, with ilmenite reserves at 39. 01 million tonnes, garnet at 29. 40 million tonnes, and sillimanite at 17. 91 million tonnes. Probe Micro-Analysis (EPMA) to determine the mineralogical composition of the heavy mineral laminations. EPMA analysis identified the heavy minerals as detrital ilmenite. Northeastern and southwestern ends of the tidal flat. NE part of this area with prominent heavy mineral lamina and SW part there are large scale aeolian dunes with heavy minerals concentrated along aeolian super-surfaces as well as in foreshore and backshore region. Rao, Sahoo, and Panda, 2001 provides a detailed evaluation of Odisha's coastal heavy mineral sand deposits, highlighting their distribution, composition, and economic significance. The research emphasizes the interplay between geological formations, coastal processes, and sediment dynamics in shaping these valuable mineral resources. The perennial (Panchpara River) and the ephemeral drainage systems (Dubdubi River) played a dominant role in transporting and supplying sediment flux consisting of radioactive mineral (monazite) assemblages in the Chandipur coast.

Summary

Heavy mineral deposits play a crucial role in various industrial applications due to their unique physical and chemical properties. These deposits, typically rich in minerals like zircon, rutile, and ilmenite, offer significant economic value, particularly in sectors such as manufacturing, electronics, and construction. However, the sustainable extraction and management of these resources remain vital for minimizing environmental impacts and ensuring long-term availability. As demand for these materials continues to rise, ongoing research into more efficient extraction methods, along with responsible mining practices, will be key to balancing economic growth with environmental stewardship. The heavy minerals are primarily found in the coastal areas of Odisha, particularly in the Ganjam and Kendrapara districts, which have been identified as key zones for mineral sands.

While Odisha's heavy mineral resources contribute significantly to the national economy, the mining and extraction processes raise environmental concerns. These include habitat destruction, coastal erosion, and pollution, which necessitate careful management and sustainable practices in the extraction industry. Hence, Odisha's heavy mineral deposits are of immense economic importance and require responsible management to ensure that environmental impacts are minimized and that the state's natural resources are used sustainably.

Acknowledgement

The author(s) acknowledge Fakir Mohan University, Balaosre for providing the platform to conduct this research from the FMU Seed Fund Grant. Ms. I. Priyadarshini thanks her mentors and team for their consistent guidance and support.

Reference

- Bhattacharjee, S., & Sarkar, S. (2018). Geochemical and Sedimentological Investigation of Unusual Heavy Mineral Lamination in Tidal Flat of Chandipur, Odisha, India: Probable Influence of Anthropological Activity. Geological Society of America Abstracts with Programs, 50(6).
- Rao, R. G., Sahoo, P., & Panda, N. K. (2001). Heavy Mineral Sand Deposits of Orissa. Exploration and Research for Atomic Minerals, 13, 23-52.
- **Rout, S. P., Ch, S., Kumar, K. R., & Raju, K. (2018).** Delineation of Mineable Heavy Placer Deposits Using Geospatial Technology Along Puri to Ichchapuram Coastal Tract of Odisha State, India. Journal of Applied Science and Computations.
- **Routray, S., Vanamu, J., & Swain, R. (2018).** Placer Deposits of Brahmagiri Coast, Odisha - A New Resource for Industrial Heavy Minerals. IOP Conference Series: Materials Science and Engineering, **338**, 012012.
- **Acharya, B. C., Nayak, B. K., & Das, S. K. (2009).** Heavy Mineral Placer Sand Deposits of Kontiagarh Area, Ganjam District, Orissa, India. Resource Geology, **59**(4), 388–399.
- Ghosal, S., Agrahari, S., & Sengupta, D. (2022). Provenance studies on the heavy mineral placers along the coastal deposits of Odisha, eastern India. Journal of Palaeogeography, 11(2), 275-285.
- Sahu, B. K., Suar, P. C., & Sahu, K. C. (1984). Heavy Minerals in Beach Sands of Chatrapur (Orissa), East Coast of India. Indian Journal of Marine Sciences, 13(3), 142-143.
- Behera, P. (2003). Heavy Minerals in Beach Sands of Gopalpur and Paradeep along Odisha Coastline, India. Indian Journal of Marine Sciences, 32(2), 172-174.

- Rao, D. S., & Sengupta, D. (2014). Electron Microscopic Studies of Ilmenite from the Chhatrapur Coast, Odisha, India. Journal of Geochemistry, 8, Article ID 192639.
- Sengupta, R., Bhattacharya, S., Rana, R. S., Mitra, S. K., & Jain, V. K. (1998). Sediment Distribution and Heavy Mineral Potential of the Shoreface Zone of Southern Orissa. Journal of Indian Association of Sedimentology*, 117*(2), 231-237.
- Chakraborty, D., Saha, B. K., & Hazra, S. (2019). Sediment Character of Beach-Dune Complex of Gopalpur Coast, Odisha. Indian Journal of Geosciences, 73(1), 25-38.

Coastal Economy from Beach Sand: Silicon the Magic Element

Namrata Singh[1] and Vibhuti Rai[2]

1. Department of Chemistry, University of Lucknow, Lucknow 226007

2. Department of Geology, University of Lucknow, Lucknow 226007

Email: namratasingh9988@gmail. Com

Abstract

Amongst the various geo-resources from the coastal region, one of the most abundant resources occur in the form of coastal sands, in which, the key components are heavy mineral placers, metallic sands, gem stones, abrasives, rare-earth elements and silica sand. Many of these are being exploited for the last hundreds of years and were broadly the part of coastal economy for the countries which have large coastal areas.

Considering the extent and vastness of coastal regions in India, where a number of coastal geomorphological units represent a huge amount of geo-resource material. We propose to explore another vast resource that occurs in the form of silica sand from which the modern technology related metalloid the silicon can be extracted at a high level for making the country Atmanirbhar for its energy and electronic industry related needs.

We also propose that the economic and technological benefits of using Odisha's beach sands, can be a resource for the production of silicon. To make silicon extraction more effective and environmentally benign, issues like energy-intensive procedures and environmental sustainability need for greater study and development.

Key words: Beach sand, silicon, Odisha coast

Introduction

The discovery of silicon was made in 1824 by Swedish chemist Jons Jacob Berzelius.

Silicon is the second most abundant element in the Earth's crust (about 27. 7% by weight) and occurs naturally in various forms. However, it is rarely found in its pure elemental state due to its high reactivity. Instead, it is most commonly found as silicates and silica compounds.

One of the most prevalent elements on Earth, silicon serves as the foundation for the growth of industry (Park et al. 2015; Riordan and Hoddeson, 1997). It is essential to several industries such as electronics, solar energy and innovative materials. Silicon's remarkable qualities such as its temperature stability and semiconducting behaviour,

make it essential to contemporary technology (Green, 2020). Coastal beach sands provide an alternate source of high-purity silica, especially in a country like India with its vast coastline. This is in addition to quartz rich rock formations of peninsular India. The coastal sands of Odisha, which are abundant in quartz and other silicate minerals, are a mostly unexplored resource that may be able to meet the silicon demands of India's expanding electronics and renewable energy industries. The present contribution focuses on the production of Silicon from vast resources of Coastal India, particularly, the Odisha state.

Geographical Distribution In Odisha State

Odisha's coastal regions, particularly in the Ganjam district, are rich in beach sand minerals including significant quantities of silica sand. The Orissa Sands Complex (OSCOM), operated by IREL (India) Limited, is a prominent facility located in Chatrapur, Ganjam district. This complex spans a mining lease area of 2, 464 hectares and produces approximately 265, 400 tonnes per annum of ilmenite and associated minerals such as rutile, zircon, sillimanite, and garnet (Indian Rare Earths Limited, n. d.).

In 2017, a joint venture between IDCOL and IRELs was established to explore and mine beach sand minerals along the Odisha coast, particularly from Gopalpur in Ganjam district to Brahmagiri in Puri district (Moneycontrol, 2018).

The reserves of silica sand and quartz can be found in coastal region of numerous districts of Odisha state named as: The Boudh, Baragada, Kandhamal, Kendujhar, Jharsuguda, Kalahandi, Mayurbhanj, Nuapada, Subarnapur, Nabrangpur, Rayagada and Koraput districts (Odisha Minerals Department, n. d.)

Quartz occurs in the form of veins and as a constituent of pegmatites. In Orissa, quartz and silica sand deposits are located in the Precambrian terrains. Quartzite occurs as beds interstratified with other meta sedimentaries. Estimated reserve in the state is 70. 30million tonnes. Ceramic, fertilizers, abrasives, electrical, paint, rubber, chemical and textile industries with different specifications are based on silicon related minerals. Transparent varieties of quartz such as rock crystals, amethyst, citrine, rose quartz and smoky quartz are used as semiprecious gem stones. Quartz is a piezoelectric mineral and is used in radio circuit, radars, ultrasonic devices, chronometers etc. Quartzites are used in refractory industry, iron and steel making, ferro-silicon industry, glass and ceramic industry.

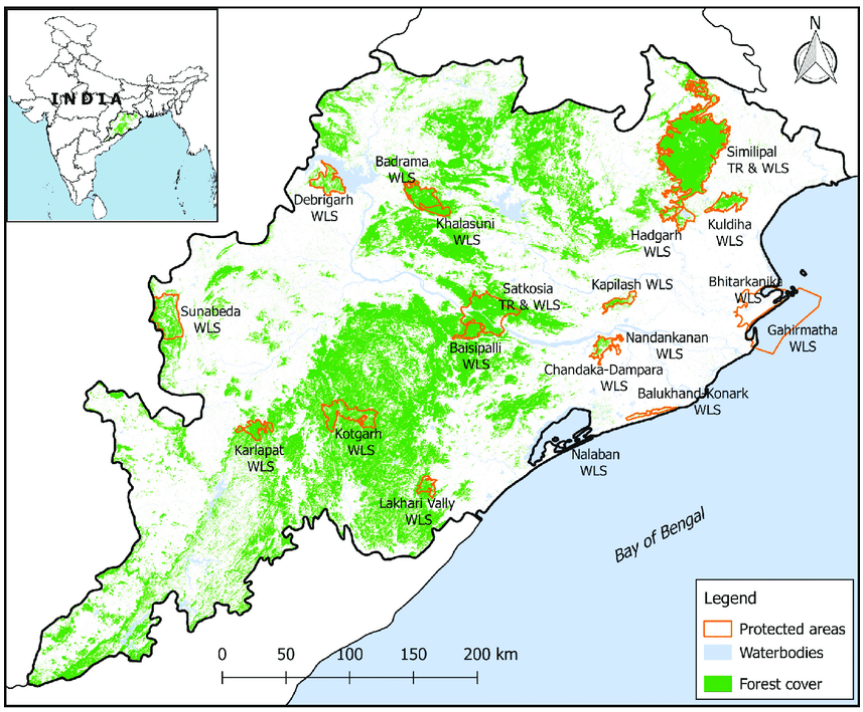

Figure 1: Coastal Districts of Odisha (after Inspired Pencil, 2023)

Silicon: Characteristics And Distribution

1. Forms of Silicon in Nature

A. Silica (SiO_2 - Silicon Dioxide)

Most common natural form of silicon. Found in quartz, sand and flint. Present in:

Quartz crystals (pure silica)

Silica sand (desert sands, beaches, riverbeds)

Opal (hydrated silica)

Chert and flint (microcrystalline silica)

Diatomaceous earth (fossilized diatoms rich in silica) (Rimstidt, 2014)

B. Silicates (SiO_4-based Minerals)

Most abundant form of silicon on Earth. Found in igneous, metamorphic and sedimentary rocks. Silicate minerals make up more than 90% of the Earth's crust (Deer et al. 2013).

Major types:

Feldspar (most abundant silicate mineral)

Mica (biotite, muscovite)

Amphibole & Pyroxene (in volcanic rocks)

Olivine (found in basalt and peridotite)

Clay minerals (kaolinite, montmorillonite) (Bergna and Roberts, 2005)

C. Native Silicon (Rare)

Found in meteorites and in trace amounts in Earth's crust.

Native silicon deposits have been reported in volcanic rocks (Klein and Dutrow, 2007).

D. Silicon in Biological Systems

Silicon is essential for plant growth, especially for species like rice and wheat.

Found in bamboo, horsetail plants and diatoms (microscopic algae with silica shells).

Present in human and animal tissues (bones, skin, cartilage) (Parks, 1990).

2. Major Geological Occurrences of Silicon

Silicon is widely distributed across different geological environments (Linsay, 1979; Goldschmidt, 1954: U. S. Geological Survey, 2022):

Quartz-rich Rocks: Found in granite, sandstone and quartzite.

Volcanic Rocks: Silicon occurs in basalt, obsidian and rhyolite.

Deserts & Beaches: Large reserves of silica sand in the Sahara, Atacama and Australian deserts.

River Systems: Rivers like the Amazon, Mississippi and Ganges carry silica-rich sediments (Moson and Moore, 1982).

History Of Silicon

Silicon has a fascinating history that spans from its early discovery to its crucial role in modern technology. Here's a brief overview:

Early Discovery and Naming (19th Century)

- 1787: French chemist Antoine Lavoisier first theorized the existence of silicon but did not isolate it.
- 1824: Swedish chemist Jöns Jacob Berzelius successfully isolated amorphous silicon by heating potassium fluorosilicate with potassium.
- 1831: Scottish chemist Thomas Thomson named the element "silicon, " combining the Latin word "silex" (meaning flint) with "-on" to align with other non-metals (Lojek, 2007).

Development of Pure Silicon (19th - 20th Century)

- 1854: French chemist Henri Sainte-Claire Deville improved silicon purification methods.
- 1900s: Further research led to the development of more refined forms of silicon, important for industrial applications.

Silicon in Electronics (20th Century)

- 1941: Russell Ohl, an engineer at Bell Labs, discovered the p-n junction in silicon, a key component for semiconductor devices (Ohl, 1941).
- 1947: The first transistor, made from germanium, was invented by John Bardeen, William Shockley and Walter Brattain (Bardeen et al. 1948).
- 1954: Texas Instruments built the first silicon transistor, replacing germanium and leading to more efficient electronic components (Sze and Ng, 2006).
- 1958: Jack Kilby of Texas Instruments developed the first integrated circuit (IC), marking the beginning of the microelectronics revolution (Kilby, 1958)

Silicon Extraction Method

Extraction of Silicon from beach sand by magnesiothermic reaction was successfully attempted (Li et al. 2017).

The magnesiothermic reduction process is an effective method for extracting high-purity silicon from silica-rich materials such as beach sand, quartz or diatomaceous earth. This method involves reducing silicon dioxide (SiO_2) using magnesium (Mg) as a reducing agent at elevated temperatures (Cheng et al. 2016; Gao et al. 2013).

Chemical Reaction

The magnesiothermic reaction follows this fundamental equation (Bao et al. 2021):

$SiO2 + 2Mg \rightarrow Si + 2MgO$

In this reaction:

Silicon dioxide (SiO_2) from beach sand is reduced by magnesium.

Magnesium oxide (MgO) is formed as a by-product.

The silicon obtained is often porous and requires further purification.

Magnesiothermic Reduction

The purified silica sand is mixed with fine magnesium powder in a stoichiometric ratio for reaction in a Furnace. The mixture is placed in an inert atmosphere (argon or vacuum) to prevent unwanted reactions. It is heated to 650–850°C for several hours to allow the reduction reaction to take place

Formation of Porous Silicon, the reaction produces silicon (Si) and magnesium oxide (MgO) as a byproduct. The silicon formed is usually amorphous or nanocrystalline (Jeon et al. 2019).

Figure 2: Silica sand and heay mineral deposited on Chilika Lake, Odisha.

Advantages of Magnesiothermic Reduction:

It is energy-efficient compared to traditional carbothermal reduction (which requires temperatures>2000°C). This method is environmentally friendly, as it does not require carbon-based reduction (avoiding CO_2 emissions).

Magnesiothermic reduction presents an energy-efficient, scalable solution suitable for decentralized production in coastal regions. Its relatively mild process conditions make it particularly appealing for processing Indian beach sands.

Figure 3: Silica sand of the Puri Beach, Odisha.

Environmental Considerations

Unregulated sand mining has already led to significant environmental degradation along India's coastline, including beach erosion, loss of biodiversity and disruption of coastal ecosystems (UNEP, 2019). Sustainable silicon extraction from beach sands will require:

- Regulated extraction volumes to maintain sediment balance.
- Monitoring of impacts on coastal ecosystems and local livelihoods.
- Post-extraction rehabilitation through habitat restoration and sand replenishment.
- Development of closed-loop processing systems to minimize waste and energy consumption.

Economic And Technological Potential

India possesses extensive reserves of beach sand rich in silica (SiO_2), particularly along its eastern and western coastlines. Extracting silicon from these sands holds substantial economic potential.

India's demand for silicon is growing due to the rise of domestic solar energy installations, semiconductor manufacturing under the "Make in India" initiative and increasing exports of advanced materials (Kumar et al. 2021). By leveraging domestic coastal resources, India can:

- Reduce dependence on imported silicon.
- Create new employment opportunities in coastal regions.
- Promote research and development in sustainable silicon extraction.

Odisha, with its high-purity beach sands and proximity to industrial hubs, could become a huge centre for silicon extraction and processing. Another important mineral resource for this mineral rich state.

Countries Exporting Silicon to India

Despite its natural reserves, India currently imports almost all of its silicon requirements. In the first half of 2024, India's silicon imports increased by 14% year-on-year, totaling 45, 665 tonnes, up from 40, 220 tonnes in the same period in 2023. The primary countries exporting silicon to India during this period include:

China: Dominates India's silicon imports, accounting for approximately 90% of the total imports. In H1 2024, imports from China surged by 27%, reaching 40, 787 tonnes. (BigMint, 2024)

Malaysia: Supplied 2, 940 tonnes in H1 2024, marking a 50% decrease compared to the previous year.

Norway: Exported 621 tonnes to India in the same period.

Angola: Entered the market with 284 tonnes of silicon exports to India in H1 2024.

Other countries collectively contribute 1, 031 tonnes, a slight decrease from 1, 125 tonnes in the corresponding period of the previous year.

Discussion And Conclusions

1. Our study indicates that there is a huge potential for exploration and exploitation of Silicon rich silica minerals in India.
2. Presently, almost all the Silicon requirement of the country is being met by import.
3. It is believed that a national level mission is to be drawn in the field of Silicon element extraction from different parts of the country as rocks containing them occur in Himalayas and in Peninsular India, besides rich silica sand deposits in the Gangetic plain as well as coastal regions of the country.
4. Innovative technologies in the field can certainly start the production at the national level with the government's support.
5. Coastal regions show a huge deposit of Silica rich sand, where using sustainable technology with proper consideration of environmental issues would certainly give rise to boost for small scale industries which would provide not only employment opportunities but would also generate fiscal alternative to states economy.
6. The coast of Odisha has the maximum potential to develop Silicon extraction industrial hub as beach sand is of very high-quality quartz and occurs in accessible terrain of the coast.
7. In the national mission of the hon'ble prime minister, it would be appropriate that innovation and resource generation for the "Atmanirbhar Bharat" is the clarion call for scientists so that the five trillion-dollar economy is achieved as per the plan.

Acknowledgements

Authors are thankful to Prof. Dhruv Sen Singh, the Head of the Department of Geology, University of Lucknow, Lucknow for providing the working facilities of the department for the present contribution. They are also thankful to CST, Uttar Pradesh for the project funding in which silicon extraction from domestic resources is the main theme. Authors are also thankful to Prof. Rosalin Das, Head of Department of Geology, Fakir Mohan University for providing an opportunity to present this paper at the International Conference on "Coastal Dynamics: Geology, Economy and Environment" held at Balasor between 8th -10th January 2025.

References

- Bao, L., Wang, T., Shen, X., & Zhang, L. (2021) Magnesiothermic reduction of silica for silicon production: A review. Journal of Materials Science 56, 11215–11231.
- Bardeen, J., Brattain, W. H., & Shockley, W. (1948). Three-electrode circuit element utilizing semiconductive materials. U. S. Patent No. 2, 524, 035.
- Bergna, H. E., & Roberts, W. O. (2005). Colloidal silica: Fundamentals and applications. CRC Press.
- BigMint. (2024). India's silicon imports up 14% in H1CY24, volumes from China dominate. Retrieved from https://www. bigmint. co/insights/detail/indias-silicon-imports-up-14-in-h1cy24-volumes-from-china-dominate-575617
- Cheng, X., Li, M., & Zhao, X. (2016). Magnesiothermic reduction of silica to silicon: A review on reaction mechanisms and synthesis strategies. Journal of Materials Chemistry A, 4(5), 1751-1766. https://doi. org/10. 1039/C5TA09415A
- Deer, W. A., Howie, R. A., & Zussman, J. (2013). An introduction to the rock-forming minerals (3rd ed.). Mineralogical Society of Great Britain and Ireland.
- Gao, X., Wu, H., & Lou, X. W. (2013). Nanostructured silicon materials: Synthesis, properties, and applications in batteries. Advanced Materials, 25(15), 215-230. https://doi. org/10. 1002/adma. 201204506
- Goldschmidt, V. M. (1954). Geochemistry. Clarendon Press.
- Green, M. A. (2020) Silicon Solar Cells: Advanced Principles & Practice. UNSW.
- Indian Rare Earths Limited (IREL). (n. d.). OSCOM – Odisha Sand Complex. Retrieved from https://www. irel. co. in/oscom
- Inspired Pencil. (2023). Odisha geographical map. Retrieved from https://ar. inspiredpencil. com/pictures-2023/odisha-geographical-map
- Jeon, J. H., Park, J., & Choi, Y. M. (2019). Extraction of nano-silicon from natural sand via magnesiothermic reduction. Journal of Alloys and Compounds, 786, 492-500. https://doi. org/10. 1016/j. jallcom. 2019. 01. 368
- Kilby, J. S. (1958). Miniaturized electronic circuits. U. S. Patent No. 3, 138, 743.
- Klein, C., & Dutrow, B. (2007). Manual of mineral science (23rd ed.). Wiley.
- Kumar, R. et al. (2021) Heavy minerals and silica in Indian beach sands: Distribution and economic potential. Indian Journal of Geology 62, 91–102.
- Lindsay, J. W. (1979). The occurrence and uses of silica sand deposits in the United States. U. S. Geological Survey Bulletin, 21(2), 45-67.
- Li, W., Liao, J., & Wang, C. (2017). Magnesiothermic reduction synthesis of porous silicon from beach sand and its application in lithium-ion batteries. Electrochimica Acta, 258, 1102-1110. https://doi. org/10. 1016/j. electacta. 2017. 11. 021

- Lojek, B. (2007). History of semiconductor engineering. Springer.
- Mason, B., & Moore, C. B. (1982). Principles of geochemistry (4th ed.). Wiley.
- Moneycontrol. (2018, January 11). IDCOL, IREL form joint venture for beach sand mining in Odisha. Retrieved from https://www. moneycontrol. com/news/india/idcol-irel-forms-joint-venture-for-beach-sand-mining-in-odisha-2450359. html
- Odisha Minerals Department. (n. d.). Geology and mineral resources of Odisha. Retrieved from https://www.odishaminerals.gov.in/Download/geology_mineral_resources_orissa. pdf
- Ohl, R. S. (1941). Light-sensitive electric device. U. S. Patent No. 2, 402, 662.
- Parks, G. A. (1990). Surface energy and adsorption at mineral-water interfaces. Reviews in Mineralogy and Geochemistry, 23(1), 133-175.
- Park, C., Lee, J., & Lee, H. (2015). Controlled magnesiothermic reduction of silica for porous silicon anodes in lithium-ion batteries. Scientific Reports, 5, 9817.
- Rimstidt, J. D. (2014). Silica mineralogy and chemistry. Elements, 10(3), 183-188.
- Riordan, M., & Hoddeson, L. (1997). Crystal fire: The birth of the information age. W. W. Norton & Company.
- Sze, S. M. & Ng, K. K. (2006) Physics of Semiconductor Devices. Wiley.
- UNEP. Sand and Sustainability: Finding New Solutions for Environmental Governance of Global Sand Resources. United Nations Environment Programme(2019)
- U. S. Geological Survey. (2022). Mineral commodity summaries: Silicon. Retrieved from https://www. usgs. gov

Coastal Vulnerability to Natural Disasters: The Smart Solution

Vibhuti Rai[1] and Namrata Singh[2]

1. Department of Geology, University of Lucknow, Lucknow 226007
2. Department of Chemistry, University of Lucknow, Lucknow 226007

Email: vibhutirai@gmail. com

Abstract

Coastal vulnerability to natural disasters is a critical issue for the sake of life and properties of the habitants of the area. The length and breadth of these disasters also affect the economy of the region as huge resource is required to safe-guard the infrastructures besides mobilizing manpower to protect the affected people and livestock. Post disaster scenario is always full of anguish and anxiety as people lose their belongings, houses and businesses.

In the light of above situation, we herewith suggest a "Smart Solution" as a preventive measure where previous data sets of various aspects would be put to Artificial Intelligence related tools and softwares to generate a viable and effective solution in order to safe-guard the life and property well in advance. This Artificial Intelligence (AI) Technology works very fast as it is based on Data patterns from millions of data sets. For differently affected regions, specific solutions could be found at the click of button.

Smart Solutions require well developed data sources from multifaceted streams hence a national level disaster mitigation centre would be needed to process data and distribute it as quickly as possible to the affected area through relief distribution systems (Vitousek et al. 2023).

Key words: Coastal disaster, solution,

Introduction

Amongst the most common natural disasters of the world, the disasters in the coastal area is probably the most rampant. The vulnerability of the coast where one side is the land and the other side being the ocean is a geomorphological setting which needs to be understood in terms of distribution of settlements, agricultural lands, habitats and infrastructure. In India, almost the entire coastal area is prone to many of the above-mentioned disasters barring earthquakes as the east coast and the west coast is made up of passive continental margin. Although the coast line occurs inside the Indian continent, the continental margins fall far away from the coast hence providing a regionally

distinctive sub oceanic terrain in which the distance from the coast line and the continental margin varies along the entire length of the Indian coast.

On an average, every year the Indian ocean side and the Bay of Bengal side are stuck by cyclones prominently in the Bay of Bengal region. Thereby affecting the life and settlements of the coastal areas in which huge amount of losses are incurred in terms of fiscal loss to the government and people in general (Das and Vincent, 2009). Since this situation is continuing every year, it is the right time to assess the situation where newer technologies are available within the country to provide a solution (Hossen and Yigitcanlar, 2021).

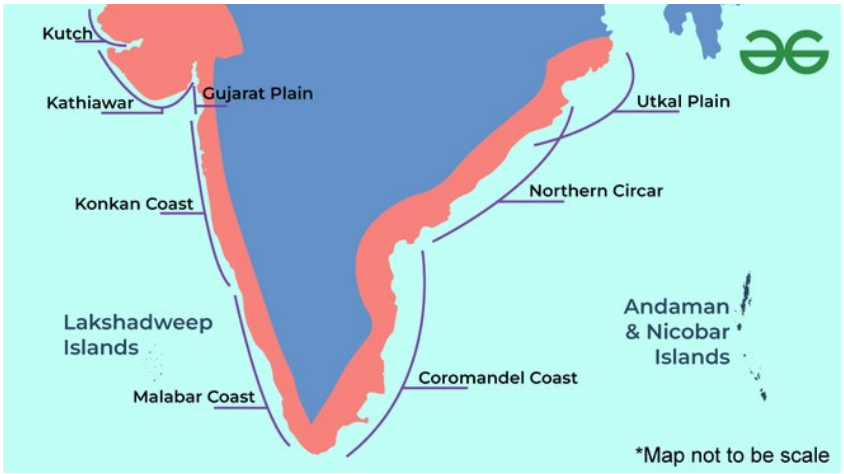

Figure. 1: Map showing distinctive coastline of India with specific coastal features (after GeeksforGeeks, n. d.)

Types Of Disasters

The key natural disasters are related to cyclones, typhoons, tsunamis, earthquakes, tides and hurricanes. Many of these can be inter-related too. Some of these can be geographically confined to restricted regions. Hence different areas of the world would require specific evaluation for their disaster issues (Bryant, 2008).

In India, coastal areas are particularly vulnerable to a range of natural disasters, including cyclones, typhoons, tsunamis, earthquakes, tidal surges, and hurricanes. These disasters often have interconnected impacts, and their severity can vary depending on the region. Cyclones and hurricanes frequently affect the eastern and western coasts of India, while tsunamis, particularly in regions like the Andaman and Nicobar Islands (Srinivasan and Gupta, 2018), pose a significant threat to coastal populations. Earthquakes can also lead to tsunamis in the Indian Ocean, amplifying the damage along the coast (Mileti, 1999).

These disasters may be geographically concentrated but can have widespread impacts. For instance, cyclones often hit the Bay of Bengal and Arabian Sea, while the western coast faces the brunt of monsoon-induced tidal surges. Similarly, earthquakes along the

Indian subcontinent, particularly near the Himalayan and Indo-Burmese regions, can trigger tsunamis affecting coastal regions (IMD, 2020 ; NDMA, 2019).

India's diverse coastal geography requires a nuanced approach to disaster management. Different regions face unique risks, and thus, targeted disaster evaluation and mitigation strategies are essential. A National Disaster Mitigation Centre would be crucial for processing real-time data from various sources to effectively address the specific vulnerabilities of India's coastal zones. This would ensure the swift distribution of relief and help minimize the devastating impact of such natural calamities. By integrating data from multiple streams, this center can enhance the country's preparedness and response systems, ultimately safeguarding lives and property in coastal areas.

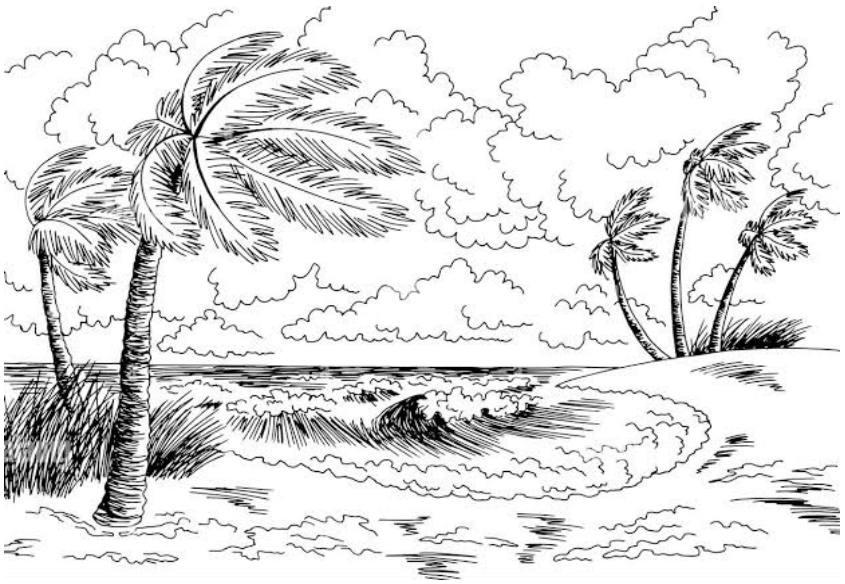

Figure 2: Coastal storm disaster sketch showing impact of big wind (after Alamy, n. d.)

Modern Day Technologies for Monitoring Coastal Disasters

1. Satellite Data

Satellites play a crucial role in monitoring coastal disasters by providing real-time images and data on weather patterns, sea levels and coastal erosion. They help track hurricanes, tsunamis and floods, offering early warning signs to minimize damage (Khan et al. 2020).

2. Remote Sensing

Remote sensing technology, including satellite imagery and aerial photography, allows scientists to observe and analyse coastal regions from a distance. It helps in detecting changes in sea surface temperature, wave patterns and land shifts which are essential for disaster prediction and management (Martino et al. 2009; Toth and Jozkow, 2016).

3. WSN (Wireless Sensor Network)

Wireless sensor networks consist of interconnected sensors placed in coastal areas to collect data on environmental conditions like temperature, humidity and water levels. These networks provide real-time monitoring and help in early detection of potential disasters such as storms and tsunamis.

4. Mobile Ad Hoc Network

Mobile Ad Hoc Networks (MANETs) are decentralized wireless networks used in disaster-prone areas where traditional communication infrastructure may be damaged. They enable emergency response teams to communicate effectively and share critical information during coastal disasters.

5. Artificial Intelligence (AI)

AI is revolutionizing disaster management by analysing vast amounts of data to predict potential coastal disasters. AI-powered models can process meteorological data, track storm development and provide real-time alerts to authorities and communities at risk.

6. Fuzzy Logic

Fuzzy logic helps in decision-making during uncertain conditions by processing imprecise or incomplete data. In coastal disaster monitoring, it is used for risk assessment, predicting flood levels and making real-time decisions for emergency response.

7. Unmanned Aerial Vehicles (UAVs)

Drones or UAVs are used for aerial surveys of coastal regions before, during and after disasters. They provide high-resolution images and videos, assess damage and assist in search-and-rescue operations without putting human lives at risk.

8. Big Data Analytics

Big Data Analytics processes massive amounts of historical and real-time data to identify disaster patterns and trends. It helps in forecasting coastal hazards, improving preparedness strategies and optimizing disaster response efforts (Abdalzaher et al. 2024).

9. Machine Learning

Machine learning algorithms analyse past disaster data and environmental factors to make accurate predictions about future coastal events. They enhance early warning systems, improve risk assessments and assist in planning effective mitigation measures.

These technologies, when combined, provide a comprehensive approach to monitoring and mitigating coastal disasters, ultimately reducing loss of life and property.

Data Collection

A centralized national-level center would be responsible for collecting, processing, and disseminating disaster-related data. The center would:

- Collaborate with meteorological agencies, geological departments and research institutions to gather multifaceted data.
- Utilize AI-powered tools to assess vulnerabilities and develop region-specific disaster preparedness plans.
- Disseminate real-time alerts and guidance through digital communication channels, ensuring swift action (Kesavan and Swaminathan, 2006).

Several countries have successfully implemented AI-based disaster mitigation strategies:

- Japan: AI-driven earthquake prediction models have improved early warning systems.
- United States: AI tools assist in hurricane tracking and emergency response planning.
- India: AI-based flood prediction systems have helped mitigate monsoon-related damage (IndiaTimes, 2021).

Smart Solution Through Artificial Intelligence (AI)

We herewith propose that an integrated approach for short-term and long-term redressal is required in the light of global climatic impact such as sea level changes as well as assessment of detailed coastal geomorphology utilizing spatially explicit information using GIS-based mapping (Kesavan and Swaminathan, 2006). Demarcating detailed coastal ecosystem for ecologically sensitive areas such as habitats of mud flats, salt marshes, mangroves, coastal grasslands, beach regions, tidal flats, estuaries, coastal lakes, rocky coasts, sand dunes, nesting sites of birds and turtles, and related ecologically sensitive areas required for that.

We also propose that the newer technologies such as space-derived data (remotely sensed) alongside the sounding data for a detailed understanding of depth profile off the coast, with the distribution of human habitats such as townships, cities, industries, agricultural lands, infrastructures such as roads and railways, water bodies etc. needs to be integrated with the data from the past occurrences of natural disasters vis-a-vis meteorological data and the extent of these disasters to be incorporated in developing a databased Integrated Management System. It would be worthwhile that all the above information can be modelled using Artificial Intelligence for the prediction and management of disaster-prone areas in order to provide a viable solution which we can call as the “Smart Solutions”.

Since Natural disaster cannot be stopped to happen, their mitigation is only possible if ample preparedness is put into operation where action can be initiated at the speed of light (pun intended), something similar to fire brigade where that becomes operational within seconds of getting information.

Discussions

- Natural Disasters are the most damaging events of nature as they leave large-scale impacts in the affected areas.
- Some of these natural disasters are almost instantaneous, like earthquakes and some leave a trail where there is a time gap from their initiation to the actual impact.
- Different parts of the coastal area represent different types of geomorphic settings including the setting beneath the sea in the vicinity of the coast.
- On account of historical reasons, the world's biggest cities have been inhabited for hundreds to thousands of years in the coastal areas. Therefore, the natural impact of these disasters affects these huge cities by impacting their economy and industrial devastation.
- On a conventional level, in the last hundred years only post-disaster relief was given to the affected masses without planning for the mitigation and minimizing the impact.
- In recent years, several new technologies have emerged, particularly space technology, aimed at minimizing the impact of natural disasters.
- In the current scenario, additional digital technologies, such as artificial intelligence (AI), which work on the basis of algorithms, can predict impending disasters by analysing and overlapping different data sets to generate patterns. This provides sufficient information in advance, allowing preventive measures to be taken through the early warning system (EWS) to safeguard the well-being of the masses.
- Artificial intelligence (AI) has lately spread its wings to provide solutions by managing millions to billions of data to generate a pattern for its futuristic impact. This multilayer data considers each and every element to provide specific results depending on the terrain, the type of disaster and time when the disaster would happen, that allows the administration to take the preventing measures so that minimum loss is there.
- We can certainly say that AI is one of the most forward-looking technologies in the field of disaster management in a sustainable way and should be part of the early warning system across the globe.

Acknowledgements

Authors are thankful to Prof. Dhruv Sen Singh, the Head of the Department of Geology, University of Lucknow, Lucknow for providing the working facilities of the department for the present contribution. They are also thankful to CST, Uttar Pradesh for the project funding to VR during which coastal sands were analyzed for Silicon resources.

References

- Abdalzaher, M. S., Krichen, M., & Falcone, F. (2024). Emerging technologies and supporting tools for earthquake disaster management: A perspective, challenges, and future directions. Progress in Disaster Science.
- Alamy. (n. d.). Sea coast storm graphic beach black white landscape sketch illustration vector. Alamy. https://www. alamy. com/sea-coast-storm-graphic-beach-black-white-landscape-sketch-illustration-vector-image366095637. html
- Bryant, E. (2008). Tsunami: The underrated hazard (2nd ed.). Springer.
- Das, S., & Vincent, J. R. (2009). Mangroves protected villages and reduced death toll during Indian super cyclone. Proceedings of the National Academy of Sciences, 106(18), 7357-7360. https://doi. org/10. 1073/pnas. 0810440106
- GeeksforGeeks. (n. d.). Coastal plains of India. Retrieved March 21, 2025, from https://www. geeksforgeeks. org/coastal-plains-of-india/
- Goodchild, M. F. (2007). Citizens as sensors: The world of volunteered geography. GeoJournal, 69(4), 211-221. https://doi. org/10. 1007/s10708-007-9111-y
- Hossen, M. A., & Yigitcanlar, T. (2021). Toward artificial intelligence in emergency management: A systematic literature review. Technological Forecasting and Social Change, 173, 121186. https://doi. org/10. 1016/j. techfore. 2021. 121186
- Indian Meteorological Department (IMD). (2020). Cyclones and their impacts on coastal regions in India. Retrieved from https://www. imd. gov. in
- IndiaTimes. (2021, October 7). Google's AI-based flood forecasting system is saving lives in India: Here's how. Retrieved March 21, 2025, from https://www. indiatimes. com/technology/news/google-ai-based-flood-forecasting-india-553906. html
- Kesavan, P. C., & Swaminathan, M. S. (2006). Managing extreme natural disasters in coastal areas. Philosophical Transactions of the Royal Society A: Mathematical, Physical and Engineering Sciences, 364(1845), 2191–2216. https://doi. org/10. 1098/rsta. 2006. 1822
- Khan, A., Gupta, S., & Gupta, S. K. (2020). Multi-hazard disaster studies: Monitoring, detection, recovery, and management, based on emerging technologies and optimal techniques. International Journal of Disaster Risk Reduction, 46, 101642. https://doi. org/10. 1016/j. ijdrr. 2020. 101642

- Martino, L., Ulivieri, C., Jahjah, M., & Loret, E. (2009). Remote sensing and GIS techniques for natural disaster monitoring. In Olla, P. (Ed.), Space technologies for the benefit of human society and Earth (pp. 279-296). Springer. https://doi. org/10. 1007/978-1-4020-9573-3_14
- Mileti, D. S. (1999). Disasters by design: A reassessment of natural hazards in the United States. Joseph Henry Press.
- National Disaster Management Authority (NDMA). (2019). Disaster management in coastal regions: A comprehensive guide. Government of India. Retrieved from https://www. ndma. gov. in
- Srinivasan, R., & Gupta, R. (2018). Tsunami preparedness in India: A case study of the Andaman and Nicobar Islands. Journal of Disaster Risk Reduction, 30, 212-224. https://doi. org/10. 1016/j. jdr. 2018. 02. 006
- Toth, C., & Jóźków, G. (2016). Remote sensing platforms and sensors: A survey. ISPRS Journal of Photogrammetry and Remote Sensing, 115, 22-36. https://doi. org/10. 1016/j. isprsjprs. 2015. 10. 004
- Vitousek, S., Buscombe, D., Vos, K., Barnard, P. L., Ritchie, A. C., & Warrick, J. A. (2023). The future of coastal monitoring through satellite remote sensing. Cambridge Prisms: Coastal Futures, 1, e10, 1–18. https://doi. org/10. 1017/cft. 2022. 4

Spatio-temporal mapping and characterization of Turbidity Maximum Zone (TMZ) of Dhamra estuary, India

Pankajini Mahanta*

P. G Department of Geology, Fakir Mohan University, Balasore

Email*- positivepankajini@gmail.com

Abstract:

The turbidity maximum zone (TMZ) is the dynamic high turbid water zone within a macro-tidal estuary. It contains significantly higher suspended solid concentrations than landward and seawards, and is a special phenomenon of suspended sediment movement and migration in estuaries worldwide. TMZ forms at the interface between riverine and ocean environments, where the transport of suspended solids is complex. The interaction of fresh water input and tidal activity leads to an increased residence time of terrestrial fine sediments resulting in formation of TMZ. Numerous processes impact its formation, structure, and movement. The dynamic changes and spatio-temporal distributions of TMZs have a profound and widespread impact on the development and evolution of sandbars, shoals, channels, and estuary morphology. In addition, TMZs significantly affect the physical, and biogeochemical processes occurring at estuarine environments. TMZ possess many threats to the surrounding ecology, water quality and economy. It is responsible for strong siltation rates near harbors or other infrastructure, necessitating regular dredging. TMZ study is the cynosure for scientific and engineering innovations among researchers, communities, engineering corporations, and government agencies. Dhamra estuary located at the confluence point of river Baitarani and Brahmani, one of the most dynamic macrotidal estuary present near the Gahiramatha sanctuary, a nesting site for olive ridley sea turtles is still least understood. Siltation problem of Dhamra estuary near Dhamra port is quite significant resulting in formation of new islands. TMZ can provide a way to understand the underlying causes behind rapid growth of island in this zone. Huge time series data is necessary to track the movement of TMZ over different time periods and varied seasons. Field observations in estuary region are notoriously hazardous, time consuming & expensive, and are also restricted to certain time periods or geographical locations. As TMZ is highly dynamic in nature, station or field data alone is not sufficient for monitoring its movement. Consequently, coupling of field and satellite observations is necessary for obtaining Total Suspended Sediment (TSS), Chl-a and TMZ variation over time. Band ratioing coupled with thresholding

successfully used for Chl-a retrieval and TMZ zone mapping using multi-sensor data in Google Earth Engine and Arc GIS platform.

Keywords: Remote Sensing, Maximum Turbidity Zone, Sentinel-2, NDTI, GEE

1. **Introduction:**

Turbidity represents the level of suspended sediments in water indicating water clarity or how clear is the water (Dewantoro et al., 2024). The trapping of suspended particles in river estuaries can often lead to the formation of highly turbid concentrations, sometimes culminating in the generation of a turbidity maximum zone (TMZ). In coastal waters, estuaries are complex environments where dissolved and particulate matter, drained by rivers in upland basins, are mixed with marine water and substances. Because of the tidal asymmetry and residual density circulation, a turbidity maximum zone is generally formed in macrotidal estuaries where most of the suspended particles are trapped (Allen et al., 1977; Arman and Daming, 2023). TMZ in an estuary commonly occurs near the upstream limits of the salinity intrusion and can be the result of the combined effects of density-driven residual circulation, tidal dynamics and erosion and deposition of fine sediments (Abascal-Zorrilla et al., 2020).

The TMZ plays an important role in biological productivity and sedimentary processes and can be a significant source of fine-grained sediment supply within and outside the boundaries of estuaries (Abascal-Zorrilla et al., 2020; Van Santen et al., 2007; Willemsen et al., 2016). Tropical rivers located between 30° N and 30° S contributes more fine-grained sediment to their estuaries than mid latitude rivers owing to high degree of chemical weathering and degree of alteration in tropics. Such tropical estuaries are commonly bordered by mangroves that trap sediment sand affect flushing rates (Wolanski, 1992; Simpson et al., 1997) thus contributing to the dynamics of the TMZ. Unfortunately, studies dealing with the TMZ in tropical estuaries are relatively scarce when compared to those devoted to the study of estuarine hydrodynamics (Abascal-Zorrilla et al., 2020). Turbidity is an expression of the light-scattering property of water caused by the presence of fine suspended matter such as clay, silt, plankton, and other microscopic organisms. The degree of scattering depends on the amount, size and composition of the suspended matter. Turbidity refers to the decreased ability of water to transmit light caused by suspended particulate matter (Boyd, 2000). Turbidity is one of the indicators of water quality and ecologically important parameter because it is associated with a light limitation for phytoplankton growth. Turbidity distribution can also be used to identify and interpret geomorphological and hydrological processes, such as sediment transport, deposition and resuspension. Identification of the source and spatial distribution of suspended matters, can help deducing relevant spatial information about the essential nutrients availability in the primary production of coastal waters. The linkage is characterized as a nutrient flow and the reduction of light penetration into the

water (Amran and Daming, 2023; Ouillon et al., 2004). Turbidity may endanger fish and other marine organisms by reducing food supplies, destroying spawning areas, and affecting the ability of fish gills to absorb dissolved oxygen. In estuarine waters with high turbidity, dissolved oxygen concentrations can decrease dramatically, which can lead to decline of marine organisms (Quang et al., 2017).

Conventional way of turbidity monitoring requires a large number of in-situ measurement points that are demanding both in time and cost. In addition, traditional methods are constrained by poor spatial and temporal scopes. Alternatively, continuous measurement strategies using point locations with data-loggers can overcome temporal variations in water turbidity at designated locations, but fail to provide synoptic representations of water dynamics. Effective mapping and monitoring of water quality in coastal environments is very difficult due to temporal and spatial variations. Many investigators have been limited by the inability to review a large coastal area as a whole at the same time so that mapping has to be done by relying on data from a series of sampling stations and then interpolating parameter values between stations or extrapolating to a wider area than the coverage of the station distribution. In recent years, marine remote sensing techniques has become a useful tool for mapping turbidity at coastal waters. The advantage of using remote sensing for water quality analysis is its ability to obtain synoptic data from the entire study area to produce continuous surface data, can shows detailed spatial variability and periodically. The use of remote sensing technology for monitoring water quality has been carried out by several researchers, and is proven to be a cost-effective method with acceptable accuracy

(Brezonik et al., 2007; Wu et al., 2015; Hu et al., 2016). The studies were to formulate the method of obtaining the quantity of water quality parameters from various sensors (Liu et al., 2003; Islam et al., 2007; Lihan et al., 2008), that show a similarity in the relationship between water quality parameters and remote sensing data, but the relationship is concluded to be locally specific (Liu et al., 2003; Sravanthi et al., 2013). Satellite remote sensing can be used to study the spatiotemporal variations of surface turbidity, and satellite-derived turbidity maps are useful tools for studying the effect of turbidity especially in shallow waters (Dogliotti et al., 2015; Quang et al., 2017). Turbidity mapping and other water quality parameters have been conducted using data from wide-swath ocean color instruments such as SeaWiFS, Aqua/MODIS and ENVISAT/MERIS medium resolution images. For small or narrow areas, however, these satellites give low precision estimates resulting mismatched because of their low spatial resolution causes many mixed pixels (Dewantoro et al., 2024). For this reason, we have selected Sentinel-2 imagery which has a higher spatial resolution of 10 m. Sentinel-2 has been successfully utilized to map turbidity patterns in water body by several researcher including Sebastiá-Frasquet et al. (2019), Arman and Daming (2013), Lizcano-Sandoval et al. (2022) and Dewantoro et al., 2024. Sentinel-2 consists of a pair

of satellites that are part of the European Union's Copernicus Program for observations of the Earth's surface. To cover the full surface of the Earth every 3–5 days, Sentinel-2A and Sentinel-2B are in the same orbit but 180 degrees apart. Sentinel-2 data is categorized according to pre-processing level. Level-0, Level-1A, and Level-1B data are primarily composed of unprocessed raw satellite data. Surface reflectance detected at the top of the atmosphere is categorized as Level-1C. Level-2A is the bottom of atmosphere reflectance is created by applying the Sen2Cor algorithm to Level-1C (Obregón et al., 2019). The best data for research purposes is Level-2A since it enables extra analysis without requiring more atmospheric corrections. Studies on turbidity distribution using remote sensing technology have been done mostly follow semi-analytic or empirical models that correlate between remote sensing reflectance with field turbidity (Ouillon et al., 2008; Doxaran et al., 2006; Doxaran et al., 2009; Petus et al., 2010; Vanhellemont & Ruddick, 2014; Dogliotti et al., 2015; Zhang et al., 2016; Chang et al., 2022). Ouma et al. (2020) have used Sentinel-2 (level-1C) to model the relationship between reflectance and turbidity of inland water reservoir. Estimation of turbidity using Sentinel-2 (level-1C) data has also been used by Katlane et al. (2020) in the Gulf of Gabes, Tunisia.

This study aims to create a model to estimate coastal waters turbidity using Sentinel-2A, surface reflectance product. An efficient characterization and mapping of the estuarine turbidity maximum zone (TMZ) is important for studying terrestrial hydrological processes (Wang et al., 2021). Although many studies relevant to the TMZ have been conducted worldwide, the extraction methods and criteria used to describe the TMZ vary significantly both spatially and temporally. The present chapter aims at (i) mapping the spatio-temporal variation and (ii) analyzing the seasonal (winter, pre monsoon, monsoon and post monsoon) and annual variation (from 2018 to 2025) of TMZ in macro-tidal estuary Dhamra using integrated Google Earth Engine and GIS based approach.

2. Study area:

The present study area Dhamra estuary is formed at the confluence of the Brahmani and Baitarani rivers is located to south of the town of Chandabali. It lies in the Bhadrak district and empties into the Bay of Bengal. To the north of its mouth is the Dhamra Port and near the mouth is the Gahiramatha sanctuary, a nesting site for olive ridley sea turtles. The Dhamra estuary forms an important component of the Bhitara Kanika marine sanctuary on the Eastern coast of India, covered with mangroves, a kind of endemic vegetation which provides breeding and spawning grounds of varieties of marine life forms. The river's mouth is as wide as 4 kilometres (2. 5 mi), and it enters the sea through two distinct river channels separated by an island formation called Kalibhanja. The two channels are further separated by another island formation in the sea called Kanika Sands which is approximately 8 kilometres (5 mi) wide.

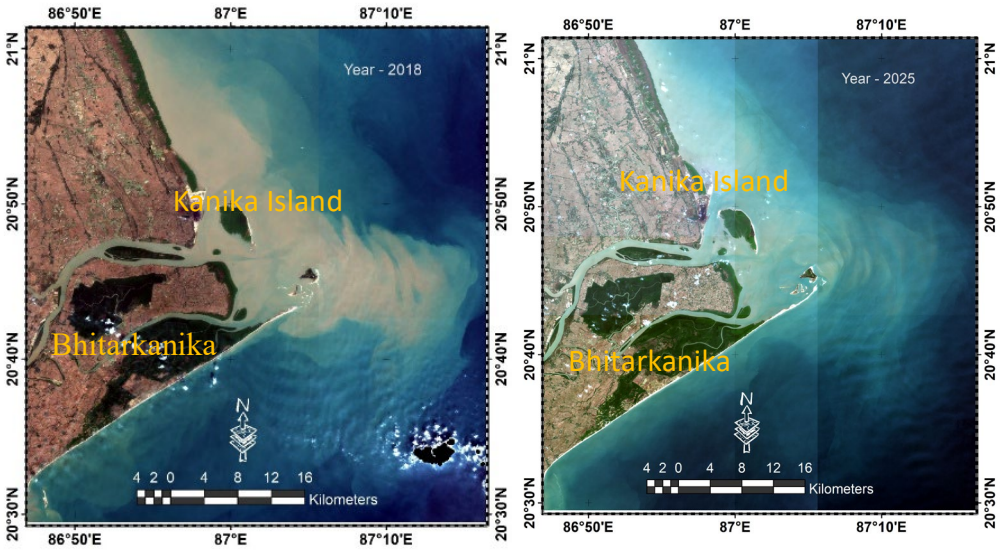

Figure-1: Sentine-2 imagery of the study area showing Dhamra macro tidal estuary for the year 2018 (a) and 2025 (b) in True Color Composite.

3. Data and Methodology:

Sentinel-2 data accessed from Copernicus has been utilized in the current study. Turbidity zone has been mapped for year from 2018 to 2025. The seasonal dynamics is also captured considering four different seasons viz. Winter, Pre-Monsoon, Monsoon and Post-Monsoon. Both the seasonal and annual variation has been understood using Google Earth Engine. Figure 2 depicts the adopted methodology to understand the variation of turbidity in the Dhamra macrotidal estuary. Turbid water was mapped using Normalized Difference Turbidity Index, where higher positive value indicates more turbid water and higher negative indicates clear water. Sentinel-2 is a wide-swath, high-resolution, multi-spectral imaging mission supporting Copernicus Land Monitoring studies, including the monitoring of vegetation, soil and water cover, as well as observation of inland waterways and coastal areas. Harmonized Sentinel 2A product has been filtered further for the cloud coverage. The data has been clipped for the area of interest using the clip (geometry) function. Normalized Difference Water Index is calculated from the sentinel image where positive value indicates water body. The water body has been masked using the NDWI threshold value 0. 1 as shown in the Figure 3. NDTI is calculated only for the masked region of water body and the product has been imported to GIS for map compilation.

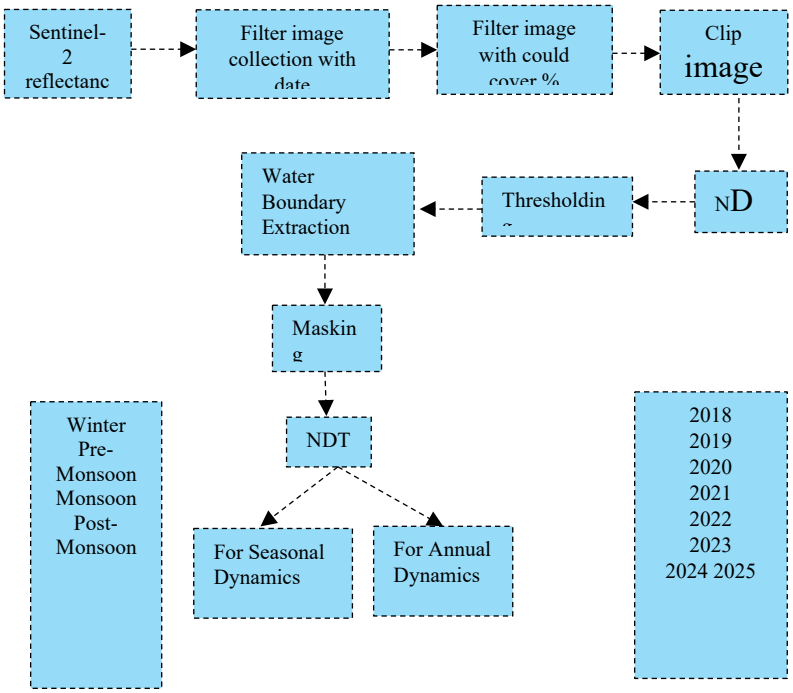

Figure-2: Flowchart depicting the data and methodology employed for the turbidity zone mapping.

4. Result and Discussion:

Google Earth Engine, a cloud-based platform integrates all the process to produce final product without the intermediate output which allow to save lot of memory of the system. GEE reduces the time of processing drastically while directly producing the final output for the area of interest. In conventional satellite image processing, this data processing produces several images, including the initial image clip from the Sentinel-2 image which is the study area for processing. Sometime more than one images required to mosaic in order to cover the study area.

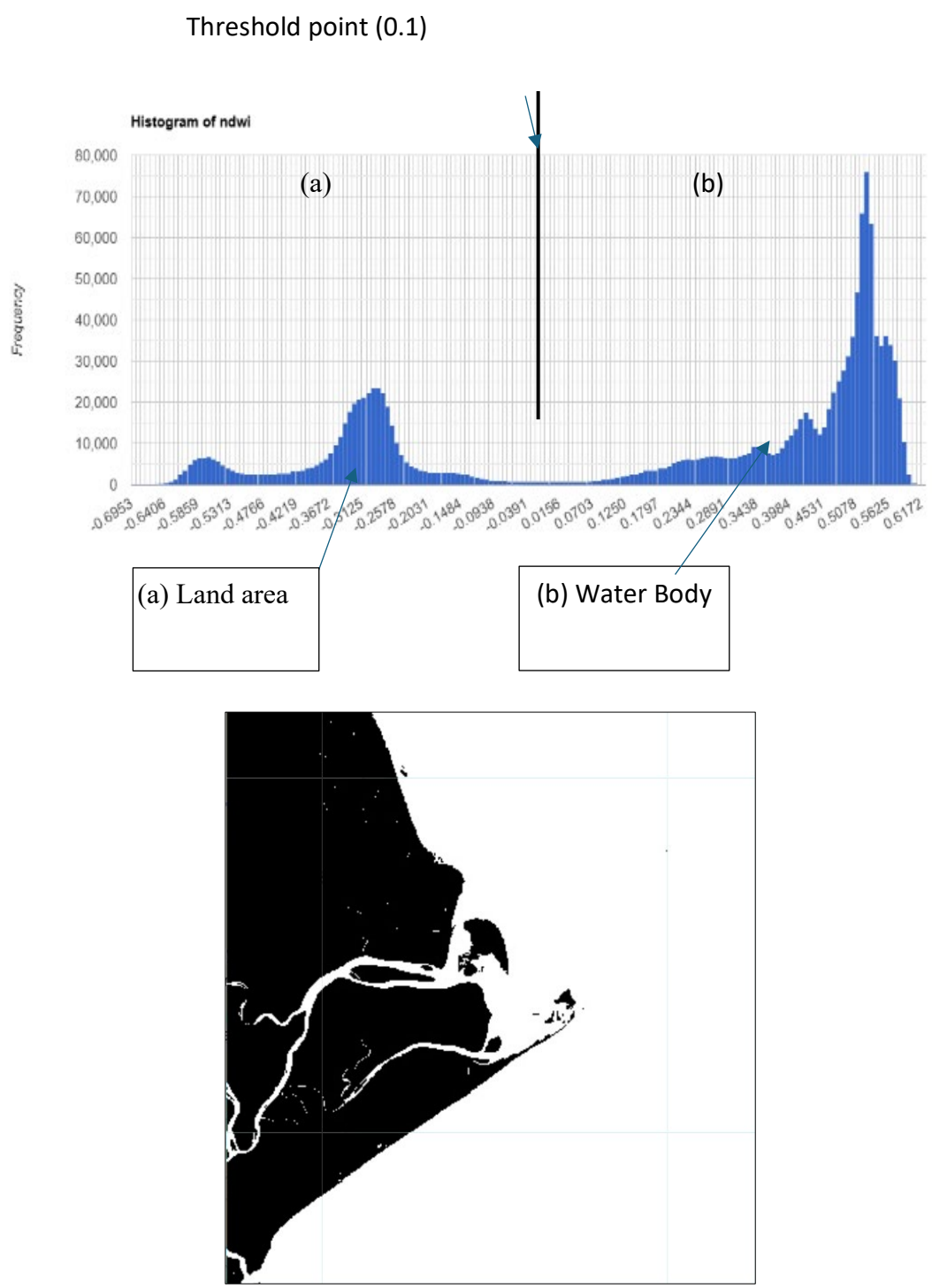

Figure-3(A): Histogram of NDWI showing two major peak separated by threshold value 0. 1 correspond to the land and water part of the image. (B) Thresholded Image highlighting water with white color and land part with black color.

The second output image is the result of NDWI extraction which is the output of the separation process between water bodies and non-water bodies, the third image is a water body with a turbidity index value and no turbidity index value, the fourth image is the final output or a water body image that only has a turbidity index value. One of the key advantages of cloud computing, especially GEE, where data processing is carried out very efficiently without burdening the memory of computer devices used for processing. In addition to this GEE provides the final output image directly without all immediate intermediate results of different processing stages.

The Normalized Difference Water Index (NDWI) have a value range between -0. 69 to 0. 61 as shown in the histogram (Fig. 3A). The histogram is bimodal in nature where two peaks correspond to land and water part of the image. Positive value indicates water body whereas negative value indicates land area. Thresholded output (Fig. 3B) classified the water pixel and land pixel two classes and highlighted the water with bright pixel and land as dark pixel. The thresholded product shown in Figure 3B is used for masking the water body and further NDTI image. The output resulted from image processing in GEE is an NDTI image with a pixel value between minus one to positive one. The NDTI index is imported to QGIS software, the range of index values can be presented in a gradual color display as shown in Figure 4. The NDTI map of the Dhamra macro-tidal estuary shows the distribution of turbidity through year 2018 to 2025. Red color indicates high turbid water, yellow indicates intermediate turbidity and green indicates the clear water with minimum turbidity. NDTI data variation is highest for the year 2018 where the minimum value is -0. 7 and maximum value is 0. 5. Maximum turbidity is observed in the year 2018 (Fig. 4a) whereas the minimum turbidity observed for the year 2021 (Fig. 4d). Throughout the years the turbidity is very high near the riverine area, mouth of the estuary and towards the northern portion of the estuary. As the rivers emptied water in the Bay of Bengal the turbidity gradually reduces from the river mouth to seawards as seen in figure 4 (a-h). This is because of the mixing of high turbid river water with the fresh sea water. Another striking observation clearly indicated from figure 4(a-h) showing the geospatial turbidity variation from 2018 to 2025 is the concentration of high turbid zone towards the northern region in compared to the southern region. The exceptionally high concentration of turbid water near the immediate vicinity of coast in further north of Dhamra estuary is observed. This northward movement of the turbid zone might be due to the impact of longshore current which needs further field validation to confirm. However, the northward migration the turbidity zone is clearly evident from the NDTI geospatial pattern.

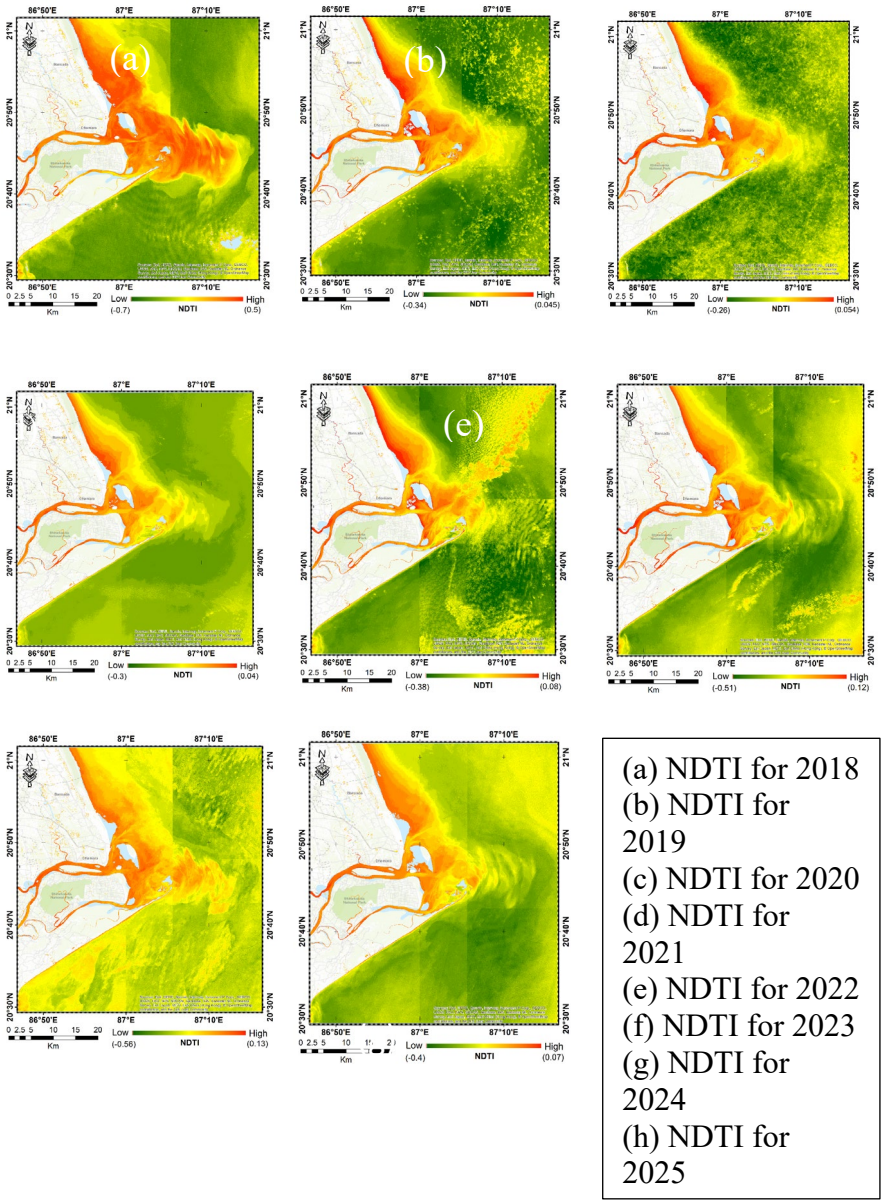

Figure-4: Variation in spatial distribution of turbid water from 2018 (a) to 2

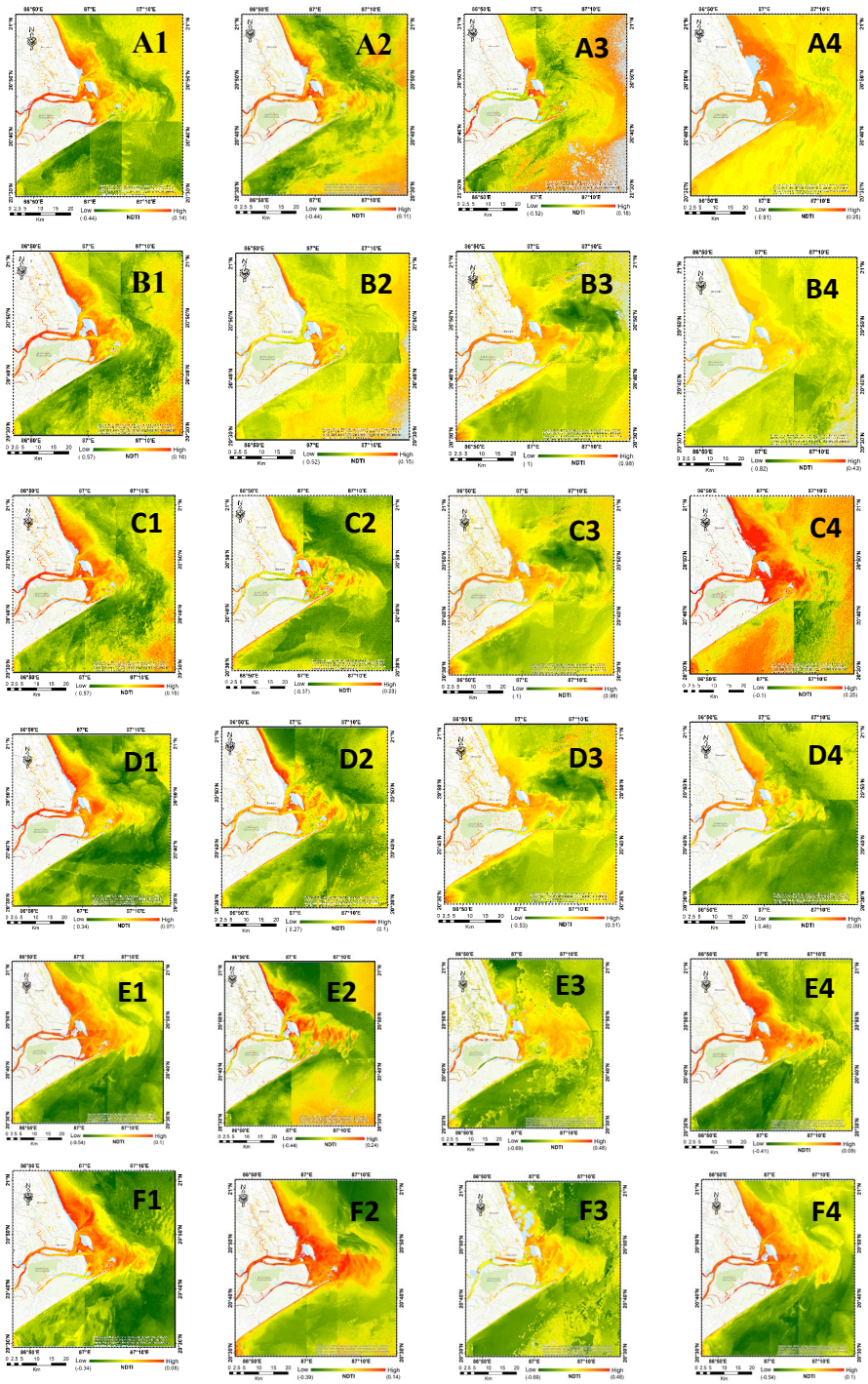

Figure-5: Seasonal variation in spatial distribution of turbid water (1-Winter, 2-Pre monsoon, 3-Monsoon, 4-Post Monsoon) from 2024 (A) to 2019 (F). Red, yellow and green color indicate high turbid water, intermediate turbid water and clear water respectively.

Temporal dynamics from 2018 to 2025 suggests the occurrence of turbidity maximum zone near mouth of Dhamra estuary surrounding the Kanika and Abudul Kamal island which extends towards north along the coastal zone depicted with red color in figure-4.

The seasonal variation of turbidity for Dhamra estuary and nearby region is shown in the Figure-5, where A to F stand for the year from 2024 to 2019 and 1 to 4 indicates four different season of a year Winter, Pre monsoon, Monsoon and Post monsoon respectively. Higher positive values indicating the high turbid water are represented with red color and higher negative values represented with green color indicates less turbid clean water (Fig. 5). Shades of yellow indicates the intermediate to low turbid water. The variation of turbidity is very high through different season of a year. The maximum turbidity is observed in post monsoon period which span from September to December followed by monsoon during the month of July and August. The minimum turbidity is observed in winter from December to March followed by Pre monsoon between April to June. The maximum value of NDTI index is obtained during the post monsoon from the year 2022 and 2023. In a particular year the NDTI index is high for Post monsoon indicating highest turbid water in year during the month of September to December. The cloud cover is very high in post monsoon spell making difficult to get cloud free image. The unwanted cloud cover giving some unwanted error as seen from figure 5 (A3 to F3). This seasonal high in turbidity might be because of the regular cyclonic event causing torrent rainfall every year during this spell in the coastal region of Bay of Bengal. Another reason can be the late arrival of monsoon to the Odisha coast. This seasonal turbidity variation of Dhamra estuary need to be correlated with the monthly rainfall data and natural disaster including cyclone for better understanding. The northward extension of the TMZ is not prominent in the post monsoon period unlike through out the year. The seasonal dynamics of TMZ can be correlated with the seasonal variation of the longshore current of the study area for better understanding which can be future scope of this work.

5. Conclusion:

The study shows that integration of Google Earth Engine and GIS can successfully map the turbidity maximum zone in a small spam of time with minimum computational requirement. It successfully utilized Sentinel 2A product and NDTI index for mapping the turbidity maximum zone. Google earth engine is an efficient platform for analyzing time series data to understand both seasonal and annual dynamics of TMZ. The spatio-temporal analysis of Dhamra estuary using GEE and Sentinel 2 dataset shows the similar trend of turbidity maximum zone throughout the year. The maximum value of turbidity index is observed during Post monsoon period and minimum value of turbidity observed during the winter season. The high amount of turbidity during Post monsoon might be resulted from the frequent cyclonic event causing torrent rainfall in this region. Although the degree of turbidity highly influenced by the seasonal change their underlying pattern

of distribution remain similar. The patterns highlight a strong influence of long-shore current in the distribution of TMZ. Northern portion of the estuary shows consistently high turbidity compared to the southern coastal region. The geomorphic processes occurring at this place need to be studied in details to identify the underlying causes for northward migration of TMZ. TMZ of Dhamra estuary located near the river mouth, islands (Kanika and Abdul Kalam) and north coast throughout the year. North ward extension of TMZ is not very prominent during Post monsoon period.

6. Acknowledgement:

The Author expresses sincere gratitude to Q-GIS and GEE platform for providing the open-source data utilized in this study. I also extend my appreciation to the various sources for making geospatial data available. A special thanks goes to the editors and reviewers for their unwavering support and effort in critically evaluating and refining our work.

References:

- Abascal-Zorrilla, N., Vantrepotte, V., Huybrechts, N., Ngoc, D. D., Anthony, E. J., & Gardel, A. (2020). Dynamics of the estuarine turbidity maximum zone from landsat-8 data: The case of the maroni river Estuary, French Guiana. *Remote Sensing*, *12*(13), 2173.
- Allen, G. P., Sauzay, G., & Castaing, P. (1977). Transport and deposition of suspended sediment in the Gironde Estuary, France. In Estuarine processes (pp. 63-81). Academic press.
- Amran, M. A., & Daming, W. S. (2023). Estimation of coastal waters turbidity using Sentinel-2 imagery. *Geodesy and Cartography*, *49*(4), 180-185.
- Boyd, C. E. (2000). Water quality: an introduction. Springer Science & Business Media.
- Brezonik, P. L., Olmanson, L. G., Bauer, M. E., & Kloiber, S. M. (2007). Measuring water clarity and quality in Minnesota lakes and rivers: A census-based approach using remote sensing techniques. Cura Reporter, 37, 3–13.
- Chang, M., Li, P., Sun, Y., Wang, H., & Li, Z. (2022). Mapping dynamic turbidity maximum zone of the yellow river estuary from 38 years of Landsat imagery. Remote Sensing, 14(15), 3782.
- Dewantoro, M. D. R., Ulfa, M., & Supatmanto, B. D. (2024, May). Water Turbidity Mapping Using Sentinel-2A Imagery and Cloud Based Google Earth Engine in Saguling Reservoir. In *IOP Conference Series: Earth and Environmental Science* (Vol. 1343, No. 1, p. 012027). IOP Publishing.
- Dogliotti, A. I., Ruddick, K. G., Nechad, B., Doxaran, D., & Knaeps, E. (2015). A single algorithm to retrieve turbidity from remotely-sensed data in all coastal and estuarine waters. Remote sensing of environment, 156, 157-168.

- Doxaran, D., Castaing, P., & Lavender, S. J. (2006). Monitoring the maximum turbidity zone and detecting fine-scale turbidity features in the Gironde estuary using high spatial resolution satellite sensor (SPOT HRV, Landsat ETM+) data. *International Journal of Remote Sensing*, *27*(11), 2303-2321.
- Doxaran, D., Froidefond, J. M., Castaing, P., & Babin, M. (2009). Dynamics of the turbidity maximum zone in a macrotidal estuary (the Gironde, France): Observations from field and MODIS satellite data. *Estuarine, Coastal and Shelf Science*, *81*(3), 321-332.
- Hu, Z., Pan, D., He, X., & Bai, Y. (2016). Diurnal variability of turbidity fronts observed by geostationary satellite ocean color remote sensing. *Remote Sensing*, *8*(2), 147–162. https://doi. org/10. 3390/rs8020147.
- Islam, M. A., Lan-Wei, W., Smith, C. J., Reddy, S., Lewis, A., & Smith, A. (2007). Evaluation of satellite remote sensing for operational monitoring of sediment plumes produced by dredging at hay point, Queensland, Australia. *Journal of Applied Remote Sensing*, *1*(1), 011506–011521.
- Katlane, R., Dupouy, C., El Kilani, B., & Berges, J. C. (2020). Estimation of chlorophyll and turbidity using Sentinel 2A and EO1 data in Kneiss Archipelago Gulf of Gabes, Tunisia. *International Journal of Geosciences*, *11*, 708–728.
- Lihan, T., Saitoh, S. I., Iida, T., Hirawake, T., & Iida, K. (2008). Satellite-measured temporal and spatial variability of the Tokachi River plume. *Estuarine Coastal and Shelf Science*, *78*(2), 237–249.
- Liu, Y., Islam, M. A., & Gao, J. (2003). Quantification of shallow water quality parameters by means of remote sensing. *Progress in Physical Geography*, *27*(1), 24–43.
- Lizcano-Sandoval, L., Anastasiou, C., Montes, E., Raulerson, G., Sherwood, E., & Muller-Karger, F. E. (2022). Seagrass distribution, areal cover, and changes (1990–2021) in coastal waters off West-Central Florida, USA. *Estuarine, Coastal and Shelf Science*, *279*, 108134.
- Obregón, M. A., Rodrigues, G., Costa, M. J., Potes, M., & Silva, A. M. (2019). Validation of ESA Sentinel-2 L2A aerosol optical thickness and columnar water vapour during 2017–2018. *Remote Sensing*, *11*(14), 1649.
- Ouillon, S., Douillet, P., & Andrefouet, S. (2004). Coupling satellite data with in situ measurements and numerical modeling to study fine suspended-sediment transport: A study for the lagoon of New Caledonia. *Coral Reefs*, *23*(1), 109–122. https://doi. org/10. 1007/s00338-003-0352-z.
- Ouillon, S., Douillet, P., Petrenko, A., Neveux, J., Dupouy, C., Froidefond, J. M., Andréfouët, S., & Caravaca, A. M. (2008). Optical algorithms at satellite wavelengths for total suspended matter in tropical coastal waters. *Sensors*, *8*(7), 4165–4185.

- Ouma, Y. O., Noor, K., & Herbert, K. (2020). Modelling reservoir chlorophyll-a, TSS, and turbidity using Sentinel-2A MSI and Landsat-8 OLI satellite sensors with empirical multivariate regression. *Journal of Sensors*, *2020*, 8858408.
- Petus, C., Chust, G., Gohin, F., Doxaran, D., Froidefond, J. M., & Sagarminaga, Y. (2010). Estimating turbidity and total suspended matter in the Adour River plume (South Bay of Biscay) using MODIS 250-m imagery. *Continental Shelf Research*, *30*(5), 379–392. https://doi. org/10. 1016/j. csr. 2009. 12. 007.
- Quang, N. H., Sasaki, J., Higa, H., & Huan, N. H. (2017). Spatiotemporal variation of turbidity based on Landsat 8 OLI in Cam Ranh Bay and Thuy Trieu Lagoon, Vietnam. *Water*, *9*(8), 570–594. https://doi. org/10. 3390/w9080570.
- Sebastiá-Frasquet, M. T., Aguilar-Maldonado, J. A., Santamaría- Del-Ángel, E., & Estornell, J. (2019). Sentinel 2 analysis of turbidity patterns in a coastal lagoon. *Remote Sensing*, *11*(24), 2926.
- Simpson, J. H. ; Gong, W. K. ; Ong, J. E. The determination of the net fluxes from a mangrove estuary system. Estuaries **1997**, 20, 103–109.
- Sravanthi, N., Ramana, I. V., Yunus Ali, P., Ashraf, M., Ali, M. M., & Narayana, A. C. (2013). An algorithm for estimating suspended sediment concentrations in the coastal waters of India using remotely sensed reflectance and its application to coastal environments. *International Journal of Environmental Research*, *7*(4), 841–850.
- Van Santen, P. ; Augustinus, P. G. E. F. ; Janssen-Stelder, B. M. ; Quartel, S. ; Tri, N. H. Sedimentation in an estuarine mangrove system. J. Asian Earth Sci. **2007**, 29, 566–575.
- Vanhellemont, Q., & Ruddick, K. (2014). Turbid wakes associated with offshore wind turbines observed with Landsat 8. *Remote Sensing of Environment*, *145*, 105–115.
- Wang, C., Wang, L., Wang, D., Li, D., Zhou, C., Jiang, H.,... & Li, Y. (2021). Turbidity maximum zone index: A novel model for remote extraction of turbidity maximum zone in different estuaries. *Geoscientific Model Development Discussions*, *2021*, 1-38.
- Willemsen, P. W. J. M. ; Horstman, E. M. ; Borsje, B. W. ; Friess, D. A. ; Dohmen-Janssen, C. M. Sensitivity of the sediment trapping capacity of an estuarine mangrove forest. Geomorphology **2016**, 273, 189–201.
- Wolanski, E. Hydrodynamics of mangrove swamps and their coastal waters. Hydrobiologia **1992**, 247, 141–161.
- Wu, G., Cui, L., Liu, L., Chen, F., Fei, T., & Liu, Y. (2015). Statistical model development and estimation of suspended particulate matter concentrations with Landsat 8 OLI images of Dongting Lake, China. *International Journal of Remote Sensing*, *36*(1), 343–360.

- Zhang, Y., Zhang, Y., Shi, K., Zha, Y., Zhou, Y., & Liu, M. (2016). A Landsat 8 OLI-based, semi analytical model for estimating the total suspended matter concentration in the slightly turbid Xin'anjiang reservoir (China). *IEEE Journal of Selected Topics in Applied Earth Observations and Remote Sensing*, *9*(1), 1–16.

Assessment of Salt Water Intrusion in Coastal District of Eastern India

Utsav Das[1] and Rosalin Das[2]

P. G. Department of Geology, Fakir Mohan University, Balasore - 756089, Odisha

Corresponding author e-mail: utsavdas1992@gmail. com

Abstract

As a result of growing urbanization, groundwater extraction, and worldwide sea level changes coastal aquifers are becoming more and more vulnerable to sea water intrusion. Historically, vulnerability to seawater intrusion has been describing using pattern diagrams, which bare the result of several hydrogeochemical processes. The geospatial study of groundwater quality is hindered by the forms of these diagrams, which restricts the capacity for spatiotemporal mapping and monitoring. This highlights the necessity of converting the data from existing pattern diagrams into a format that can be easily utilized to identify locations that are susceptible seawater intrusion within a GIS framework. In all 60 groundwater samples are collected during May 2022 and their ionic characteristics examined. Four coastal area of Balasore block viz Chandipur, Rasalpur, Inchudi, Rupsa assessed for seawater intrusion. These blocks were located from seashore to 25 km inland distance. Based on hydro geology parameters and molar ratio all the four villages were associated with saltwater intrusion. The high Mg/Ca ratio (> 5. 5) may be indicative of saltwater contaminations in these villages. According to Cl /CO_3^{2-} +HCO_3^- ratio (>6. 6) the given locations have high seawater intrusion near to coastal area. Based on Na/Cl ratio (<0. 86), the contamination is due to marine source of origin. Thus construction of small check dams and artificial impermeable barrier in these areas across the river at frequent intervals will assist in mitigation the problem of saltwater intrusion by improving groundwater recharge.

Keyword: coastal area, groundwater, ionic concentration, seawater intrusion

Introduction

Seawater intrusion endangers freshwater supplies globally along the shore, making groundwater unfit for human use and invariably forcing well abandonment or requiring costly treatment system. Additionally this vulnerability is also expected to exacerbate by future climate change and sea level rise (Taylor et al. 2013). Sea water and fresh water both have different hydrochemistry, with the former nearly uniform chemistry where chloride (Cl) and sodium(Na^+) make up of 84% of total ionic composition.

Whereas freshwater composition varies widely with calcium (Ca^{2+}) and bicarbonate (HCO^{-}_{3}) are dominate ions. Mixing of these is generally identified by elevated in Cl^{-} concentration with in the aquifers that can be traceable due to conservative nature of anion. Likewise, a frequent elevated in total dissolved solids (TDS) or electrical conductivity (EC) used as indicator to identify salinity in groundwater (Singhal and Gupta 2010). Intrusion of sea water is a complex process due to influences of hydro geochemical reactions, shoreline geomorphology, aquifer flow and biological process. Processes indicative of seawater intrusion include cation exchange reaction, calcite dissolution; carbonate digenesis, dolomitization and sulphate reduction. Over exploitation of groundwater resource for domestic, irrigation and industrial purpose leads to ingress of seawater in freshwater aquifers in these regions. The people of these regions are engaged with fishing, oil refineries, harbor works and industrial activities like fertilizer manufacturing, pesticides and pharmaceuticals are responsible for over extraction of groundwater resources of Balasore district of Odisha, India

Study area

The study area of the present research comprises Balasore and Remuna revenue blocks Odisha in the eastern part of India (Fig. 1). It lies between the north latitudes 21° 16′ 22″– 21° 39′ 27″ and east longitudes 86° 46′ 20″ – 87° 11′ 19″ falling in toposheets NF45O14, NF45O15, NF45P2 and NF45P3). These two rural to suburban blocks consists of two small towns Balasore and Remuna and 560 villages covering an area of about 786 Km^2. The area is drained by Budhabalanga, Panchpara, Sunai (Sono) and their tributaries. The drainage pattern is sub-dendritic and prominent geomorphic features are meandering patterns of Budhabalanga and Panchpara rivers with development of ox-bow lakes (Fig. 1), which suggest very low gradient of the drainage area with more residence time of groundwater. The region enjoys a humid subtropical climate with average annual rainfall of about 1450 mm, most of which takes place by southwest monsoon during June to September. The water table occurs at 4 – 6. 5 m depth below the ground level during pre-monsoon season (March – May).

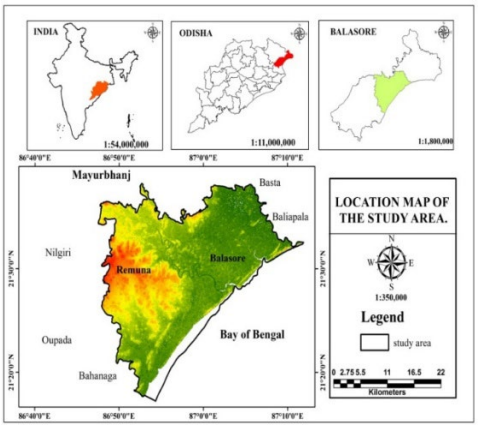

Fig. 1. Location map of Study area

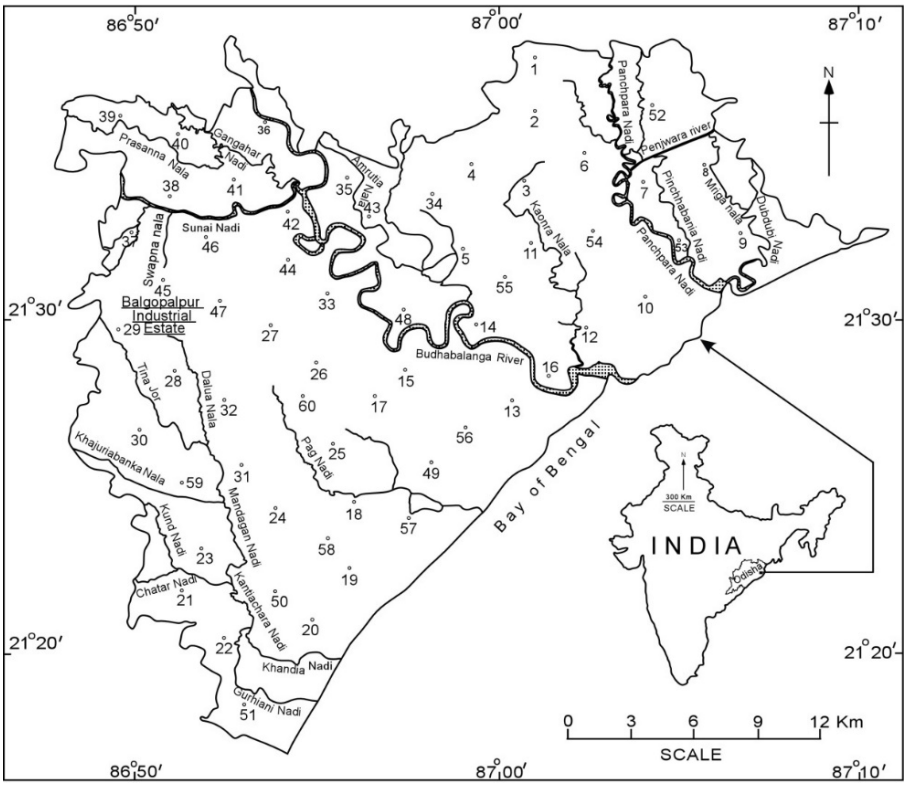

Fig. 2. Study area showing drainage and groundwater sample locations

Materials and Methods

A total of 60 groundwater samples were collected from hand pumps and dug wells during the pre-monsoon season (March-April 2022). The samples were analyzed for physico-chemical parameters such as pH, electrical conductivity (EC), total dissolved solids (TDS), alkalinity, hardness, nitrate, chloride, fluoride, by standard analytical procedure (APHA 2012). The EC and pH are measured insitu using handheld pH and EC meter (HANNAHI-9828). Ca^{2+}, HCO_3^{-}, Mg^{2+}, Cl^{-} and TDS by volumetric titration method. Na^{+}, K^{+} ion is measured by flame photometer while F^{-} and SO^{2-}_4 determined by Spectro-photometric techniques. Quality parameters like SAR and RSC were calculated by using the formula of (Richards 1954; Eaton 1950). Screeing of groundwater samples for their sutibality for irrigation is done on the basis of EC, SAR, RSC values. The collected data was processed using the Geographical Information System (GIS) software. The spatial distribution of physico-chemical parameters was mapped using the Kriging interpolation method. The interpolation surfaces were classified based on the Standard for Drinking Water (WHO) to identify the areas with poor water quality. Based on groundwater quality map prepared, the groundwater fell under saline and alkali classes are alone taken for sea water intrusion studies. Four coastal area in Balasore district viz Chandipur, Inchudi, Rasalpur, Srijang villages are more vulnerable to sea water intrusion.

Table 1 Criteria for recognition of seawater intrusion in groundwater

Ionic Ratios			
Sl. No.	**Parameters**	**Critical limit**	**References**
1.	Cl /HCO_3	> 1- Sea water intrusion	Soni & Pujari, 2010
2.	Na / Cl	<0. 86–Salinity due to sea water intrusion 0. 86 -1. 0 Fresh ground water >1- Anthropogenic activities	Jones *et al*., 1999
3.	Cl /(CO_3+HCO_3)	0. 05 - Fresh ground water 0. 05 to 1. 30 - Slightly contaminated ground water 1. 30 to 2. 80 - Moderately contaminated ground water 2. 80 to 6. 60 - Injuriously contaminated ground water 6. 6 to 15. 5 - Near sea water>200 - Sea water	Mohan Babu *et al*., 2013
4.	Cl/Br	Cl/Br ratio = 297 mg/l - Seawater (where Cl = 19, 500 mg/l, Br = 67. 3 mg/l) Hyper saline brine >297 mg/l (from remains of evaporated seawater) up to 800 mg/l - anthropogenic sources (sewage effluents or agriculture-returnflows) >1000) - evaporate–dissolution products	Morris & Riley, 1966
5.	Ca/Mg	Ca/Mg ratio low due to Sea water intrusion 'Mg' is the dominant ion in ocean	Mohan Babu *et al*., 2013)
6.	Cl> Na	Sea water intrusion	Mondal et al., 2010 & 2011
7.	Kelly's ratio	<1 – Safe >1 – Unsafe	Kelley, 1951
8.	Mg/Ca	4. 5 to 5. 2 – Seawater (with an excess of Mg)	Jones *et al*., 1999

Individual ionic concentration			
9.	Ca^{2+}	75 to 200 mg/ l	USDA Handbook, vol. 60
10.	Mg^{2+}	50 to 150 mg/l	USDA Handbook, vol. 60
11.	Cl^{-}	260 to 1600 mg/L	USDA Handbook, vol. 60
12.	SO_4^{2-}	150 to 400 mg/l	USDA Handbook, vol. 60
13.	TDS	>2000mg/l – Sea water mixing 500 to 1500 ppm - Normal ground water	USDA Handbook, vol. 60
14.	NO_3^{-}	45 mg/l	USDA Handbook, vol. 60
15.	F^{-}	0. 6 to 1. 5 mg/l	
16.	Electrical Conductivity	>5000 µS/cm	Kim *et al*., 2005
17.	Total hardness (TH) mg/l of equivalent CaCO3	< 75 - soft 75 to 150 – Moderately hard 150 to 300 - Hard >300 – Very hard	Sawid & Issa, 2015
18.	Magnesium hazard (MH)	<50 – Suitable >50 – Unsuitable	Eaton, 1950
19.	PermeabilityIndex (PI)	Class I – Good Class II – PermissibleClass III – Unsuitable	Richards, 1954
20.	Seawater mixing index(SMI)	SMI - >1 (possibility of sea water intrusion)	Park *et al*., 2005

Sea water Mix index

In order to determine SMI, the relative concentration proportions of Na, Mg, Cl, and SO4 were represented by the constants a, b, c, and d (a = 0. 31, b = 0. 04, c = 0. 57, d = 0. 08, respectively). TNa, TMg, TCl, and TSO4 stand for threshold values of Na, Mg,

Cl, and SO4 that were derived from the interpretation of cumulative probability curves, whereas CNa, CMg, CCl, and CSO4 indicate concentrations of Na, Mg, Cl, and SO4 detected in groundwater samples expressed in mg/l.

Result and Discussion

The groundwater samples collected from the coastal area of Balasore district was analysed for irrigation purpose. Four coastal villages namely Chandipur, Rasalpur, Inchudi, Rupsa were suspected for seawater intrusion from their hydro geology parameters and molar ratio. Bicarbonate and chloride were dominating anion; Magnesium and Sodium were dominating cations based on above mentioned locations. The groundwater is dominantly Ca-HCO_3however Na-Cl facies also dominate in the four coastal villages.

The high Mg/Ca ratio (>5. 4) may be a sign of salt water pollution in certain areas with regard to sea water intrusion. The screened sites have severely contaminated ground water (near sea water) based on the Cl/CO^{2-}+HCO^{-}ratio (>6. 6). The Na/Cl ratio (<0. 86) suggests that the contamination could have come from a marine source. Cations such as Na+, anions such as Cl- and HCO3-, and ionic ratios such as Na/Cl (<0. 86) (Nair et al., 2012), Cl /CO3+HCO3 (> 6. 6) (Mohan Babu et al., 2013), and Mg/Ca (> 5. 4) (Jones et al., 1999) are more abundant than other ions in ground water samples. The villages of Chandipur, Rasalpur, Inchudi, and Rpusa of the Balasore district were suspected of having seawater intrusion, according to the Seawater Mixing Index (>1) and Water Quality Index (>100) (Krishnamoorthy & Athimoolam, 2015). SMI values greater than one suggested that anthropogenic contamination and seawater mixing were causing the ground water to become salinized. In addition to the previously stated cause, the primary causes of seawater intrusion in the Balasore district were the drought and excessive groundwater use Kerrou et al. (2010), Furuya (2009), Wicks and Herman (1996), Omonona et al. (2014), and Jankowski and Jacobson (1991) all endorsed this. The geochemical trend of groundwater is shown in a box plot (Fig. 3) and demonstrate that sodium is the dominate cataion ($Na > Ca^{2+} > Mg^{2+} > K^{+}$) and chloride is the dominate anaion ($Cl^{-} > HCO_3 > so_4^{-} > CO_3^{-} > NO_3^{-} > F^{-}$) point out that saline water ingress.

Table. 2 Screening of Sea water intruded well locations of Balasore district, Odisha

Blocks / Villages		Geo coordinates	Distance from sea (Km)	Na^+ (m. eq. /lit)	Cl^- (m. eq. /l)	HCO_3^- (m. eq. /l)	Na/Cl	$Cl/CO_3^{2-}+HCO_3^-$	Mg^{2+}/Ca^{2+}	WQI	Rating	S MI	Rating
1.	**Chandipur**	21°25'48" N 87°0'36" E	4	90.47	190.0	16.00	0.48	7.92	7.55	177.20	Unfit for drinking	15.11	Sea water intrusion
2.	Rasalpur	**21°19'48"N 86°52'48"E**	8	84.83	160.0	14.00	0.53	7.27	9.69	160.67	Unfit for drinking	13.06	Sea water intrusion
3.	**Inchudi**	**21°19'48"N 86°53'24"E**	10	86.93	90.00	16.00	0.51	7.08	8.03	134.42	Very poor	8.55	Sea water intrusion
4.	Rupsa	**21°37'48"N 87°4'48"E**	11	99.24	210.0	16.00	0.47	8.75	9.70	225.05	Unfit for drinking	16.53	Sea water intrusion

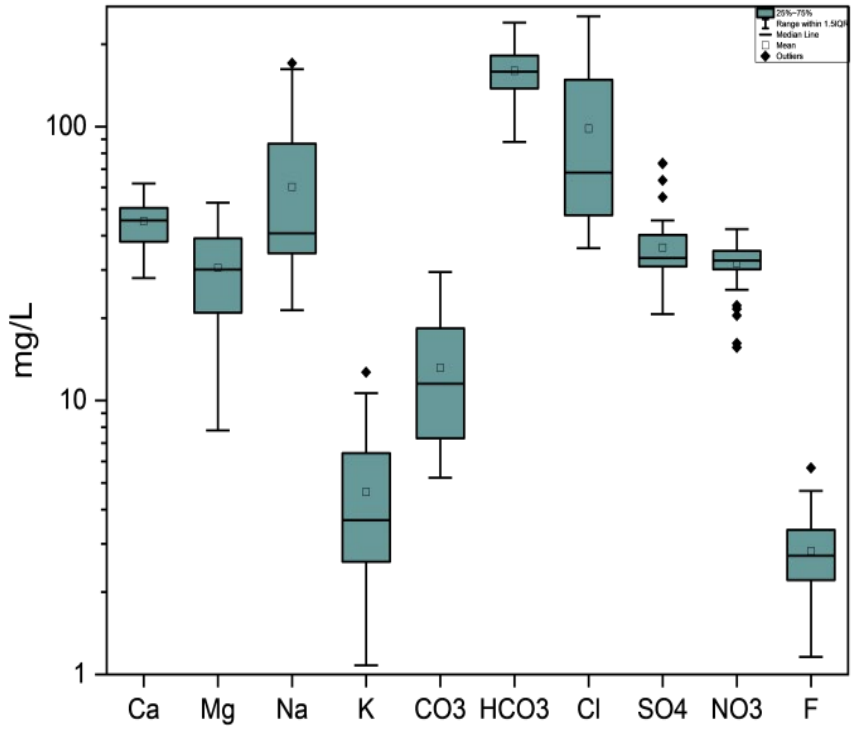

Fig. 3 Box plot for the maximum, minimum and average for the chemical constitution in groundwater in study area, Balasore district Odisha state, India

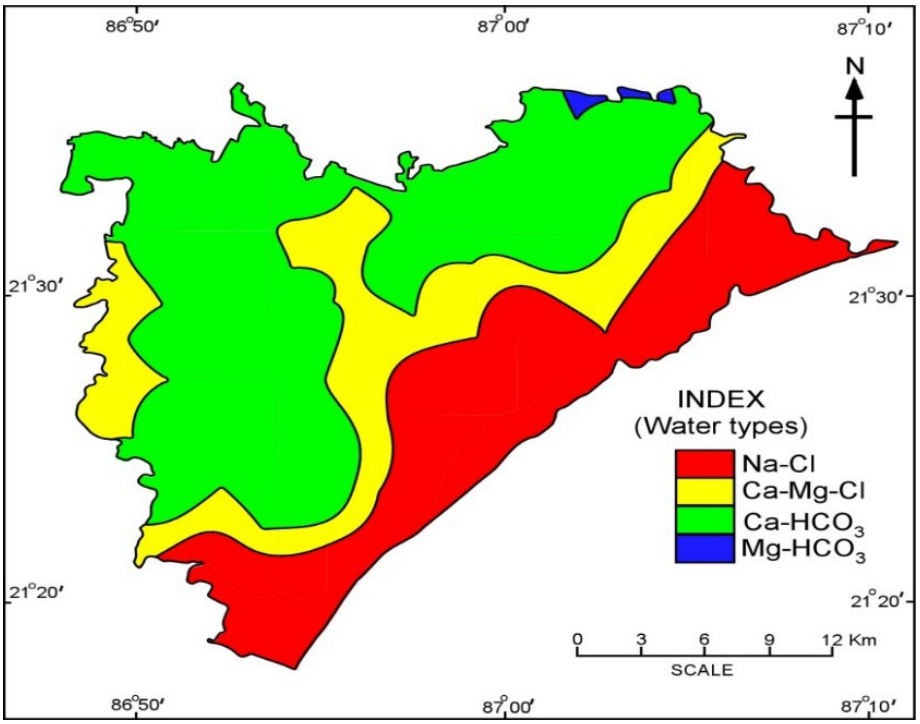

Fig. 4 spatial distribution map showing hydro geochemical facies

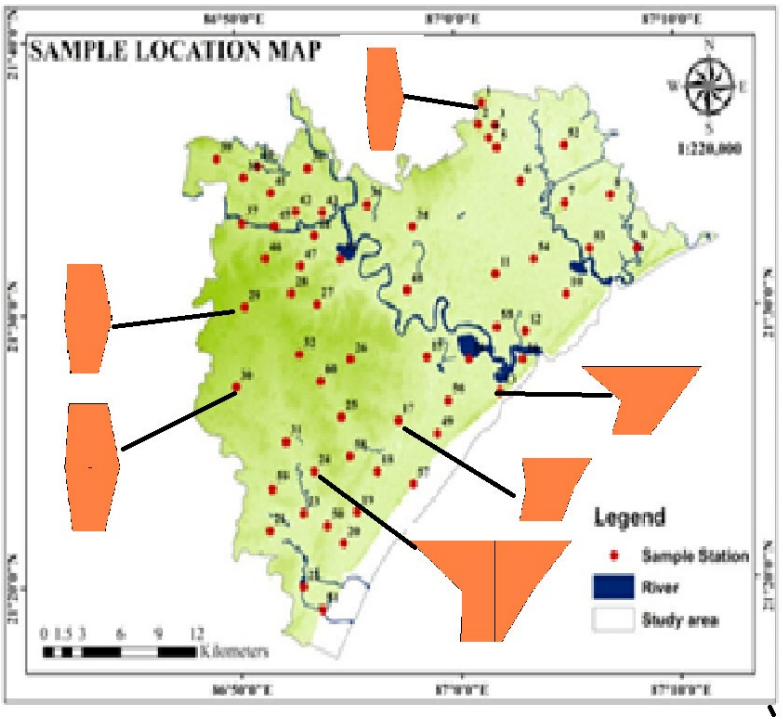

Fig. 5 map showing saline water intruded area

Conclusion

This coastal part of Odisha is densely populated and sustains intense agricultural activity, as a result of which the coastal aquifers are affected by geogenic, anthropogenic and seawater intrusion processes including fluorosis problem. The impact of seawater intrusion in the research area is shown by the change in groundwater types from Ca-HCO3 (fresh water) to Ca-Mg-Cl and Na-Cl (saline water), as well as an increase in TDS in a seaward direction. The impact of non-geogenic sources is often superimposed on the geogenic factors resulting in wide variation of the groundwater chemistry. Sea water mixing index of the villages Hnadipur, Rasalpur, Inchudi, and Rupsa were identified for seawater intrusion from Na/Cl (< 0. 86), Cl /CO_3^{2-} +HCO_3^- ratio (>6. 6), Mg/Ca ratio (> 5. 5), Cl^-/ HCO_3^- (>1), salt water intrusion in these Water quality index (>100), and seawater mixing index (>1). Construction of check dams, impermeable barriers and simultaneously periodic monitoring, artificial recharge of groundwater and rain water harvesting is necessary to mitigate villages.

References

- Anandhan P (2005). Hydrogeochemicalstudiesin and around Neyveli mining region, Tamilnadu, India. Ph. D Thesis, Department of Earth Sciences, Annamalai University, 189p.
- Appelo, C. A. J., Postma, D., 2005. Geochemistry, Groundwater and Pollution. CRCPress.

- Arslan, H., Cemek, B., Demir, Y., 2012. Determination of seawater intrusion viahydrochemicals and isotopes in Bafra Plain, Turkey. Water Resour. Manag. 26 (13), 3907- 3922.
- Central Ground Water Board, 2009. TechnicalReport Series, District Ground waterBrochure, Cuddalore District, TamilNadu. Govt. of India. Ministry of Water Resources, CGWB, South Eastern Coastal Region, Chennai.
- Durov, S. K., 1948. Natural waters and graphic representation of their compositions. Dokl. Akad. Nauk. SSSR 59, 87 - 90.
- Edmond JM, Palwer MR, Measures CF, Grant B, Stallard RF (1995). The fluvial geochemistry and denudation rate oftheGuayana Shield in Venezuela, Colombia and Brazil, GeochimCoscochimActa. 59:3301-3323.
- Elango L, Kannan R, Senthil Kumar M(2003). Major ion chemistry andidentification of hydrogeochemical processesof ground waterin a part of KanchipuramDistrict, Tamil Nadu, India. EnvironmentalGeosciences, 10(4): 157- 166.
- Gibbs RJ (1970). Mechanisms controllin gworld's water chemistry, Science, 170:1088- 1090.
- Hanshaw, B. B., Back, W., 1979. Major geochemical processes in the evolution of carbonate aquifer systems. J. Hydrology 43, 287 - 312.
- Mohan Babu, M., Viswanadh, G. K., Venkateswara Rao, s., 2013. Assessment ofsaltwater intrusion along coastal areas of Nellore district, A. P. International journal of Scientific &Engineering Research, 4 (7) PP:173 -178
- Panteleit, B., Hamer, K., Kringel, R., Kessels, W., Schulz, H., 2011. Geochemical processesin the saltwater - freshwater
- Piper, A. M., 1944. A graphic procedure in the geochemical interpretation of wateranalyses. Trans. Am. Geophys. Union 25, 914-928.
- Schoeller, H., 1964. La classification geochimique des eaux. TASH Publication, Iahs. Info, pp. 16-24.
- Singhal, B., Gupta, R. P., 2010. Applied Hydrogeology of Fractured Rocks. Springer.
- Stiff, H., 1951. The interpretation of chemical water analysis by means of patterns. J. Pet. Technol. 3 (10).
- Taylor, R. G., Scanlon, B., Doll, P., Rodell, M., Van Beek, R., Wada, Y., Edmunds, M., 2013. Ground water and climate change. Nat. Clim. Change 3, 322-329.
- ShereneJenitaRajammalT, P. Balasubramania mandM. J. Khaledhonkar.

2021. Assessment ofgroundwater quality in Kanyakumari district, Tamil Nadu, using ionic chemistry. Currentscience121. No. 5. pp:676 -681

- ShereneJenitaRajammal, T. P. Balasubramaniam, M. J. Khaledhonkar. and V. Ravikumar. 2020. Sea water intrusion appraisalthrough ground water chemistry in coastal (Cuddalore) district of TamilNadu, India. Journal of Soil and Water Conservation 19(2): pp: 142-148 ; DOI: 10. 5958/2455-7145. 2020. 00019. 3
- Suguna, S and Sherene, T. 2019. Assessment of Sea Water Intrusion in Ground Water Samples of Selected Blocks of Cuddalore District, Tamil Nadu, India. Madras Agric. J., ;106 | 7-9 | pp: 470 -476 doi:10. 29321/MAJ 2019. 000295
- Suguna, S, Sherene, T, P. Balasubramaniam and V. Ravikumar. 2018. Assessment ofseawater intrusion through ionic ratios along coastal areas of Cuddalore district, Tamil Nadu. *Green Farming* Vol. 9 (5) : 906-909 ; September-October, 2018

Analysing Land Use/Land Cover Changes in Angul District's Industrial Zone: A Spatio-Temporal Approach Using GEE

Susanta Kumar Das[1], Rosalin Das*, Barsarani Mallick[1], Santosh Kumar Rout[1], Subhadrarani Das2, Department of Geology, Fakir Mohan University, Balasore

E-mail: susantakdas.geology@gmail.com

Abstract

The proposed study area in Angul district, Odisha, spans 3, 088. 4 km² and includes five blocks: Angul, Banarpal, Talcher, Kaniha, and Chendipada. Known for its industrial prominence, it hosts thermal power plants, steel manufacturing, aluminum smelting, and cement production. Talcher features 8 opencast and 3 underground coal mines. The Tikarpada Wildlife Sanctuary, covering 795. 52 km², is located within the picturesque Satkosia gorge and is home to endangered species like crocodiles. The region's soil is predominantly Alfisols, including red sandy, red loamy, and mixed red-black soils. Angul district, the industrial hub of Odisha, has undergone significant land use and land cover (LULC) changes due to extensive coal and mineral mining. This study examines LULC transformations from 2009 to 2024 using multi-temporal satellite imagery analyzed the Google Earth Engine (GEE) platform. Key LULC classes—forest, agriculture, settlements, water bodies, fallow land, and mining zones were mapped and quantified using GIS techniques across three phases: 2009, 2014, 2019, and2024. Results reveal major shifts driven by expanding mining and industrial activities. Forest cover declined from 38% in 2009 to 30% in 2024, primarily due to deforestation for mining infrastructure. Agricultural land decreased by 12%, converted into mining and urbanized zones. Settlements expanded by 15%, reflecting industrial growth and population influx. Mining areas increased by 25%, encroaching on forests and farmland. Water bodies grew marginally by 3%, associated with reservoirs and ponds supporting mining. Fallow land declined, indicating limited vegetative recovery in mined-out zones. These findings highlight the environmental impacts of mining in Angul, underscoring the need for sustainable practices, effective reclamation strategies, and balanced management policies to restore degraded landscapes and promote ecological stability alongside economic growth.

Key Words – LULC, GEE, Industrial, Angul

Introduction

Global forest cover has been undergoing significant and unprecedented changes due to various anthropogenic activities such as timber extraction, industrialization, agricultural expansion, mining, and urbanization (Geist and Lambin, 2002; Reddy et al., 2013; Kim et al., 2014; Maus et al., 2020). Among these, mining activities are considered one of the primary drivers of forest cover loss (FCL), especially in tropical regions of developing countries (Emiru et al., 2018; Thonfeld et al., 2020). In these tropical areas, FCL is influenced by a range of factors, including mining, population pressure, migration, unemployment, lack of property rights, and agricultural and infrastructure development (Seymour and Harris, 2019; Edwards and Laurance, 2015; Ranjan, 2019).

The Earth's surface has undergone significant transformations due to both natural phenomena, such as global warming and the greenhouse effect, as well as anthropogenic activities, including the cultivation of marginal lands, deforestation, mining, industrialization, and overgrazing (Rathore and Wright, 1993; Hurtt et al., 2011; Areendran et al., 2013). Changes in land use/land cover (LULC) can have both positive and negative impacts on natural resources at local, regional, and global scales, making LULC monitoring a priority for policymakers, land managers, and researchers (Malaviya et al., 2010; Mousivand and Arsanjani, 2019). Negative consequences of LULC changes, such as deforestation, mining, and land degradation, have contributed to climate change, biodiversity loss, and alterations in biophysical characteristics (Li et al., 2016; Mahmood et al., 2016).

In many developing countries, regional ecosystems are increasingly degraded due to unplanned land use activities, such as unregulated urban expansion, shifting cultivation, and illegal mining operations (Mukhopadhyay et al., 2017; Awotwi et al., 2018). While mineral resources are vital to the economic development of any nation (Sekerin et al., 2019), unregulated mining practices can lead to significant environmental harm, including deforestation, land degradation, displacement of local populations, and air pollution (Patra and Sethy, 2014; Awotwi et al., 2017).

Odisha State, located on the eastern coast of India, is of particular significance due to its rich mineral deposits, making it one of the most resource-abundant regions in the country. Mining activities in Odisha contribute significantly to both the state's and India's Gross Domestic Product. Recent trends show an increase in mineral production and the number of workers engaged in mining activities (Hota and Behera, 2015; Ranjan, 2019).

Several studies have employed geospatial technologies and open-source remote sensing data to analyze the relationship between mining activities and FCL. For instance, Swenson et al. (2011) examined the impacts of gold mining in the Peruvian Amazon, while López-Carr and Burgdorfer (2013) studied the role of population growth,

migration, and land-use changes in deforestation. Sonter et al. (2017) reported that mining alone was responsible for 11, 670 km² of deforestation in the Brazilian Amazon between 2005 and 2015. Other studies, such as those by Austin et al. (2019) in Indonesia, Tsai et al. (2019) in southern Ghana, and Feng et al. (2020) in Shenzhen Bay, China, have similarly investigated the impacts of mining on forest cover. Additionally, studies by Ang et al. (2021) and Yang et al. (2021) focused on the socio-environmental effects of mining in Malaysia and China, respectively.

In India, Lele and Joshi (2009) analyzed forest cover changes in North-East India from 1972 to 1999, while Deb et al. (2018) assessed mining-related deforestation in the Indian Himalayan region. Ranjan (2019) explored the contribution of mining to deforestation across more than 300 districts in India, highlighting coal, iron ore, and limestone mining as the most significant contributors to FCL. However, limited studies have investigated the long-term impacts of mining on forest cover at the district level, particularly in Odisha (Rath and John, 2018).

Temporal land use/land cover (LULC) studies are essential for monitoring and mapping mine reclamation activities, such as afforestation and land restoration, as well as for quantifying the environmental impacts of mining operations (Turner et al., 2007; Ranjan et al., 2021). Traditional methods for regular LULC monitoring and map generation are often time-consuming, expensive, and labor-intensive. Additionally, ground surveys can be challenging in certain areas due to difficult terrain (Prakash and Gupta, 1998). Furthermore, user-based image classification may lead to issues such as insufficient sample sizes and poor generalization of results (Zhao and Du, 2016).

Google Earth Engine (GEE) has emerged as a widely used platform for LULC classification, offering the advantage of leveraging Google's vast computing infrastructure and storage capabilities. Its self-programming classification algorithms enable automated LULC classification with high computational efficiency (Stromann et al., 2020; Pan et al., 2021). Numerous global studies have employed GEE for LULC mapping. For example, Xiong et al. (2017) generated a cropland map for Africa using Sentinel-2 and Landsat-8 data, Kumar et al. (2021) utilized Sentinel-2 level-1C data in the RUSLE model for LULC analysis, Pan et al. (2021) classified LULC in Australia and the United States using MCD12Q1 Version 6 global land data, and Praticò et al. (2021) employed Sentinel-2 time-series data to classify Mediterranean forest habitats.

Study Area

The industrial landscape of India is a dynamic amalgamation of diverse sectors spanning manufacturing, technology, and infrastructure. From bustling metropolitan centers to remote rural regions, industrial areas are the backbone of the nation's economy, driving growth, innovation, and employment opportunities.

Over the past few decades, Odisha has witnessed a significant surge in industrial growth, with numerous industries being established. The proposed study area, located in the Angul district, stands out as a prominent industrial hub within Odisha. Encompassing five blocks of the Angul district - Angul, Banarpal, Talcher, Kaniha, and Chendipada. The area spans approximately 3088. 4 square kilometers. The study area falls under Survey of India toposheet number 73C/15, 73G/3, 73C/12, 73C/16, 73G/4, 73G/8, 73D/13, 73H/1, 73H/5, 73D/10, 73D/14, 73H/2 (1:50, 000 Scale), between 20° 31′N and 21° 40′ N and longitudes of 84° 15′ E and 85°23′ E. The diverse array of industrial setup includes thermal power plants, steel manufacturing, aluminium smelting, and cement production, Angul serves as a cornerstone of industrial prowess in the region. Noteworthy establishments like NALCO, CPP, NTPC, TTPS, JSPL, JITPL, Heavy water project at Talcher and Shree metallics limited at Mukundapur. The Talcher industrial block consists of 8 opencast and 3 underground coal mines in its 5 coal areas namely - Jagannath area, Bharatpur area, Lingaraj area, Hingula area, and Talcher area. Additionally, Angul is home to key dams like Rengali, derjang and Tikarpada, crucial for irrigation and hydroelectric power generation. The Tikarpada Wildlife Sanctuary in Angul district, Odisha, spans 795. 52 km² and is famed for its diverse flora and fauna. Situated amidst the stunning Satkosia gorge, it shelters endangered species like crocodiles. It has been observed that the major part of the area is occupied by Alfisols which includes red sandy soil, red loamy soil and mixed red and black soils.

Brahmani and Mahanadi are the two major rivers of the district. Both these rivers have numerous perennial and non-perennial tributaries. The Brahmani River which is the second longest river in Orissa flows through Talcher subdivision. The major portion of the district is drained by Brahmani River and its tributaries. The Brahmani flows in a general SE direction, broadly parallel to the general strike trends of the prevalent rock formations, but locally guided by major joints and faults. The major tributaries of Brahmani are Tikra Jhor, Singhara Jhor, Samakoi, Nandira Jhor, Gambhira, Nigra, Bade Jhor etc. These major streams show a general right-angle pattern while joining with the river Brahmani. The major tributaries of this river are Karandi Jhor, Ghosar Jhor, Sindol Jhor, Chanagorhi and Malia Jhor etc., all flow from the northern side of the river originating in Atthamalik and Angul subdivisions.

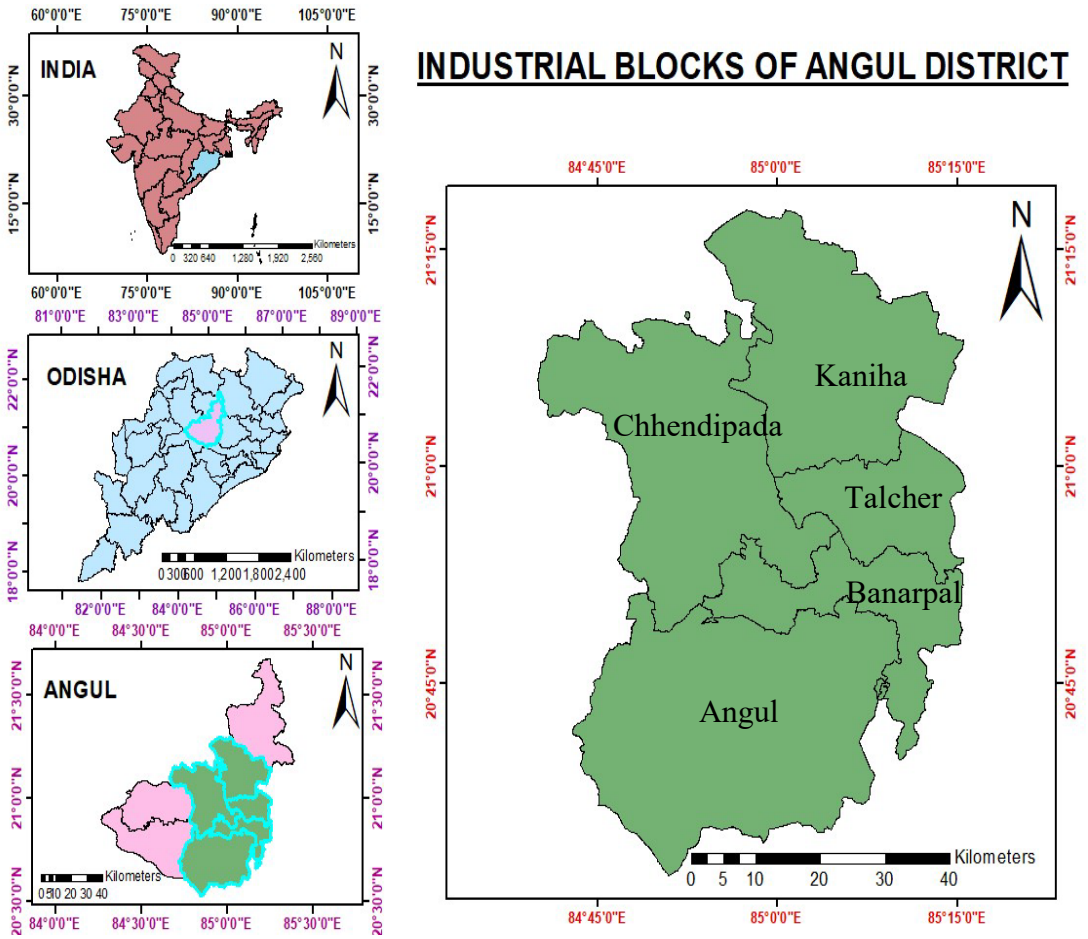

Fig:1 Study Area Map of Industrial Blocks of Angul District

Methodology

The analysis of Land Use and Land Cover (LULC) change in Angul district, Odisha, was conducted using Landsat satellite imagery, specifically Landsat 5 (2009) and Landsat 8 (2014, 2019, 2024). This study employed Google Earth Engine (GEE) and Geographic Information System (GIS) techniques to process, classify, and assess the accuracy of satellite data. The methodology involved several key steps to ensure a systematic and reliable evaluation of LULC transformations over time.

Image Processing

The initial phase involved acquiring and preprocessing Landsat imagery to enhance data consistency and accuracy. Georeferencing was performed to align all datasets with a common coordinate system, ensuring spatial consistency across different years. Radiometric calibration was applied to correct sensor and atmospheric distortions, thereby standardizing pixel values to reflect actual surface conditions. Additionally, cloud masking was employed to remove atmospheric noise and improve classification accuracy.

Image Classification

A hybrid classification approach was implemented, combining both unsupervised and supervised classification techniques. Initially, unsupervised classification was performed to categorize pixels into preliminary clusters based on spectral similarities, aiding in the identification of broad land cover types. Subsequently, supervised classification was conducted by selecting training samples representative of key LULC classes, including forest, agricultural land, settlements, water bodies, fallow land, and mining zones. A machine learning-based classification algorithm, such as Random Forest, was applied to accurately delineate LULC categories.

LULC Change Detection

After classifying land use and land cover (LULC) for the selected years (2009, 2014, 2019, 2024), change detection maps are generated to analyze temporal variations. Post-classification comparison is employed to identify transitions between different land cover categories. These maps highlight significant shifts, such as urban expansion, deforestation, and agricultural growth. Change detection involves overlaying classified images and computing differences to quantify the extent and nature of transformations. Spatial analysis techniques, including GIS-based change detection and accuracy assessments, ensure reliable results. This approach helps identify patterns of environmental change, supporting sustainable land management. The final LULC change maps provide a visual representation of landscape dynamics over time, facilitating informed decision-making in land-use planning and conservation efforts.

Accuracy Assessment

To ensure the reliability of the LULC classification, an accuracy assessment is conducted by comparing the classified maps with reference data, such as ground truth observations or high-resolution satellite imagery. This assessment quantifies classification performance using key statistical measures, including overall accuracy, producer's accuracy, user's accuracy, and the kappa coefficient. The overall accuracy reflects the proportion of correctly classified pixels, while producer's and user's accuracy assess errors of omission and commission, respectively. The kappa coefficient evaluates classification agreement beyond chance, providing a robust measure of accuracy.

Table:1 Flow chart of Methodology

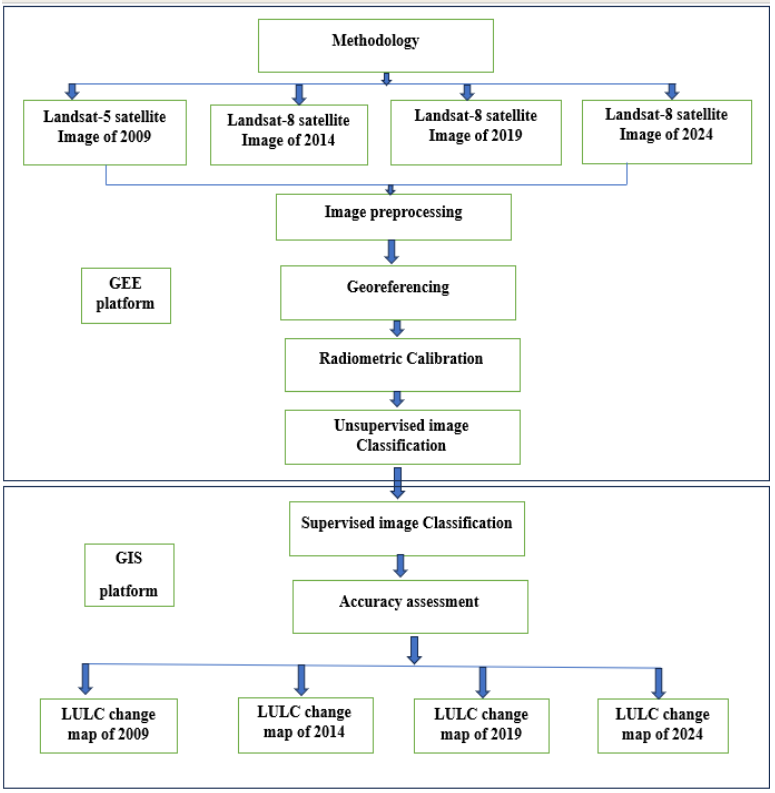

This validation process enhances the credibility of LULC change analysis, ensuring that detected land cover transitions are reliable. By integrating accuracy assessment, this methodology offers a systematic and effective framework for monitoring LULC dynamics, supporting sustainable land-use planning and environmental management decisions.

Result And Discussion

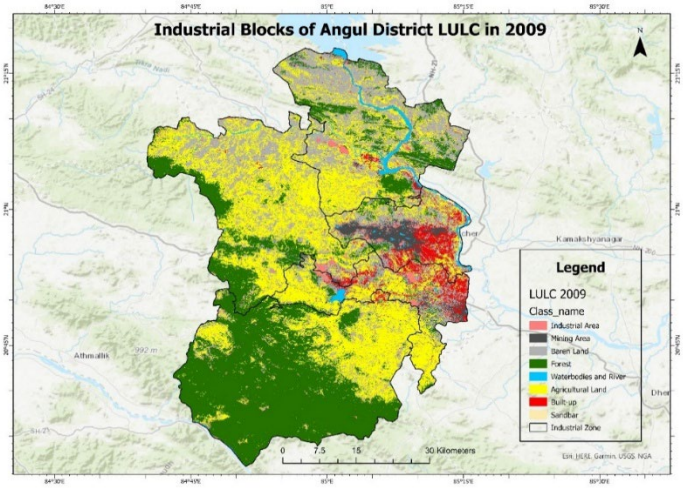

Fig:2 Land Use Land Cover Map of Industrial Blocks of Angul District in 2009

The provided land use and land cover (LULC) map of Angul District in 2009 illustrates the spatial distribution of various geological and anthropogenic features. The geological composition of the region comprises diverse landforms, including extensive forested areas (green), agricultural land (yellow), and barren land (gray). The industrial and mining areas, prominently marked in red and dark gray, indicate significant anthropogenic modifications to the landscape. These mining zones likely represent coal or mineral extraction sites, which contribute to geomorphological changes such as land subsidence, erosion, and alteration of natural drainage patterns.

Waterbodies and rivers (blue) traverse the region, signifying active fluvial processes that shape the terrain through sediment transport and deposition. The presence of sandbars along the river courses suggests high sediment load and periodic deposition, characteristic of dynamic river systems influenced by monsoonal flow variations. Built-up areas (brown) indicate urban expansion, often associated with increased impervious surfaces, leading to altered hydrological cycles, reduced groundwater recharge, and enhanced surface runoff.

The juxtaposition of industrial zones and agricultural lands highlights potential environmental challenges such as soil degradation, groundwater contamination, and air pollution due to industrial emissions. The presence of extensive forested regions in the southern part of the district underscores the ecological significance of these areas in maintaining regional biodiversity and stabilizing the soil structure. Overall, the map reflects a landscape undergoing rapid transformation due to industrialization and resource extraction, necessitating sustainable land management practices to mitigate adverse geological and environmental impacts.

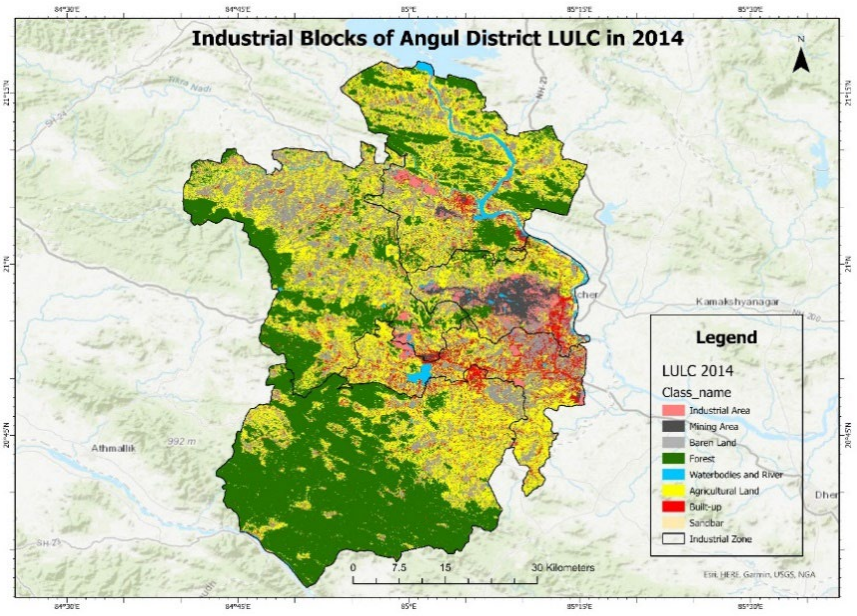

Fig:3 Land Use Land Cover Map of Industrial Blocks of Angul District in 2014

The land use and land cover (LULC) map of Angul District in 2014 illustrates significant geological and geomorphological transformations over time. The expansion of industrial and mining areas (red and dark gray) highlights intensified resource extraction, contributing to landscape degradation through deforestation, soil erosion, and land subsidence. The barren land (gray) indicates exposed geological formations and loss of vegetative cover, potentially leading to increased surface runoff and sediment transport in fluvial systems.

The riverine networks (blue) continue to play a crucial role in shaping the region's sedimentary dynamics, with sandbars forming in depositional zones due to alluvial processes. Agricultural land (yellow) remains extensive but shows signs of fragmentation, possibly due to encroaching industrial activities and urbanization (brown). The persistence of dense forest cover in the southern region (green) suggests a stable geological setting, acting as a critical buffer against soil erosion and hydrological alterations.

The presence of industrial zones near major waterways raises concerns about hydrogeological contamination, including groundwater depletion and pollution from industrial effluents. The ongoing transformation of the land cover highlights the necessity for sustainable geological resource management to mitigate adverse effects such as land degradation, habitat loss, and alteration of natural drainage patterns.

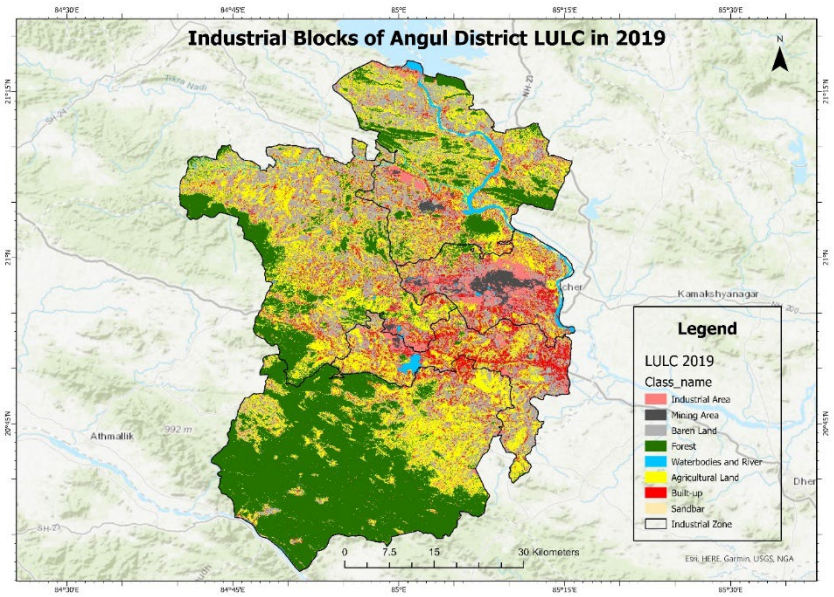

Fig:4 Land Use Land Cover Map of Industrial Blocks of Angul District in 2019

The 2019 land use and land cover (LULC) map of Angul District reveals significant geological transformations driven by industrialization, mining, and urban expansion. The continued expansion of industrial (gray) and mining areas (red) indicates intensified extraction of geological resources, likely including coal and minerals, leading to

increased geomorphological disturbances such as land subsidence, erosion, and terrain alteration.

Barren land (gray) has expanded, suggesting increased stripping of topsoil, which exposes bedrock and alters the region's natural geomorphology. Agricultural land (yellow) shows a decline due to encroachment by industrial and built-up areas (brown), highlighting a shift in land use patterns. The persistence of large-scale deforestation (green reduction) impacts soil stability and groundwater recharge, increasing susceptibility to desertification and hydrological changes.

The river systems (blue) continue to shape the geological landscape, with sandbars indicating sediment deposition processes influenced by hydrodynamic variations. Waterbodies remain crucial in maintaining regional hydrogeological balance, but proximity to industrial areas raises concerns about contamination from heavy metals and pollutants.

The rapid transformation of land cover necessitates sustainable geological and environmental management to mitigate adverse effects such as soil degradation, loss of biodiversity, and groundwater depletion, ensuring long-term ecological stability in the region.

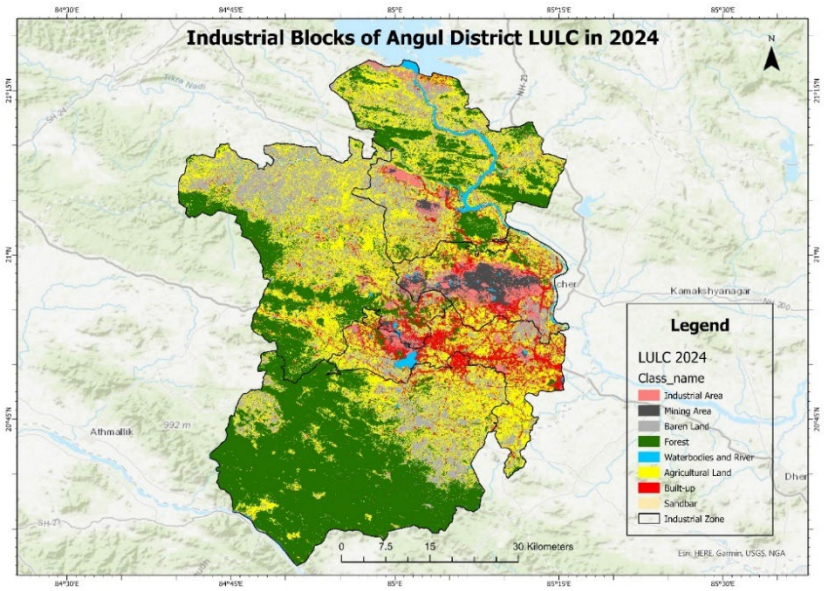

Fig:5 Land Use Land Cover Map of Industrial Blocks of Angul District in 2024

The 2024 land use and land cover (LULC) map of Angul District showcases significant geological and geomorphological changes, primarily driven by industrial expansion, mining activities, and deforestation. The continuous proliferation of mining areas (red) has further altered the region's lithology, exposed subsurface strata and accelerated land degradation. The expansion of barren land (gray) suggests severe erosion, depletion of soil fertility, and exposure of parent rock formations.

Deforestation (reduction in green forested areas) continues, influencing regional pedogenesis by reducing organic matter input, thereby affecting soil composition and increasing susceptibility to desertification. The increasing built-up area (brown) and industrial zones indicate intensified anthropogenic influences, leading to alterations in drainage patterns and increased impervious surfaces, which impact groundwater recharge and fluvial processes.

The river systems (blue) remain vital in sediment transport, with noticeable changes in sandbar (beige) formations due to variations in fluvial dynamics and deposition patterns. The presence of waterbodies suggests potential hydrogeological shifts, possibly linked to surface water extraction for industrial use.

These ongoing geological transformations highlight the need for sustainable land management practices, as the depletion of geological resources and changes in soil structure may trigger long-term environmental consequences, including increased geohazards such as land subsidence and water scarcity.

Fig:6 Pie Chart shows the Land Use Land Cover of 2009 to 2024

The pie charts depict the temporal variations in land use and land cover (LULC) from 2009 to 2024, showcasing geological and environmental transformations within the Angul District. Over this period, significant shifts in landforms, soil composition, and anthropogenic activities have influenced regional geomorphology.

The decline in agricultural land from 33% in 2009 to 18% in 2024 suggests soil degradation, reduced fertility, and possible overexploitation of groundwater, altering the hydrogeological balance. Simultaneously, the increase in fallow land (from 24% in 2009

to 31% in 2024) indicates potential soil erosion and declining pedogenesis, affecting topsoil stability and sediment transport.

Vegetation cover has fluctuated, peaking at 35% in 2014 and 2024, which might be linked to afforestation efforts or shifts in lithological properties affecting soil-water interactions. The expansion of industrial zones and settlement areas reflects rapid urbanization and increased impervious surfaces, influencing hydrological cycles, infiltration rates, and groundwater recharge.

Mining activities have slightly fluctuated but remain a key factor in land degradation, exposing bedrock, altering sediment deposition, and contributing to land subsidence. The negligible change in water bodies and sandbars suggests a relatively stable fluvial system despite anthropogenic pressures. These trends highlight critical geological implications for sustainable land management.

Table:2 Percentage of LULC Parameters

Parameters	2009	2014	2019	2024
Industry	1. 736496	2. 899958	6. 154009	3. 698479
Mining	2. 607173	1. 947849	1. 395278	1. 89286
Vegetation	32. 496	35. 30284	31. 87288	35. 16281
Fallow	24. 18021	18. 18589	21. 69485	31. 16516
Agricultural land	33. 39055	32. 29588	28. 36226	18. 04264
Waterbody	1. 614131	1. 785978	1. 588982	2. 203778
Sandbar	0. 308328	0. 310277	0. 332901	0. 39588
Settlement	3. 667121	7. 271331	8. 59884	7. 438387

The tabulated data illustrates the spatiotemporal variations in land use and land cover (LULC) from 2009 to 2024, emphasizing significant geological and environmental transitions in the region. The fluctuation in vegetation cover, from 32. 49% in 2009 to a peak of 35. 16% in 2024, suggests dynamic ecological succession and possible changes in lithospheric composition influencing soil stability and fertility.

The sharp decline in agricultural land from 33. 39% in 2009 to 18. 04% in 2024 indicates a geomorphic shift driven by soil erosion, potential desertification, and declining groundwater recharge, altering pedological processes. Conversely, the increase in fallow land (from 24. 18% in 2009 to 31. 16% in 2024) suggests reduced land productivity, possibly due to anthropogenic pressures, leaching of essential minerals, or altered fluvial deposition patterns.

The settlement expansion (from 3. 66% to 7. 43%) and industrial growth correlate with increased surface imperviousness, disrupting natural drainage, exacerbating surface runoff, and influencing hydrogeological processes. Mining fluctuations, reducing from 2. 60% in 2009 to 1. 89% in 2024, might reflect shifting extraction strategies or resource depletion, impacting regional geomorphology through land subsidence and altered sediment deposition.

The increase in water bodies (from 1. 61% to 2. 20%) suggests hydrological modifications, possibly due to reservoir construction or altered precipitation trends, affecting groundwater recharge and sediment transport dynamics.

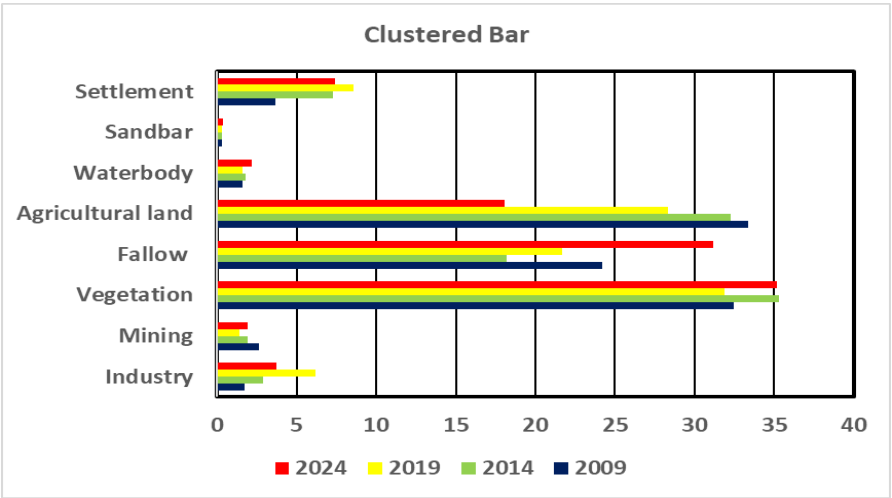

Fig: 7 Bar Diagram shows Land Use Land Cover (LULC) in (2009, 2014, 2019, 2024)

The clustered bar chart illustrates the temporal variation in land use and land cover (LULC) across four distinct years (2009, 2014, 2019, and 2024), depicting significant geological and geomorphological changes. The observed decline in agricultural land over time suggests soil degradation, reduced fertility due to excessive leaching, and possible anthropogenic influences, such as urbanization and industrial expansion.

Vegetation cover, an indicator of ecological stability, exhibits minor fluctuations but remains dominant, signifying a relatively stable lithological composition and moderate weathering processes. The increase in fallow land from 2009 to 2024 hints at shifting pedogenic conditions, possibly linked to changes in soil moisture retention, groundwater depletion, or increased sediment erosion.

The mining sector shows varying trends, with a decline in more recent years, potentially due to resource exhaustion or stricter environmental regulations. Mining-induced subsidence, alteration in local topography, and lithospheric stress distribution could also be factors affecting its spatial extent.

The expansion of industrial and settlement areas correlates with increasing surface impermeability, altering infiltration rates, and exacerbating runoff, thereby affecting

regional hydrogeological dynamics. The gradual rise in water bodies suggests shifts in the hydrological cycle, possibly influenced by climate variability, fluvial geomorphology, or reservoir development.

Conclusion

This study comprehensively analysed the land use and land cover (LULC) changes in Angul district, Odisha, from 2009 to 2024, focusing on the impacts of extensive coal mining, industrialization, and urban expansion. Using multi-temporal satellite imagery and Google Earth Engine (GEE) analysis, the study quantified transformations in key LULC classes, including forests, agricultural land, settlements, water bodies, fallow land, and mining zones. The results provide critical insights into the environmental consequences of rapid industrial development in this region.

Findings indicate significant LULC shifts driven by escalating mining and industrial activities. Forest cover, which accounted for 38% of the land area in 2009, declined to 30% by 2024 due to widespread deforestation for mining infrastructure and industrial expansion. The loss of forested areas not only threatens biodiversity but also disrupts ecological stability, affecting carbon sequestration and local climate patterns. The conversion of dense forests into mining zones has led to habitat fragmentation, particularly impacting wildlife species within the Tikarpada Wildlife Sanctuary and the broader Satkosia Gorge ecosystem.

Agricultural land exhibited a notable decline of 12% over the study period, primarily converted into mining sites and urbanized areas. The reduction in cultivable land raises concerns about food security and the livelihoods of local communities dependent on agriculture. The increase in built-up settlements by 15% underscores the region's industrial boom, attracting a growing workforce and leading to urban sprawl. While economic opportunities have expanded, unplanned urbanization poses challenges such as inadequate infrastructure, water scarcity, and increased pollution.

Mining areas expanded by 25%, encroaching upon forests and farmlands, illustrating the scale of resource extraction in Angul district. The dominance of mining zones underscores the pressing need for effective land reclamation strategies to mitigate adverse environmental effects. Although water bodies increased marginally by 3%, mainly due to artificial reservoirs and ponds created to support mining and industrial operations, this growth is insufficient to counterbalance the depletion of natural water sources. The decline in fallow land suggests limited vegetative recovery in mined-out areas, highlighting the long-term consequences of land degradation.

These findings emphasize the urgent need for sustainable land management practices to balance industrial development with environmental conservation. Effective policies should focus on afforestation, soil restoration, and the reclamation of abandoned mining sites to enhance ecological resilience. Additionally, adopting cleaner mining

technologies and enforcing stricter environmental regulations can mitigate the adverse effects of resource extraction. Integrated planning that considers both economic growth and ecological sustainability is crucial to ensure long-term environmental health in Angul.

Furthermore, community engagement in conservation initiatives, afforestation drives, and sustainable agricultural practices can foster environmental stewardship. Policymakers, industries, and local stakeholders must collaborate to implement land-use policies that promote a harmonious coexistence between industrial activities and natural ecosystems.

In conclusion, while Angul district in industrial area remains a vital industrial hub, the extent of LULC changes over the past 15 years highlights the pressing need for responsible land management and conservation efforts. A strategic, well-regulated approach is essential to restore degraded landscapes, safeguard biodiversity, and ensure sustainable development for future generations.

References

- Ang, M. L. E., Arts, D., Crawford, D., Labatos Jr., B. V., Ngo, K. D., Owen, J. R., Gibbins, C., Lechner, A. M., 2021. Socio-environmental land cover time-series analysis of mining landscapes using Google Earth Engine and web-based mapping. Remote Sens. Appl. : Soc. Environ. 21, 100458.
- Areendran, G., Rao, P., Raj, K., Mazumdar, S., Puri, K., and Gandhi, I. (2013). Land use/land cover change dynamics analysis in mining areas of Singrauli district in Madhya Pradesh, India. Tropical Ecology, 54, 239-250.
- Austin, K. G., Schwantes, A., Gu, Y., Kasibhatla, P. S., 2019. What causes deforestation in Indonesia? Environ. Res. Lett. 14 (2), 024007.
- Awotwi, A., Anornu, G. K., Quaye-Ballard, J. A., and Annor, T. (2018). Monitoring land use and land cover changes due to extensive gold mining, urban expansion, and agriculture in the Pra River Basin of Ghana, 1986–2025. Land degradation & development, 29(10), 3331-3343.
- Awotwi, A., Anornu, G. K., Quaye-Ballard, J., Annor, T., and Forkuo, E. K. (2017). Analysis of climate and anthropogenic impacts on runoff in the Lower Pra River Basin of Ghana. Heliyon, 3(12) 1-25, https://doi. org/10. 1016/j. heliyon. 2017. e00477.
- Deb, S., Debnath, M. K., Chakraborty, S., Weindorf, D. C., Kumar, D., Deb, D., Choudhury, A., 2018. Anthropogenic impacts on forest land use and land cover change: modelling future possibilities in the Himalayan Terai. Anthropocene 21, 32–41.
- Edwards, D. P., Laurance, W. F., 2015. Preventing tropical mining disasters. Science 350, 1482-1482.

- Emiru, T., Naqvi, H. R., Athick, M. A., 2018. Anthropogenic impact on land use land cover: influence on weather and vegetation in Bambasi Wereda, Ethiopia. Spat. Inf.
- Feng, Z., Tan, G., Xia, J., Shu, C., Chen, P., Wu, M., Wu, X., 2020. Dynamics of mangrove forests in Shenzhen Bay in response to natural and anthropogenic factors from 1988 to 2017. J. Hydrol. 591, 125271.
- Geist, H. J., Lambin, E. F., 2002. Proximate causes and underlying driving forces of tropical deforestation. Bioscience 52, 143–150.
- Hota, P., Behera, B., 2015. Coal mining in Odisha: an analysis of impacts on agricultural production and human health. The Extr. Indust. Soc. 2 (4), 683–693.
- Hurtt, G. C., Chini, L. P., Frolking, S., Betts, R. A., Feddema, J., Fischer, G., and Wang, Y. P. (2011). Harmonization of land-use scenarios for the period 1500–2100: 600 years of global gridded annual land-use transitions, wood harvest, and resulting secondary lands. Climatic change, 109(1), 117-161.
- Kim, D. H., Sexton, J. O., Noojipady, P., Huang, C., Anand, A., Channan, S., Feng, M., Townshend, J. R., 2014. Global, Landsat-based forest-cover change from 1990 to 2000. Remote Sens. Environ. 155, 178–193.
- Kumar, R., Deshmukh, B., and Sathunuri, K. (2021). RUSLE Model based assessment of soil erosion in Parbati River Basin, Central India using Google Earth Engine and GIS. In EGU General Assembly conference abstracts.
- Lele, N., Joshi, P. K., 2009. Analyzing deforestation rates, spatial forest cover changes and identifying critical areas of forest cover changes in North-East India during 1972- 1999. Environ. Monit. Assess. 156, 159–170.
- Li, W., Ciais, P., MacBean, N., Peng, S., Defourny, P., and Bontemps, S. (2016). Major forest changes and land cover transitions based on plant functional types derived from the ESA CCI Land Cover product. International Journal of Applied Earth Observation and Geoinformation, 47, 30-39.
- Lopez-Carr, D., Burgdorfer, J., 2013. Deforestation drivers: population, migration, and´ tropical land use. Environ. : Sci. Policy Sustain. Develop. 55 (1), 3–11.
- Mahmood, R., Pielke, R. A., and McAlpine, C. A. (2016). Climate-relevant land use and land cover change policies. Bulletin of the American Meteorological Society, 97(2), 195202.
- Malaviya, S., Munsi, M., Oinam, G., and Joshi, P. K. (2010). Landscape approach for quantifying land use land cover change (1972–2006) and habitat diversity in a mining area in Central India (Bokaro, Jharkhand). Environmental Monitoring and Assessment, 170(1), 215-229.

- Maus, V., Giljum, S., Gutschlhofer, J., da Silva, D. M., Probst, M., Gass, S. L. B., Luckeneder, S., Lieber, M., McCallum, I., 2020. A global-scale data set of mining areas. Sci. Data 7, 1–13.
- Mousivand, A., and Arsanjani, J. J. (2019). Insights on the historical and emerging global land cover changes: The case of ESA-CCI-LC datasets. Applied Geography, 106, 82-92.
- Mukhopadhyay, S., George, J., and Masto, R. E. (2017). Changes in polycyclic aromatic hydrocarbons (PAHs) and soil biological parameters in a revegetated coal mine spoil. Land Degradation and Development, 28(3), 1047-1055.
- Pan, X., Wang, Z., Gao, Y., Dang, X., and Han, Y. (2021). Detailed and automated classification of land use/land cover using machine learning algorithms in Google Earth Engine. Geocarto International, 1-18.
- Patra, H. S., and Sethy, K. M. (2014). Assessment of impact of opencast mine on surrounding forest: a case study from Keonjhar district of Odisha, India. Journal of Environmental Research and Development, 9(1), 249-254.
- Prakash, A., and Gupta, R. P. (1998). Land-use mapping and change detection in a coal mining area-a case study in the Jharia coalfield, India. International Journal of Remote Sensing, 19(3), 391-410.
- Praticò, S., Solano, F., Di Fazio, S., and Modica, G. (2021). Machine learning classification of Mediterranean forest habitats in Google Earth Engine based on seasonal Sentinel2 Time-Series and Input Image Composition Optimisation. Remote Sensing, 13(4), 586.
- Ranjan, A. K., Sahoo, D., and Gorai, A. K. (2021). Quantitative assessment of landscape transformation due to coal mining activity using earth observation satellite data in Jharsuguda coal mining region, Odisha, India. Environment, Development and Sustainability, 23, 4484-4499.
- Ranjan, R., 2019. Assessing the impact of mining on deforestation in India. Res. Pol. 60 (1), 23–35.
- Ranjan, R., 2019. Assessing the impact of mining on deforestation in India. Res. Pol. 60 (1), 23–35.
- Rath, S., John, R., 2018. What factors influence the abundance and distribution of sacred forests in Odisha, a densely forested state in eastern India? Int. J. Environ. Stud. 75, 553–564.
- Rathore, S. and Wright, R. (1993). Monitoring environmental impacts of surface coal mining, International Journal of Remote Sensing, 14(6), 1021-1042.
- Reddy, C. S., Jha, C. S., Dadhwal, V. K., 2013. Assessment and monitoring of long-term forest cover changes in Odisha, India using remote sensing and GIS. Environ. Monit. Assess. 185, 4399–4415.
- Res. 26, 427–436.

- Sekerin, V., Dudin, M., Gorokhova, A., Bank, S., and Bank, O. (2019). Mineral resources and national economic security: current features. Mining of Mineral Deposits, 13(1), 72-79.
- Seymour, F., Harris, N. L., 2019. Reducing tropical deforestation. Science 365 (6455), 756–757.
- Sonter, Laura J., Herrera, Diego, Barrett, Damian J., Galford, Gillian L., Moran, Chris J., Soares-Filho, Britaldo S., 2017. Mining drives extensive deforestation in the Brazilian Amazon. Nat. Commun. 8 (1), 1–7.
- Stromann, O., Nascetti, A., Yousif, O., and Ban, Y. (2020). Dimensionality reduction and feature selection for objectbased land cover classification based on Sentinel-1 and Sentinel-2 time series using Google Earth Engine. Remote Sensing, 12(1), 76.
- Swenson, J. J., Carter, C. E., Domec, J. -C., Delgado, C. I., 2011. Gold mining in the Peruvian Amazon: global prices, deforestation, and mercury imports. PLoS One 6 (4), e18875.
- Thonfeld, F., Steinbach, S., Muro, J., Hentze, K., Games, I., Naschen, K., Kauzeni, P. F., ¨ 2020. The impact of anthropogenic land use change on the protected areas of the Kilombero catchment, Tanzania. ISPRS J. Photogramm. Remote Sens. 168, 41–55.
- Tsai, Y. H., Stow, D. A., Lopez-Carr, D., Weeks, J. R., Clarke, K. C., Mensah, F., 2019. ´ Monitoring forest cover change within different reserve types in southern Ghana. Environ. Monit. Assess. 191.
- Turner, B. L., Lambin, E. F., and Reenberg, A. (2007). The emergence of land change science for global environmental change and sustainability. Proceedings of the National Academy of Sciences, 104(52), 20666-20671.
- Xiong, J., Thenkabail, P. S., Tilton, J. C., Gumma, M. K., Teluguntla, P., Oliphant, A., and Gorelick, N. (2017). Nominal 30-m cropland extent map of continental Africa by integrating pixel-based and object-based algorithms using Sentinel-2 and Landsat-8 data on Google Earth Engine. Remote Sensing, 9(10), 1065.
- Yang, L., Shen, F., Zhang, L., Cai, Y., Yi, F., Zhou, C., 2021. Quantifying influences of natural and anthropogenic factors on vegetation changes using structural equation modeling: a case study in Jiangsu Province, China. J. Clean. Prod. 280, 124330.
- Zhao, W., and Du, S. (2016). Learning multiscale and deep representations for classifying remotely sensed imagery. ISPRS Journal of Photogrammetry and Remote Sensing, 113, 155-165.

Impact of Coal Trading Activity on Groundwater Quality in Paradeep Municipality of Odisha

Rosalin Das*, Rabindra Nath Hota[2] and Susanta Kumar Das[2]

P. G. Department of Geology, Fakir Mohan University, Balasore, Odisha

*Email: rosalindas. geology@gmail. com

Abstract

This study investigates the impact of coal trading and port activities on groundwater quality in Paradeep municipality, Odisha, a major industrial and coastal hub. The region faces significant environmental challenges due to coal storage, handling, and transportation. Hydrogeochemical analysis of 32 groundwater samples revealed elevated concentrations of sodium, fluoride, chloride, sulfate, and nitrate, rendering 71. 9% of the samples unsuitable for drinking. Water hardness analysis classified 80% of the samples as moderate to hard and 6% as very hard. Hydrochemical facies, determined using Piper's diagram, indicated Na+-Cl--HCO3−, Na+-Cl−, and Na+-Cl—-SO4− water types, with geospatial mapping identifying contamination hotspots near coal storage areas.

To assess coal-related contamination, six samples from coal storage sites were analyzed for polycyclic aromatic hydrocarbons (PAHs), revealing the presence of phenanthrene, fluoranthene, pyrene, and indeno(1, 2, 3-cd) pyrene. These compounds correlated with sulfate levels, confirming coal's contribution to groundwater pollution. The detection of carcinogenic PAHs poses significant health risks, including respiratory issues and skin irritation. Additionally, coal dust exacerbates soil degradation and acidification of water bodies, further threatening aquatic ecosystems. These findings underscore the urgent need for stringent dust control measures, continuous groundwater monitoring, and alternative water sources to mitigate risks and protect public health in Paradeep.

Introduction

Groundwater quality is a critical concern in coastal industrial regions, where anthropogenic activities significantly impact water resources. Paradeep municipality, located in Odisha's Jagatsinghpur district, is a major seaport and industrial hub, hosting numerous chemical industries and handling extensive coal trading operations. The Paradeep Port Trust (PPT) manages approximately 25 million metric tons of coal annually, making it the largest handler of dry fuel in India. However, improper coal

storage, handling, and transportation practices contribute to severe environmental pollution, particularly groundwater contamination.

Coal dust and particles, dispersed by wind, cyclones, and monsoon rains, infiltrate water bodies, altering water chemistry and posing risks to both human health and ecosystems. Over-extraction of groundwater exacerbates salinization and pollution risks. This study aims to assess the impact of coal-related activities on groundwater quality in Paradeep by analyzing hydrogeochemical parameters and detecting polycyclic aromatic hydrocarbons (PAHs). Findings will aid in formulating strategies for sustainable groundwater management and pollution control.

Study area

Paradip Municipality, located in the Jagatsinghpur district of Odisha, lies within the Mahanadi delta, characterized by deltaic alluvial soils with NE-SW trending horst-graben structures influencing sediment deposition. The geomorphology is shaped by active and defunct distributary channels, ancient beach ridges, tidal flats, swamps, and parallel sand dunes sloping towards the Bay of Bengal. The region's drainage is dominated by the Mahanadi River and its distributaries, exhibiting an anastomosed, braided, and dendritic drainage pattern, with tidal streams and saline marshes influencing coastal hydrology. The area's geological and geomorphological features play a vital role in infrastructure development, flood management, and environmental conservation.

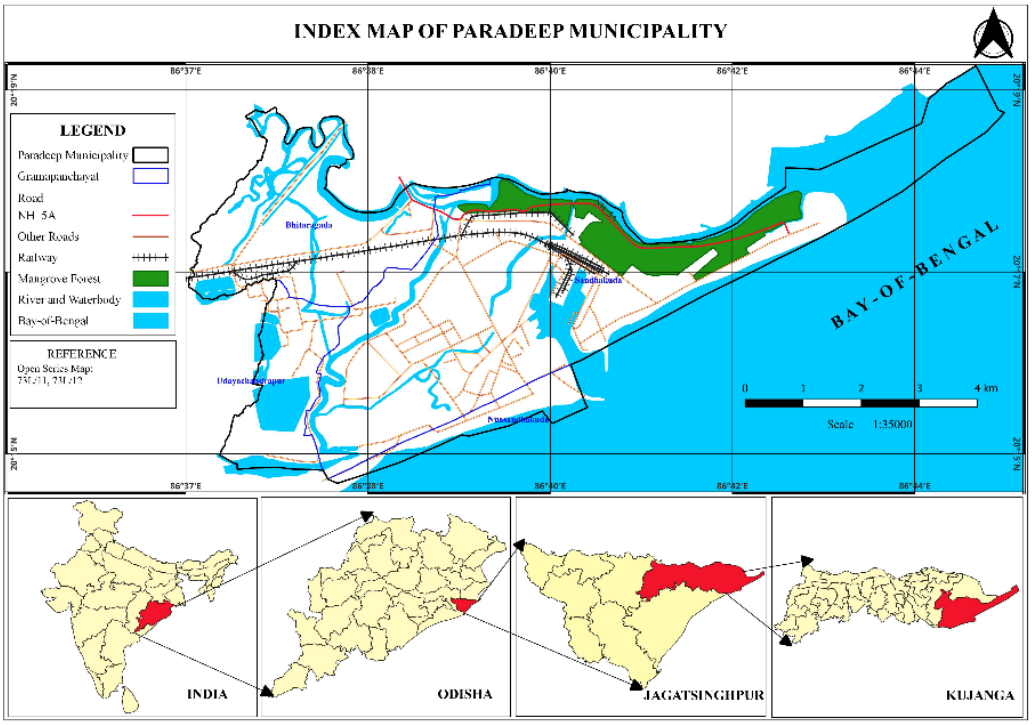

Figure 1: Index Map of Paradeep Municipality

Methodology

2. 1 Groundwater Sampling and Analytical Procedures

Groundwater sampling and analytical procedures were conducted in May 2023 during the pre-monsoon season. A total of thirty-two groundwater samples were collected from tube wells. The samples were analysed for pH, electrical conductivity (EC), total dissolved solids (TDS), major cations and anions by adopting standard analytical procedures (Das, 2022; Das et al, 2015, 2016, 2023; APHA, 2005). Electrical conductivity (EC) and pH were measured using digital meters (Systronics) immediately after sampling. Ca^{2+}, Mg^{2+}, HCO_3^-, CO_3^{2-}, Cl^- and TDS were analysed by volumetric titrations. Flame photometer (Systronics Model No. 128) used to measure Na^+ and K^+ ions. nitrate (NO_3^-), and fluoride (F^-) concentrations were measured using a UV-visible spectrophotometer (Systronics Model No. 2701). Poly Cyclic Aromatic Hydrocarbon (PAH) analysis of water samples has been carried out and analysed in State pollution Control Board Laboratory, Bhubaneswar.

To assess the accuracy of the chemical analyses, the ionic balance error (IBE) was calculated using Equation-1, as proposed by Subba Rao (2017):

$$IBE = \frac{\sum TCC - \sum TCA}{\sum TCC + \sum TCA} \times 100 \quad (1)$$

where ΣTCC represents the total concentration of cations in meq/L, and ΣTCA represents the total concentration of anions in meq/L. The ionic balance errors for all groundwater samples were found to be within ±5%, indicating reasonable accuracy in the analyses. The fig. 2 represents the sampling location and geomorphology map of the study area,

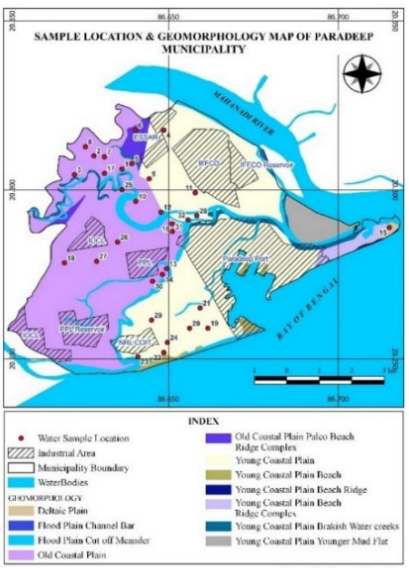

Fig. 2 Sampling Location And Geomorphology Map Of The Study Area

Result and Discussion

Water Chemistry

The groundwater's physicochemical parameters were evaluated against the WHO guidelines to determine their suitability for drinking. (Table: 3) The pH of water may be used as an indicator of its cleanliness and geochemical stability. (Hem, 1985). The pH ranges between 6. 35 -7. 49 is consistent with moderately acidic to slightly alkaline groundwater. Based on the projected EC of 882 to 5286 S/cm, the predicted total dissolved solid (TDS) concentrations are 573 - 3436 mg/l. The total alkalinity might be anywhere between 170 and 450, while the hardness can be anywhere from 80 to 520 mg/l. The most prevalent major cations are calcium (12–1158 mg/l) and magnesium (8. 45–91. 71mg/l), with sodium (132–1057 mg/l) and potassium (0. 23–62 mg/l) present at lower amounts. Bicarbonate, which is produced from carbon dioxide released during organic decomposition in soil and has a high concentration in solution (50-742mg/l), is the most abundant anion (Todd, 1980). Chloride concentrations range between (172-1386 mg/l) may be found in the groundwaters. Sulphate ranges between (22 -144 mg/l) and nitrates with a range of (28-62 mg/l) Temperatures may be between 26. 81- and 36. 4 -degrees Fahrenheit, while iron levels can be anywhere from 0. 56 to 0. 1. 43 mg/l.

Table 1: Descriptive Statistics of Physico-Chemical Parameters

	Minimum	Maximum	Mean	Std. Deviation	WHO standard	Exceeding
pH	6. 35	7. 49	7. 0856	. 32818	6. 5–8. 5	
EC	882. 00	5286. 00	2365. 1875	1285. 92358	750	100%
TDS	573. 00	3436. 00	1537. 3750	835. 87473	500	100%
TA	170. 00	450. 00	311. 2500	70. 65363	-	
TH	80. 00	520. 00	212. 1875	109. 75734	-	
Ca^{2+}	12. 00	62. 00	36. 1875	14. 36042	75	
Mg^{2+}	8. 45	91. 71	29. 6541	20. 11291	50	12. 5%
Na^{+}	132. 00	1057. 00	428. 0937	276. 47101	200	81. 25%
K^{+}	. 23	62. 00	12. 3687	16. 36792	30	18. 75%
Fe	. 19	1. 38	. 5125	. 25177	1	3. 12%
HCO_3^{-}	50. 00	742. 00	320. 6875	178. 82185	100	92%
Cl^{-}	172. 00	1386. 00	562. 5313	357. 99531	200	92%
SO_4^{2-}	22. 00	144. 00	96. 5625	28. 07816	200	
NO_3^{-}	28. 00	62. 00	42. 5313	6. 62831	45	22%
F^{-}	. 56	1. 43	1. 0631	. 26217	1	43. 75%

*Units of all parameters except pH (no unit) and EC (µS/cm) are mg/L.

The abundance sequence of cations in the groundwater is $Na^+ > Ca^{2+} > Mg^{2+} > K^+$. The dominance of Na^+ in groundwater points to the prolific weathering and dissolution of the basement rocks as well as anthropogenic inputs and saline water intrusion. The decreasing order of abundance of anions is $Cl^- > HCO_3^- > F^- > SO_4^{2-}$. The highest concentration of HCO_3^- suggests the prevalence of mineral dissolution in the groundwater system (Subba Rao, 2018). Wide range of standard deviation values of the chemical parameters indicate varied distribution of the salts in groundwater (Subba Rao et al. 2017).

Hydrochemical Facies

Piper's ternary diagram: The Piper's ternary diagram (Piper, 1953) is used to infer hydrogeochemical facies of the study area. These plots include two triangles, one for cations and the other for plotting anions. The cation and anion fields are combined to show a single point in a diamond-shaped field, from which inference is drawn on the basis of hydro geochemical facies concept (Das et al, 2023). A Piper trilinear diagram (Fig. 3) displaying the water samples reveals distinct groupings based on their chemical compositions. The 12 samples of Na^+-Cl^- type water cluster near the sodium and chloride vertices, indicating saline ingression in the region. The 18 samples of Na^+-Cl^--HCO_3^- type water are spread between the chloride and bicarbonate vertices, showing mixed dominance with high sodium. A single sample near the port, characterized as Na^+-Cl^--SO_4^- type water, is positioned near the sodium and chloride vertices but closer to sulfate. In the central diamond field, the Na^+-Cl^- type samples are in the upper right, the Na^+-Cl^--HCO_3^- type samples occupy the central upper area, and the Na^+-Cl^--SO_4^- type sample leans towards the sulfate region, where the groundwater may be impacted due to the coal import activity. This distribution illustrates the varying water chemistries and their potential sources.

The predominant cation present in the samples was sodium. As a result, the water quality of Paradeep municipality area was classified as either Na^+-Cl^--HCO_3^- or Na^+-Cl^- type, and Na^+-Cl^--SO_4^- type.

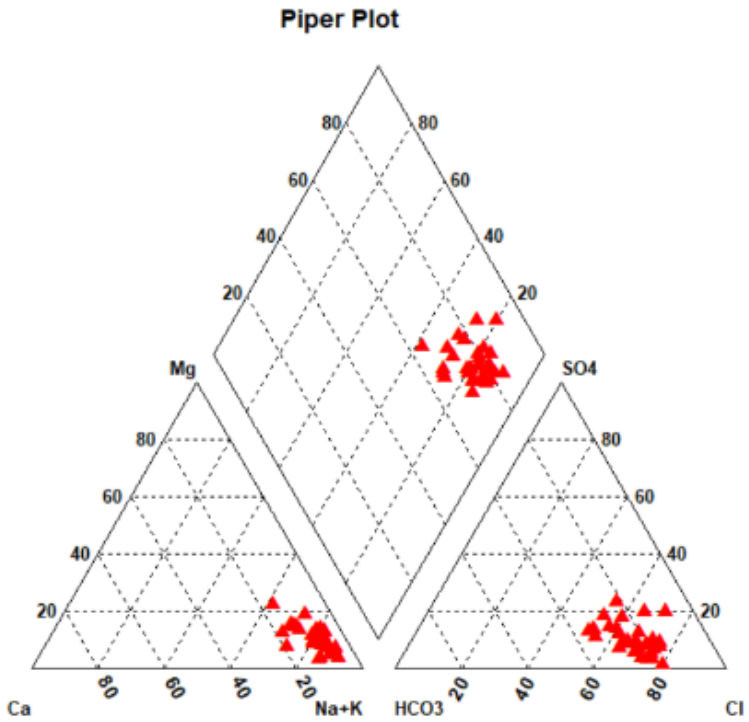

Figure 3: Piper's Ternary Diagram

Recent Statistics of Coal Import activity and it's impact:

The Paradip port has become the highest cargo handling major port of the country in the financial year 2023-24 (Ministry of Ports, Shipping and Waterways, April 2024). In 2023-24, the Paradip port handled 145. 38 million metric tons (MMT) of cargo. It handled 10. 02 million metric tons more cargo than 2022, registering a growth of 7. 4 percent. The port has capacity to handle 289 million metric tonnes.

Based on the observations in Table 2, it is inferred that from June 2022 to June 2023, a total of 43, 119, 845 tons of coal were traded, whereas from July 2023 to June 2024, the coal trading increased to 44, 328, 808 tons. This indicates a significant rise in coal trading at the port, which is likely contributing to increased environmental pollution due to the accumulation of coal dust.

Table 2: Monthly Coal traffic during the observation period

	2024	**2023**	**2022**
June	3880758	3526008	
May	3755092	3828213	
April	3821524	3774048	
March	4154287	4390768	

February	3764292	3882283	
January	4372040	3536455	
December		3419770	3787291
November		3570845	3214815
October		3594484	2870909
September		3627477	3073686
August		3075384	3708402
July		3292855	3526967
June		3526008	

Polycyclic Aromatic Hydrocarbons (PAH) Analysis of Groundwater of Study area

To assess the impact of coal on water quality, six samples were collected from various locations within Paradeep municipality. These samples were analyzed for the presence of polycyclic aromatic hydrocarbons (PAHs) at the State Pollution Control Board laboratory. PAHs are known to persist in the environment and tend to accumulate in sediments and biota rather than dissolving in water. The rate at which PAHs migrate from the surface to groundwater is influenced by soil type and permeability; for instance, sandy or loosely packed soils allow faster infiltration. Additionally, local hydrological factors, such as the depth of the water table and groundwater flow patterns, play a key role in determining PAH dispersion and concentration in groundwater.

Result and Discussion

The analysis conducted aimed to detect the presence of polycyclic aromatic hydrocarbons (PAHs) in water samples. Out of the 13 PAHs tested, phenanthrene, fluoranthene, pyrene, and indeno (1, 2, 3-cd) pyrene were identified, as shown in Table 2. Studies suggest that PAHs originating from coal can infiltrate groundwater through leaching, especially in areas with intensive coal-related activities such as processing and storage. The graph (Fig. 3) illustrates the concentration levels of these PAHs in various water samples. The presence of indeno (1, 2, 3-cd) pyrene in groundwater and fluoranthene in surface water within the Paradip Port area is largely attributed to coal import operations. These activities encompass the storage, handling, transportation, and combustion of coal. To manage and mitigate such contamination, it is crucial to implement effective monitoring, ensure regulatory compliance, and adopt pollution prevention and remediation strategies, protecting both the environment and public health.

Table: 3 Groundwater analysis for Polycyclic aromatic hydrocarbons (PAHs)

PAH	SW1	GW20	GW26	GW7	GW16	GW19
Phenanthrene	0.00013	0.00009	0.00008		0.00014	0.00012
Fluoroanthracene	0.2921	0	0		0	0
Pyrene	0	0	0		0.00011	0
Indeno(123-cd) pyrene	0	0.11308 PPM	0.20012 PPM		0	0

Environmental Impact and Health Concerns

Human Health: Both Indeno(1, 2, 3-cd) pyrene and fluoranthene are carcinogenic and can cause other health issues, including respiratory problems and skin irritation, upon exposure. Ecosystem Damage: These PAHs are toxic to aquatic life and can affect the overall health of ecosystems, potentially leading to bioaccumulation in the food chain.

Conclusion

The study highlights the significant impact of coal trading activities on groundwater quality in Paradeep municipality, Odisha. Hydrogeochemical analysis of groundwater samples reveals elevated concentrations of sodium, chloride, fluoride, sulfate, and nitrate, with a majority of samples exceeding permissible drinking water limits. The presence of polycyclic aromatic hydrocarbons (PAHs), including phenanthrene, fluoranthene, pyrene, and indeno(1, 2, 3-cd) pyrene, further confirms coal-related contamination, particularly in areas near storage and handling sites. The correlation between PAH and sulfate concentrations indicates that coal dust and leachate contribute to groundwater pollution, posing serious environmental and public health risks.

The increasing coal trading volume at Paradeep Port underscores the urgency of implementing stringent environmental management strategies. Effective dust control measures, improved coal handling procedures, and continuous groundwater monitoring are essential to mitigate pollution risks. Additionally, alternative water supply solutions should be explored to ensure safe drinking water for the local population. This research emphasizes the need for proactive policy interventions and sustainable groundwater management practices to safeguard environmental and human health in the region.

Reference:

- Piper, A. M. (1953) A graphic procedure in the geo-chemical interpretation of water analysis. USGS Groundwater Note No. 12.
- Subba Rao, N. (2017) Hydrogeology - Problems with solutions. PHI Learning Pvt. Ltd., Delhi.

- Das, U., Hota, S. R., Das, R. and Hota, R. N. (2023) Statistical and geochemical evaluation of fluoride-rich groundwater from north coastal part of Odisha. Journal of the Geological Society of India, v. pp. 1705-1715. https://doi. org/10. 1007/s12594-023-2526-3
- Das, U. and Das, R. (2023) Aquifer salinization: A groundwater appraisal of northeast coast of Odisha using water quality index (WQI) and geospatial interpretation; Ec0. Env. &Cons. 29(3):2023; pp. (1086-1095) DOI No. :http://doi. org/10. 53550/EEC. 2023. v29i03. 011
- Das, R. 2022. Monitoring the seasonal variation of groundwater chemistry and quality assessment for agricultural and industrial purpose of Athgarh basin, India, Journal of Environment, Ecology and Conservation, Eco. Env. & Cons. 28 (1), pp. 298-309, Copyright@ EM International, ISSN 0971–765X, DOI No. : http://doi. org/10. 53550/EEC. 2022. v28i01. 043
- APHA (2012) Standard methods for the examination of water and wastewater, 19th edn. American Public Health Association, Washington DC.
- Das, R., Das, M. and Goswami, S. 2016. Groundwater quality Assesment for drinking and industrial purpose of Rourkela, Sundergarh District, Odisha, India. International Journal of Earth Science and Engineering. (6), pp. 314-321.
- as, R., Goswami, S., Das, S., Das, M. 2015. Hydrogeochemistry and Groundwater quality assessment for irrigation purpose in and around Rayagada Town, Odisha, India. International Journal of Earth Science and Engineering 8 (2), pp. 611- 616. (SJR:0. 15) (ISSN:0974- 5904), http://cafetinnova. org/journals/ ijee/about- journal/) SCOPUS UGC No. 2901

Oil Spills and Coastal Sustainability: A multidimensional Perspective on Biodiversity and Economy

Sayan Kumar Manna, Asim Amitabh Pradhan* and Satyabrata Nayak

Department of Geology, Fakir Mohan University, Balasore

*Email: asimgeology@gmail.com

Abstract:

Disaster is a sudden, devastating event which causes significant damage or loss of life. It may be natural or manmade but, in both cases, destruction is the only result. Increasing marine traffic in sea creates possible chances of spill. Oil is mainly transported through ships and pipes. So, a huge quantity of oil is transferred through water ways. Oil spill refers to the sudden release of oil to water surface that may be on sea /ocean or land surface. It may be released by vessels, ships, failure of oil rig or breakdown of pipes etc. Oil spill is considered as one of the disturbing disasters as it harms coastal ecosystems, coastal communities as well as economy. It causes a wide range of impacts in the marine environment and emerged as 'environmental disasters'. The costal ecosystem comprises of diverse flora, fauna and marine animals which are highly vulnerable to oil spill due to their ecological complexity and interdependence. It can't cause sudden death of organisms but can impact the physiology and behaviour of animals. It has great impact on coast changing its characteristics and soil condition. It affects sandy or muddy beaches, mangroves, wetlands and nearby forests. In addition to poisoning, oil reaching coastal wetlands can smoother plants by cutting off oxygen from the plants' root systems and turn contribute to wetland erosion. Apart from this oil spill impacts to communities as well as economy of a country. Immediate impacts include beach, water and fisheries closure resulting in lost and diminished user days to beach access, fishing, boating and other activities that boosts economy. Closure of these activities can have monetary losses. Besides these beach and wetland recreational area closures lead to additional economic, cultural and social losses to local communities and tourism. The simultaneous impact on biodiversity and the economy highlights the critical need for preventive measures, fast response mechanisms and long-term restoration projects. Protecting coastal ecosystems is critical not only for environmental resilience, but also for ensuring the economic well-being of people that rely on them.

Key Words: Biodiversity, Coast, Economy, Ecosystem, Oil Spill

Introduction:

Offshore oil spills have a disastrous impact on marine and coastal ecosystems (Gilbert 1999; Chang *et. al*. 2014). Disasters are one of the brutal incidents both for human and organisms. It may be happened due to manmade or natural causes. Starting from drinking to transportation oil is the prime source. But when it comes to transportation the crude oil is taken into consideration. Depending upon increasing rate of use of oil the possible chances of oil spill increases (Michel and Fingas, 2016). It is extracted from both off-shore and on-shore region. The extracted oil is named as crude oil as it contains many other substances along with oil (Punati and Raju, 2017). The products of crude oil are Petroleum, LPG (Liquified Petroleum Gas) and feedstock for the petrochemical Industries. Most of the world's production of crude oil is transported through sea, where 48% of the marine oil pollution is due to fuels and 29% due to crude oil (Vethamony, *et. al.,* 2007). Fig-1 shows the significant rise of oil spill has increased in 2023 in comparison to last five years. Globalisation has increased dependence on maritime transport, which is responsible for almost 90% of world trade (UNCTAD, 2020). Exploration and transportation of oil and gas carry the risk of leakage or spill accidents (Zabbey and Olsson, 2017).

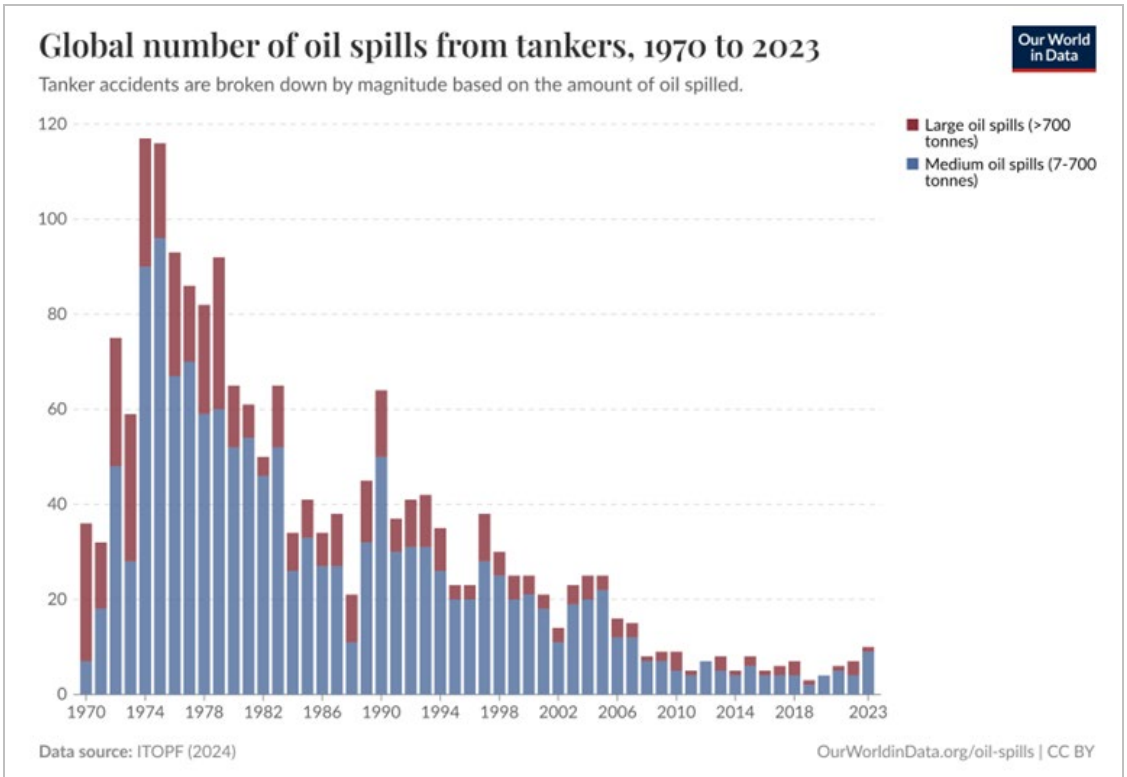

Fig-1 Global number of oil spill, 1970-2023 (Our world in data)

Oceans are being used extensively for oil exploration, navigation, marine transportation, and other oil-related activities due to the ever-growing demand for energy in our society (Kankara and Subramanian, 2007). oil spills resulting from maritime disasters or operational incidents have become a worrying environmental problem that can have lasting repercussions on marine ecosystems (Peterson et. *al*., 2003). The economic consequences of oil spills are also considerable. The loss of income in sectors such as fishing, tourism, and the maritime industry can be massive and long-term (Cohen, 1995). Oil spill is the leakage or release of oil, probably crude oil, into the environment especially to marine ecosystem. It can be due to the leakage in off-shore pipeline, collision between oil tankers in ocean or release of oil from oil industries due to technical failures etc. When the oil spills into the water surface, it undergoes various physio-chemical changes in oil viscosity, density, and interfacial tension (Daling and Strom, 1999). It includes spreading, evaporation, and dispersion like physio- chemical processes. Evaporation, dispersion, and emulsification depend on the chemical properties of oil and various environmental factors (Sebastio and Guedes, 1995). Continued dependence on oil and shipping creates a tension between economic growth and environmental protection, a complex dynamic that requires careful study (Etkin, 2000).

Oil Spill:

An oil spill refers to the sudden release of oil from pipelines or ships into the surface of sea or ocean water. In other words, "Oil spill is the sudden release of oil from vessels, tankers and oil barrels into the water surface which is very hazardous to the surrounding ecosystem and human habitat" (Othumpangat and Castranova, 2014). This oil spill generally associated with marine water as most of the crude oil is transported through route as it is one of the convenient modes of transportation. The crude oil consists of various products like LPG, petroleum which creates marine pollution and hazard. It is one of the disastrous incidents on marine water which has significant impact on marine, organism, surrounding environment, marine water, human habitat and economy (Hettithanthri *et. al.,* 2024)

History of Oil Spill:

Depending upon necessity of crude oil to the society a huge amount of Oil gets transported through Ocean which uses smaller to larger ships. In recent times increase in oil tanker movement is reported from the Bay of Bengal (Desa *et. al*., 2002). The ascending order of ships in ocean creates oil spill and pose threat to future spill. Maritime transport along this sensitive coastal region points at oil spill risk for several reasons like accident, leaking, or grounding ships (Carpenter, 2019). Yet, the world has been racked by many disastrous and major oil spills which have a great impact on organisms as well as humans. They are-

- The world's largest oil spill 'Gulf war oil spill' was not an accident it's a result of War between Iraq and USA. In this connection, huge gallons of oil are believed to have discharged into Persian Gulf (Michel, 2011).
- 'Deep water Horizon' or' Gulf Mexico Oil Spill' also a major oil spill happened due to explosion of Oil rig. About 4. 9 million barrels of oil flowed on Gulf of Mexico (Griggs, 2011).

Oil Spill in India and Odisha:

Indian cost also recorded several numbers of oil spill which also had an adverse as well as hazardous effect on organisms followed by humans. These are-

- On 28th Jan, 2007, an oil spill took place outside the Kamjor Port in Ennore near Chennai (Begum *et. al.,* 2022).

In few recent times Odisha have not faced major oil spills. But there are some minor cases of oil spill are found which are not so hazardous but pose threat to living organisms. They are-

- Crude oil pipeline of Indian Oil Corporation connecting Haldia- Paradip line got leaked near Paradip Port. Since, no casualties reported.
- Two minor oil spill was done by MV Black Rose ship at Paradip Port Anchorage and MV Malavika at Gopalpur beach (Passen, 2015).

Causes and Effects of Oil Spill:

Oil spill can happen both land and water surface. But off-shore oil spills have a disastrous impact on marine and coastal ecosystems (Gilbert, 1999; Chang *et. al*., 2014). Exploration and transportation of oil and gas carry the risk of leakage or spill accidents (Zabbey and Olsson, 2017). Oil spills have numerous causes that impact on surrounding ecosystem and biodiversity but here are mainly two causes for which oil spill happens (Ismila *et. al*., 2020). One is natural Cause and another one is human cause. Natural cause is very negligible where as manmade cause has significant impact on various sources.

Natural Cause- Sometime oil comes out to surface from deep ocean due to sedimentary rock degradation and rupture of rocks. But this process is quite negligible.

Human Cause- This is the main source of oil spill causes which are highly vulnerable and risky to natural resources as well as ecosystem. Large vessels like tankers can cause oil spills due to the following factors (Zabbey and Olsson, 2017):

- Poor storage management
- Heavy water traffic from massive oil transport
- Human error and negligence

- Tanker collisions
- Improper routine operations
- Rig failures or accidents
- Illegal industrial activities
- Machinery failures in refineries
- Natural disasters (earthquakes, tsunamis)

Equipment malfunctions or breakages in oil exploration, extraction, or transportation also contribute to spills.

Effects of Oil spill:

Oil spill has very hazardous impact on marine ecosystem as well as human being (Chang *et. al*., 2014). They are-

- ✓ It pollutes marine environment and its surrounding eco-system as it contains toxic substances.
- ✓ It causes death of aquatic marine organisms. It is fatal for birds, marine mammals (whale, dolphins, seals), fish (eggs get disposed to water and get destroyed), wildlife habitat and breeding grounds (Sea turtles) etc.
- ✓ It poisons the sea food.
- ✓ It destroys mangroves and other vegetation surrounding the beach.

Background of the study:

Odisha is a coastal district of India where its coast extends about 574. 7 km. In the recent report from the Union Ministry of Home Affairs, India shows that Odisha's coast gets a significant extension of about 96 km which shows the importance of Odisha as a coastal district. Odisha has six coastal districts starting from Balasore to Ganjam (Fig-2). Odisha has rich source of various minerals as a result numerous industries like mining, refineries, automobile have established and for smooth transportation of goods some ports have been established (Govt. of Odisha, Report). Out of them Paradip port is significant one. But to manage the workload there are other two ports have been proposed one in Balasore, and one is in Ganjam. They are one of the finest ports after Paradip port. The most interesting thing is that the coastal sites and port sites of Odisha have significant biodiversity and mangrove habitat (Shyamal, 2023). These are very sensible and vulnerable to oil spill. Odisha can be highly affected by the impact of oil spill and will be highly impact on economy as well as tourism of the state. So, it is very important to assess the immediate and long-term impacts of oil spills on coastal and marine biodiversity, including species and habitat degradation. There should be a sustainable policy proposal that strike a balance between industrial activity, environmental conservation, and community welfare.

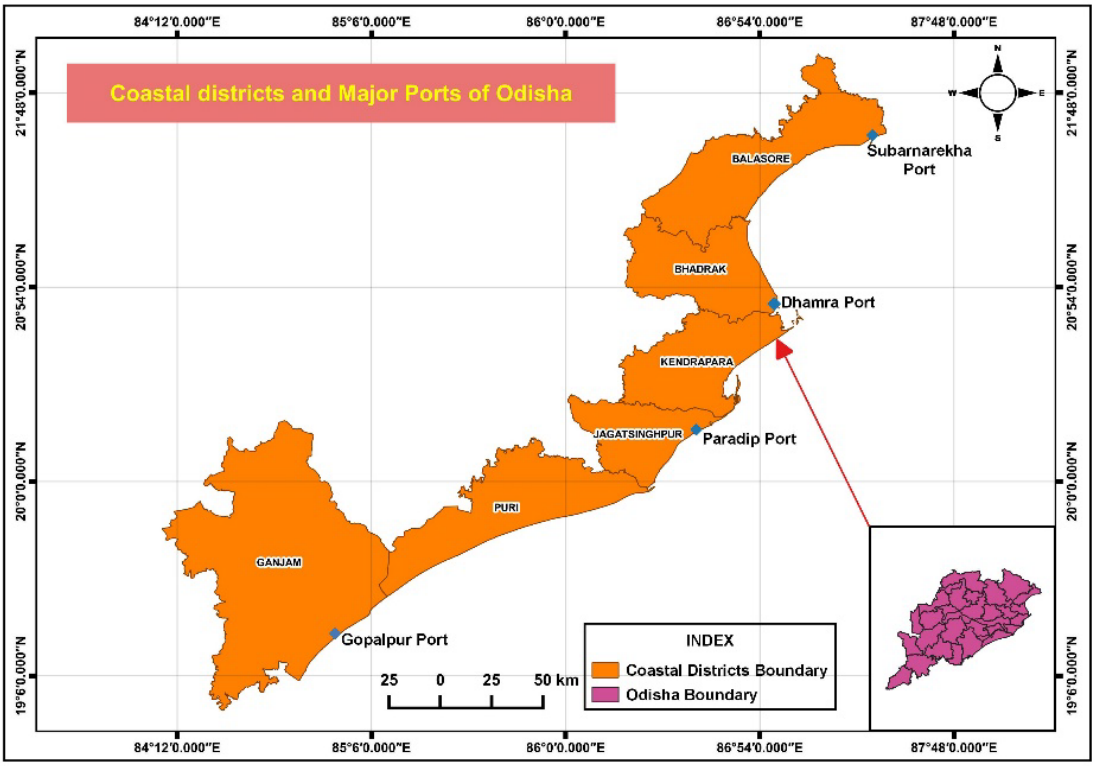

Fig-2 Coastal districts and ports of Odisha

Environmental Impact of Oil Spill:

Oil spilled on shorelines can cause major habitat damage and pose serious threats to all living organisms living on and within shorelines (Michel *et. al*., 2017). Oil spills represent one of the most catastrophic forms of environmental devastation, with immediate and visible ramifications for marine and coastal ecosystems. According to Leighton 1993, these spills can cause significant mortality in marine flora and fauna. Seabirds, which are particularly vulnerable, often suffer from hypothermia and poisoning as a result of the degradation of the insulating and buoyant properties of their plumage (VanBlaricom, 1990). Fish fauna is also directly influenced by oil spills, with adverse effects on growth, reproduction, and (Heintz *et. al*., 1999). Coastal habitats, particularly mangroves and salt marshes, are particularly vulnerable to oil spills. It damages the marine living organisms like mammals, turtles, crabs etc. It has also diverse impact on land organisms like birds, common dwelling organisms, cows, ships, goat etc. Coral reefs, salt marshes, mangrove plants get oiled which leads to death of them (Asif *et. al*., 2022). Mangroves are the ultimate defender of the nature, damage of these may lead to instability of biodiversity.

Impact of Oil spill on Economy:

Oil spills have profound and wide-ranging economic consequences that affect several sectors, and understanding these economic impacts is essential for management, planning, and legislation in regions exposed to such risks (Moussaoui and Idelhakkar, 2023). Odisha is considered as good source of revenue generator due to the presence of number of beaches. As beaches are the good source of revenue booster. Odisha has extensive beaches and islands like Chandipur beach, Astarang beach, Puri beach, Gopalpur beach whereas Puri beach is named as blue flagged beach. These beaches attract huge number of tourists every year which plays a vital role in revenue generation and boost country's economy. Oil spill on this area can damage the beaches and may be the reason of closure of beaches. It also polluted the soil of the surrounding areas of the beach which may causes closure of the area (Rout and Sharma, 2013). It can also pollute the underground water and can create several health problems. If oil spill happens these activities will be highly affected.

Policies and Regulations:

Oil spill is a hazardous incident that has great impact on surrounding environment and living organisms. Timely and highly efficient responses can lead to more hopeful outcomes with less overall damage to the environment. Even though preventing oil spills is the ideal goal, approaches for controlling and cleaning need to be taken seriously with rapid and effective implementations (Lee *et. al*., 2015). To protect these resources and organisms' proper response plan and strategies are required. Indian coast guards are the first authority to tackle an oil spill in India. Besides them there are many NGOs, Policy makers are present who consciously look over the oil spill incident and put proper policies and management plant to prevent the impact of Oil Spill. Government of India has many regulations and policies which should highly applicable to industries norms and policy maker norms. There should be affective management plan to be prepared by the district administration and the local industry people to manage oil spill incident and to protect the vulnerable and sensible resources.

Conclusion:

Oil strengthens a country's economy as it improves country's GDP and economy too. Oceans are considered as store house of all types of minerals and other substance. Oceans are used as transportation of goods, navigation and oil exploration. Transportation of oil and gas creates possible chance of oil spill. Oil spill creates hazardous impact on ecology, surrounding biodiversity causing death of aquatic as well as marine organisms. It also effects on economy and destroys beaches which directly impacts on tourism sector. To protect all the vulnerable and sensible resources there should be proper policy, regulations and management plan be prepared to tackle the spill at earliest keeping the resources safe and secure. So, regulations and policies should be

strictly implemented by the government and the response planner should aware on these to prepare an effective management plan.

Reference

- Asif, Z., Chen, Z., An, C. and Dong. J. (2022). Environmental impacts and challenges associated with oil spill on shorelines. *J. Mar. Sci. Eng. v. 10, no. 6, p. 762.*
- Begum, M, Ezhilarasan, P., Muthukumar, C., Gopinath, G., Panda, U. S., Naik, S., Sura, A. N., Karthikeyan, P., Dash, S. K., Mishra, P., Pradhan, U. K., Bharathi, M. D., Iyyappan. M., Usha, T. and Murthy M. V. R. (2022). Assessment of Ennore Oil Spill 2017 on Chennai Coastal Water and Biota. Conference Proceedings. DOI:10. 1109/OCEANSChennai45887. 2022. 9775218
- Carpenter, A. (2019). Oil pollution in the North Sea: the impact of governance measures on oil pollution over several decades. Hydrobio-logia, v. 845, pp. 109–127. https://doi. org/10. 1007/s10750-018-3559
- Chang, S. E, Stone J., Demes, K. and Piscitelli, M. (2014). Consequences of oil spills: a review and framework for informing planning. Ecol Soc, v. 19, no2, p. 26. https://doi. org/10. 5751/ES-06406-190226
- Chang, S. E., Stone, J., Demes, K. W. and Doshkov, M. A. P. (2014). Consequences of oil spills: A review and framework for informing planning (2014). Ecology and Society. v. 19, no. 2, p. 26. DOI:10. 5751/ES-06406-190226
- Cohen, M. (1995). Technological disasters and natural resource damage assessment: An evaluation of the Exxon Valdez oil spill. Land Economics, v. 71, no. 1, pp. 65-82.
- Desa, E., Zinged, M. D. and Vethamony, P. (2002). Marine Environmental Man agement Strategies for the Gulf of Kachchh. Report No. NIO/ SP-13/2003 National Institute of Oceanography, Goa.
- Etkin, D. S. (2000). Analysis of oil spill trends in the United States and worldwide. International Oil Spill Conference Proceedings, v. 2000, no. 1, pp. 1291-1296.
- Geology and Mineral Resources of Odisha. Odishaminerals. gov. in.
- Gilbert, T. D. (1999). Oil spills in the Australian marine environment: environmental consequences and response technologies. In: Proceedings of the Australian oil and gas conference, Perth, 22–23 Apr 1999.
- Griggs, J. W. (2011). BP Gulf of Mexico oil spill. Energy Law Journal, v. 32, no. 57.
- Heintz, R. A. (1999). Delayed effects on growth and marine survival of pink salmon Oncorhynchus gorbuscha after exposure to crude oil during embryonic development. Marine Ecology Progress Series, v. 208, pp. 205-216.

- Hettithanthri, O., Nguyen, T. B. T., Fiedler, T., Phan, C., Vithange, M., Pallewatta, S., Nguyen, T. M. L., Nguyen, P. Q. A. and Bolan, N. (2024). A review of oil spill dynamics: Statistics, impacts, countermeasures, and weathering behaviors. Asia-Pacific Jour of Chem Eng. v. 19, no. 6. DOI: https://doi. org/10. 1002/apj. 3128
- Ismila, C., Ishak, I. C., Arof, A. Md. and Zoolfakar, M. D. R. (2020). The Causes of the Oil Spill Incident: A Review Paper. Conference Proceedings.
- Kankara, R. S. and Subramanian, B. R. (2007). Oil Spill Sensitivity Analysis and Risk Assessment for Gulf of Kachchh, India, Using Integrated Modelling. J of Coast Res, v. 23, no. 5, pp. 1251-1258. DOI: 10. 2112/04-0362. 1
- Lee, K., Boufadel, M., Chen, B., Foght, J., Hodson, P. and Swanson, S. (2015). The behaviour and environmental impacts of crude oil released into aqueous environments. Ottawa: The Royal Society of Canada.
- Leighton, F. A. (1993). The toxicity of petroleum oils to birds. Environmental Reviews, v. 1, no. 2, pp. 92-103.
- Michel, J. (2011). 1991 Gulf War Oil Spill. Oil Spill Science and Technology, pp. 1127–1132. DOI:10. 1016/b978-1-85617-943-0. 10037-1
- Michel, J. and Fingas, M. (2016). Oil Spills: Causes, Consequences, Prevention, and Countermeasures. Fossil Fuel., pp. 159–201.
- Michel, J., Fegley, S. R., Dahlin, J. A. and Wood, C. Oil spill response-related injuries on sand beaches: When shoreline treatment extends the impacts beyond the oil (2017). Mar. Ecol. Prog. Ser., v. 576, pp. 203–218.
- Moussaoui, N. EL and Idelhakkar, B (2023). The impact of oil spills on the economy and the environment. Euro Jour of Eco and fin res. v. 7, no. 4.
- Othumpangat, S. and Castranoda, V. (2014). Oil Spills. Encyclopedia of Toxicology, pp. 677-681. DOI:10. 1016/b978-0-12-386454-3. 00359-6
- Our World in Data (https://ourworldindata. org/oil-spills)
- Peterson, C. H. (2003) Long-term ecosystem response to the Exxon Valdez oil spill. Science, v. 302, no. 5653, pp. 2082-2086.
- Punati, N. and Raju, R. (2017). Determinants of Crude Oil Prices in India. International journal of economics and Management studies. v. 4, no. 10, pp. 1-9.
- Rout, C. and Sharma, A. (2013). Oil Spill in Marine Environment: Fate and Effects. International conference on ESTEEM.
- Sebastiao, P. and Guedes, S. C. (1995). Modelling the fate oil spills at sea. Spill Sci Technol Bull, v. 2, pp. 121-131.
- Shyamal, B. (2023). Bhitarkanika: Biodiversity Hotspot of Unique Mangrove Ecosystem on Brahmani, Baitarani & Dhamra Delta, Orissa, India. Int Jour of creative res and thought. v. 11, no. 5.

- UNCTAD. Review of Maritime Transport (2020). United Nations Conference on Trade and Development.
- Van Passen, L. A., Vardon, P. J. and Jeffery, P. (2015). Cargo liquefaction in bulk carriers: a review. Yearbook Mijnbouwkundige Vereeniging. Conference Proceedings.
- VanBlaricom, G. R. (1990). Capture of lightly oiled sea otters for rehabilitation: a review of decisions and issues. Biological Report, v. 90, p. 130.
- Vethamony, P., Sudheesh, K., Babu, M. T., Jayakumar, S., Manimurali, R. and Saran, A. K., Sharma L. H., Rajan, B. and Srivastava, M. (2007). Trajectory of an Oil spill off Goa, eastern Arabian Sea: field observations and simulations, Environmental Pollution v. 148 no. 2, pp. 438-444. DOI: 10. 1016/j. envpol. 2006. 12. 017
- Zabbey, N. and Olsson, G. (2017). Conflicts—oil exploration and water. Glob Chall (Hoboken, NJ), v. 1, no. 5, pp. 1-2. DOI:1600015. https ://doi. org/10. 1002/ gch2. 201600015

Spatial and Morphometric Analysis of the Ghodahada River Basin, Odisha Using GIS and Remote Sensing

Santosh Kumar Rout[1], Rosalin Das*, Susanta Kumar Das[1], Barsarani Mallick[1] and Subhadrarani Das[2]

Department of Geology, Fakir Mohan University, Balasore

*E-mail: santosh. rout07@gmail. com

Abstract

The Rushikulya River basin, covering 8, 402 km², is located in southern Odisha, India, along the eastern coast, bordering the southern edge of Chilika Lake. Surrounded by the Eastern Ghats, it opens to the Bay of Bengal. This study focuses on the Ghodahada sub-basin, within Ganjam and Gajapati districts. Geomorphic analysis of the sub-basin was conducted using Survey of India topographical sheets (74A/6 to 74A/11) at a 1:50, 000 scale to understand its evolution and characteristics. Morphometric analysis is crucial for understanding hydrological processes and stream network dynamics, essential for effective water resource management. This study utilizes remote sensing satellite data and advanced GIS techniques to conduct a comprehensive morphometric analysis of the Ghodahada River basin, aneighth-order basin primarily composed of lower-order streams. Key drainage parameters, including linear, aerial, and relief aspects, were examined to evaluate the basin's morphology. Predominantly dendritic to sub-dendritic drainage patterns indicate uniform lithological characteristics. First-order streams dominate the basin's stream order frequency, decreasing with higher orders. The basin's maximum relative relief of 1, 239. 68 meters and slopes up to 45° suggest a predominantly flat to gently sloping terrain with localized steep regions. A total of 2, 268 stream segments were mapped, comprising 1, 037 first-order streams and one seventh-order stream. The stream frequency is 1. 80 km/km², and the drainage density is 1. 36 km/km², reflecting moderate drainage and resistant, permeable subsurface materials. The relief ratio is 0. 98, and the longest seventh-order stream spans 65. 56 km, indicating a mature geomorphic stage. This study underscores the effectiveness of remote sensing and GIS in detailed basin analysis, providing critical insights for hydrological studies and sustainable resource management.

Keywords- Morphometric, Ghodahada Basin, Gis, Remote Sensing, Dem

Introduction

Morphometry involves measuring and mathematically analyzing the shape, configuration, and dimensions of the Earth's surface and its landforms (Clarke 1996; Agarwal 1998; Obi Reddy et al. 2002). Morphometric analysis is effectively carried out by measuring the linear, aerial, and relief characteristics, as well as the gradient of the channel network and the contributing ground slope of the basin (Nautiyal 1994; Nag and Chakraborty 2003; Magesh et al. 2012b). A well-established principle of morphometry is that the morphology of a drainage basin reflects the influence of various geological and geomorphological processes over time, as demonstrated by numerous studies (Horton 1945; Strahler 1952, 1964; Muller 1968; Shreve 1969; Evans 1972, 1984; Chorley et al. 1984; Merritts and Vincent 1989; Ohmori 1993; Cox 1994; Oguchi 1997; Burrough and McDonnell 1998; Hurtrez et al. 1999).

It is well established that drainage morphometry plays a crucial role in understanding landform processes, soil physical properties, and erosional characteristics. The analysis of drainage is incomplete without a systematic approach to understanding the development of the drainage basin in the area. Drainage lines in an area not only reveal the current three-dimensional geometry of the region but also provide insights into its evolutionary processes (Singh 1980).

Drainage offers a fundamental basis for understanding the initial gradient, variations in rock resistance, structural controls, and the geological and geomorphological history of a drainage basin or watershed. Evaluating morphometric parameters involves analyzing various drainage features, including stream ordering, basin area and perimeter, channel length, drainage density (Dd), bifurcation ratio (Rb), stream length ratio (RL), and relief ratio (Rh). Additionally, the quantitative analysis of the drainage system is a crucial aspect of watershed characteristics (Strahler 1964). It plays a key role in hydrological investigations, including groundwater potential assessment, groundwater management, basin management, and environmental evaluation.

Hydrologic and geomorphic processes take place within the watershed, and morphometric characterization at this scale provides insights into the formation and development of land surface processes (Singh 1992, 1995; Dar et al. 2013). The drainage characteristics of various river basins and sub-basins worldwide have been examined using conventional methods (Horton 1945; Strahler 1957, 1964; Krishnamurthy et al. 1996). The surface runoff and flow intensity of a drainage system can be estimated by analyzing the geomorphic features associated with morphometric parameters (Ozdemir and Bird 2009). In Strahler's classification system, a stream segment with no tributaries is designated as a first-order stream. When two first-order stream segments merge, they form a second-order stream segment, and this process

continues for higher orders. The goal of morphometric analysis of a drainage basin is to obtain precise data on the measurable features of its stream network.

Hydrological phenomena can be correlated with the physiographic characteristics of a drainage basin, such as its size, shape, slope, drainage density, and the size and length of its contributories (Rastogi and Sharma 1976; Magesh et al. 2012a). Remote sensing is a convenient method for morphometric analysis, as satellite images offer a comprehensive view of large areas and are highly effective for analyzing drainage basin morphometry.

Emerging spatial information technologies such as remote sensing, GIS, and GPS offer effective tools for addressing many challenges in land and water resources planning and management, surpassing the capabilities of conventional data processing methods (Rao et al. 2010). GIS-based evaluations using Shuttle Radar Topographic Mission (SRTM) and Advanced Spaceborne Thermal Emission and Reflection Radiometer (ASTER) data provide a precise, rapid, and cost-effective method for analyzing hydrological systems (Smith and Sandwell 2003; Grohmann 2004). The processed DEM was effectively used to generate the stream network and other supporting layers (Mesa 2006; Magesh et al. 2011). A digital elevation model (DEM) of the area was created to determine morphometric parameters such as drainage basin area, drainage density, drainage order, relief, and network diameter within a GIS environment.

The integration of remote sensing satellite data with hydrological and spatial analysis in a GIS environment simplifies the process of identifying and distinguishing drainage areas (Pirasteh et al. 2010).

The geographic and geomorphic characteristics of a drainage basin are crucial for hydrological investigations, including the assessment of groundwater potential. The present study aims to utilize remote sensing and GIS technology to calculate various morphometric parameters of the Kanhar River watershed. This aligns with the recent developments and research referenced above.

Study Area

The Rushikulya River basin, spanning 8, 402 km², is located on the eastern coast of India in southern Odisha, bordering the southern edge of Chilika Lake. The basin is surrounded by the Eastern Ghats in a semi-circular manner, extending towards the northeast, north, west, and south. It opens up towards the Bay of Bengal in the east.

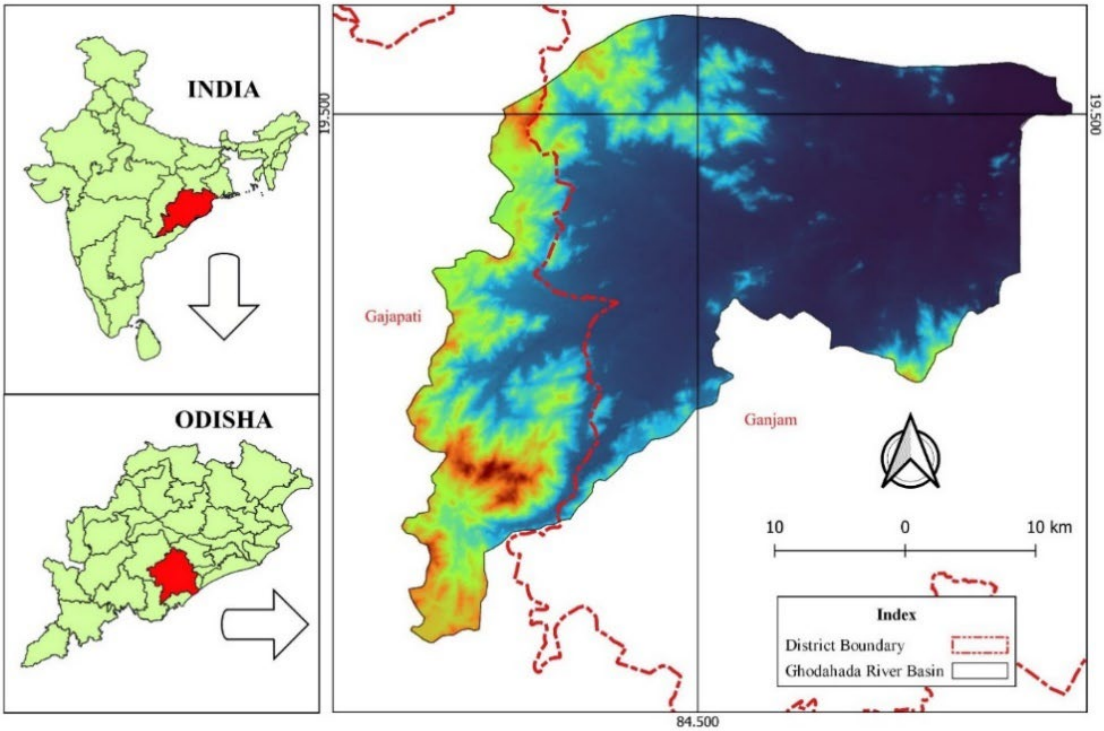

Fig:1 Index Map of Ghodahada River Basin

This study centres on the Ghodahada sub-basin, which is a smaller catchment area within the larger Rushikulya basin. The Ghodahada basin is situated within specific geographical coordinates, including longitudes and latitudes. It covers the administrative districts of Ganjam and Gajapati. An analysis has been conducted on the geomorphic evolution and characteristics of the sub-basin using Survey of India topographical sheets (74A/6, 74A/7, 74A/8, 74A/10, and 74A/11) at a scale of 1:50, 000.

Geology & Geomorphology

Ghodahada River sub-basin is mostly composed of Archaean-era metamorphic rocks from the Eastern Ghats group, and it is situated in the southern portion of the Rushikulya River basin (Dikshit, 1981). Quartzite, khondalite, gneiss, charnockite, and granite is all part of this geological category. In addition, the region is cut across by huge denudational hills and ridges formed by igneous rocks gabbro, norite, diorite, khondalite, granite and other rocks.

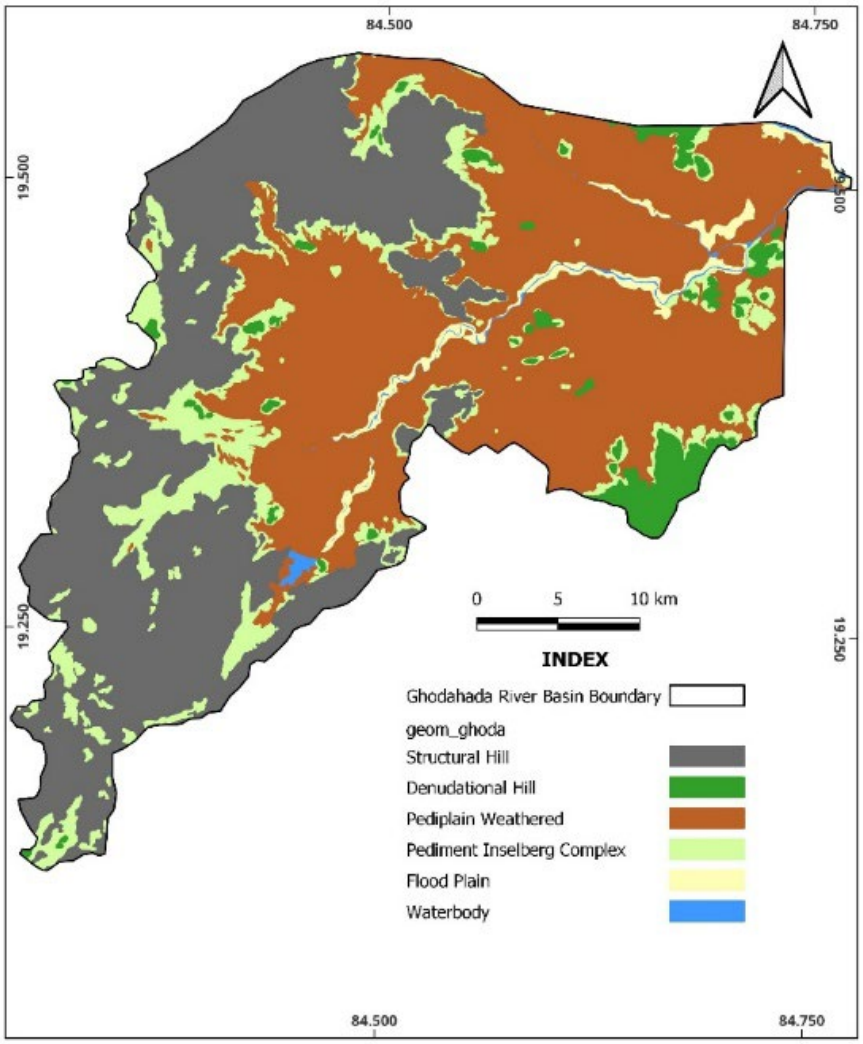

Fig:2 Geomorphology Map of Ghodahada River Basin

Structured hills, denudation hills, weathered pediplains, pediplain-inselberg complexes, floodplains, and bodies of water are all part of the Ghodahada River sub-basin's geomorphology. Plutonic rocks, mostly granite and gneiss, characterize the terrain of the sub-basin's southern region. Because it has never been significantly folded, disturbed, or submerged under water, this area has been quite stable. It is possible that the schists here predate the earliest sedimentary strata of the Archaean group, suggesting that the plutonic rocks here are among the oldest formations on earth.

The area has a complicated structure, with a geometric pattern of surface expressions that shows two generations of fold axes superimposed on top of each other at almost right angles. Polycyclic erosion and neotectonics uplift may have occurred in the past, according to the present physiography, which is characterized by rough mountainous terrains interspersed with flat, low-lying sections (Vaidyanathan, 1964).

Table-1 Stratigraphic Sequence of the Rushikulya Basin (Mohanty, B. K. and Devdas, V. Geological mapping of Quaternary formations in Rushikulya river basin in parts of Ganjam District, Orissa, Records Geological Survey of India, 122(3), pp. 5-6.)

Geological Age	Formation	Outcrops
Recent to sub-recent	Alluvial, laterite and laterite gravels Unconformity	Sand, clay, silt of various grades
	Younger intrusions	Gabbro, Norite, Diorite Syenite, Anorthosite Granite
	Granite suite	Prophyroblastic, Biotite Bearing and Granetiferous Granite gneiss, Pegmatite and Quartz veins
Archean (Eastern Ghat)	Charnockite suite	Acid, Intermediate, Basic/UltrabasicCharnockite
	Khondalite suite	Quartz, Garnet, Sillimanite
		Gneiss and schist, Garnetiferrous quartzite
	Base	
	Unknow	

Methodology

To address the challenges associated with manual extraction of drainage networks and stream ordering from topographic maps and georeferenced satellite data, this study utilizes automatic extraction techniques to evaluate morphometric parameters for the Ghodahada River basin, a sub-basin of the Rushikulya River basin. The primary aim is to extract and analyze the river basin/watershed boundary and drainage/stream network from CARTOSAT DEM data, with the data projected in the regional coordinate system (WGS-1984, UTM Zone 45N).

Table 2. Flow Chart of Methodology

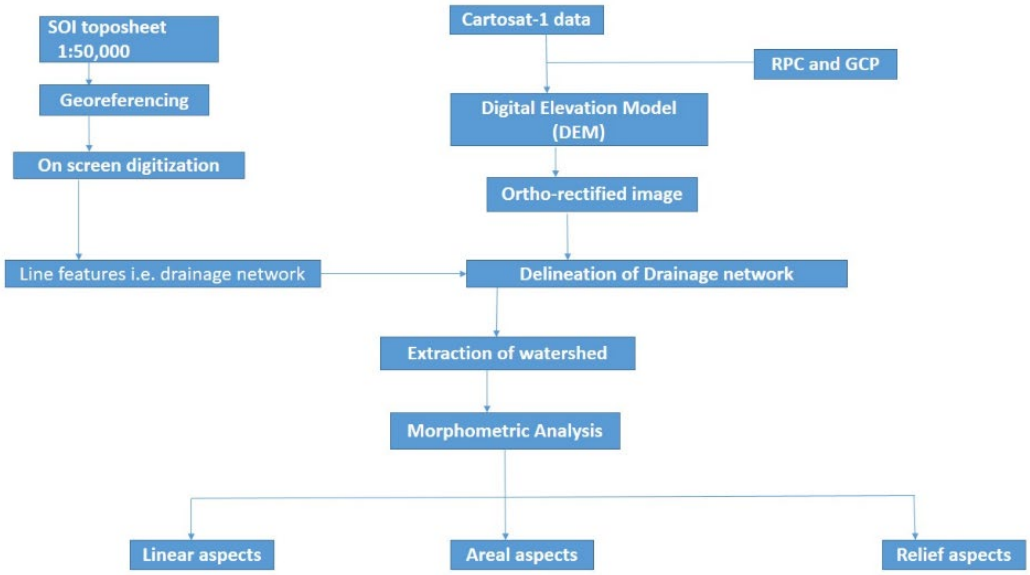

Data Acquisition and Processing

1. Data Sources: The study employs CARTOSAT DEM data from BHOONIDHI portal of NRSC.
2. Software Utilized: QGIS software was used for the processing and analysis of DEM and SOI toposheet data.
3. Automatic Extraction: The extraction of the river basin and stream networks was performed using automated techniques within QGIS. This included delineation of the watershed boundary and the identification of drainage networks.

Morphometric Analysis

1. Classification and Analysis: The extracted watershed and drainage networks were analyzed using quantitative morphometric characteristics. The watershed was classified based on several parameters: Aspects, Slope, Drainage, Relief, and Stream Order.
2. Hypsometric Analysis: To perform the hypsometric analysis, the line feature class in QGIS was utilized to generate contour lines. These contours were processed using the hydrology toolset to derive the necessary attributes. The attribute tables recorded the height, length, area, and perimeter of each contour, along with the enclosed catchment areas.
3. Hypsometric Curve: The hypsometric curve for the catchment was plotted based on the recorded data from the attribute feature classes. This curve was used to assess the distribution of elevations within the catchment area.

The integration of remote sensing (RS) and geographic information systems (GIS) methodologies facilitated the efficient extraction and analysis of morphometric parameters for the Ghodahada River basin. The automated techniques not only reduced the time and effort required for manual extraction but also provided a comprehensive framework for evaluating the watershed's morphometric characteristics.

Table-3 linear relief and areal morphometric parameters used for Ghoadahada river basin

S. no.	Parameter	Formula	References
1	Stream order (U)	Hierarchial rank	Strahler (1964)
2	Stream length (Lu)	Length of the stream	Horton (1945)
3	Mean stream length (Lsm)	Lsm = Lu/Nu	Strahler (1964)
4	Stream length ratio (RL)	RL = Lu/ (Lu - 1)	Horton (1945)
5	Bifurcation ratio (Rb)	Rb = Nu/Nu + 1	Schumm (1956)
6	Mean bifurcation ratio (Rbm)	Rbm = average of bifurcation ratios of all order	Strahler (1957)
7	Drainage density (Dd)	Dd = Lu/A	Horton (1945)
8	Drainage texture (T)	T= Dd 9 Fs	Smith (1950)
9	Stream frequency (Fs)	Fs = Nu/A	Horton (1945)
10	Elongation ratio (Re)	Re =D/L= 1. 128HA/L	Schumm (1956)
11	Circulatory ratio	Rc = $4pA/P^2$	Strahler (1964)
12	Form factor (Ff)	Ff =A/L^2	Horton (1945)
13	Length of overland flow (Lg)	Lg = 1/D9 2	Horton (1945)
14	Relief	R=H-h	Hadley and Schumm (1961)
15	Relief ratio	Rr =R/L	Schumm (1963)

The morphometric parameters examined in this study encompass stream order, bifurcation ratio, stream frequency, drainage density, drainage texture, length of overland flow, and slope. The parameters, as well as the longitudinal and cross profiles of the main river, were thoroughly analysed to evaluate stream development and the formation of related landforms.

Result & Discussion

The morphometric parameters for the Ghodahada River basin have been calculated, and the results are presented in Table 2. The total drainage area of the Ghodahada River basin is 1, 258. 469 km². The basin exhibits a dendritic drainage pattern, which is influenced by the region's topography, geology, and rainfall conditions. Slope, aspect, and contour maps were prepared using CARTOSAT DEM data. Based on stream order, the Ghodahada basin is classified as a seventh-order basin, with the corresponding morpho-dynamic parameters detailed in Table 1. (Horton 1932, 1945; Smith 1950; Schumm 1956, 1963; Hadley and Schumm 1961; Strahler 1964; Sreedevi et al. 2005; Mesa 2006).

Table-4 Results of morphometric analysis of Ghodahada river basin

Sl. no.	Parameters	Stream orders							
		I	II	III	IV	V	VI	VII	VIII
1	Stream order (U)	1307. 00	656	328	128	116	2	2	1
2	Stream length (LU)(km)	846. 65	389. 78	202. 44	85. 78	93. 65	16. 69	62. 09	7. 88
3	Mean stream length (km) (Lsm)	0. 65	0. 59	0. 62	0. 67	0. 81	8. 35	31. 05	7. 88
4	Stream length ratio (RL)	II/I	III/II	IV/III	V/IV	VI/V	VII/VI	VIII/VII	
		0. 46	0. 52	0. 42	1. 09	0. 18	3. 72	0. 13	
5	Bifurcation ratio (Rb)		I/II	II/III	III/IV	IV/V	V/VI	VI/VII	
			1. 99	2. 00	2. 56	1. 10	58. 00	1. 00	2. 00
6	Mean bifurcation ratio (Rbm)	8. 58							
7	Perimeter (P) (in km)	203. 72							
8	Basin length (Lb) (km)	65. 56							
9	Basin area (km^2)	1258. 47							
10	Total relief (R) (m)	1239. 68							
11	Relief ratio (Rh)	0. 98							
12	Length of over land flow (Lg)	0. 37							
13	Drainage density (D) (km/km^2)	1. 35							
14	Stream frequency (Fs)	2. 02							
15	Texture ratio (Rt)	6. 42							
16	Form factor (Rf)	0. 29							
17	Circulatory ratio (Rc)	0. 38							

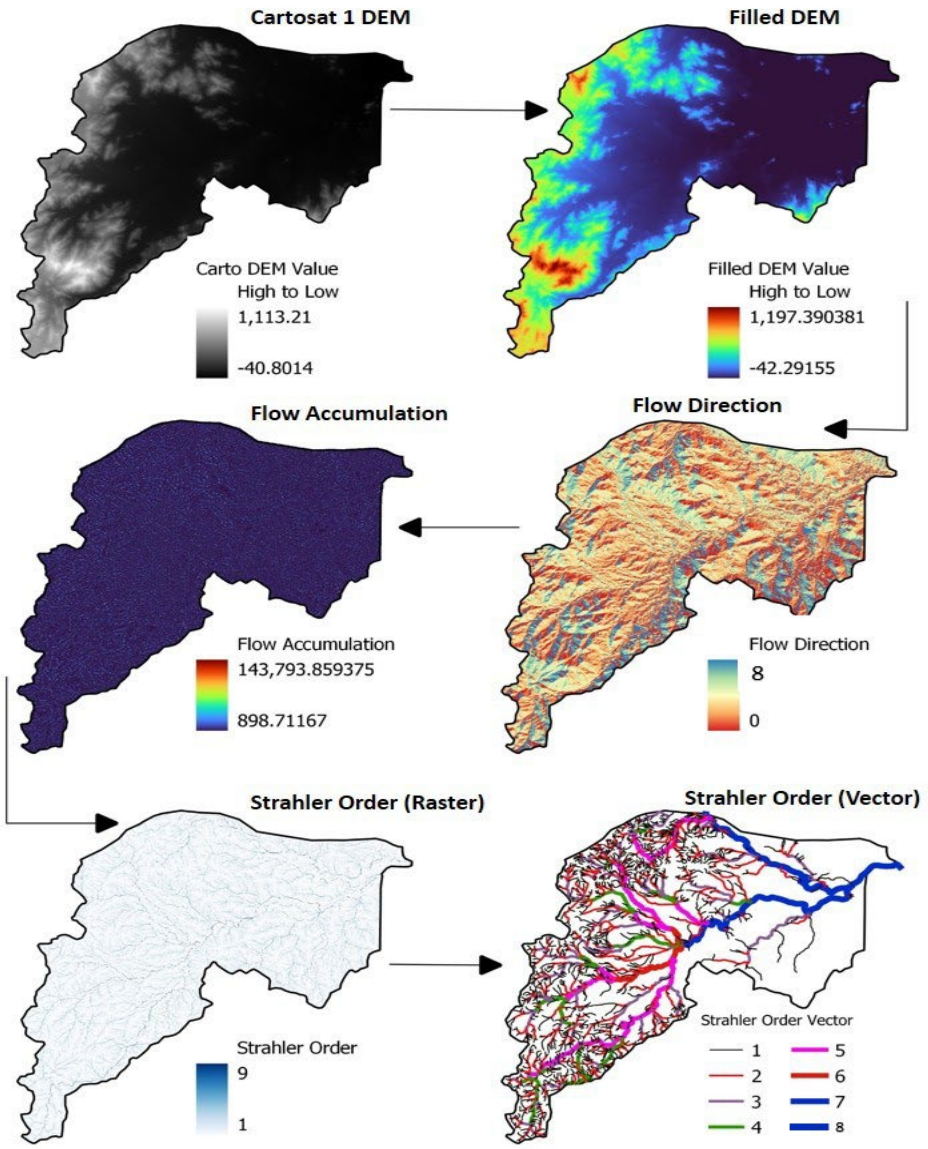

Fig:3 Stream Extract Map of Ghodahada RiverBasin

Aspect

Aspect refers to the direction that a mountain slope faces. It significantly impacts local climate conditions, as the sun's rays are most intense from the west during the afternoon. Consequently, west-facing slopes tend to be warmer compared to east-facing slopes, which are more sheltered and cooler. This temperature difference can significantly affect the distribution of vegetation within the Ghodahada River basin. The output raster data set provides values that represent the compass direction of the aspect, as detailed by

Magesh et al. (2011). The study area is clearly seen that southeast facing slopes mainly occur. Thus, these slopes have a higher moisture content and lower evaporation rate.

Slope

Slope analysis is a crucial parameter in geomorphological studies, particularly for watershed development and morphometric analysis. Slope elements are influenced by climatomorphogenic processes and the varying resistance of underlying rock types (Magesh et al., 2011; Gayen et al., 2013). In this study, a slope map of the area was generated using CARTOSAT DEM data and the spatial analysis tool in QGIS. The slope grid in the study area reaches a maximum value of 45°. Steeper slopes are associated with increased runoff and higher erosion rates, which can lead to greater soil loss and reduced groundwater recharge potential.

Relative Relief

Relative relief is a key morphometric variable for assessing the morphological characteristics of topography (Gayen et al., 2013). In the Ghodahada River basin, the highest relative relief is measured at 1, 239. 68 meters. The generally low relief in the basin indicates that the terrain is predominantly flat to gently sloping. This topographic feature makes the area suitable for agricultural activities, particularly along the stream sides, due to its flat nature and good water accessibility.

Stream Order (U)

In this study, streams in the Ghodahada basin have been ranked according to the method proposed by Strahler (1964). The classification extends up to the seventh order. The Ghodahada River is identified as an Eighth-order stream. Analysis of the stream orders reveals that the highest frequency is observed for first-order streams, followed by second-order streams. There is a noticeable decrease in stream frequency with increasing stream order, indicating a general decline in the number of streams as the order increases.

Stream Number

Stream order refers to the classification of stream channels based on their hierarchical position within a drainage basin. According to Horton's Law (1945), the number of streams of different orders in a given drainage basin tends to follow an inverse geometric series, where the first term is unity and the ratio is the bifurcation ratio. This principle implies that as stream order increases, the number of streams of each order decreases.

In this study, the number of streams for each order was plotted on a logarithmic scale on the y-axis against stream order on an arithmetic scale on the x-axis. Stream counts for different orders and the total number of streams in the basin were determined using GIS platforms. The analysis showed a gradual decrease in the number of streams as the order increases. This variation in stream order and the size of tributary basins is influenced by the physiographical, geomorphological, and geological conditions of the region.

In the Ghodahada River basin, a total of 2, 540 stream segments were identified, including the Ghodahada River. The breakdown is as follows: 1, 307 first-order streams, 656 second-order streams, 328 third-order streams, 128 fourth-order streams, 116 fifth-order streams, 2 sixth-order streams, 2 seventh-order and eighth-order 1 stream.

Stream Length (Lu)

GhoAccording to Horton (1945), the lengths of stream segments for each successive order in a basin generally follow a direct geometric series, with the first term being the average length of the first-order streams. Stream length provides insights into the hydrological characteristics of the bedrock and the extent of drainage. In regions with permeable bedrock and formations, fewer but longer streams are typically present in well-drained watersheds. Conversely, areas with less permeable bedrock and formations develop a larger number of shorter streams (Sethupathi et al., 2011).

In the Ghodahada River basin, it is observed that the cumulative stream length is greatest for first-order streams and diminishes with increasing stream order. The longest stream segment, representing the highest order (seventh-order) for the Ghodahada River, measures 62. 09 km.

Stream Length Ratio

Horton's Law (1945) on stream length suggests that the mean length of stream segments for each successive order in a basin approximates a direct geometric series, with stream length generally increasing as the stream order increases.

Bifurcation Ratio

Horton (1945) regarded the bifurcation ratio (Rb) as an index of relief and dissection, while Strahler (1957) noted that Rb generally exhibits only minor variation across different regions, except where strong geological controls are present. Schumm (1956) defined the bifurcation ratio (Rb) as the ratio of the number of stream segments of a given order to the number of segments of the next higher order. As a dimensionless property, Rb reflects the degree of integration among streams of various orders within a drainage basin. In the Ghodahada basin, the bifurcation ratio (Rb) ranges from 1 to 58.

Relief Ratio

According to Schumm (1956), the relief ratio is defined as the maximum vertical relief relative to the horizontal distance along the basin's longest dimension, parallel to the principal drainage line. This ratio measures the difference in elevation between the highest point of the basin and the lowest point on the valley floor, known as the total relief of the river basin. Schumm (1963) further explained that the relief ratio is a dimensionless height-to-length ratio, equivalent to the tangent of the angle formed by the intersection of two planes at the basin's mouth: one plane is horizontal, and the other

passes through the highest point of the basin. In the study area the total relief area is 1239. 68km^2 and the relief ratio is 0. 98.

Drainage Density

Drainage density measures the total length of streams within a given basin relative to the basin's total area (Strahler, 1964). It is influenced by factors that determine the characteristic length of the watershed, including valley density, channel head source areas, relief, climate, vegetation (Moglen et al., 1998), as well as soil and rock properties (Kelson and Wells, 1989), and landscape evolution processes. The drainage density of the Ghodahada basin is 1. 35 km/km², indicating that the basin features highly resistant permeable subsurface materials, intermediate drainage, and low to moderate relief.

Stream Frequency

Stream frequency (Sf) is defined as the total number of stream segments of all orders per unit area (Horton, 1932). According to Reddy et al. (2004), low values of stream frequency suggest the presence of permeable subsurface materials and low relief. Although enumerating channel segment numbers per unit area can be challenging (Singh, 1980), an attempt was made to calculate the stream frequency for the Ghodahada basin. The stream frequency for this basin is 2. 02 km/km². Stream frequency is largely influenced by the basin's lithology and reflects the texture of the drainage network. The positive correlation between stream frequency (Sf) and drainage density in the Ghodahada basin indicates that as drainage density increases, so does the stream population.

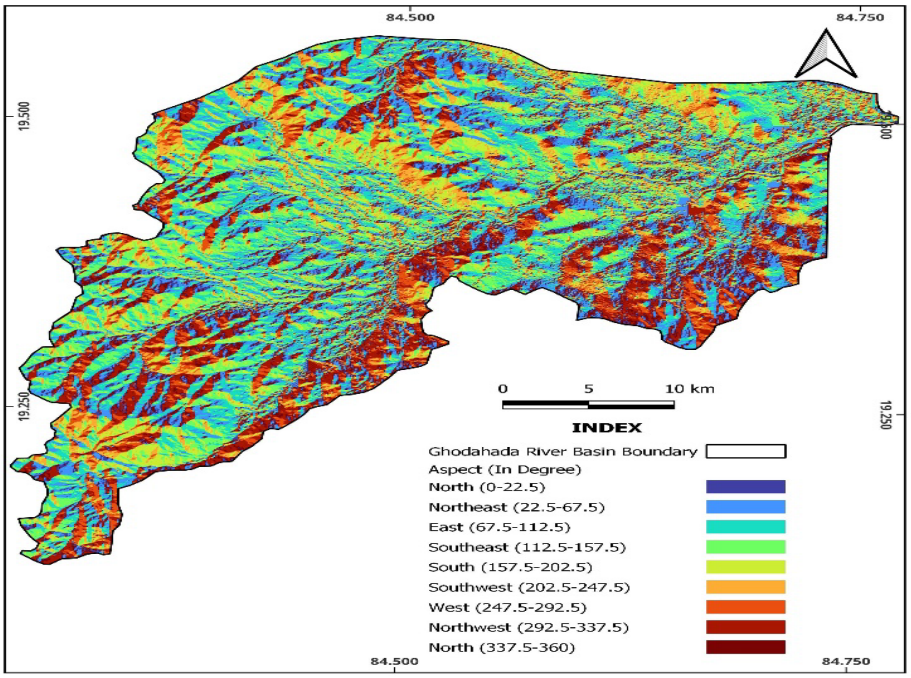

Fig:4 Aspect Map of Ghodahada River Basin

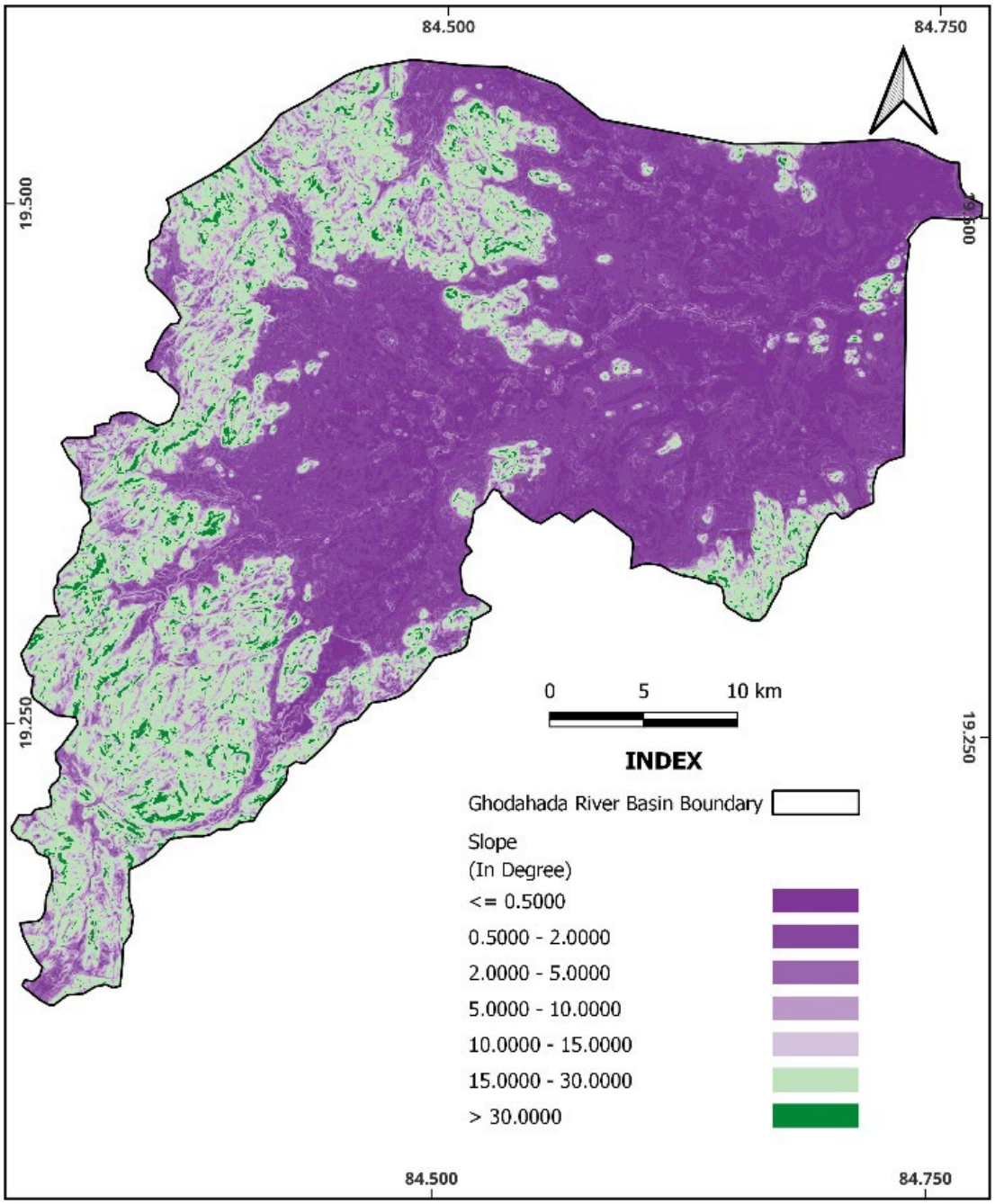

Fig:5 Slope Map of Ghodahada River Basin

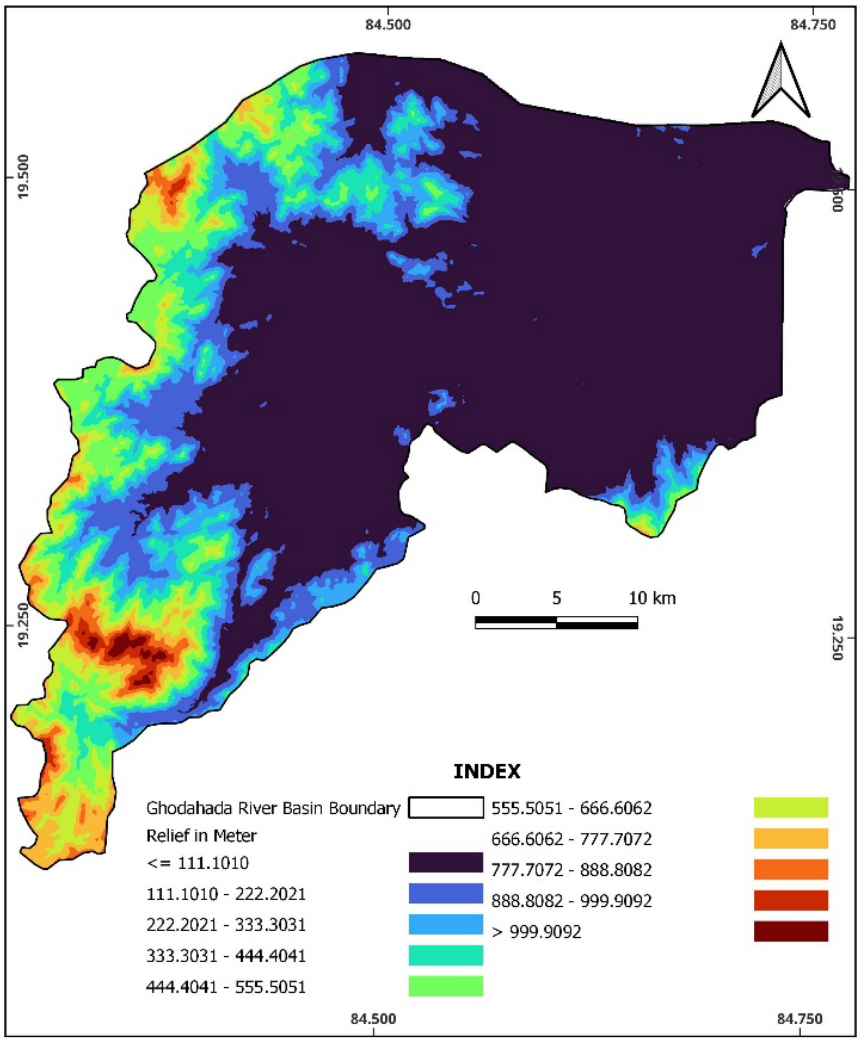

Fig:6 Relief Map of Ghodahada River Basn

Conclusion

Morphometric analysis of the Ghodahada River basin, utilizing remote sensing satellite data and advanced GIS tools, has provided a comprehensive understanding of the basin's drainage system. The study confirms that the Ghodahada River basin is classified as a seventh-order basin, predominantly characterized by lower-order streams. The analysis encompasses various drainage parameters, including linear, aerial, and relief aspects, revealing significant insights into the basin's morphology.

The study identifies dendritic to sub-dendritic drainage patterns, indicating a relatively homogeneous lithology across the basin. The highest stream order frequency occurs in first-order streams, with a decreasing frequency observed in higher orders. The basin exhibits a maximum relative relief of 1, 239. 68 meters, suggesting that the terrain is largely flat to gently sloping. The slope grid reaches up to 45°, while a total of 2, 540

stream segments were mapped, including the Ghodahada River itself. The distribution includes 1, 307 first-order streams, 656 second-order streams, 328 third-order streams, 128 fourth-order streams, 116 fifth-order streams, 2 sixth-order streams, 2 seventh-order and 1 eighth-order stream.

The stream frequency in the Ghodahada basin is 2. 02 km/km², reflecting the basin's lithological characteristics and drainage network texture. The drainage density, at 1. 35 km/km², indicates the presence of highly resistant permeable subsurface materials, intermediate drainage, and low to moderate relief. The total relief area is 1, 239. 68 km², with a relief ratio of 0. 98. The bifurcation ratio (Rb) ranges from 1 to 58, and the longest stream segment, representing the highest order (seventh-order), measures 62. 09 km.

These findings offer valuable insights for developing effective water usage strategies and managing the watershed in the Ghodahada River basin. The detailed morphometric analysis can aid in informed decision-making for sustainable water resource management and land use planning in the region.

Refernces

- Agarwal CS (1998) Study of drainage pattern through aerial data in Naugarh area of Varanasi district, U. P. J Indian Soc Remote Sens 26:169–175.
- Burrough PA, McDonnell RA (1998) Principles of geographical information systems. Oxford University Press Inc., New York.
- Chorley RJ, Schumm SA, Sugden DE (1984) Geomorphology. Methuen, London.
- Clarke JI (1996) Morphometry from Maps. Essays in geomorphology.
- Cox RT (1994) Analysis of drainage-basin symmetry as a rapid technique to identify areas of possible quaternary tilt-block tectonics: an example from the Mississippi embayment. Geol Soc Am Bull 106:571–581.
- Dar RA, Chandra R, Romshoo SA (2013) Morphotectonic and lithostratigraphic analysis of intermontane Karewa basin of Kashmir Himalayas, India. J Mt Sci 10(1):731–741.
- Dikshit, K. R. (1981) *The Western Ghats: a geomorphic overview*. In Singh, L. R. (ed) NewPerspective in Geography, Thinkers Library, Allahabad: 1–25.
- Elsevier publication. Co., New York, pp 235–274.
- Evans IS (1972) General geomorphometry, derivatives of altitude, and descriptive statistics. In: Chorley RJ (ed) Spatial analysis in geomorphology. Harper and Row, New York, pp 17–90.
- Evans IS (1984) Correlation structures and factor analysis in the investigation of data dimensionality: statistical properties of the Wessex land surface, England. In: Proceedings of the Int. Symposium on Spatial Data Handling, Zurich., v 1. Geograph- isches Institut, Universitat Zurich-Irchel. pp 98–116.

- Grohmann CH (2004) Morphometric analysis in geographic infor- mation systems: applications of free software GRASS and R. Comput Geosci 30:1055–1067.
- Horton RE (1932) Drainage basin characteristics. Am Geophys Union Trans 13:348–352.
- Horton RE (1945) Erosional development of streams and their drainage basins; hydrophysical approach to quantitative mor- phology. Bull Geol Soc Am 56:275–370.
- Hurtrez JE, Sol C, Lucazeau F (1999) Effect of drainage area on hypsometry from an analysis of small-scale drainage basins in the Siwalik hills (central Nepal). Earth Surf Process Landform 24:799–808.
- Krishnamurthy J, Srinivas G, Jayaram V, Chandrasekhar MG (1996) Influence of rock type and structure in the development of drainage networks in typical hard rock terrain. ITC J 4(3):252–259.
- Magesh NS, Chandrasekar N, Kaliraj S (2012a) A GIS based automated extraction tool for the analysis of basin morphometry. Bonfring Int J Ind Eng Manag Sci 2(1):32–35.
- Magesh NS, Chandrasekar N, Soundranayagam JP (2011) Morpho- metric evaluation of Papanasam and Manimuthar watersheds, parts of Western Ghats, Tirunelveli district, Tamil Nadu, India: a GIS approach. Environ Earth Sci 64(2):373–381.
- Magesh NS, Jitheshlal KV, Chandrasekar N, Jini KV (2012b) GIS based morphometric evaluation of Chimmini and Mupily watersheds, parts of Western Ghats, Thrissur District, Kerala. India Earth Sci Inform 5(2):111–121.
- Merritts D, Vincent KR (1989) Geomorphic response of coastal streams to low, intermediate, and high rates of uplift, Mendocino junction region, northern California. Geol Soc Am Bull 101:1373–1388.
- Mesa LM (2006) Morphometric analysis of a subtropical Andean basin (Tucuman, Argentina). J Environ Geol 50(8):1235–1242.
- Muller JE (1968) An introduction to the hydraulic and topographic sinuosity indexes. Ann Assoc Am Geogr 58:371–385.
- Nag SK, Chakraborty S (2003) Influence of rock types and structures in the development of drainage network in hard rock area. J Indian Soc Remote Sens 31(1):25–35.
- Nautiyal MD (1994) Morphometric analysis of a drainage basin, district Dehradun, Uttar Pradesh. J Indian Soc Remote Sens 22(4):251–261.
- Obi Reddy GE, Maji AK, Gajbhiye KS (2002) GIS for morphometric analysis of drainage basins. GIS lndia 4(11):9–14.

- Oguchi T (1997) Drainage density and relative relief in humid steep mountains with frequent slope failure. Earth Surf Process Landf 22:107–120.
- Ohmori H (1993) Changes in the hypsometric curve through mountain building resulting from concurrent tectonics and denudation. Geomorphology 8:263–277.
- Ozdemir H, Bird D (2009) Evaluation of morphometric parameters of drainage networks derived from topographic maps and DEM in point floods. Environ Geol 56:1405–1415.
- Pirasteh S, Safari HO, Pradhan B, Attarzadeh I (2010) Litho morphotectonics analysis using Landsat ETM data and GIS techniques: Zagros Fold Belt (ZFB), SW Iran.
- Rao NK, Swarna LP, Kumar AP, Krishna HM (2010) Morphometric analysis of Gostani River Basin in Andhra Pradesh State, Indian using spatial information technology. Int J Geomat Geosci 1(2):179–187.
- Rastogi RA, Sharma TC (1976) Quantitative analysis of drainage basin characteristics. J Soil Water Conserv India 26(1–4):18–25.
- Shreve RW (1969) Stream lengths and basin areas in topologically random channel networks. J Geol 77:397–414.
- Singh KN (1980) Quantitative analysis of landfroms and settlement distribution in southern uplands of eastern Uttar Pradesh (India). Vimal Prakashan, Varanasi.
- Singh S (1992) Quantitative geomorphology of the drainage basin. In: Chouhan TS, Joshi KN (eds) Readings on remote sensing applications. Scientific Publishers, Jodhpur.
- Singh S (1995) Quantitative analysis of watershed geomorphol- ogy using remote sensing techniques. Ann Arid Zone 34(4): 243–251.
- Smith B, Sandwell D (2003) Accuracy and resolution of shuttle radar topography mission data. Geophys Res Lett 30(9):20–21.
- Strahelr AN (1952) Hypsometric (area-altitude) analysis of erosional topography. Bull Geol, Soc Am 63.
- Strahler AN (1957) Quantitative analysis of watershed geomorphol- ogy. Trans Am Geophys Union 38:913–920.
- Strahler AN (1964) Quantitative geomorphology of drainage basins and channelnetworks. In: Chow VT (ed) Handbook of applied hydrology. McGraw-Hill, New York, pp 439–476

Tracking Coastal LULC Transformations in Puri District, Odisha through GIS and Remote Sensing on GEE

Barsarani Mallick[1], Rosalin Das*, Susanta Kumar Das[1], Santosh Kumar Rout[1], Subhadrarani Das

Department of Geology, Fakir Mohan University, Balasore

Corresponding Author E-mail: *rosalindas.geology@gmail.com, [1]barsaranimallick31@gmail.com

Abstract

The coastal land use and land cover (LULC) of the eastern Puri coast is influenced by both natural and anthropogenic factors, with marine dynamics playing a pivotal role. This study examines LULC transformations over 16 years, using Landsat 5 imagery from 2009 and Landsat 8 data from 2014, 2019, and 2024. Analysis was conducted on the Google Earth Engine (GEE) platform, complemented by QGIS software for field calculations. LULC classes include dune vegetation, general vegetation, agriculture, built-up areas, water bodies, rivers, the sea, and beach zones. Significant transitions were observed, notably the conversion of sandy beaches, dunes, plantations, agricultural fields, and barren lands into built-up areas. Between 2009 and 2024, dune vegetation showed consistent decline due to frequent cyclones, particularly the 2019 Fani cyclone, while vegetation cover increased marginally. Built-up areas expanded by 1. 234%, driven by urbanization. Barren land exhibited fluctuations, peaking in 2014 and decreasing by 2024. Water bodies remained relatively stable, increasing from 2009 to 2019 before declining slightly. Beach area and sea extent notably expanded in 2019. This study underscores the dynamic interplay of natural events and human interventions in shaping coastal LULC. The findings highlight the need for sustainable land-use practices to mitigate environmental impacts and balance developmental goals.

Keywords- Land Use and Land Cover (LULC), GIS, Remote Sensing

Introduction

Natural hazardous events can escalate into disasters when environmental changes or human activities alter the local landscape (Adger et al., 2001). Each year, meteorological, hydrological, and climate-related disasters result in significant loss of life while severely impacting economic and social development. Climate-induced and water-related hazards, including floods, storm surges, and tsunamis, pose substantial

threats by rendering vast regions uninhabitable due to prolonged inundation. Extreme weather events such as cyclones and tornadoes lead to widespread destruction of infrastructure, displacement of populations, and resource depletion (UN-HABITAT, 2010). While wind and tidal forces impose immediate impacts, long-term consequences such as erosion and saltwater intrusion persist, exacerbating environmental degradation over extended periods (Wisner et al., 2004).

Disasters such as floods, droughts, and tropical cyclones can lead to severe biological and epidemiological consequences as secondary impacts (Wisner et al., 2004). In addition to natural disasters, land-use and land-cover (LULC) changes are a significant global concern, as they interact with disasters, intensifying their effects. LULC changes alter ecosystem functions, affecting biodiversity and essential resources such as food, fiber, and water, which are crucial for both present and future human societies (Chase et al., 2000). Unsustainable land-use practices directly contribute to biodiversity loss, while natural disasters also influence land-use patterns (Dale, 1997). Socio-ecological systems undergo modifications in response to environmental changes, and in turn, LULC changes may exacerbate vulnerability to disasters. For instance, in coastal Bangladesh, the conversion of traditional paddy fields into shrimp ponds is a well-established land-use transformation (Ali, 2006; Rahman et al., 2011, 2013). These coastal areas experience intensive land use for agriculture, human settlements, forestry, shrimp farming, fisheries, salt production, industrial expansion, infrastructure development, and tourism (Islam, 2006). Understanding the complex interplay between disasters and LULC changes is essential for sustainable land management and disaster risk reduction.

Coastal zones are dynamic transitional areas between terrestrial and marine environments, characterized by high resource availability and ecological complexity. Approximately 23% of the global population, around 1. 2 billion people, reside within 100 km of the coast and at elevations below 100 m above sea level (Nicholls and Small, 2002; Nicholls, 2003). Given the geomorphic and ecological changes occurring in these regions, site-specific research is essential to assess and predict coastal transformations, considering their complexity at the regional level (Mani Murali and Dinesh Kumar, 2015). The existing land use/land cover (LULC) of coastal areas is shaped by the interaction of natural and anthropogenic factors. Rapid urbanization and the extensive exploitation of natural resources significantly alter coastal landscapes, necessitating a comprehensive understanding of LULC changes. Monitoring these transformations is critical to mitigating unplanned and unsustainable alterations in LULC patterns, which can have long-term environmental and socio-economic implications (Alphan, 2003; Muttitanon and Tripathi, 2005; Ioannis and Meliadis, 2011; Knorr et al., 2011).

Choudhary et al. (2013) conducted shoreline detection studies along the western coast of India, from Karwar to Gokarna, while Gupta (2014) utilized LISS III datasets to monitor shoreline changes in the Gulf of Khambhat between 1966 and 2004. The

successful application of remote sensing data for land use/land cover (LULC) change detection and shoreline monitoring is contingent upon a comprehensive understanding of landscape features and the selection of an appropriate information extraction methodology, particularly for shoreline delineation. In LULC studies, key challenges include selecting suitable satellite imagery with optimal spatial and temporal resolution, establishing a standardized classification scheme, and applying methods relevant at national and regional scales (Gilani et al., 2015). Among the various methodologies employed for LULC studies, pre- and post-classification assessments are widely utilized (Coppin et al., 2004; Singh, 1989). Pre-classification techniques include image differencing, band ratios, vegetation indices, principal component analysis, change vector analysis, and direct multi-date classification, all of which leverage temporal variations in pixel reflectance values to detect changes (Toll, 1985; Nelson, 1983; Townshend and Justice, 1995; Fung and LeDrew, 1987; Johnson and Kasischke, 1998; Li and Yeh, 1998). While these methods effectively identify LULC changes, they present limitations in capturing the underlying nature and drivers of these transformations (Ridd and Liu, 1998).

The selection of study years aims to highlight decadal variations in land use/land cover (LULC) changes within the region. Accuracy assessment is conducted using a combination of reference ground points, Google Earth imagery, and ancillary data to ensure the reliability of the derived LULC maps. The decadal changes in LULC classes from 2009 to 2024 analyzed, and the overall transformation over the 16-year period (2009–2024) is determined using change detection techniques. Additionally, based on LULC analysis and studies (Gupta, 2014; Manek and Balaji, 2014; Mahapatra et al., 2013; INCOIS, 2009), it is evident that shorelines in these districts are particularly susceptible to erosion due to both natural and anthropogenic factors. In this context, shoreline changes are further examined using GIS techniques to delineate erosion-prone zones along the coastline. The primary objective of this study is to generate LULC can serve as essential tools for coastal zone management, facilitating the development of effective conservation and mitigation strategies.

Study Area

The east coast of Odisha is highly vulnerable to a variety of environmental challenges, including unpredictable monsoon rainfall, frequent cyclones, flooding, salinity hazards, and crop failures. The study area is located along this coastal stretch, characterized by predominantly flat terrain with sandy beaches, sand dunes, and expansive mudflats. Despite its relatively short geological history, the coast remains in a state of ongoing formation, continuously shaped by the dynamic interaction between terrestrial and marine processes. The shoreline undergoes constant changes due to natural factors such as erosion, sedimentation, sea-level fluctuations, and the impact of cyclonic storms and floods.

The region's vulnerability to environmental hazards is compounded by its geographic location and exposure to the Bay of Bengal. The coastal areas of Puri, known for its rich cultural heritage, are also prone to salinity intrusion and water contamination, which significantly affect agriculture and human health. Puri is home to historic landmarks like the Jagannath Temple and the Konark Sun Temple, in addition to the scenic Chilika Lake, making it a major tourist destination. Spanning an area of 2358. 31 km², the study area falls within the Survey of India toposheet numbers 74E/3, 74E/2, 74E/6, 74E/5, 74E/10, 74E/9, 74E/13, 74I/1, 73L/4, 74I/5, 73L/8, and 73H/16 (1:50, 000 scale). The geographic coordinates of the study area range between 19°28′ and 20°10′ N latitude and 85°09′ and 86°25′ E longitude. The region is bordered by Jagatsinghpur and Cuttack districts to the north, the Bay of Bengal to the east, Ganjam district to the south, and Khordha district to the west.

Within Puri district's coastal blocks, several rivers, including the Kushabhadra, Daya, Bhargavi, Kadua, Prachi, and Devi, flow from the Mahanadi River and empty into the Bay of Bengal. These rivers play a vital role in the hydrology of the region and are integral to the livelihoods of local communities. The research focuses on the coastal blocks of Puri district, specifically Krushnaprasad, Brahmagiri, Puri Sadar, Gop, Kakatapur, and Astaranga blocks. These areas are not only famous for their cultural and ecological significance but are also increasingly facing challenges such as water salinization, fluoride contamination and land use land cover also.

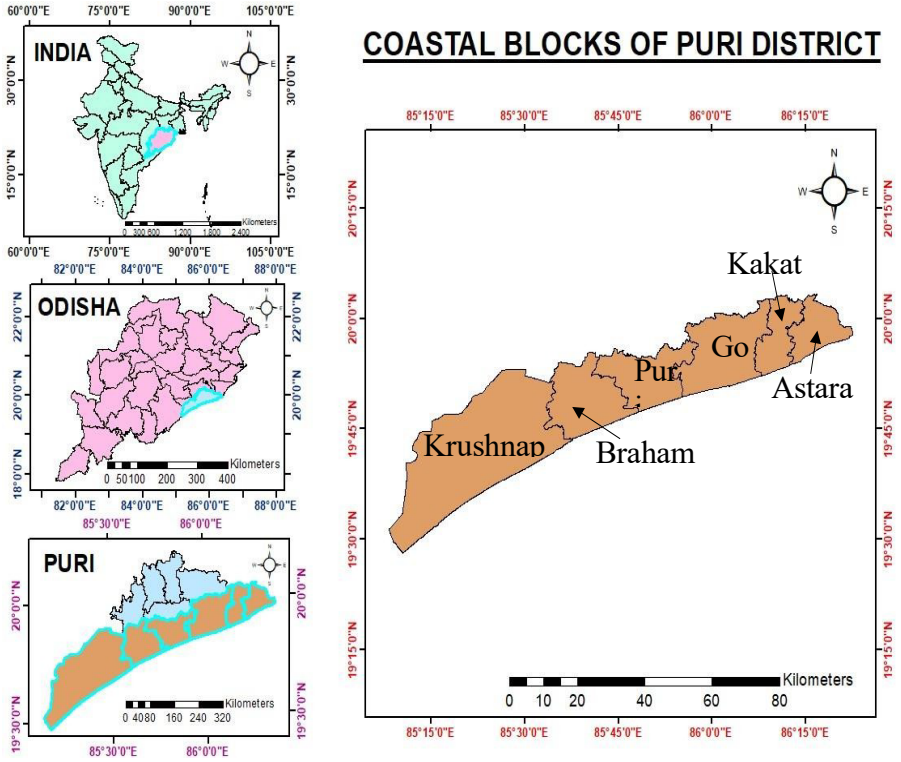

Fig: 1 Study Area Map of Coastal Blocks of Puri District

Methodology

The methodology for analyzing Land Use and Land Cover (LULC) change using Landsat satellite imagery involves several systematic steps, primarily utilizing Landsat 5 (2009) and Landsat 8 (2014, 2019, 2024) data. This process is carried out through Google Earth Engine (GEE) and Geographic Information System (GIS) platforms, integrating image preprocessing, classification, and accuracy assessment techniques.

1. **Image Preprocessing:** The first step involves the acquisition and preprocessing of Landsat data. This includes the georeferencing of images to align them with the Earth's coordinate system, ensuring that all datasets from different years are spatially consistent. Radiometric calibration is then performed to adjust the images for sensor and atmospheric distortions, allowing for accurate pixel values that reflect true surface conditions.
2. **Image Classification:** The next step involves the classification of land cover. Initially, an unsupervised classification approach is applied to categorize the image into different clusters based on pixel values, such as vegetation, water bodies, and built-up areas. This process helps in the identification of distinct land cover types without prior knowledge. Following this, supervised classification is performed, where training samples for different land cover classes (e. g., forest, urban, agricultural land) are manually selected, and a classification algorithm is applied to classify the entire image into predefined land use categories.
3. **LULC Change Detection:** After classification, LULC change maps are generated for each selected year (2009, 2014, 2019, 2024). These maps highlight the differences in land cover types over time, allowing for the detection of areas experiencing changes such as urbanization, deforestation, or agricultural expansion.
4. **Accuracy Assessment:** To evaluate the reliability of the LULC classification, an accuracy assessment is performed. This typically involves comparing the classified maps with reference data, such as ground truth or high-resolution imagery, to compute overall accuracy, producer's accuracy, user's accuracy, and kappa coefficient.

This methodology provides a comprehensive and efficient framework for monitoring LULC changes over time, offering valuable insights into environmental dynamics and land management.

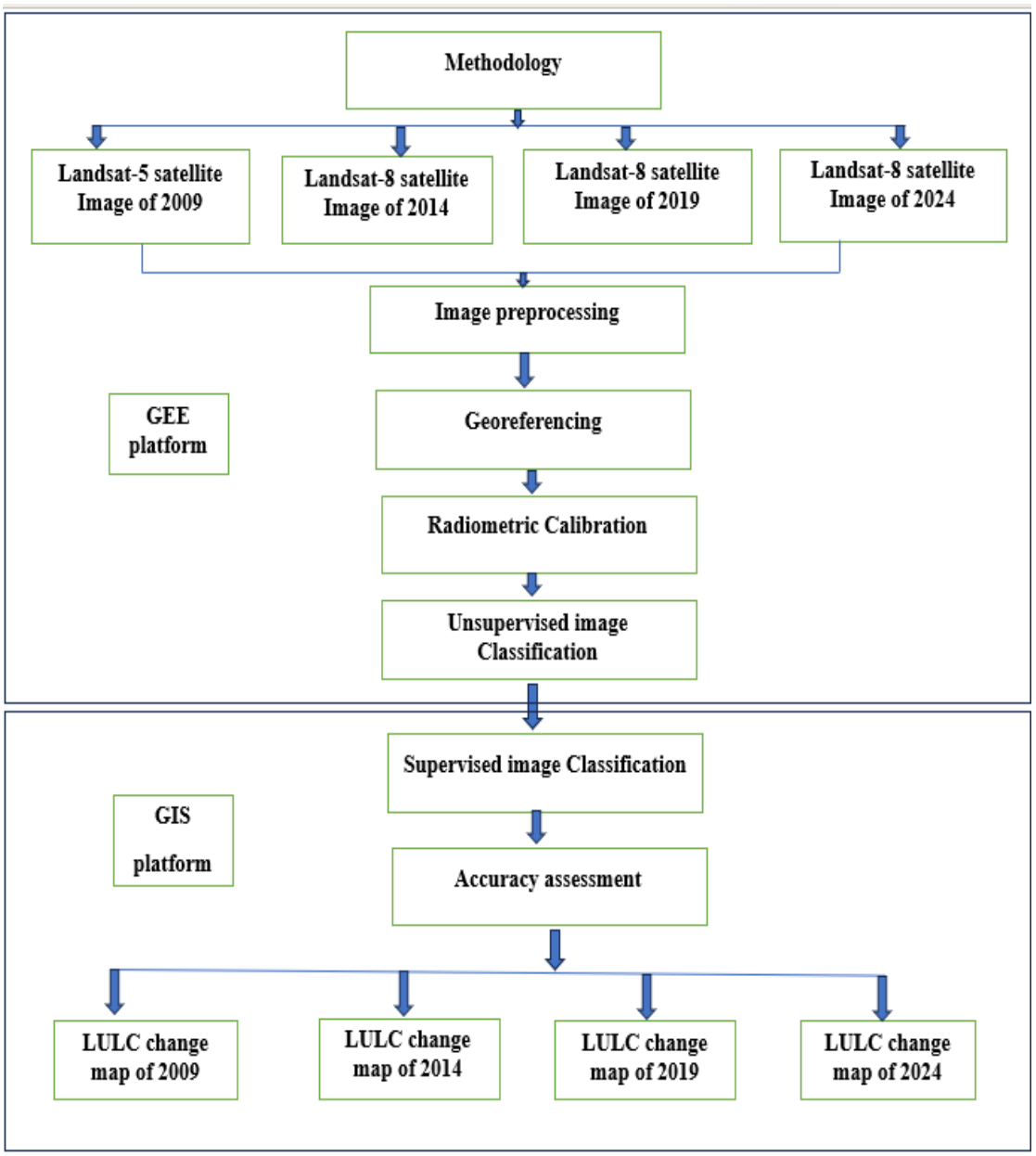

Table: 1 Flow Chart of Methodology

Result and Discussion

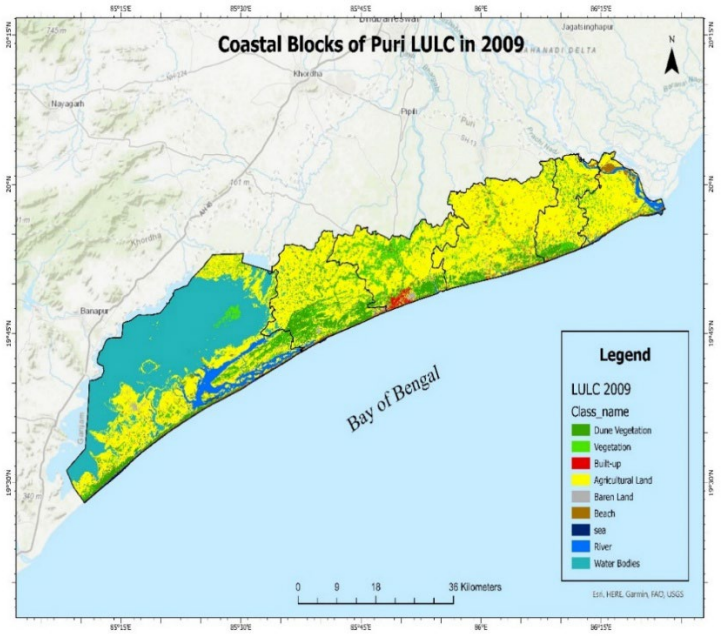

Fig:2 Land Use Land Cover (LULC) in 2009

The map depicts the coastal blocks of Puri's Land Use Land Cover (LULC) in 2009, highlighting various classifications like vegetation, agricultural land, built-up areas, rivers, and the sea. It uses different colours to represent each category, with the Bay of Bengal at the bottom. The legend explains the classifications clearly.

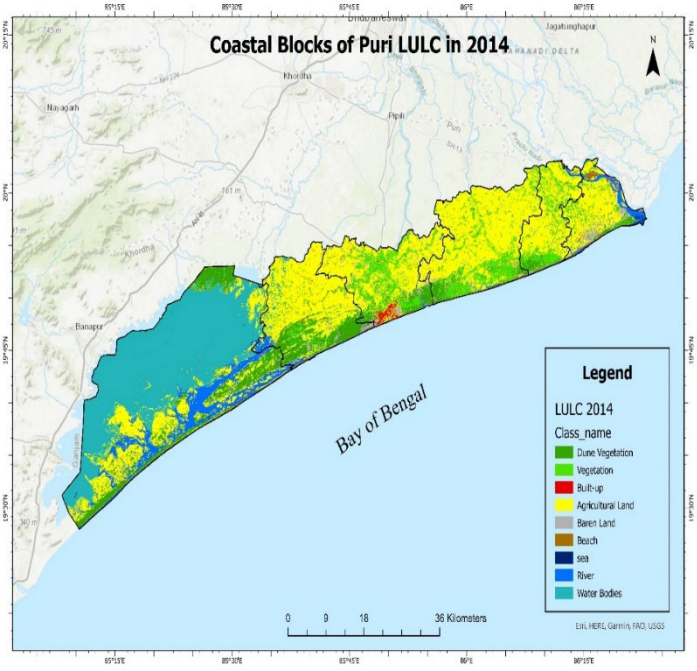

Fig: 3 Land Use Land Cover (LULC) in 2014

The map displays the coastal land use and land cover (LULC) of Puri in 2014. It categorizes areas using different colours, representing vegetation, built-up regions, agricultural land, barren land, dune vegetation, water bodies, and the sea. The Bay of Bengal borders the southern coastline, with major towns and rivers marked.

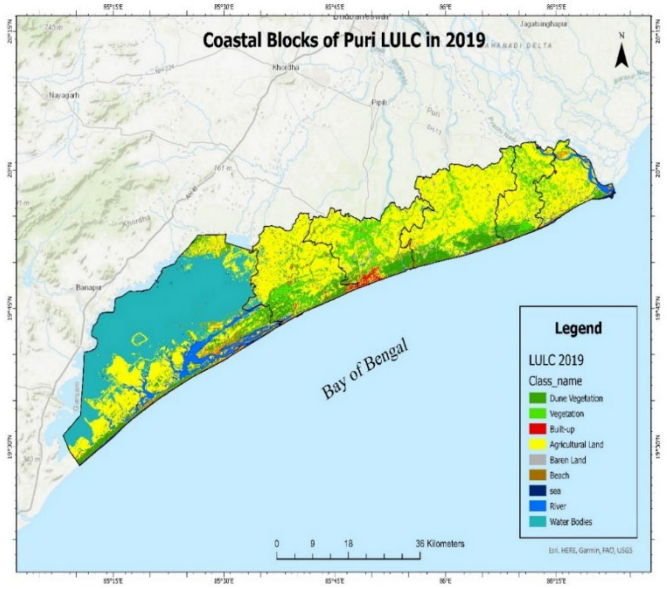

Fig:4 Land Use Land Cover (LULC) in 2019

The map represents the coastal land use and land cover (LULC) of Puri in 2019. It categorizes areas into vegetation, built-up land, agricultural land, barren land, dune vegetation, water bodies, and the sea. The Bay of Bengal is along the coast, with major settlements and rivers clearly marked.

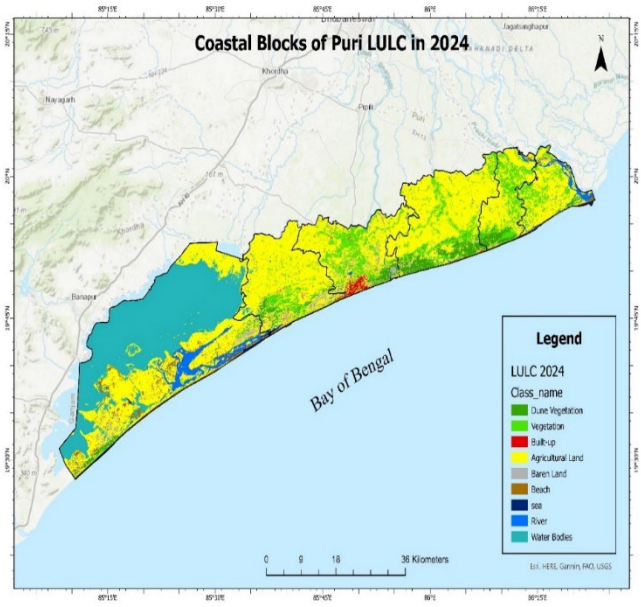

Fig:5 Land Use Land Cover (LULC) in 2024

The map illustrates the coastal geomorphology and land use/land cover (LULC) of Puri in 2024. It delineates various lithological units such as dune vegetation, fluvial deposits, agricultural plains, and urbanized terrains. Coastal dynamics are evident with sediment transport along the shoreline, estuarine systems, and hydrological features like rivers, lagoons, and tidal inlets influencing landscape evolution.

Table: 2 Percentage of LULC Parameters

PARAMETERS	2009	2014	2019	2024
Dune Vegetation	10. 87603	10. 83589	9. 382598	3. 94738
Vegetation	4. 544582	8. 490663	8. 918928	9. 964852
Agriculture	51. 97391	43. 44677	45. 79285	51. 81458
Built-up	1. 234894	0. 542157	1. 025875	0. 795533
Barren land	0. 829235	1. 899895	0. 856531	2. 521819
Water	24. 83524	26. 60322	25. 97917	24. 71527
River	3. 994318	6. 93884	4. 488683	3. 388587
Sea	0. 619367	0. 569883	1. 179863	0. 826672
Beach	1. 092423	0. 672684	2. 375509	2. 025303

The table illustrates the temporal variation in land use/land cover (LULC) parameters in the coastal region of Puri from 2009 to 2024, showcasing significant geological and environmental transformations. One of the most notable changes is the decline in dune vegetation, which suggests increasing coastal erosion and sediment displacement due to natural and anthropogenic influences. Vegetation cover fluctuates over time, reflecting changes in land management and ecological succession. Agricultural land exhibits a dynamic trend, decreasing in 2014 before rebounding in later years, potentially due to shifts in land use practices or soil fertility variations.

The built-up area shows inconsistent patterns, indicating phases of urban expansion and contraction, possibly linked to developmental projects and regulatory policies. Barren land undergoes sporadic increases, highlighting shifting land cover dynamics caused by climatic variations and human interventions. Hydrological processes influence river morphology and water bodies, shaping sediment transport, deposition, and erosion mechanisms. Changes in sea and beach areas suggest ongoing shoreline modifications driven by tidal forces, wave action, and marine transgression.

Overall, the data reflect the interplay of fluvial, marine, and aeolian processes shaping the region's geomorphology. These patterns highlight the need for sustainable coastal management to mitigate environmental impacts and preserve ecological stability.

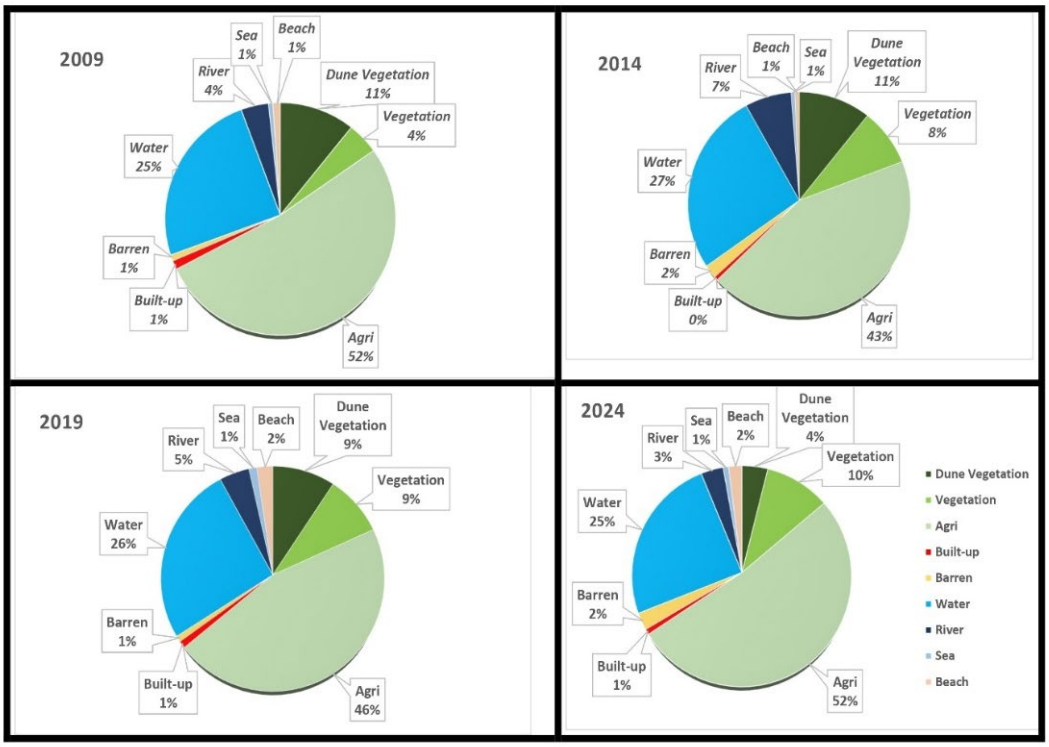

Fig:6 Pie Charts shows Land Use Land Cover (LULC) in (2009, 2014, 2019, 2024)

The series of pie charts illustrate the temporal variations in land use/land cover (LULC) patterns in Puri's coastal region from 2009 to 2024. These changes reflect dynamic geological and environmental processes influenced by coastal erosion, sediment transport, fluvial dynamics, and human activities.

Dune vegetation, which plays a critical role in coastal stabilization, has significantly declined over time, decreasing from 11% in 2009 to 4% in 2024. This indicates intensified erosion, possibly due to rising sea levels, increased wave action, and anthropogenic encroachments. Vegetation cover shows fluctuations, peaking at 10% in 2024, which may indicate afforestation efforts or shifts in land-use patterns.

Agricultural land exhibits notable variations, reducing in 2014 but recovering to 52% in 2024, suggesting soil fertility changes, water availability, or human interventions. The built-up area remains minimal, showing an erratic pattern, likely due to zoning regulations or infrastructure development.

Barren land, river systems, and water bodies reflect geomorphological changes influenced by hydrological processes such as sediment deposition and erosion. River coverage peaked in 2014 but declined in 2024, hinting at channel modifications. Coastal processes, including marine transgression and beach erosion, are evident in the fluctuating beach and sea proportions. These trends highlight complex coastal dynamics requiring sustainable management strategies.

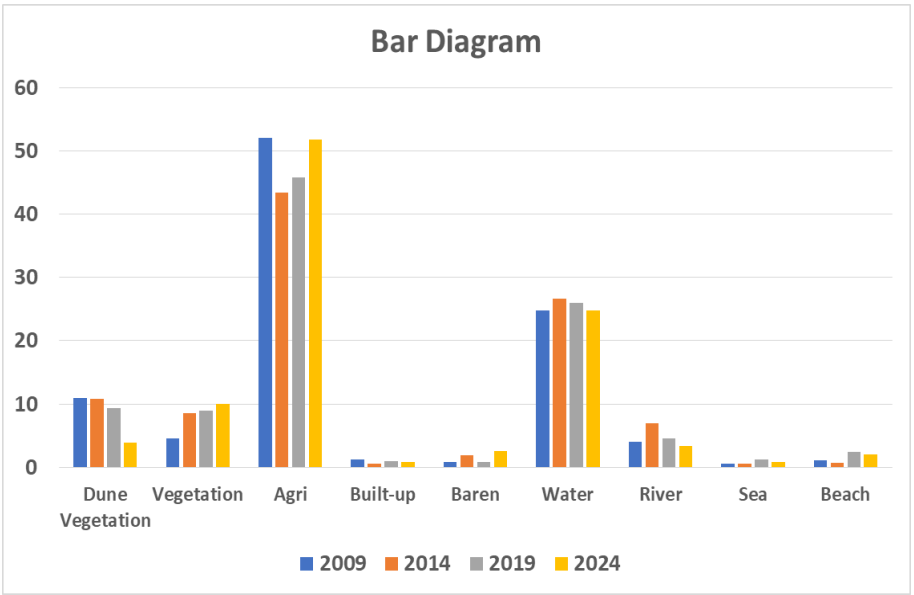

Fig: 7 Bar Diagram shows Land Use Land Cover (LULC) in (2009, 2014, 2019, 2024)

The bar diagram illustrates the temporal variations in land use/land cover (LULC) categories in Puri's coastal region from 2009 to 2024. Key geological and environmental changes are evident in parameters like dune vegetation, agriculture, water bodies, and built-up areas.

Dune vegetation has consistently declined, indicating intensified coastal erosion and increased anthropogenic pressure. Vegetation shows a gradual increase, suggesting possible reforestation or land-use shifts. Agricultural land fluctuates, dipping in 2014 but rising again in 2024, highlighting the impact of soil fertility, water availability, and farming practices.

Water bodies and rivers exhibit variations due to hydrodynamic processes such as sediment deposition, erosion, and tidal influence. The built-up area remains minimal

with inconsistent trends, possibly due to regulatory policies or changing development patterns.

Fluctuations in barren land, beach areas, and sea levels indicate ongoing coastal geomorphological changes driven by marine transgression and wave action. These trends emphasize the dynamic interactions shaping the coastal landscape.

Table:3 The Framework of tourism-led land use changes and their environment effect in Coastal Blocks

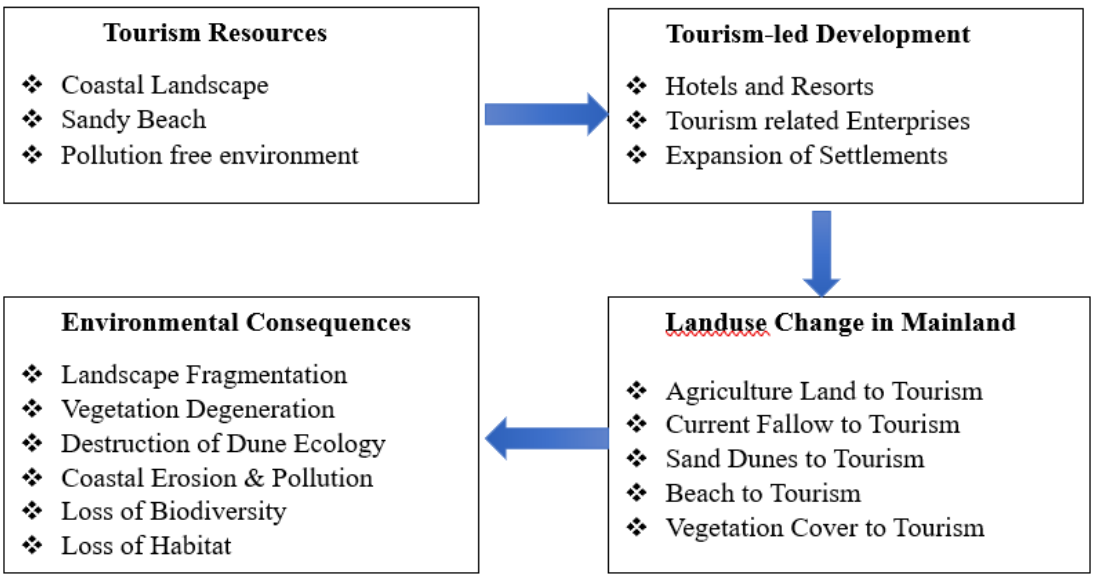

The diagram illustrates the interconnection between tourism development and environmental consequences in coastal regions, emphasizing geological and geomorphological transformations.

Tourism resources such as coastal landscapes, sandy beaches, and pollution-free environments attract large-scale tourism-led development. This results in the construction of hotels, resorts, and tourism-related enterprises, leading to urban expansion. Such infrastructural growth significantly alters coastal geomorphology, accelerating landscape modification.

Land use change in the mainland is a direct consequence, wherein agricultural land, fallow land, sand dunes, beaches, and vegetated areas are converted into tourism infrastructure. The transformation of sand dunes and vegetation into built-up areas disrupts natural sediment transport, exacerbating coastal erosion. Additionally, beaches, which act as buffers against wave action, undergo morphological changes, leading to increased vulnerability to marine transgression and storm surges.

Environmental consequences include landscape fragmentation, vegetation degeneration, and dune ecology destruction. Sand dunes, vital for coastal stability, are eroded due to excessive human activities. The depletion of vegetation cover impacts sediment

stabilization, leading to enhanced soil erosion and altered hydrological regimes. Coastal erosion, pollution, and biodiversity loss further destabilize the fragile ecosystem, affecting habitat availability for flora and fauna.

The ongoing modifications highlight the dynamic interplay between anthropogenic activities and geological processes. As tourism-driven expansion continues, sustainable coastal zone management becomes imperative to mitigate habitat loss, prevent shoreline retreat, and maintain the delicate equilibrium of sedimentary processes. Conservation measures, such as dune restoration and afforestation, can help minimize the adverse impacts of tourism-induced land use changes in the coastal environment.

Conclusion

The analysis of coastal land use and land cover (LULC) changes along the eastern Puri coast over the past 16 years highlights the significant impact of both natural and anthropogenic factors. Utilizing multi-temporal Landsat imagery from 2009, 2014, 2019, and 2024, this study provides a comprehensive assessment of LULC transformations driven by marine dynamics, urban expansion, and extreme weather events. The integration of remote sensing techniques via Google Earth Engine (GEE) and QGIS facilitated accurate classification and quantification of LULC changes, offering valuable insights into coastal dynamics.

One of the most striking findings is the continuous decline in dune vegetation, primarily attributed to frequent cyclonic events, particularly the 2019 Fani cyclone. These extreme weather conditions have led to significant erosion and the degradation of coastal vegetation, underscoring the vulnerability of dune ecosystems. Despite this decline, general vegetation exhibited a marginal increase, possibly due to conservation efforts, afforestation programs, or shifts in land use. However, these gains are not sufficient to counteract the rapid depletion of coastal greenery, necessitating more effective management strategies.

Urban expansion emerged as a dominant driver of LULC changes, with built-up areas increasing by 1. 234% between 2009 and 2024. The conversion of sandy beaches, dunes, plantations, agricultural fields, and barren lands into urban infrastructure reflects the region's growing developmental pressures. The increasing built-up footprint poses challenges such as habitat loss, increased surface runoff, and a higher risk of flooding, particularly in low-lying coastal zones. Sustainable urban planning is crucial to mitigate these risks and ensure balanced coastal development.

Barren land displayed notable fluctuations over the study period, peaking in 2014 before declining by 2024. This variability suggests that land-use practices and climate conditions significantly influence the extent of barren land. A reduction in barren land could indicate reforestation, agricultural reclamation, or increased development

activities. However, it also raises concerns about land degradation and soil erosion, particularly in areas with fragile coastal topography.

Water bodies remained relatively stable throughout the study period, with a slight increase from 2009 to 2019, followed by a minor decline. This stability suggests that hydrological conditions in the region have remained largely unchanged, although localized shifts may have occurred due to seasonal variations, storm surges, or infrastructure developments. Notably, the expansion of the beach area and sea extent in 2019 indicates the impact of storm surges and tidal fluctuations, reinforcing the need for coastal protection measures.

Overall, this study underscores the dynamic interplay between natural forces and human interventions in shaping the coastal landscape of the eastern Puri coast. The findings highlight the urgent need for sustainable land-use practices, integrated coastal zone management (ICZM), and climate-resilient infrastructure development. Future policies should prioritize the conservation of dune ecosystems, implement strict zoning regulations to control urban sprawl, and enhance coastal defence mechanisms to mitigate erosion and flooding risks.

As climate change continues to amplify the frequency and intensity of extreme weather events, proactive planning and adaptive strategies are essential to balance developmental goals with environmental sustainability. The insights from this study serve as a valuable resource for policymakers, urban planners, and environmentalists, guiding efforts toward a more resilient and ecologically sustainable coastal future.

Reference

- Adger WN, Kelly PM, Nguyen HN (2001) Living with environmental change: social vulnerability, adaptation and resilience in Vietnam, 1st edn. Routledge, London.
- Ali AMS (2006) Rice to shrimp: land-use/land-cover changes and soil degradation in Southwestern Bangladesh land-use. Policy 23:421–435
- Alphan, H. (2003). Land-use change and urbanization of Adana, Turkey. Land Degradation and Development, 14(6), 575– 586.
- Chase TN, Pielke RA, Kittel TGF, Nemani RR, Running SW (2000) Simulated impacts of historical land cover changes on global climate in northern winter. Clim Dyn 16:93–105.
- Choudhary, R., Gowthaman, R., & SanilKumar, V. (2013). Shoreline change detection from Karwar to Gokarna-South West coast of India using remotely sensed data. International Journal of Earth Sciences and Engineering, 6(3), 489–494.

- Coppin, P., Jonckheere, I., Nackaerts, K., Muys, B., & Lambin, E. (2004). Review article digital change detection methods in ecosystem monitoring: a review. International Journal of Remote Sensing, 25(9), 1565–1596.
- Dale VH (1997) the relationship between land-use change and climate change. Ecol Appl 7:753–769
- Fung, T., & Ledrew, E. (1987). Application of principal components analysis to change detection. Photogrammetric Engineering and Remote Sensing, 53(12), 1649–1658.
- Gilani, H., Shrestha, H. L., Murthy, M. S. R., Phuntso, P., Pradhan, S., Bajracharya, B., & Shrestha, B. (2015). Decadal land cover change dynamics in Bhutan. Journal of Environmental Management, 148, 91–100.
- Gupta, M. (2014). Monitoring shoreline changes in the Gulf of Khambhat, India during 1966–2004 using RESOURCESAT1 LISS-III. OpenJournal ofRemote Sensingand Positioning, 1(1), 27–37.
- Gupta, M. (2014). Monitoring shoreline changes in the Gulf of Khambhat, India during 1966–2004 using RESOURCESAT1 LISS-III. OpenJournal ofRemote Sensingand Positioning, 1(1), 27–37.
- INCOIS (2009). Indian National Centre for Ocean Information Services. Report on use of satellite data for detection of violation of land use along the coastal regulation zone and impact of port structures on shoreline changes.
- Ioannis, M., & Meliadis, M. (2011). Multi-temporal Landsat imageclassification andchange analysis of land cover/useinthe prefecture of Thessaloiniki, Greece. Proceedings of the International Academy of Ecology and Environmental Sciences, 1(1), 15–25.
- Islam MR (2006) Managing diverse land-uses in coastal Bangladesh: institutional approaches. Program Development Office for Integrated Coastal Zone Management, Dhaka, Bangladesh
- Johnson, R. D., & Kasischke, E. S. (1998). Change vector analysis: a technique for the multispectral monitoring of land cover and condition. International Journal of Remote Sensing, 19(3), 411–426
- Knorr, W., Pytharoulis, I., Petropoulos, G. P., & Gobron, N. (2011). Combined use of weather forecasting and satellite remote sensing information for fire risk, fire and fire impact monitoring. Computational Ecology and Software, 1(2), 112–120.
- Li, X., & Yeh, A. G. O. (1998). Principal component analysis of stacked multi-temporal images for the monitoring of rapid urban expansion in the Pearl River Delta. International Journal of Remote Sensing, 19(8), 1501–1518.
- Mahapatra, M., Ratheesh, R., & Rajawat, A. S. (2013). Shoreline change monitoring along the South Gujarat coast using remote sensing and GIS

techniques. International Journal of Geology, Earth and Environmental Sciences, 3(2), 115–120. Mahapatra, M., Ratheesh, R., & Rajawat, A. S. (2014). Shoreline change analysis along the coast of South Gujarat, India, using digital shoreline analysis system. Journal of the Indian Society of Remote Sensing, 42(4), 869–876.

- Manek, N. P., & Balaji, R. (2014). Assessment of shoreline oscillations along South Gujarat coastline, India. Indian Journal of Marine Sciences, 43(7).
- Mani Murali, R., & Dinesh Kumar, P. K. (2015). Implications of sea level rise scenarios on land use/land cover classes of the coastal zones of Cochin, India. Journal of Environmental Management, 148, 124–133.
- Muttitanon, W., & Tripathi, N. K. (2005). Land use/land cover changes in the coastal zone of Ban Don Bay, Thailand using Landsat 5 TM data. International Journalof Remote Sensing, 26(11), 2311–2323.
- Nelson, R. F. (1983). Detecting forest canopy change due to insect activity using Landsat MSS. Photogrammetric Engineering and Remote Sensing, 49, 1303–1314.
- Nicholls, R. J., & Small, C. (2002). Improved estimates of coastal population and exposure to hazards released. Eos, Transactions American Geophysical Union, 83(28), 301–305.
- Nicholls, R. J. (2003). Case study on sea-level rise impacts. In OECD Workshop on the Benefits of Climate Policy: Improving Information for Policy Makers. 9, 69–86.
- Rahman MH, Lund T, Bryceson I (2011) Salinity impacts on agrobiodiversity in three coastal, rural villages of Bangladesh. Ocean Coast Manag 54(6):455–468
- Rahman MR, Andob K, Takedaa S (2013) Development of shrimpbased cropping systems in the coastal area of Bangladesh: a village-level study in Satkhira district. Journal of Land-use Science Rowsell ECP, Sultana P, Thompson P (2013) The 'last resort'? Population movement in response to climate-related hazards in Bangladesh. Environ Sci Policy 27:S44–S59
- Ridd, M. K., & Liu, J. (1998). A comparison offour algorithms for change detectioninanurban environment. RemoteSensingof Environment, 63(2), 95–100.
- Singh, A. (1989). Review article digital change detection techniques using remotely-sensed data. International Journal of Remote Sensing, 10(6), 989–1003.
- Toll, D. L. (1985). Effect of Landsat thematic mapper sensor parameters on land cover classification. Remote Sensing of Environment, 17(2), 129–140.

- Townshend, J. R. G., & Justice, C. O. (1995). Spatial variability of images and the monitoring of changes in the normalized difference vegetation index. International Journal of Remote Sensing, 16(12), 2187–2195.
- UN-HABITAT (2010) Land and natural disasters: guidance for practitioners. United Nations Human Settlements Programme (UN-HABITAT).
- Wisner B, Piers B, Cannon T, Davis I (2004) At risk: natural hazards, people's vulnerability and disasters, 2nd edn. Routledge, London.

Utilizing Remote Sensing techniques to investigate beach placer minerals along the coastal zones of Odisha, India

Suman Acharya* and Smruti Rekha Sahoo

Department of Geology, Fakir Mohan University, Balasore, Odisha -756089

*Corresponding Email: acharyasuman171@gmail.com

Abstract

The state of Odisha, surrounded by Jharkhand in the north, Chhattisgarh in the west, Andhra Pradesh in the south and the Bay of Bengal in the east, has a long coastline of 480 km. Odisha is recognized as one of the leading producers of placer minerals in India. In light of this, it is proposed to study the heavy minerals of the Odisha coast. Applications of remote sensing data are wide and unique in the mapping of different lithologies, mineral resources, and ore deposits. Satellite images are capable in discriminating rock types useful for geological applications and are significantly used in the identification of mineral resources. The absorption characters of multi-spectral bands of Landsat-8 (OLI) images are analyzed using image enhancement techniques such as geometric correction, FLAASH (Fast Line-of-Sight Atmospheric Analysis of Hypercubes module) atmospheric correction, band math, and band ratios to demonstrate the sensor capability for mapping heavy mineral deposits. The combination of remote sensing and field investigations can lead to generating a high accuracy mineralogical map.

Keywords: Remote Sensing, Heavy Mineral, Coast, Odisha

Introduction

The Odisha coast is known for its placer deposits associated with the Eastern Ghats Mobile Belt, which includes granite, migmatite, khondalite, and charnockite rock types, potentially influencing the composition of beach placer minerals. Heavy minerals such as ilmenite, rutile, zircon, monazite, tourmaline are very essential deposits having high economic and industrial importance. These are having high specific gravity (> 2. 85), resistant to abrasion, chemically stable. In the coastal areas of Odisha, heavy minerals with beach placer deposits are abundant, where beach placer and river placer are the two main types of placer minerals. Advances in remote sensing have developed digital image processing algorithms for mapping heavy minerals on the earth`s surface. Remotely sensed data are nowadays, frequently used for mineral exploration around the

world. This study will boost methods for mineral exploration as an eco-friendly technique of natural resources. High potential of multispectral satellite data can be used for exploration and mapping.

Geological Setting of the Study area

The coastal plains of Odisha are the sedimentary landforms of recent origin. Geologically they are of Paleogene and Neogene age. This region stretches from the Subarnarekha basin in the north to the Rushikulya basin in the south. A major part of this region is formed by deltas of the six major rivers i. e. the Mahanadi, the Brahmani, the Budhabalanga, the Subarnarekha, the Baitarani, and the Rushikulya. This has given rise to the names such as the "Gift of Six Rivers" or the "Hexadeltaic region".

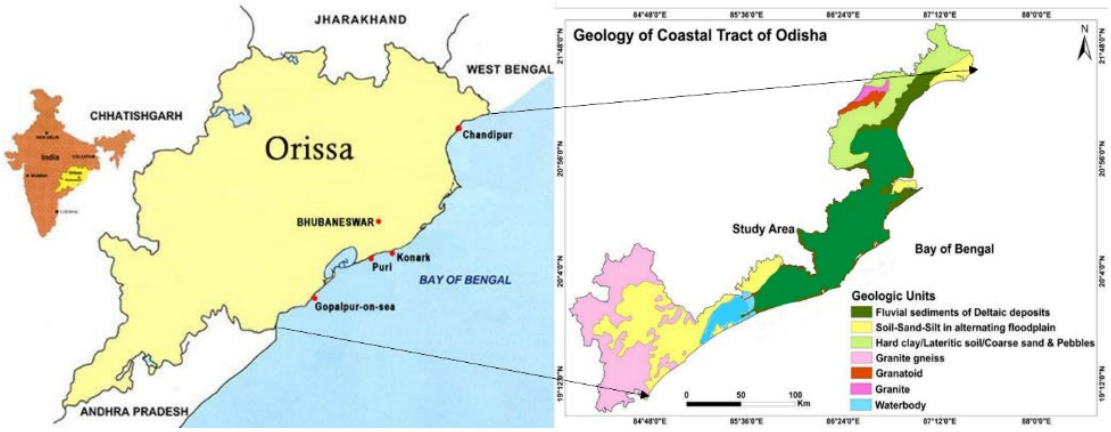

Fig. 1 Location map of the study area (Geological map of the coastal districts)

This region is rich in alluvial soils. The coastal region of Talsari at Balasore, Ramchandi at Puri, Chhatarpur at Ganjam possess heavy mineral deposits like monazite, zircon, tourmaline, rutile. So, the present study focuses on the capability of the potential of multispectral remote sensors in the direction of heavy mineral targeting.

Mineral deposit mapping is essential for sustainable and eco-friendly exploitation of natural resources. Currently the beach sands are extracted for export entirely in raw form without any value addition. Due to unsustainable sand mining, there are negative environment impacts, which lead to various coastal hazards such as erosion, salinization and sea-water intrusion. To initiate the focus on mapping of mineral deposits along this area, standardized hyperspectral analysis has been carried out using Landsat satellite data and Environment for Visualizing Images (ENVI) software (Lillesand, Keifer and Chipman, 2015). The selected endmembers are identified by comparing the spectral signatures with predefined spectral plots from the United States Geological Survey (USGS) spectral library. Finally, the endmembers are mapped with ENVI's spectral angle mapper (SAM). The minerals which show significant variation in reflectance at different spectral bands can be effectively mapped by using multispectral data. Ground verifications performed to assess the accuracy of classification were mostly in agreement

with the obtained results. This study has opened up new areas for inland heavy mineral exploitation and leads to eco-friendly exploitation of natural resources along the study area. It also illustrates the high potential of multispectral satellite data for exploration and mapping of mineral resources (Chandrasekhar, N., et al. 2014).

Methodology and Data Used

The different image attribute extracting techniques, spectral enhancement methods is applied on the satellite image data to prospect heavy minerals. The Landsat satellite images are analysed using image enhancement techniques such as geometric correction, atmospheric correction, band math, band ratios, as a preliminary exploration tool. The aspects of image processing and spectral enhancement applied to satellite imagery, particularly for heavy mineral exploration using Landsat data.

Geometric Correction

Geometric correction is applied to ensure that the satellite image accurately represents the Earth's surface. This step is essential when comparing images from different periods or integrating satellite data with other spatial datasets (like maps). Geometric correction aligns image pixels to geographical coordinates using ground control points (GCPs), rectifying distortions caused by the sensor's perspective, Earth curvature, or satellite movement (Hutchinson and Bowering, 2005).

Atmospheric Correction

Atmospheric correction is used to remove the effects of the atmosphere (e. g., scattering, absorption) that can distort the radiometric values recorded by the satellite sensor. Without this correction, the reflected radiance captured by the sensor may not accurately represent the Earth's surface features (Mumby et al., 2002). Atmospheric correction techniques like the Dark Object Subtraction (DOS), Empirical Line Method (ELM), or radiative transfer models can be employed to adjust for atmospheric interference.

Band Math and Band Ratios

- **Band Math**: This refers to mathematical operations applied to the raw satellite data from multiple bands (e. g., adding, subtracting, multiplying bands, or applying more complex functions). Band math can help highlight specific features of interest by combining or transforming bands to enhance the visibility of those features.
- **Band Ratios**: Band ratios are particularly useful in remote sensing to highlight differences in surface features. By dividing the reflectance values of one band by another, band ratios emphasize specific mineral characteristics or vegetation types. For mineral exploration, certain ratios can highlight areas where heavy minerals like iron oxide or clay minerals are present (Kharat and Tripathy, 2016). Common band ratios in Landsat data include:

- **NIR/Red**: Often used to detect vegetation or soil moisture.
- **SWIR/NIR**: Useful for identifying clay minerals, altered rocks, or moisture content in minerals.
- **Red/Green or Blue/Green**: Can be used for detecting mineral composition and differentiating between land cover types.

Spectral Enhancement Techniques

These techniques aim to improve the visibility of certain features or materials in the satellite image that might not be clearly distinguishable from the original data. Common spectral enhancement methods include:

- **Contrast Stretching**: Enhances the contrast in the image by stretching the range of pixel values.
- **Histogram Equalization**: Adjusts the pixel values of an image to distribute them more evenly across the intensity range, making subtle features more visible.
- **Principal Component Analysis (PCA)**: A statistical method used to reduce the dimensionality of the data, while retaining the most important spectral information. PCA can enhance features that are harder to detect in individual bands.

Satellite images, particularly those from Landsat, provide valuable data for exploring mineral deposits.

Summary

This study has concentrated on the physical properties, identification, and abundance of the heavy minerals fraction in sediments collected from the study area. Satellite imagery Landsat-8 OLI was used for remote sensing verifications. The image processing and crucial analysis carried out using Environment for Visualizing Images (ENVI) and QGIS software. Coastal areas adjacent to Odisha has a very significant amount of heavy mineral reserves. The study has identified around several variety of heavy minerals from the collected samples in the study area. Ilmenite, Kyanite, Garnet, Rutile, Zircon, Magnetite, Augite, Hornblende, Enstatite, Epidote, Andalusite, Hypersthene, Diopside and Cassiterite have been found the most abundant in the entire study area. The Coastline of Odisha was surveyed completely through literature survey to map the heavy minerals which are potential resources for national economy (Gazi, Y. Md., et al. 2019). Thus, the present study summarises that spectral remote sensing is much more capable for mineral targeting. Advance remote sensing techniques can be used to investigate heavy mineral placers in the coastal areas of Odisha, which is also eco-friendly. The combination remote sensing and field investigations can lead to generate the high accuracy mineralogical map.

References

- N. Chandrasekar, P. Sheik Mujabar & G. V. Rajamanickam, 2014. Investigation of heavy-mineral deposits using multispectral satellite data, *International Journal of Remote Sensing.*
- Md. Yousuf Gazi, Khandakar Tahmida Tafhim, Md. Kawser Ahmed, Md Atikul Islam, 2019. Investigation of heavy-mineral deposits using multispectral satellite imagery in the eastern coastal margin of Bangladesh, *Earth Sciences Malaysia (ESMY)*.
- Mumby, P. J., & Edwards, A. J. (2002). "Mapping coral reef habitat using high resolution remote sensing imagery. " *Coral Reefs*, 21(1), 44-53.
- Hutchinson, I., & Bowering, E. (2005). "Satellite remote sensing for mineral exploration. " *Exploration Geophysics*, 36(4), 282-289.
- Kharat, K. M., & Tripathi, S. (2016). "Remote Sensing for Mineral Exploration. " *Mineral Resources and Ore Reserves*, 1(1), 49-59.
- Lillesand, T., Kiefer, R. W., & Chipman, J. (2015). "Remote Sensing and Image Interpretation" (7th Edition).

Geomorphic and Hydrogeologic Condition of the Baitarani Rivershed in Anandapur Block, Keonjhar District: A GIS Approach

Sradhasuman Sahoo and Rosalin Das

Fakir Mohan University, Balasore, Odisha

Abstract:

The present study investigates the groundwater quality and hydrogeological characteristics of the Anandapur Block, Odisha, using an integrated approach of field surveys, GIS-based thematic mapping, and physicochemical analysis of water samples. The research involves the preparation of thematic maps, including geological formations, land use patterns, drainage networks, elevation variations, and lithology using QGIS. These maps provide insights into the spatial distribution of hydrogeological features, aiding in the assessment of groundwater resources.

A total of seventy groundwater samples were collected during the pre-monsoon season (April–May 2024) from various locations across the Anandapur Block to analyze key water quality parameters. The physicochemical analysis includes pH, electrical conductivity (EC), total dissolved solids (TDS), total hardness (TH), major cations (Ca^{2+}, Mg^{2+}, Na^{+}, K^{+}), and anions (Cl^{-}, NO_3^{-}, HCO_3^{-}, SO_4^{2-}). The results were compared with WHO drinking water standards to assess the potability and potential health risks. The findings indicate that most water quality parameters fall within permissible limits, though variations in alkalinity and hardness were observed. GIS mapping proved instrumental in integrating hydrogeological data, offering a comprehensive understanding of groundwater recharge patterns and hydrological connectivity. The study provides valuable insights for sustainable groundwater management and informed decision-making to address water quality and resource conservation in the region.

Introduction:

The availability of clean water is crucial for the proper functioning of ecosystems and the development of human civilization, agriculture, and industry. The Baitarani Rivershed in Anandapur Block, Keonjhar District is an area of significant hydrological importance. Originating from the Guptaganga hills (Gonasika) of Keonjhar District, the Baitarani River enters the delta plain at Anandapur, characterized by its highly meandering course (Mishra et al., 2019). Heavy mining activities and shifts in cultivation practices contribute large quantities of sediment during the monsoon season,

reducing the river system's carrying capacity and causing frequent floods even with moderate rainfall. The presence of shallow aquifers, lack of drainage, and extensive waterlogged areas exacerbate flooding (CWC, 2014). This article focuses on the preparation of thematic maps, laying the foundation for subsequent project stages by providing a comprehensive overview of the environmental factors influencing groundwater dynamics. Hydrological data, gathered through a combination of field surveys and open sources, offers insights into precipitation patterns, surface water flows, and lithology.

Study area

The proposed study area spreads over 708 Sq. Kms between 21^0. 07'-$21^0$33'N latitude and $85^0$58'-$86^0$15' longitude. Baitarani is the main river in this block with the major tributaries like Musal and Kusei rivers. A significant part of the block is covered by denudational hills in the middle part. The prominent hydro-geomorphic units including pediments, buried pediments and quaternary alluvium cover the rest of the block area in the northern and southern parts.

Geology

Entire block is occupied by the Singhbhum Granites. In the northern part, there are several linear basic dolerite dykes intersecting the country rock. Approximately 85% of the block exhibits a ground slope of less than 10%, facilitating effective groundwater recharge through soil infiltration. The soil composition consists of red sandy soil (alfisol), red lateritic soil (ultisol), and alluvial soil (alfisol), contributing to the diverse ecological makeup of the area. CGWB (2020)

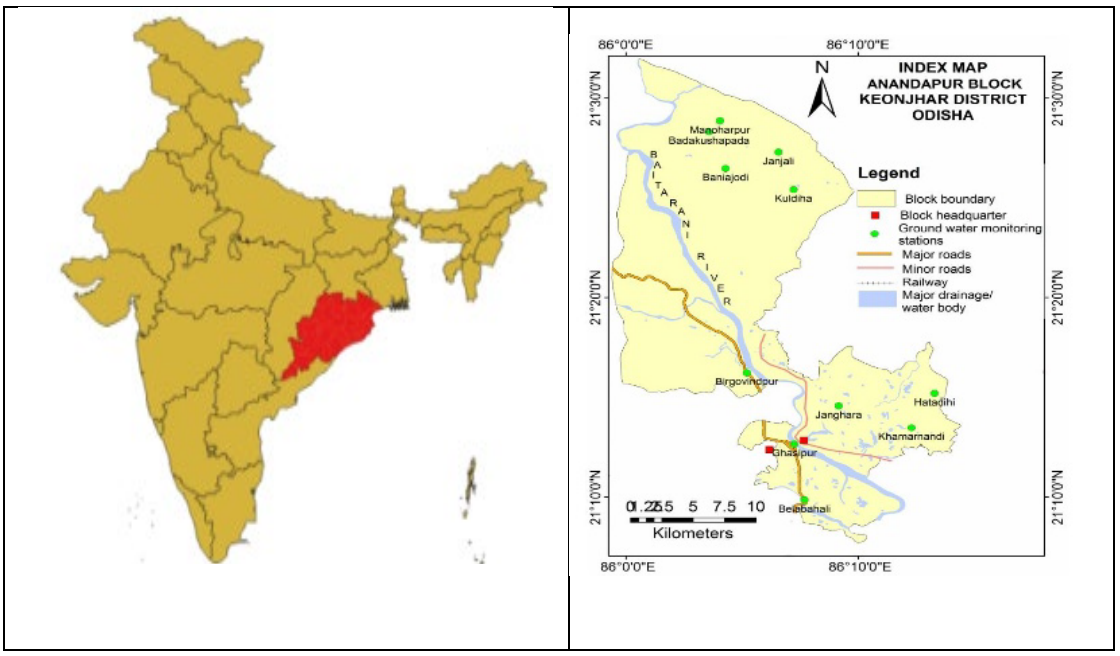

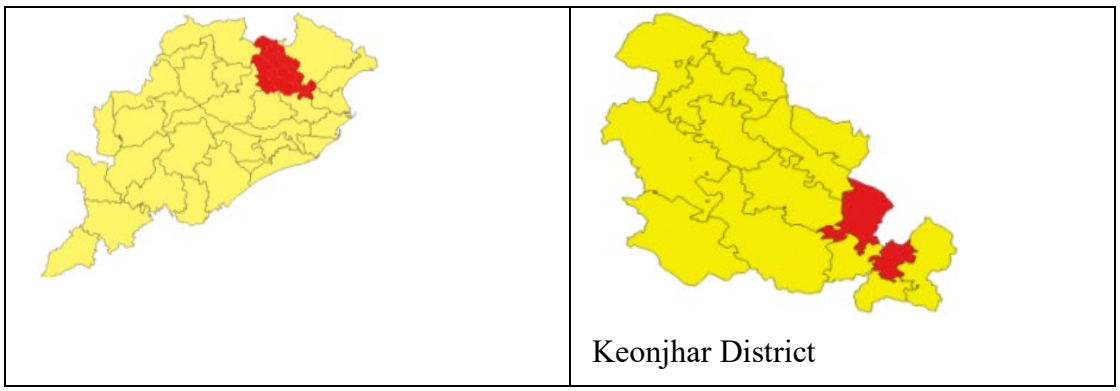

Fig. 1 Location map of the study area

Drainage

The length of the Baitarani River within Anandapur Block of Keonjhar District is approximately 65 kilometers. The river within Anandapur block showcases a dendritic drainage pattern, functioning as the primary drainage network for the region. This pattern is characterized by smaller streams and tributaries like Musal and Kusei, which converge into the Baitarani as they descend towards the main river channel. The overall drainage dynamics are influenced significantly by topography, climate conditions, and the underlying geological formations of the area. These factors collectively shape the flow patterns and distribution of water within the watershed, impacting local ecosystems and human activities reliant on water resources.

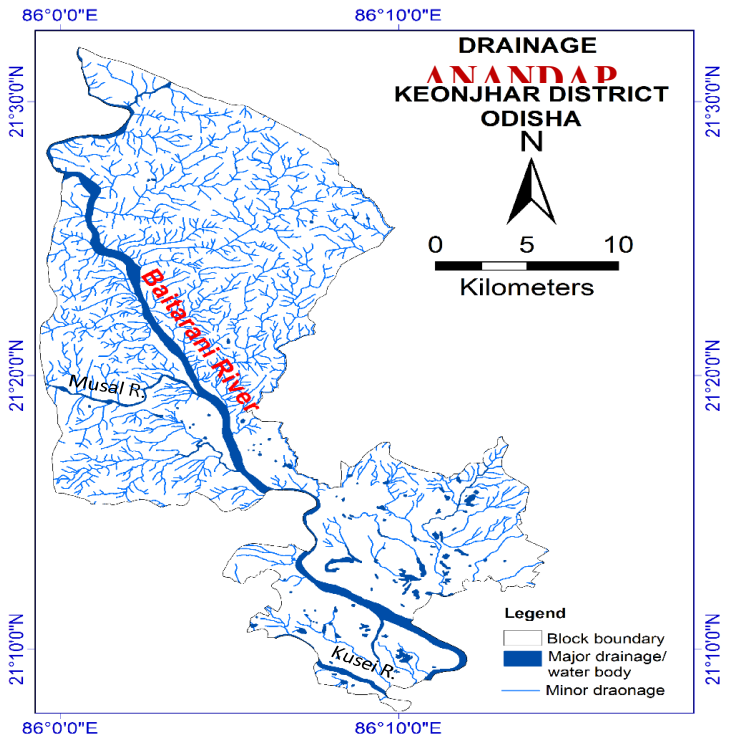

Fig. 2 Drainage map of Andapur Block

Geomorphology

In Anandapur Block, the geomorphological map highlights various landforms, geological features, and the distribution of natural resources. The map features gently rolling hills such as pediments and buried pediments, dominated by the Baitarani River basin and its tributaries. The block contains several small hills, including residual hills, structural hills, and denudational hills, formed as a result of erosion and sedimentation. Intermontane valleys, carved by rivers and streams, are where sediments are deposited during high water flows. Alluvial soil is found near riverbanks, providing fertility and supporting agriculture. Other soil types, like laterite, are found in uplands and are less fertile, contributing to the region's diverse geomorphology.

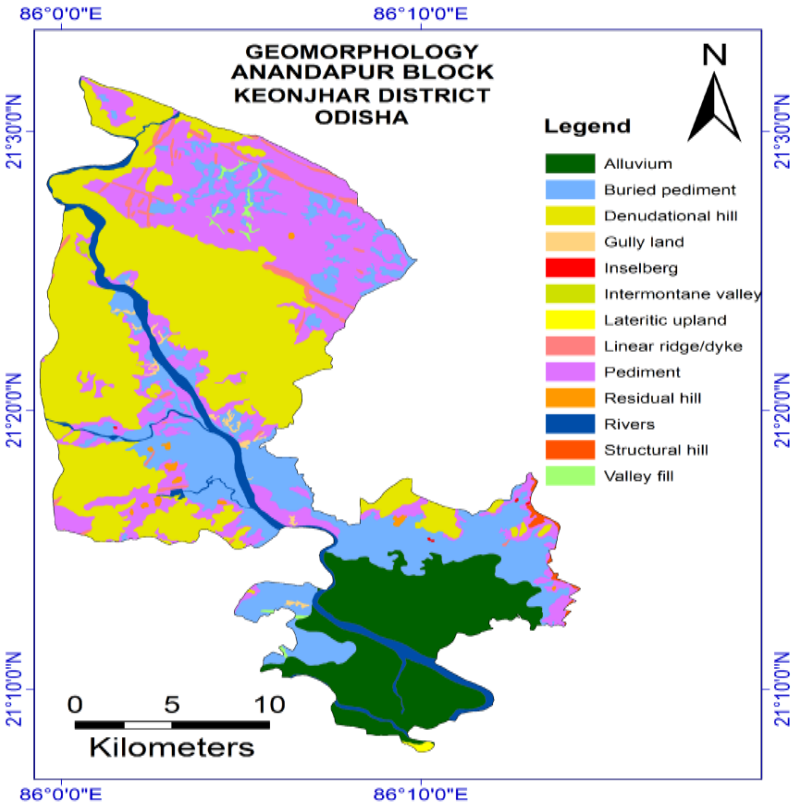

Fig. 3 Geomorphology map of Andapur block

Lithology

The lithology of Anandapur Block includes various rock types such as granite, granitic gneiss, gneiss, quartzite, banded hematite jasper (BHJ), banded hematite quartzite (BHQ), and some alluvial soils. The area is also characterized by several linear dolerite dykes cutting across the northern parts, influencing the distribution and formation of these country rocks. The iron-rich BHJ/BHQ formations provide significant importance to the southeastern end of the area. This geological diversity plays a crucial role in the region's hydrological dynamics.

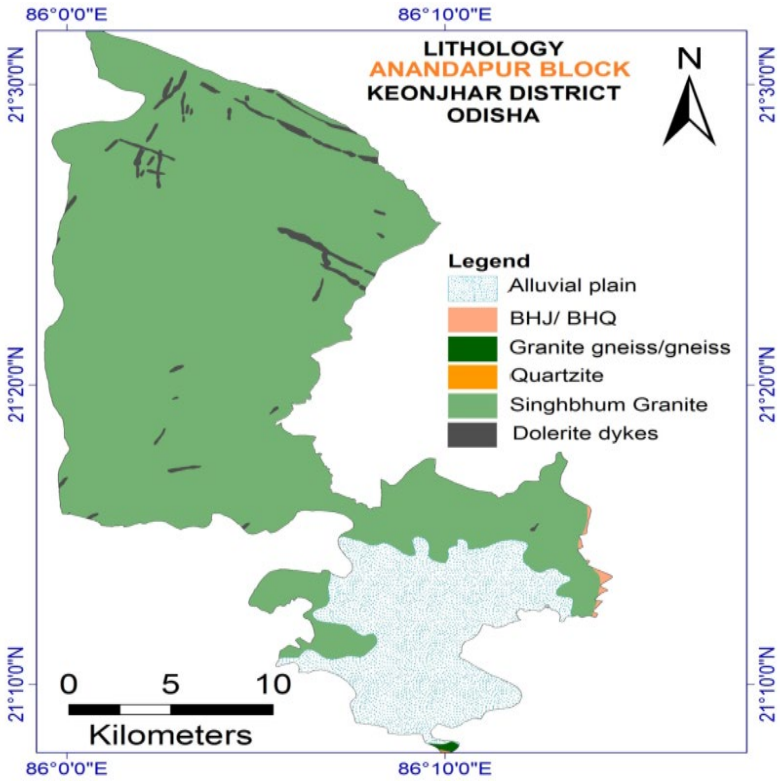

Fig. 4 Lithology of the study area

Hydrology

The hydrogeology of Anandapur Block is characterized by diverse geological formations that influence groundwater dynamics in the region. Groundwater in Anandapur Block is primarily stored in shallow aquifers, influenced by the permeability and porosity of the underlying rocks and sediments. Alluvial soils near riverbanks enhance groundwater recharge and storage, providing vital support to agricultural activities. Conversely, regions with lateritic soils in uplands generally exhibit lower groundwater availability due to reduced permeability.

The hydrological regime is further shaped by the drainage patterns, predominantly controlled by the Baitarani River and its tributaries like Musal and Kusei. Seasonal variations in precipitation and surface water flows significantly affect groundwater recharge rates and quality. Human activities such as mining and agriculture also impact hydrogeological conditions, influencing groundwater levels and contaminant transport. The weathered residum in the Precambrian rocks at shallow depth and the fracture zones at deeper depths form groundwater repositories in the hard rock areas of the block. The Singhbhum Granites possess low to moderate yield potential varying between 3-10 lps. Hilly areas with very poor aquifers indicate very low water yield.

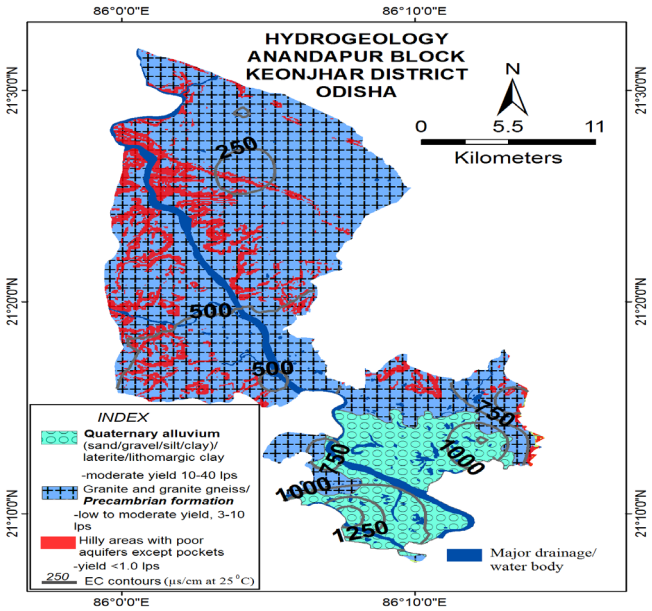

Fig. 5 Hydrogeology of the study area (source:CGWB)

Slope

Approximately 85% of the block features ground slopes of less than 10%, which promote effective groundwater recharge through soil infiltration. The terrain varies from relatively flat in the plains to moderately steep gradients in hilly areas. Steeper slopes (>40%) are typically found in the hilly regions, while gentle slopes (<10%) are common in plains and valleys. Areas with steeper slopes facilitate faster runoff and drainage, influenced by downhill water flows, and are more susceptible to soil erosion during heavy rainfall events.

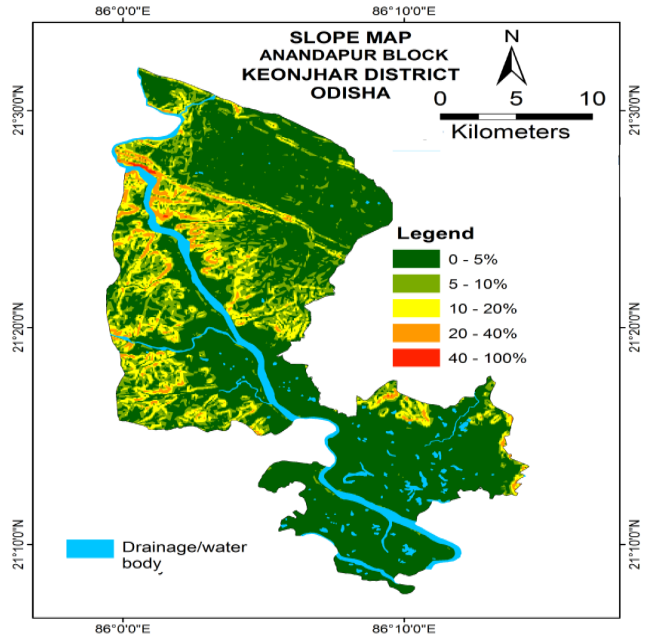

Fig. 6 Slope map of the study area.

Methodology

The present research work has been carried out with field survey, preparation of thematic maps using GIS, collection and analysis of groundwater samples of the study area. The thematic mapping is a crucial step in understanding the spatial distribution of various features within the study area. This includes preparation of location maps of geological formations, land use patterns, and hydrological features, drainage map, elevation map, lithological variations using QGIS. Water samples were collected to infer water chemistry of the study area.

Seventy water samples were collected during pre-monsoon (April -May) season of 2024 from different parts of Anandapur block and analyzed using standard laboratory methods proposed by APHA (2012) and used by Das et. al (2013, 2015, 2016 and Das 2022. Electrical conductivity (EC) and PH of the water samples were measured by digital meters immediately after sampling. Major cations (Na+, K+, Ca^{2+} and Mg^{+2}) and anions (CO_3^{2-}, $HCO3^-$, Cl^- and SO_4^{2-}, NO_3^-) including total hardness (TH) and alkalinity (TA) of the water samples were determined following standard analytical procedures. Ca^{2+}, CO_3^{2-}, HCO_3^- and Cl^- determined by volumetric titrations. Na^+ and K^+ were estimated by flame photometer and SO_4^{2-} was estimated by spectrophotometer. Total dissolved solid (TDS) was estimated from EC and Mg^{2+} was calculated from TH and Ca^{+2} by employing standard equations.

Result and discussion

Water Chemistry

Water is a universal solvent. The salts present in it are primarily derived from the rocks and soils through which it travels to arrive at the well. The analysis provides the concentration of different parameters of the ground water. The pH of water is an indicator of its quality and geochemical equilibrium (Hem, 1985). In the study area it varies from 7. 1 to 7. 7 suggesting mild saline to slightly alkaline nature of the groundwater. The electrical conductance (EC) varies from 325 to 1050µs/cm from which the amounts of total dissolved solid are estimated to be 208 to 672 mg/l. Total alkalinity and hardness values vary from 100 - 395 and 89. 9 - 360 mg/l respectively. Out of the major cations, Ca^{+2} (15 - 100 mg/l) dominates over Mg^{+2} (9. 7 – 36. 45 mg/l), while Na^+ and K^+ are present in subordinate amounts being 21. 8 – 65. 2 and 0. 3 – 3. 6 mg/l respectively. CO_3^{2-}(0 – 48 mg/l) has been reported from few of the water sample, perhaps due to absence of limestone and dolomite in the study area. Bicarbonate is the dominant anion (49 - 300mg/l) which is possibly derived from carbon dioxide released by organic decomposition in the soil (Todd, 1980). Sulphate, varying from 17 - 99 mg/l is subordinate to chloride (40 – 85 mg/l). $NO3^-$ (nitrate) varies from (3. 2 – 12. 6 mg/l). Fluoride content will be within the permissible limit that varying from 0. 2 – 0. 35 mg/l that suggest that within this period the water will be free from fluoride contaminations.

Table. 1 resents the water quality of the area compared with the water quality standard given by WHO.

Table 1: Comparison of water quality with WHO standard

Parameter	**Range in Study Area**	**WHO Standard**	**Remarks**
pH	7. 1 - 7. 7	6. 5 - 8. 5	Slightly alkaline, within permissible limits
EC (µS/cm)	325 - 1050	1500	Within limits
TDS (mg/L)	208 - 672	500 (desirable), 1500 (max)	Mostly within acceptable range
Total Alkalinity (mg/L)	100 - 395	No specific guideline	Higher values may affect taste
Total Hardness (mg/L)	89. 9 - 360	100 - 500	Generally within limits
Ca^{2+} (mg/L)	15 - 100	75 (desirable), 200 (max)	Mostly within acceptable limits
Mg^{2+} (mg/L)	9. 7 - 36. 45	50	Within permissible limits
Na^{+} (mg/L)	21. 8 - 65. 2	200	Well below limit
K^{+} (mg/L)	0. 3 - 3. 6	No specific guideline	Within safe range
CO_3^{2-} (mg/L)	0 - 48	No specific guideline	Reported in few samples
HCO_3^{-} (mg/L)	49 - 300	No specific guideline	Dominant anion, influenced by organic matter decomposition
SO_4^{2-} (mg/L)	17 - 99	250	Within safe limits
Cl^{-} (mg/L)	40 - 85	250	Within permissible limits
NO_3^{-} (mg/L)	3. 2 - 12. 6	50	Well below permissible limit
F^{-} (mg/L)	0. 2 - 0. 35	1. 5	Within safe limits

Conclusion

The groundwater quality in the study area largely falls within WHO permissible limits. However, variations in alkalinity and hardness are observed, while carbonate presence

remains limited due to geological factors. Fluoride contamination is minimal, and nitrate levels are well below hazardous thresholds, indicating overall safe water quality.

Furthermore, the geomorphic and hydrogeological survey of Anandapur Block, conducted using GIS technology, provides crucial insights into the region's landscape and water resources. The study identifies diverse landforms such as pediments, residual hills, and intermontane valleys, showcasing the area's complex geological evolution. The hydrogeological assessment reveals groundwater distribution influenced by formations including granite, gneiss, and alluvial soils. GIS mapping has been instrumental in integrating field data with spatial analysis, offering a comprehensive understanding of groundwater recharge patterns and hydrological connectivity. These findings serve as a foundation for sustainable water management and informed decision-making to address groundwater depletion and environmental sustainability challenges in Anandapur Block.

References

- APHA (2012) Standard methods for the examination of water and wastewater, 19 th edn. American Public Health Association, Washington DC.
- Central Water Commission (2014) Govt. of India, Ministry of Water Resources, Brahmani Baitarani Basin, Version 2. 0.
- Das, R. 2022. Monitoring the seasonal variation of groundwater chemistry and quality assessment for agricultural and industrial purpose of Athgarh basin, India, Journal of Environment, Ecology and Conservation, Eco. Env. & Cons. 28 (1), pp. 298-309, Copyright@ EM International, ISSN 0971–765X, DOI No. : http://doi. org/10. 53550/EEC. 2022. v28i01. 043
- Das, R., Das, M. and Goswami, S. 2013. Groundwater quality assessment for irrigation uses of Banki Sub-division, Athgarh Basin, Odisha, India. Journal of Applied Geochemistry. 15 (1), pp. 88-97.
- Das, R., Das, M. and Goswami, S. 2016. Groundwater quality Assesment for drinking and industrial purpose of Rourkela, Sundergarh District, Odisha, India. International Journal of Earth Science and Engineering. (6), pp. 314-321.
- Das, R., Goswami, S., Das, S., Das, M. 2015. Hydrogeochemistry and Groundwater quality assessmentfor irrigation purpose in and around Rayagada Town, Odisha, India. International Journal of EarthScience and Engineering 8 (2), pp. 611- 616. (SJR:0. 15) (ISSN:0974- 5904), http://cafetinnova. org/journals/ ijee/about- journal/) SCOPUS UGC No. 2901
- Devi, A. B., & Nair, A. M. (2021). Effects of urbanisation in a shallow coastal aquifer: An integrated GIS-based case study, India. Groundwater for Sustainable Development, 15, 100656
- Mishra S. P. et al (2019) Delta Partitioning, Geospatial Changes, Anastomosis of Mahanadi Tri-delta, India; IJEE, DOI:10. 21276/ijee. 2019. 12. 0103

- Sahu S. (2020) DOI:10. 13140/RG. 2. 219583. 02729. https://www. researchgate. net/publication/341598509